I. En Route to the Synthesis of the Heterocorannulenes

II. Synthesis and Study of Silver (I) and Copper (I) Complexes of Diazafluoranthene Derivatives

Dissertation

zur

Erlangung der naturwissenschaftlichen Doktorwürde (Dr. sc. nat.)

vorgelegt der

Mathematisch-naturwissenschaftlichen Fakultät

der

Universität Zürich

von

Nelli Rahanyan

aus Armenien

Promotionskomitee:

Prof. Dr. Jay S. Siegel (Vorsitz)

Prof. Dr. Reto Dorta

Prof. Dr. Kim K. Baldridge

Zürich, 2010

Die vorliegende Arbeit wurde von

der Mathematisch-naturwissenschaftlichen Fakultät

der Universität Zürich im November 2010

als Dissertation angenommen

Promotionskomitee:

Prof. Dr. Jay S. Siegel (Vorsitz)

Prof. Dr. Kim K. Baldridge

Prof. Dr. Reto Dorta

Universität Zürich, 2010

TABLE OF CONTENTS

LIST OF FIGURES

LIST OF SCHEMES

LIST OF TABLES

ACKNOWLEDGEMENTS

Prof. Dr. Jay S. Siegel
Prof. Dr. Kim K. Baldridge
PD Dr. Anthony Linden
PD Dr. Nathaniel S. Finney

UNIZH NMR Service
UNIZH MS Service

Asst. Prof. Dr. Yoshizumi Yasui (Kyoto University, Japan)
Dr. Michael Löpfe
Dr. Simon Duttwyler
Derik Frantz
Anna Butterfield

All Siegel and Baldridge group members past and present

CURRICULUM VITAE

Nelli Rahanyan

Organic Chemistry Institut, University of Zurich
Winterthurerstrasse 190, CH-8057 Zurich, Switzerland
rahanyan@oci.uzh.ch

Educational Qualification

2005-2010	Ph.D. Studies in Organic Chemistry, University of Zurich, Switzerland
1997-1999	Master of Science, Post-Graduate School, State Engineering University of Armenia, Yerevan, Armenia
1993-1997	Bachelor of Science, Diploma of Chemical Engineer, State Engineering University of Armenia, Yerevan, Armenia

Work Experience

1997-2004	Research fellow at the laboratory of natural products. Institute of Organic Chemistry National Academy of Sciences of the Republic of Armenia
2002–2003	IAESTE exchange programme. Laboratory for Sensory and Chemical Analysis, Iggesund, Sweden
2004	IAESTE exchange programme. Company: Clariant Ltd, Reinach BL, Switzerland

Teaching Experience

2005-2010	Monitoring and supervising undergraduate medical students in first-year laboratory experiments as well as evaluating and correcting their written reports.
Poster Presentation	12th International Symposium on Novel Aromatic Compounds (ISNA–12), **2007**, Awaji Island, Japan
	12th European Symposium on Organic Reactivity (ESOR 12), **2009**, Haifa, Israel
Oral Presentation	Swiss Chemical Society Meeting (SCS), **2008**, Zürich, Switzerland

List of Publications

1. Rahanyan, N.; Duttwyler, S.; Linden, A.; Siegel, J. S. "*Molecular grids. Silver (I) and copper (I) complexes of diazafluoranthene derivatives.*" Manuscript in preparation.
2. Rahanyan, N.; Linden, A.; Baldridge, K.; Siegel, J. S. "*Heterocorannulenes – novel aromatic systems, challenging synthetic targets.*" Manuscript in preparation.
3. Rahanyan, N.; Linden, A.; Baldridge, K.; Siegel, J. S. *"Diels-Alder reactions of 3,6-disubstituted 1,2,4,5-tetrazines. Synthesis and X-ray crystal structures of diazafluoranthene derivatives." Org. Biomol. Chem.* **2009**, *7*, 2082-2092.
4. Karapetyan, A. A.; Tamazyan, R. A.; Mikaelyan, A. R.; Rahanyan, N. P. *"X-ray investigation of (E)-2-phenyl-1-chlorocyclopropane-1-carboxylic acid – a convenient synthon for transamine synthesis." J. Struc. Chem.* **2004**, *45*, 352.

ABSTRACT OF THE DISSERTATION

I. En Route to the Synthesis of the Heterocorannulenes

II. Synthesis and Study of Silver (I) and Copper (I) Complexes of Diazafluoranthene Derivatives

by

Nelli Rahanyan

University of Zurich, 2010

Professor Jay S. Siegel, Chair

I. Non-planar polyarenes represent a growing class of aromatic compounds possessing unique electronic properties, which can be attributed to their special molecular structure. Corannulene $C_{20}H_{10}$, the smallest curved subunit of fullerene, has many structural and electronic parallels to C_{60}. Incorporation of heteroatoms into fullerene architectures manifests special electronic and physical properties. An open question is how this parallel withstands heteroatom substitution into the corannulene scaffold. Heterocorannulenes are interesting objects of study with regard to photophysical, metal binding, and stereodynamic properties. The first part of this dissertation is dedicated to the synthetic work aimed at the formation of such bowl-shaped heteroaromatics. Two basic areas of research are addressed: 1) to the synthesis of a novel 1,2-diazacorannulenes and 2) construction of 1,6-dithiacorannulenes.

Attempts at the synthesis of the first nitrogen-containing heterobuckybowl led to the isolation of two series of 8,9-diazafluoranthenes. Synthesis of these compounds has been accomplished using an inverse electron demand [2 + 4] cycloaddition strategy. The crystal structures of 17 members of this series of diazafluoranthenes are reported. Stereochemical analysis shows that diazafluoranthenes, substituted across the bay region, are helically-twisted strained aromatic molecules. The dihedral angle between pyridazyl *vs* naphthyl rings ranges from 0.5° to 20.9°, and follows the degree of steric congestion in the bay region. The crystal structures are compared to computational structures

determined using density functional theory, with the M06-2X/cc-pVDZ method.

Synthesis of dithiatetrahydrocorannulenes proceeds via 1,6-dibromo-7,10-bis(bromomethyl)fluoranthene or 1,6-dibromo-7,10-bis(bromomethyl)-3,4-dichlorofluoranthene – key intermediates in this synthesis. The former was synthesized from naphthalene-2,7-diol in 8 steps, whereas the later comes from acenaphthene in 5 steps. Ring closure was accomplished by an intramolecular copper-catalyzed C–S coupling reaction. Interconversion barriers between bowl/flat structures as well as relative energies for different structural conformations have been determined using density functional theory, with the M06-2X/TZVP method.

II. Metallosupramolecular chemistry, the chemistry of metal ion-ligand association, allows one to synthesize complexes of different leitmotifs, including rotaxanes, catenanes, cages and grids. The second part of this dissertation describes complexation reactions of 7,10-disubstituted diazafluoranthene derivatives with three different silver salts and $[Cu(CH_3CN)_4][PF_6]$. Expected [2 x 2] grid-like molecular association was obtained from the reaction of 2,5-di-*tert*-butyl-7,10-di-(pyrimidin-2-yl)-8,9-diazafluoranthene with $[Cu(CH_3CN)_4][PF_6]$. In the case of the sterically-hindered ligand 2,5-di-*tert*-butyl-7,10-di(pyridin-2-yl)-8,9-diazafluoranthene, butterfly-like tetrameric complex $[Cu_4(L)_4][PF_6]_4$ was obtained from the system acetone/pentane. The reaction of 2,5-di-*tert*-butyl-7,10-di(pyridin-2-yl)-8,9-diazafluoranthene with Ag^I salts affords complexes of two structural motifs. The use of relatively small anions, namely $[PF_6]^-$ and $[SbF_6]^-$, leads to the formation of tetranuclear complexes, differing from grid-type structures, whereas the larger anion $[CHB_{11}Cl_{11}]^-$ favors the formation of a wave-type dimeric structure. 2,5-di-*tert*-butyl-7,10-di-(pyrimidin-2-yl)-8,9-diazafluoranthene and 2,5-di-*tert*-butyl-7,10-di(thiazol-2-yl)-8,9-diazafluoranthene, which are less hindered in terms of H–heterocycle repulsion, afford crystals of dinuclear and polymeric complexes with $AgPF_6$ and $AgSbF_6$.

ZUSAMMENFASSUNG

I. En Route to the Synthesis of the Heterocorannulenes

II. Synthesis and Study of Silver (I) and Copper (I) Complexes of Diazafluoranthene Derivatives

von

Nelli Rahanyan

Universität Zurich, 2010

Professor Jay S. Siegel, Vorsitz

I. Nicht planare Polyarene stellen eine wachsende Klasse an aromatischen Verbindungen dar und besitzen spezielle elektronische Eigenschaften. Corannulen, $C_{20}H_{10}$, die kleinste Untereinheit der Fullerene (C_{60}), besitzt verschiedenste strukturelle und elektronische Parallelen zu C_{60}-Molekülen. Die Einführung von Heteroatomen in einem fulleren-ähnlichen Aufbau bietet neuartige elektronische und physikalische Eigenschaften. Eine bisher ungeklärte Frage stellt die Position der Heteroatome im Corannulengerüst dar. Heterocorannulene spielen eine wichtige Rolle hinsichtlich photosphysikalischen, metallbindenden und stereodynamischen Eigenschaften. Der erste Abschnitt dieser Dissertation konzentriert sich auf die synthetische Arbeit bezüglich des Aufbaus und der Synthese solcher gebogenen schalenförmige Heterocorannulene. Zwei Hauptziele werden in dieser Arbeit ausgeführt: 1) die Synthese von neuartigen 1,2-Diazocorannulenen und 2) der Aufbau von 1,6-Dithiacorannulenen.

Versuche zur Synthese der ersten stickstoffhaltigen Heterocorannulene führte zum Erhalt zweier Reihen von 8,9-Diazafluoranthenen. Um diese Komponenten zu erhalten, wurde eine [2+4] Cycloaddition mit inversem Elektronenbedarf verwendet. Die Kristallstrukturen der 17 Mitglieder dieser Serie von Diazafluoranthenen wurden bestimmt. Stereochemische Analysen zeigen, dass nur die Moleküle der Diazafluoranthenen, welche an der Stelle der Bay-Region substituiert sind, helikal verdreht sind.

Der Torsionswinkel zwischen Pyridazyl- *vs* Naphthyl-Ringen variieren zwischen 0.5° bis 20.9° und folgen dem Grad der sterischen Hinderung in der Bay-Region. Die Kristallstrukturen hierzu wurden durch ein Berechnungsverfahren, der sogenannten Dichtefunktionaltheorie (DFT) mit der M06-2X/cc-pVDZ Methode bewiesen.

Die erfolgreiche Synthese des Dithiatetrahydrocorannulens erfolgte über 1,6-Dibromo-7,10-bis(bromomethyl)fluoranthen beziehungsweise über 1,6-Dibromo-7,10-bis(bromomethyl)-3,4-dichlorofluoranthen – die Schlüsselzwischenstufen dieser Synthese. Das zuerst erwähnte Intermediat wurde in acht Stufen ausgehend von Naphthalen-2,7-diol synthetisiert, das Zweite innerhalb 5 Stufen ausgehend von Acenaphtene als Vorläufer. Der Ringschluss wurde durch eine intramolekulare Kupfer-katalysierte C-S Kupplung erreicht. Interkonversionsbarrieren zwischen der schalenförmige und der flachen Struktur, sowie relative Energien von verschiedenen strukturellen Konformationen wurden durch Dichtefunktionaltheorie per M06-2X/cc-pVDZ Methode bestimmt.

II. Metallosupramolekulare Chemie, oder ebenso die Chemie der Metallion-Liganden-Bindung, bietet die Möglichkeit zur Herstellung von Komplexen aus unterschiedlichsten Leitmotiven wie z.b. Rotaxane, Catenane, Käfige und Gittergerüste. Der zweite Teil der Dissertation befasst sich mit Komplexbildung von Derivaten der disubsituierten 7,10-Diazofluoranthene mit drei verschiedenen Silbersalzen sowie $[Cu(CH_3CN)_4][PF_6]$. Die erwartete [2 x 2] gerüstähnliche molekulare Assoziation wurde durch die Reaktion von 2,5-Di-*tert*-butyl-7,10-di-(pyrimidin-2-yl)-8,9-diazafluoranthen mit $[Cu(CH_3CN)_4][PF_6]$ erhalten. Bei Verwendung des sterisch gehinderten Liganden 2,5-Di-*tert*-butyl-7,10-di(pyridin-2-yl)-8,9-diazofluoranthene, wurde ein schmetterlings-ähnlicher tetramerischer Komplex $[Cu_4(\mathbf{L})_4][PF_6]_4$ in Aceton/Pentan gewonnen. Die Reaktion von 2,5-Di-*tert*-butyl-7,10-di(pyridin-2-yl)-8,9- diazofluoranthen mit Ag (I) Salzen brachte Komplexe mit zwei unterschiedlichen strukturellen Bausteinen hervor. Durch Verwendung von relativ kleinen Anionen, $[PF_6]^-$ sowie $[SbF_6]^-$, werden vierkernigen Komplexe gebildet, die sich von den Strukturen des Gittergerüsts unterscheiden. Hingegen werden durch grössere Anionen $[CHB_{11}Cl_{11}]^-$ bevorzugt wellenähnliche dimere Strukturen gebildet. 2,5-Di-*tert*-butyl-7,10-di-(pyrimidin-2-yl)-8,9-diazafluaranthen und 2,5-Di-*tert*-butyl-7,10-di(thiazol-2-yl)-8,9-diazafluoranthen sind

bezogen auf die *H*-heterozyklische Abstossung weniger sterisch hindernd und führen zu diatomaren und polymerischen Komplexen mit $AgPF_6$ und $AgSbF_6$.

Chapter 1. Polycyclic Aromatic Hydrocarbons (PAHs) and Heteroatom Derivatives

1.1 Introduction

Polycyclic aromatic hydrocarbons (PAHs) can be found in a diverse class of organic compounds, and some of them have shown carcinogenic, mutagenic, and teratogenic properties.[1-3] PAHs exist in oil, air, fat, foods, wood, tobacco, water and were also detected in the interstellar medium, in comets and in meteorites.[4-9] Catalytic reforming and carbonization of hard coal are two important industrial processes for the production of PAHs.[10] Technological applications of PAHs are associated with plastic and dye industry, as well as in liquid crystals,[11] optoelectronic devices,[12] organic superconductors,[13] molecular wires,[14] and solar cells.[15]

Balaban recently noted: "*Of approximately 20 million chemical compounds identified by the end of the second millennium, more than two-thirds are fully or partially aromatic, and approximately half are heteroaromatic*."[1d] Antimalarial,[16] antineoplastic,[17,18] antiallergic,[19] antiinflammatory,[20] fungicidal,[21] and antiviral[22] properties of heterosubstituted PAHs make them important core components in the synthesis of many drugs, and biochemical processes. Antimalarial properties of quinine were already known in the sixteenth century, and this compound was used to treat malaria until the 1940s, when discovery of other drugs replaced it.[23,24] Indole, another important heteroaromatic molecule,[25] is the major constituent in the skeleton of many important drugs such as indomethacin, strychnine and LSD. The structure of many coenzymes, for example nicotinamide adenine dinucleotide (NAD)[26] and flavin adenine dinucleotide (FAD),[27] also consist of heteroaromatics.

Described herein are the syntheses of a series of polycyclic aromatic hydrocarbons and heteroatom derivatives. Along with the synthesis of these compounds, structural data and any reported physical properties are discussed. Research into the synthesis, structure and dynamics of such PAHs will advance our knowledge and provide a better understanding of the chemistry of carbon based materials and heteroaromatics in general. Represented below are naphthalene (and its monoheteroatom derivatives) and seven examples of non-planar polycyclic aromatic and heteroaromatic hydrocarbons.

1.2 Naphthalene and its heteroatom analogues

Naphthalene (**1**) (Figure 1.1), bicyclo[4.4.0]deca-1,3,5,7,9-pentene is the smallest representative of PAHs and was first isolated from coal tar in 1819. Identification of the chemical structure of **1** was carried out by the two famous scientists Michael Faraday, who established the chemical formula of naphthalene,[28] and Emil Erlenmeyer, who suggested the structure of two fused benzene rings.[29] Industrial importance of naphthalene is associated with production of phthalic anhydride,[30] mothballs and in the synthesis of 2-naphthol, used for the preparation of various dyestuffs, pigments, and pharmaceuticals.[31]

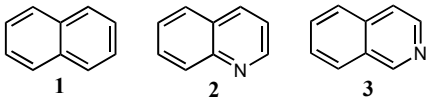

Figure 1.1 Naphthalene (**1**), quinoline (**2**), isoquinoline (**3**)

Quinoline (**2**) and isoquinoline (**3**) – heteroanalogs of naphthalene, are of great interest in pharmacy and industry. They have been used as fungicidal,[32] bactericidal,[33] insecticidal,[34] and algicidal[35] agents, as well as in preservatives for leather, textiles, plastics, coatings, paper pulp, and seeds. Similar to naphthalene, quinoline and isoquinoline were first isolated from coal tar in 1834 and 1885 respectively.[36] Owing to the more basic properties of isoquinoline (pKa 5.5) in comparison to quinoline (pKa 4.9), Weissgerber (1934) has developed new route to this compounds using selective extraction method.[37] Being a fundamental sub-unit of many PAHs, polycyclic heteroaromatics, graphenes, buckminsterfullerenes, as well as carbon nanotubes, naphthalene, quinoline and isoquinoline can be precursors to construct such aromatics.

1.2.1 Synthesis

Despite many synthetic routes to naphthalene, quinoline and isoquinoline, coal tar is still the main resource for the industrial production. It contains about 10% naphthalene by weight, and produce ≈1 million tons annually.[31] Approximately 0.3% quinoline and 0.2% of isoquinoline can be isolated from high-temperature coal tar.

Mixture of quinoline and isoquinoline can be further isolated from the methylnaphthalene fraction by extraction with sulfuric acid, and followed rectification of the crude base mixture (quinoline bases) allows to separate quinoline from isoquinoline (*bp* 6 °C higher).[38] Production of **2** and **3** can be also accomplished in laboratory, using various methods. Synthesis of quinoline via Skraup,[39] Friedländer,[40] Combes[41] and Knorr[42] methodology is well known and described in literature. Some of these methods are given below.

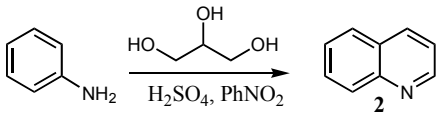

Scheme 1.1 Skraup quinoline synthesis

According to the Skraup method, quinoline was synthesized by heating aniline and glycerol with sulfuric acid in the presence of a dehydrogenating agent (Scheme 1.1). Base-catalyzed condensation of 2-aminobenzaldehydes with ketones supports the formation of quinoline derivatives and bares the name of Friedländer synthesis (Scheme1.2).

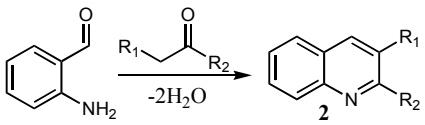

Scheme 1.2 Friedländer quinoline synthesis

Synthesis of isoquinoline derivatives can be carried out via several methods, but only a few direct pathways have been developed for unsubstituted product **3**. An efficient method for the preparation of isoquinoline is Pomeranz-Fritsch reaction[43] (Scheme 1.3). Isoquinoline, prepared in this way, include the acid catalyzed reaction of a benzaldehyde and aminoacetoaldehyde diethyl acetal. The same results can be achieved using benzylamine and a glyoxal acetal.

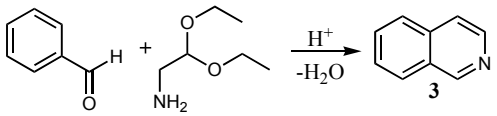

Scheme 1.3 Pomeranz-Fritsch isoquinoline synthesis

Bischler-Napieralski,[44] Pictet-Gams[45] and the Pictet-Spengler[46] reactions are alternative methods for the synthesis of isoquinoline derivatives. In spite of many synthetic routes to quinoline and isoquinoline, these syntheses are not yet industrially important because sufficient quantities of **2** and **3** can be produced from coal tar.

1.2.2 Structures and properties

Compounds **1**, **2** and **3** were found to adopt planar, fused ring systems. Naphthalene was one of the first substances studied by X-ray method in 1921 by William Bragg. The first report on the structure of naphthalene gave a clear picture about the shape and size of the molecule. More comprehensive data were later received, based on the investigations of thermal motion in crystalline naphthalene using X-ray diffraction data.[47]

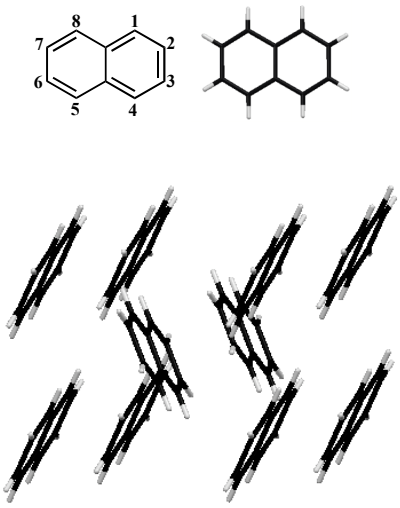

Figure 1.2 Crystal structure and packing in naphthalene[47g]

The asymmetric unit of **1** consists of two centrosymmetric molecules, (monoclinic, space group *P21/a*), the herringbone packing of 1 is shown in Figure 1.2.

Three different carbon-carbon bonds length in naphthalene comes from the presence of three resonance structures. The bond lengths between C_1–C_2, C_3–C_4, C_5–C_6 and C_7–C_8 carbons are about 1.38 Å, whereas the other carbon-carbon bonds are about 1.42 Å.

Analogous to benzene, naphthalene can undergo electrophilic aromatic substitution (Friedel-Crafts reaction), which leads to the formation of two products, alpha and beta isomers.[48] Oxidation of naphthalene with CrO_3, $KMnO_4$ or O_2 in the presence of vanadium catalyst gives phthalic acid.[49] High pressure catalytic hydrogenation of naphthalene form tetraline ($C_{10}H_{12}$) or decaline ($C_{10}H_{18}$).[50]

The first report on quinoline structure was not published until 2001.[51] The difficulty to obtain a suitable single crystal of quinoline, which is liquid at room temperature, explains the delay in structural analysis. Quinoline crystallizes in the space group *P2₁/c*, with the asymmetric unit comprising two molecules (Figure 1.3). These molecules are linked via two types interactions; C-H···N interractions into two orthogonal sets of chains and edge-to-face C–H···π interactions.

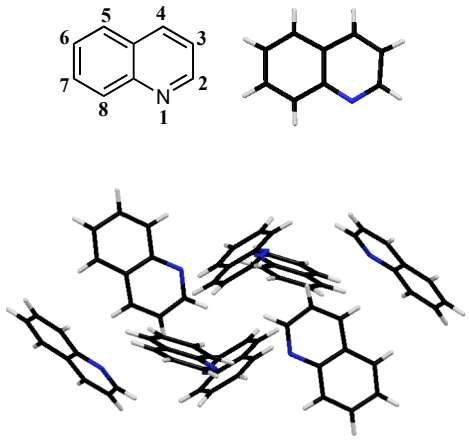

Figure 1.3 Crystal structure and packing in quinoline

Since the pyridine ring in quinoline is π-electron deficient, nucleophilic attack takes place at the 2- and 4-positions. Substitution of electrophilic reagents preferably takes place at the 5- and 8-positions. Catalytical hydrogenation of quinoline leads to 1,2,3,4- or 5,6,7,8-tetrahydroquinoline, and further to decahydroquinoline.[52] Depending on the oxidizing agent and the reaction conditions, oxidation of quinoline leads to quinoline *N*-oxide, 2-quinolinol or 2-quinolinone, quinolinic acid (pyridine-3-carboxylic

acid), or nicotinic acid.

Isoquinoline (**3**), a structural isomer of quinoline, best known as a subunit of the isoquinoline based alkaloids,[53] crystallizes in the monoclinic space group $P2_1/c$, with the asymmetric unit comprising one molecule (Figure 1.4).[54] Analogous to quinoline, isoquinoline molecules are linked via C-H···N and C–H···π interactions. Isoquinoline (**3**) is a colorless, hygroscopic liquid that crystallizes on solidifying. Catalytical hydrogenation of **3** lead to the 1,2,3,4- or 5,6,7,8-tetrahydroisoquinoline and further to decahydroisoquinoline.[52c] Oxidation in the liquid or vapor phase lead to a mixture of nicotinic and isonicotinic acids, the use of peroxyacids gives isoquinoline *N*-oxide.[55]

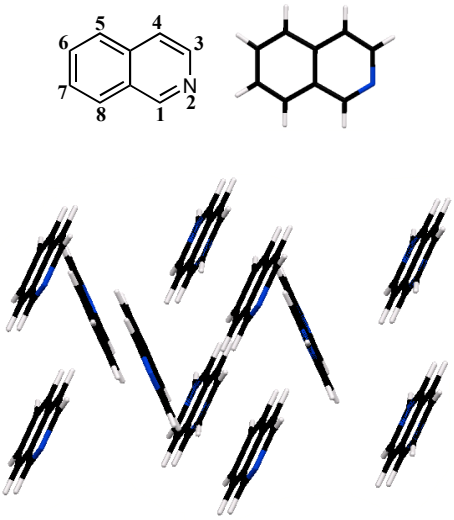

Figure 1.4 Crystal structure and packing in isoquinoline (**3**)

Isoquinoline (**3**) as well as quinoline (**2**) and naphthalene (**1**) are 10 π-electron aromatic systems, with resonance energies of 143, 198 and 255 kJ/mol.[56] They are weak bases, slightly more basic than pyridine. Compared to isoquinoline (2.60 D), quinoline has lower dipole moment (2.10 D, Figure 1.5).

The differences in the C-C bonds lengths in **2** and **3** are similar to those in naphthalene, for which they were calculated by averaging the three resonance structures.

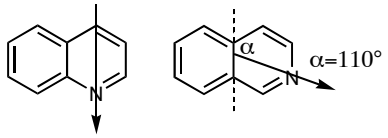

Figure 1.5 Dipole moment in quinoline and isoquinoline

In a case of quinoline, the shorter bonds ca. 1.38 Å are all bonds that are double-bonds in two of the three resonance structures, while the longer are double bonds only in one out of the three resonance structures.[57]

1.3 Helicenes

The helicene family constitutes a class of molecules with many intriguing characteristics such as chirality, building of columnar systems in the solid state, the ability to behave as organic conductors, etc.[58-60] Despite their aromaticity, these molecules can not be planar for steric reasons. Since the first synthesis of [*n*]helicenes,[61] numerous works have been carried out on helicenes containing only C-atoms.[58,62] In the recent years, particular interest was paid, e.g., to thiohelicenes, molecules with fused thiophene and benzene rings. These compounds show an interesting properties – assembling behaviour in the solid state.[63] The use of heteroaromatic compounds, containing N-atoms in the complexation process, leads to the formation of large supramolecular complexes with new intriguing properties, the field of study for many research groups.[64]

1.3.1 Synthesis

Connection and annelation are usually two key synthetic steps in the synthesis of [*n*]helicenes. Multiple annelation is the most efficient approach to the [*n*]helicenes, and allows to form two or more rings in one synthetic step. The synthetic route to the the first [*n*]helicenes, [*6*]pyrrohelicene and [*5*]helicenes (Figure 1.6), was reported in the early 1930s.[65] Twenty years later (1956) Newman and Lednicer described the synthesis of the first non-racemic [*n*]helicene - [6]helicene.[61] Photochemical synthesis of [14]helicenes and [15]thiahelicenes - the longest helicenes to date, was developed during the 1960s and 1970s.[58,66] Nonphotochemical approaches to the [*n*]helicenes includ different methods:

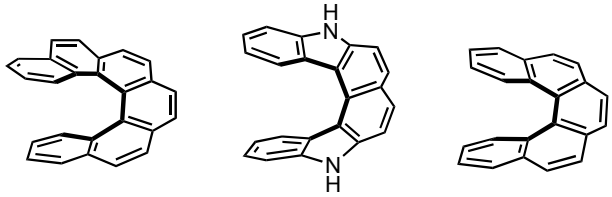

Figure 1.6 [*n*]Helicenes

electrochemical or chemical ($FeCl_3$) oxidation,[67] annelations via Diels-Alder reaction[68] or Friedel-Crafts acylation,[61] synthesis via oxy-Cope rearrangement,[69] McMurry coupling,[70] etc.

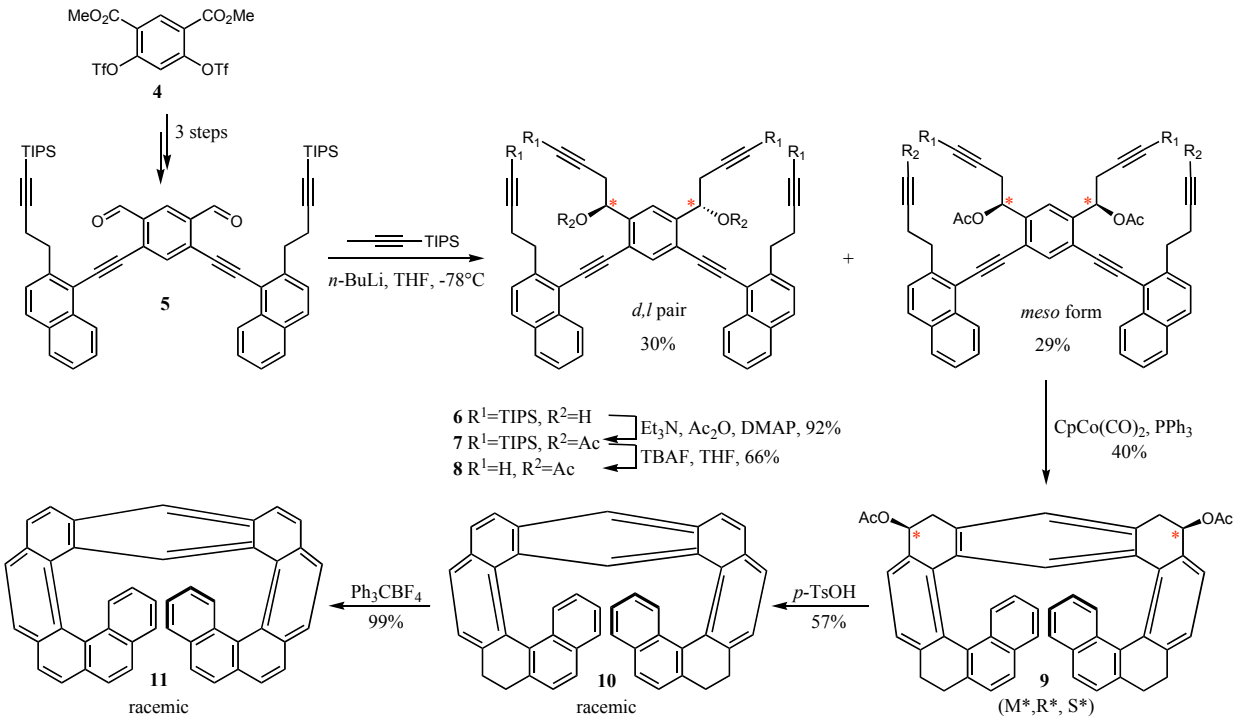

Scheme 1.4. Synthesis of racemic [11]helicene

Described below are examples of photochemical and organometallic syntheses of [11]helicene and hexathia[11]helicene. The organometallic approach to the [11]helicene is based on intramolecular cobalt – catalysed [2 + 2 + 2] cycloisomerization reaction of the corresponding triynes, which leads to the closure of 6 new rings in a single

reaction (Scheme 1.4).[71] Synthesis of dialdehyde **5** was carried out in 3 steps, starting from the known compound **4**.[72] Reaction with lithiated propyne, and followed double addition to **5** led to a 1:1 mixture of *d,l* pair (*R**,*R**)-**6** and the *meso* form (*R,S*)-**6**. Diastereomers, formed in this step, were separated by column chromatography, and further transformed in to the (*R**,*R**)-**8** and (*R,S*)-**8**. [2 + 2 + 2] cycloisomerization of (*R**,*R**)-**8** afforded mixture of diastereomers (*M**,*R**, *S**)-**9** and (*P**,*R**, *R**)-**9**. Cyclisation of *meso* hexayne (*R,S*)-**8** was carried out at 140 °C in the presence of $CpCo(CO)_2$ and PPh_3, and led to the racemic [11]helicene derivative (*M**,*R**,*S**)-**9** (up to 40%). Synthesis of racemic [11]helicene (**11)** was completed by acid-catalyzed aromatization of (*M**,*R**,*S**)-**9**, and dehydrogenation with trityl tetrafluoroborate.

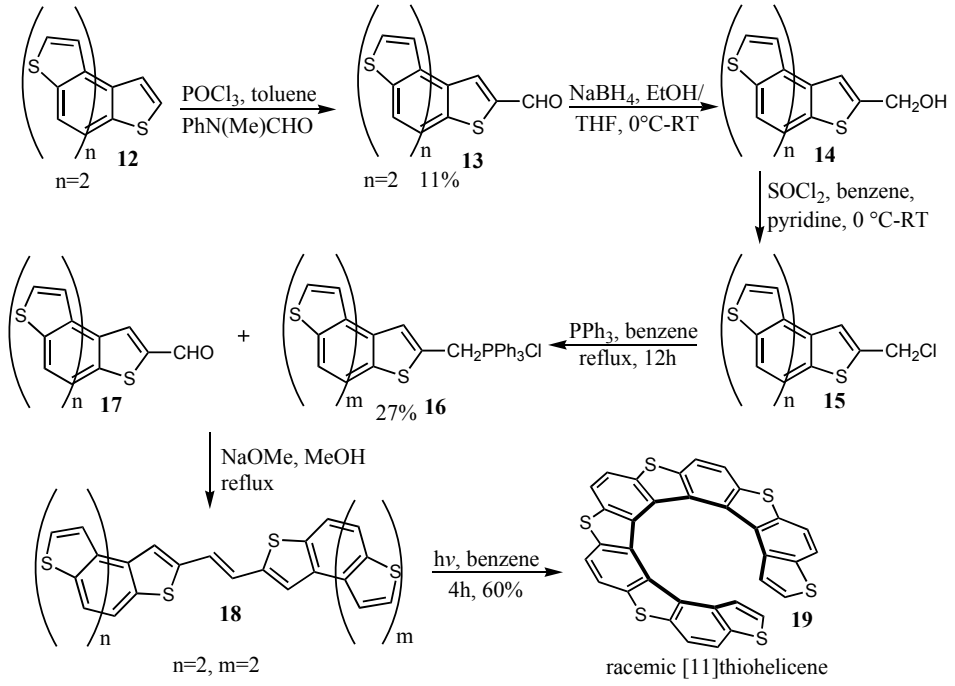

Scheme 1.5 Synthesis of hexathia[11]helicene **19**

Photochemical synthesis of a racemic thiohelicenes series containing 5, 7, 9, and 11 rings was reported by Caronna *et al*. in 2000.[73] The crucial step in the synthesis of this compounds is photocyclization of 1,2-diheteroarylethylene.[74] Synthetic approach to the [11]thiahelicene **19** (Scheme 1.5) starts by the reaction of [5]thiahelicene **12** with

Vilsmeier reagent ($POCl_3$ and $PhNCH_3CHO$), in order to obtain the corresponding 2-carboxyaldehyde **13**. Reduction of **13** with sodium borohydride followed by chlorination of **14** with thionyl chloride at 0 °C gave **15** in quantitative yield. The next step, formation of phosphonium salt **16,** was accomplished by the reaction with PPh_3 in refluxing benzene (yield 27%). Compound **16** was later converted to the corresponding 1,2-diheteroarylethylene **18** via Wittig reaction between the phosphonium salt **16** and the 2-carboxyaldehyde of the [5]thiahelicene **13**. The desired [11]thiahelicene **19** can be easily synthesized by the photoinduced cyclodehydrogenation of 1,2-diheteroarylethylene **18**.

Both racemic and enantiomeric forms of substituted thiohelicenes can also be obtained by chemical synthesis. Annelation of racemic or nonracemic intermediates,[75] and asymmetric synthesis[76] are two major approaches of nonphotochemical synthesis.

1.3.2 Structures and Properties

[11]helicene (**11)** is a stable molecule and is well soluble in various organic solvents. Higher solubility of **11** comes from limited face-to-face π-π stacking interactions between the individual molecules of **11**. No structural data on [11]helicene (**11)** has been reported.

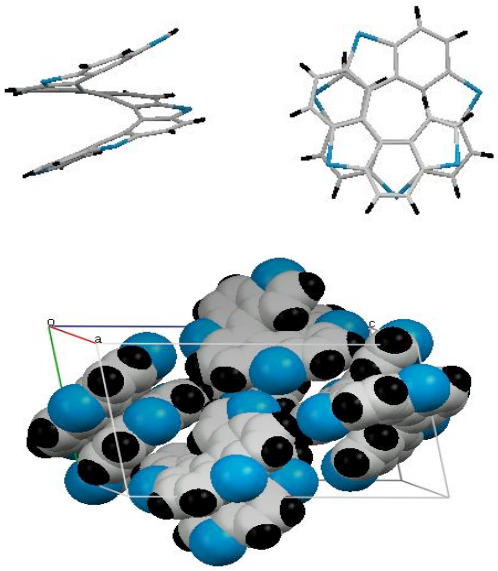

Figure 1.7 Molecular structure, side view and packing of [11]thiohelicene **19**

Figure 1.7 shows the molecular structure and the packing of the eleven-membered thiahelicene **19**, which were obtained by single-crystal X-ray diffraction. The asymmetric unit of **19** formed by two complete molecules (triclinic, space group *P1)*. In the packing environment of **19** four nonequivalent short S···S and S···H interaction are found. These specific interactions, involving also sulfur and hydrogen atoms in the central ring in **19**, play a predominant role in the aggregation process. [11]thiahelicene (**19**) as well as all other members of thiahelicene family has C_2 molecular symmetry. The conformation and the crystal architecture of [11]thiahelicene **19** shows ring distortions smaller than in [11]carbohelicene **11**.

1.4 Corannulene and fullerenes

1.4.1 Introduction

Another representative of a non-planar PAH is corannulene (**20**), which is considered as a member of a class of [*n*]circulenes.[77] This bowl-shaped polyaromatic hydrocarbon consists of five fused six-membered rings connected around the cyclopenthane ring (Figure 1.8). The presence of the curvature in the molecular scaffold of **20** provide this molecule dynamic behavior, bowl inversion.[78] The discovery of a 5-step solution phase synthesis of corannulene has stimulated much interest in the chemistry of this geodesic polyarene and its derivatives, due to their potential applications in liquid crystals,[79] dendrimers,[80,81] single-wall nanotubes,[82] light emitters,[83] chemical capsids,[84] cyclophanes,[85] molecular clefts etc.

The skeleton of corannulene constitutes 1/3 of the fullerene **21**, and has many structural and electronic parallels to C_{60}, which is the smallest stable member of the fullerene family.[86] Spherical, closed network of fullerene molecules containing a conjugated π- system consist of fused hexagons and pentagons. Unique chemical properties, as well as technological applications of buckyballs in materials science, electronics, and nanotechnology have been the subject of interest of many research groups.[87]

Increasing interest in the chemistry of fullerenes[88] and production of bulk quantities of **21** has stimulated development of chemical modifications of C_{60}.[89] Substitu-

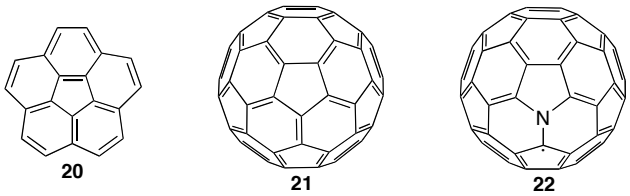

Figure 1.8 Corannulene (**20**), buckminsterfullerene (**21**) and azafullerene (**22**)

tion of one or more carbon atoms of fullerenes by heteroatoms, such as silicon, nitrogen or boron form heterofullerenes. Azafullerene **22** ($C_{59}N$),[90] the first and only known heterofullerene to date that can be prepared synthetically, has similar structure as C_{60}. Heterofullerene chemistry is quite a new discipline and is in active development.

1.4.2 Synthesis

Synthesis of corannulene (**20**) was first accomplished in 1966 by Lawton and Barth,[91] and included 16-step process. Significant innovation in the chemistry of **20** was done by Scott and Siegel groups, who suggested two different approaches to this non-planar hydrocarbon.[92,93] According to the Scott methodology, production of corannulene was carried out using flash vacuum pyrolysis method (FVP), which allowed to synthesize **20** in three steps (Scheme 1.6). The use of this strategy led to number important fullerene fragments such as cyclopentacorannulene, and semibuckminsterfullerene.[77a] Although production of **20** via FVP includes the small number of steps,[92] this strategy has several drawbacks: 1) modest yields, 2) high temperature rearrangements, leading to the formation of side products,[94] and 3) low scale reactions.

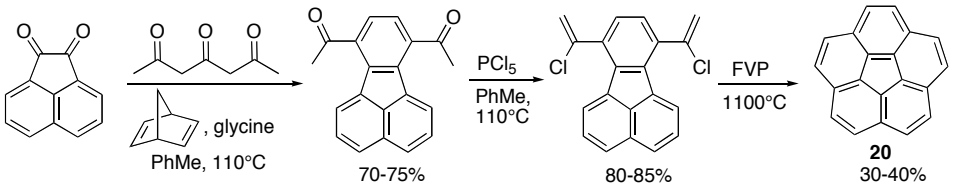

Scheme 1.6 Three step gas-phase synthesis of **20**

The solution-phase approach to **20** was pioneered by Siegel group, and after subsequent refinement of the method, corannulene can be now synthesize in five steps,

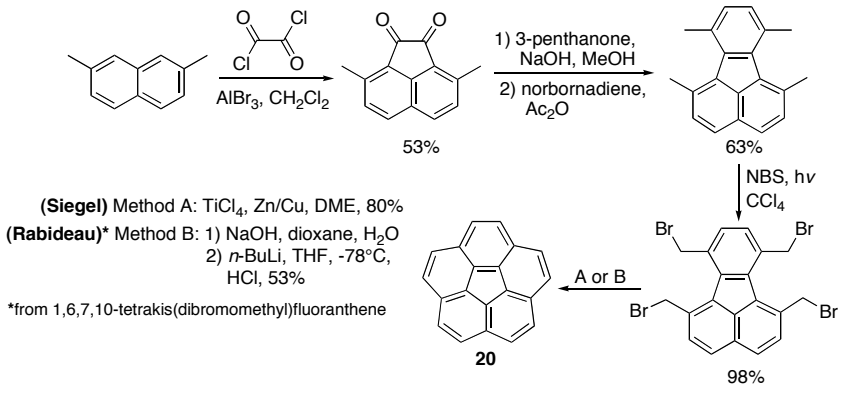

Scheme 1.7 Five step solution-phase synthesis of **20**

and allows the synthesis of **20** in kilogram scale (Scheme 1.7).[77b, 95]

The existence of spherical I_h-symmetric structure of C_{60} (**21**) was first proposed by Osawa in 1970.[96] Fifteen years later, this idea was confirmed by experimental discovery of **21** by Kroto, Smalley, and Curl[86] (the Nobel Prize in Chemistry 1996, "*for discovery of fullerenes*"). The stable ion C_{60}^+ was received by vaporization of graphite, and was detected by mass spectrometry. This molecule was popularized under the name "buckminsterfullerene" in honour of famous architect Buckminster Fuller. A significant breakthrough in the fullerene chemistry was done by Krätschmer and Huffman in 1990 after the discovery of preparative scale synthesis of **21** and other fullerenes from graphite.[88] This discovery led to a number of new carbon allotropes including carbon nanotubes and higher fullerenes.[97] At the same time, progress toward the synthesis of **21** has generated renewed interest in the chemistry of corannulene, when short and practical synthetic methods were reported by Scott, Rabideau, and Siegel.[77]

In spite of the chemical synthesis of **21** via flash vacuum pyrolysis (FVP) method (Scheme 1.8),[98,99] production of **21** is mainly done by vaporization of graphite,[88,100,101] or fuel-rich combustion of simple hydrocarbons.[102] These technologies remain the main resources for the industrial production of **21** on a metric ton scale. Accessibility of **21** from cheap starting materials allows the synthesis of a series derivatives of fullerene and investigation of many applications of **21**.

Heterofullerenes constitute a growing class of modified fullerenes, with exciting and unique physical and chemical properties. Although the existence of many heterofullerenes was already discovered, azafullerene $C_{59}N$ (**22**) remains the only member

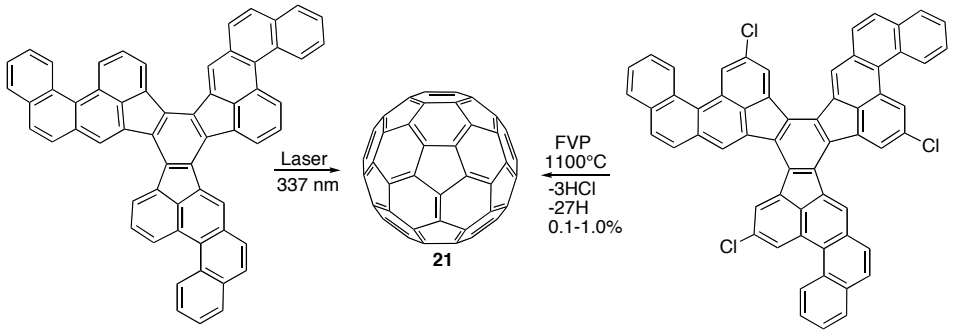

Scheme 1.8 Laser induced generation and first isolable quantities of C_{60} (**21**)

of this class of compounds that can be prepared synthetically, and its stable form is a C–C bonded dimer $(C_{59}N)_2$ (Figure 1.9).[103] Azafullerene $C_{59}N$ was first isolated by Wudl and co-workers in 1995, and one year later the Hirsch group reported an alternative synthetic route.[104] Crystalline form of monomeric cation $[C_{59}N]^+$ has been isolated as a salt with various counteranions.[105]

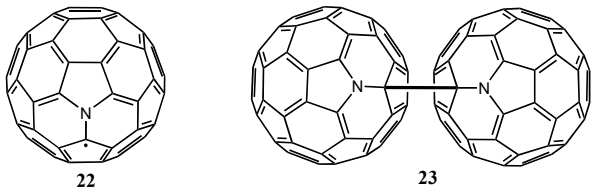

Figure 1.9 Aza[60]fullerenyl radical **22** and the stable bi(aza[60]fullerenyl) **23**

The synthetic route to **23** proceeds via construction of triazoline **24**, formed as a result of 1,3-dipolar cycloaddition between C_{60} and MEM-azide (Scheme 1.9). High temperature nitrogen extrusion in **24** formed a mixture of three different products. Isolation of the relatively stable [5,6] adduct **25** and further photooxygenation led to the exclusive formation of C_{60}N-MEM-oxo-lactam **26**, which was later converted into the 1,3-oxazetidinium system **27** by acid-catalyzed cleavage of the MEM group. The loss of formaldehyde and CO group supported formation of the aza[60]fullerenium ion ($C_{59}N^+$, **29**), which was reduced to the $C_{59}N\cdot$ monomer (**22**), and undergoes dimerization to the bisazafullerenyl **23**. Synthesis of the first azafullerene derivatives - hydroazafullerene C_{59}HN and diphenylmethane $C_{59}(CHPh_2)N$, confirmed the above described mechanism.[106]

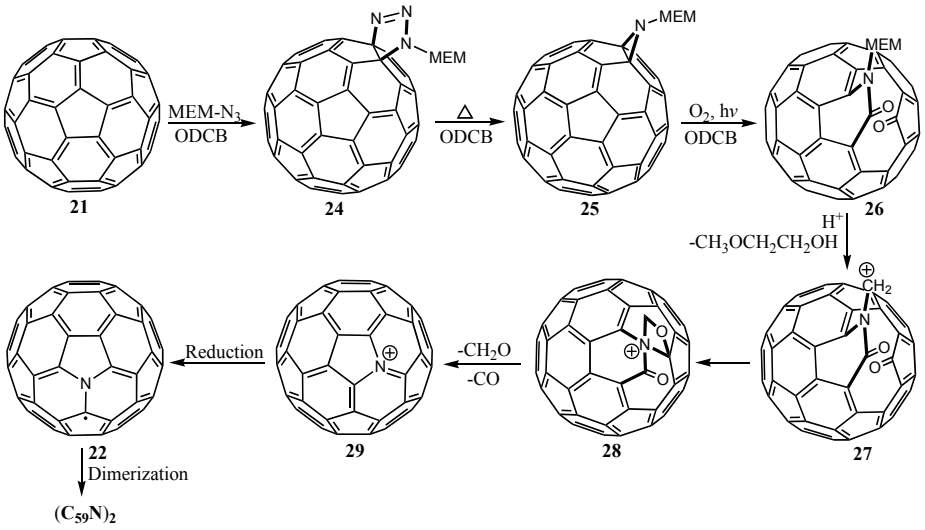

Scheme 1.9. Synthesis of $(C_{59}N)_2$ via **25** and **26**

1.4.3 Structure and properties

The bowl-shaped structure of corannulene **20** was already predicted by Lawton and Barth in 1966,[91] and as it was mentioned by them: *"Within its structural framework is an unusual strain resulting from the geometrical requirement that the bond angles deviate appreciably from the normal values found for benzenoid compounds."* The five-fold symmetrical structure of **20** shows a bowl depth of 0.875 Å (Figure 1.10).[107] The corresponding distance in **21** is 1.50 Å.[108] Four different C-C bond lengths (1.45 Å (flank), 1.38 Å (rim), 1.38 Å (spoke), and 1.42 Å (hub) have been found in the structure of corannulene, whereas C_{60} has only two types of C-C bond length 1.38 Å and 1.45 Å.

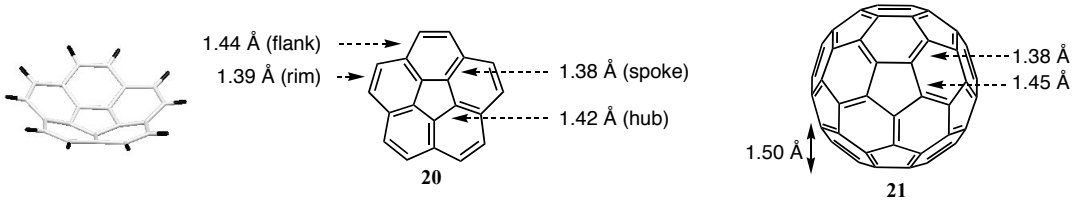

Figure 1.10 Structure of **20** and **21**

The degree of curvature in corannulene was characterized by POAV (π-orbital axis vector) pyramidalization angle (Figure 1.11), which was proposed by Haddon.[109]

According to the general definition of POAV, it is a hypothetical vector, which makes equal angles between the three bonds of the carbon atom. It was found to be 0° for planar sp^2 atoms, and in the case of curved structures like **20** or **21**, ϕ_{POAV} = 11.6° for **21**,[109] and the POAV angles of **20** are 8.7° (hub), 5.5° (spoke), and 1.1° (rim), respectively.[107]

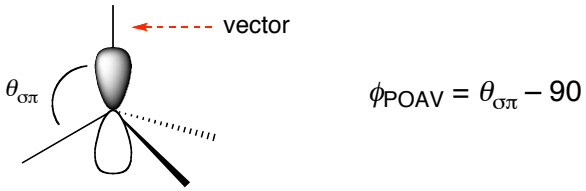

Figure 1.11 Definition of POAV angle

Crystals of corannulene (space group $P2_1/c$, monoclinic) were obtained by sublimation under reduced pressure. Two types of intermolecular interactions were found in the crystal packing of **20**, a convex-concave interaction and convex-convex interaction (Figure 1.12).

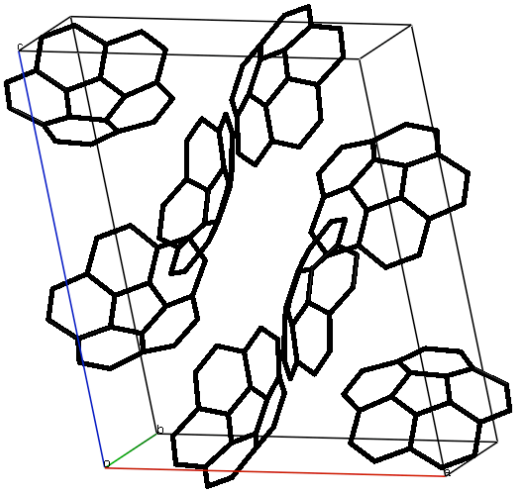

Figure 1.12 Crystal packing of **20**

In contrast to the static fullerene **21**, corannulene **20** is a dynamic molecule. Inversion of the bowl form (ground state) to flat form (transition state) is shown in Figure 1.13. The dynamic stereochemistry of several corannulene derivatives has been studied

using variable temperature NMR technique, and based on those measurements the inversion barrier of **20** was finally estimated as 11.5 kcal/mol.[78,110]

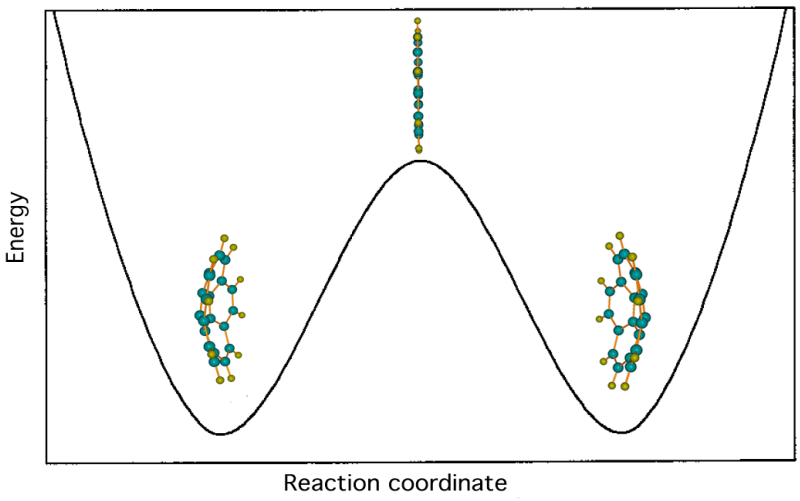

Figure 1.13 Energy diagram of the bowl-to-bowl inversion process of **20**

The structure of azafullerene **22** was confirmed by X-ray crystallography method. Aza[60]fullerenium ion was prepared by oxidation of dimeric structure $(C_{59}N)_2$ with the radical cation hexabromo(phenyl)carbazole ($HPPC^{\cdot+}$) in *o*-dichlorobenzene (using silver (I) complex carborane ion as a counterion).[90,105] Dark green crystals of $[C_{59}N]^+[Ag(CB_{11}H_6Cl_6)_2]^-$ salt were grown from the mixture hexane/*o*-dichlorobenzene, and X-ray analysis of $[C_{59}N]^+$ shows structural similarity to the C_{60}, including bond lengths (Figure 1.14).

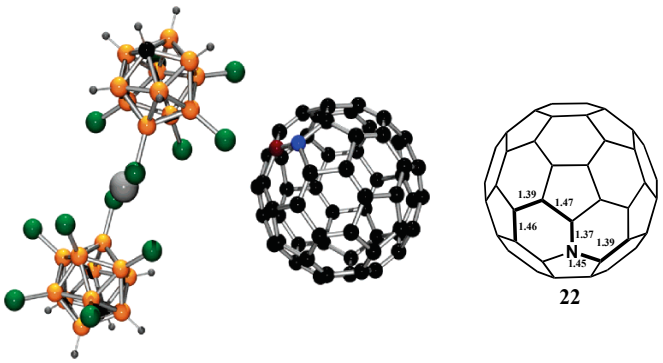

Figure 1.14 X-Ray single-crystal structure of $[C_{59}N]^+[Ag(CB_{11}H_6Cl_6)_2]^-$

1.4.3.1 Electrochemistry[111]

Reduction of **20** with excess litium metal (-78°C, THF-d_8) produced mono-, di-, tri- and tetraanions.[112] Formation of these intermediates was confirmed by NMR and EPR.[113] Three different colors changes (green, purple and brownish-red) were observed corresponding to the each reduction stages. Tetraanion of **20** was observed as a stable species, owing to the formation of sandwiche-type molecular aggregation of four lithium atoms between the two corannulene tetraanions.[113]

Like corannulene reduction, of **21** was done in several steps and lead to the formation of a series fullerene anions C_{60}^{2-},[114] C_{60}^{3-},[115] C_{60}^{4-},[116] C_{60}^{5-},[117] and C_{60}^{6-}.[118] Followed cyclic voltametric experiments (CV) showed six reversible electron reductions –0.98, –1.37, –1.87, –2.35, –2.85, and –3.26 V.[118] Oxidation of C_{60} was first reported by Echegoyen in 1993.[119] According to the voltammetric studies 1-electron oxidation of **21** occurs at +1.26V, and shows two accessible oxidation states.

1.4.3.2 Reactivity

Reactivity of corannulene comes from the aromatic nature of **20**, which does not directly satisfy Hückel's rule of aromaticity. The aromatic nature of corannulene can be explained with a so-called annulene-within-an-annulene model,[91a] representing the resonance form of **20** (Figure 1.15). Such a model was suggested by Barth and Lawton: "*This polar resonance form is unique in that it contains two charged concentric conjugated systems, the inner cyclopentadienyl anion and the outer cyclopentadecaheptenyl cation, each of which satisfies the requirements of Hückel's 4n + 2 rule.*"

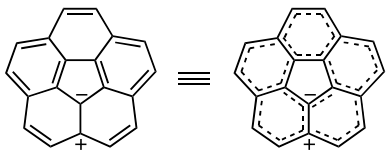

Figure 1.15 Polar resonance form of **20**

Corannulene undergoes traditional electrophilic aromatic substitution reactions such as nitration, electrophilic bromination, Friedel-Crafts acylation and Friedel-Crafts

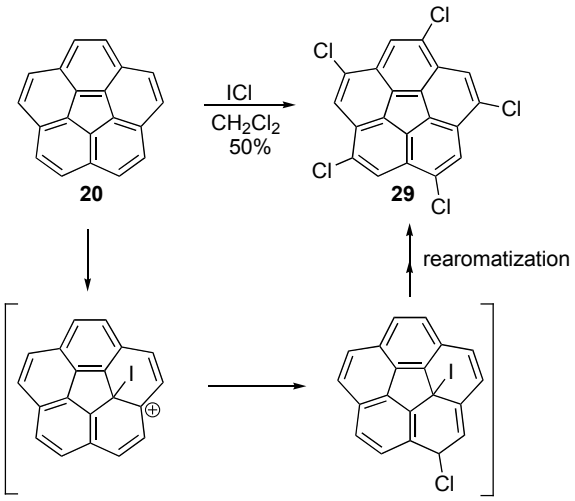

Scheme 1.10 Unique chlorination with iodine monochloride

alkylation. Unique reactivity of corannulene can be presented with a number of reactions, not characteristic for other PAHs. As an evidence of such reactivity is the reaction of **20** with iodine monochloride, which leads to formation of 50% *sym*-pentachlorocorannulene **29** (Scheme 1.10).[120] Owing to the lower electronegativity of the iodine in comparison to that of chlorine, iodine first reacts with a hub carbon of **20**, and followed addition of chloride at a rim position and rearomatization complete the synthesis of *sym*-pentachlorocorannulene.

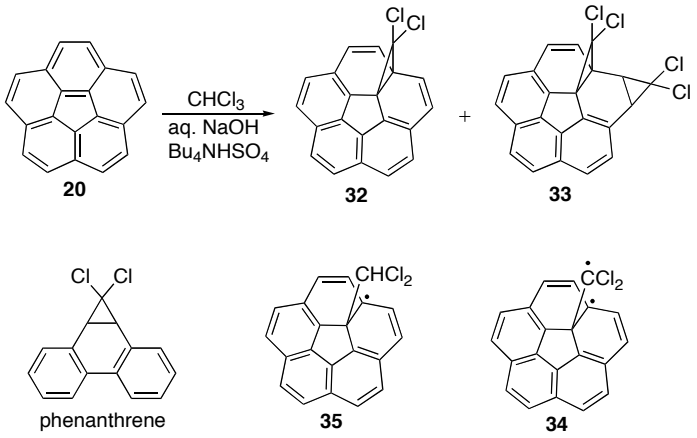

Scheme 1.11 Reaction of **20** with dichlorocarben

Reaction of corannulene with dichlorocarbene (Scheme 1.11), is another

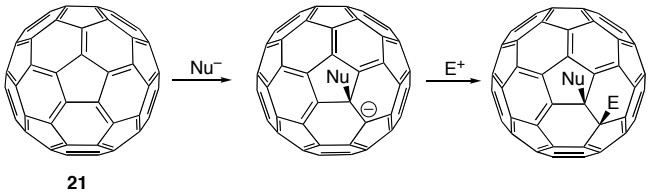

Scheme 1.12 Typical addition reaction of **21**

example of unusual reactivity of **20**, which was expected to anticipate phenanthrene-like addition.[121] However in a case of **20**, the dichlorocarbene first reacts with the fused 6,6 bond, forming monoadduct **32**, and further addition of a second dichlorocarbene gives diadduct **33**. This reaction was characterized as a fullerene type reaction.

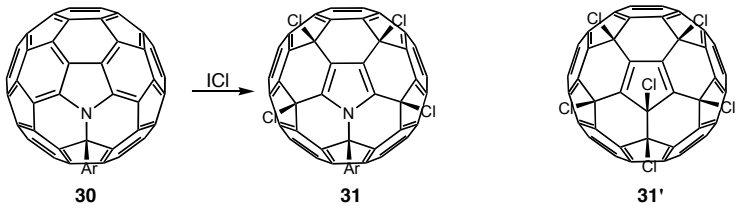

Scheme 1.13. Chlorination of $ArC_{59}N$

C_{60} can be characterized as electron-deficient polyalkene.[122] Redox chemistry and addition reactions (Scheme 1.12) are the two main chemical transformations of **21**.[123] Similar to corannulene, the main reactions of **21** occurs at the 6,6-double bonds. The reaction of C_{60} with an excess of ICl was first reported by Birkett *et al*. and leads to the quantitative formation of $C_{60}Cl_6$ (**31′**).[124] In C_s symmetrical $C_{60}Cl_6$ five Cl atoms are attached in 1,4 positions at the outer perimeter of a corannulene substructure and the sixth Cl has been used to quench pentadiene radical (Scheme 1.13). Consequently, the reaction with azafullerene derivatives $ArC_{59}N$ **30** with ICl in CS_2 leads to the related tetrachlorinated species $Cl_4ArC_{59}N$ **31**, containing unreacted pyrrole moiety of the fullerene cage[125] (Scheme 1.13).

1.5 Circumtrindene $C_{36}H_{12}$

1.5.1 Synthesis

Another bowl-shaped PAH $C_{36}H_{12}$ (**37**), represents the largest subunit (60%) of the buckminsterfullerene C_{60} so far synthesized. Its first synthesis was described by Scott *et al*. subjecting decacyclene **36** (X = H), a commercially available hydrocarbon $C_{36}H_{18}$, to flash vacuum pyrolysis at 1200-1300 °C (Scheme 1.14).[126] This triple-cyclodehydrogenation method was not very efficient and leads to the extremely low yield (0.2% to 0.6%) of **37**.

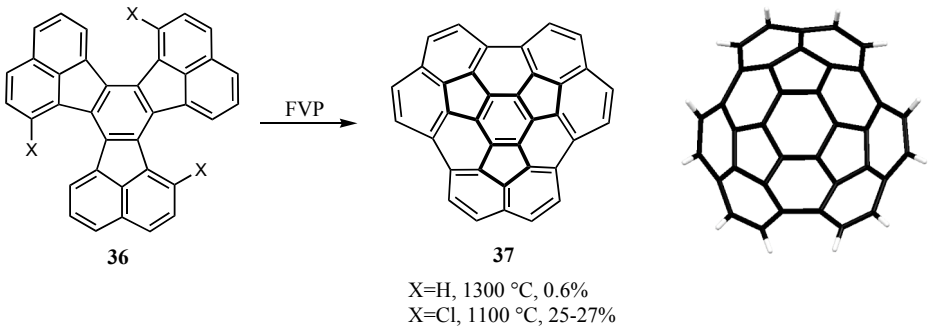

Scheme 1.14. Scott's synthesis of a $C_{36}H_{12}$ bowl **37**

A more rational synthetic route to this geodesic polyarene was reported four years later by Ansems and Scott, and was based on FVP of trichlorodecacyclene (**36**, X=Cl, Scheme 1.15).[127] This strategy allowed the synthesis of **37** in a 45% yield.

1.5.2 Structure and Properties

The curved structure of **37** shows many similarities to C_{60} (Figure 1.16).[128] Single crystal of **37** was obtained by the slow diffusion of *n*-hexane into a chloroform solution. This C_3 symmetrical molecule (slightly distorted from C_{3v} symmetry) crystallized in an uncommon space group (*R3c*). Bowl depth in **37** was defined as 4.07 Å, and similar to the structure of C_{60} the average C–C distance at 6,6 ring junction is 1.38 Å, and at a 6,5 ring junction is 1.45 Å (Figure 1.17). Similar to the curved structure of C_{60} (ϕ_{POAV} = 11.6°), the most pyramidalized carbons of **37** have the POAV angles (11.9° and

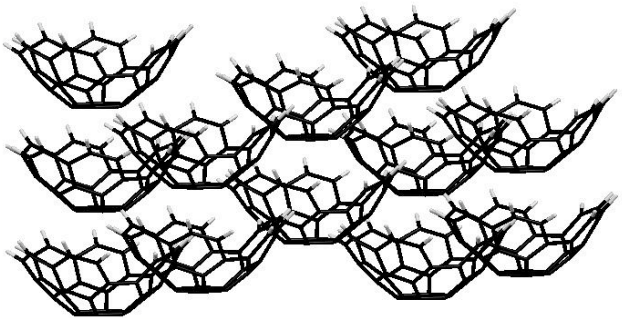

Figure 1.16 Crystal packing in **37**

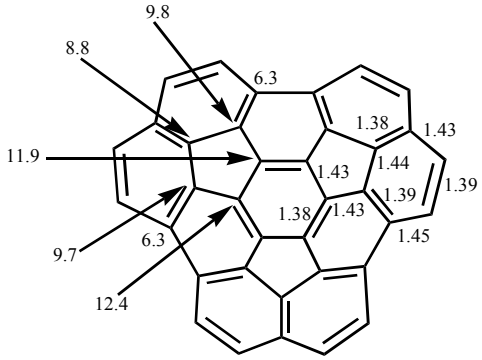

Figure 1.17 POAV angles and bond lengths of **37**

12.4°). In the crystal packing of **37** linear stacks with the convex face of one molecule nested into the concave face of the adjacent molecule were observed. The shortest intermolecular distances between bowls in a stack are 3.36 Å, 3.43 Å and 3.51 Å, however a distance of 5.16 Å was observed between the bottom of adjacent bowls.

1.6 Sumanene and triphenylenotrithiophene

1.6.1 Synthesis

Sumanene (**40**) is another symmetric subunit of C_{60} with a bowl structure. In 2003, Sakurai *et al*. reported the first synthesis of **40** from norbornadiene.[129] The synthesis included four steps and was started from trimerization of norbornadiene under catalytic condition to afford *syn*- and *anti*-**38** (ratio 1:3, Scheme 1.15), from which *syn*-**38**

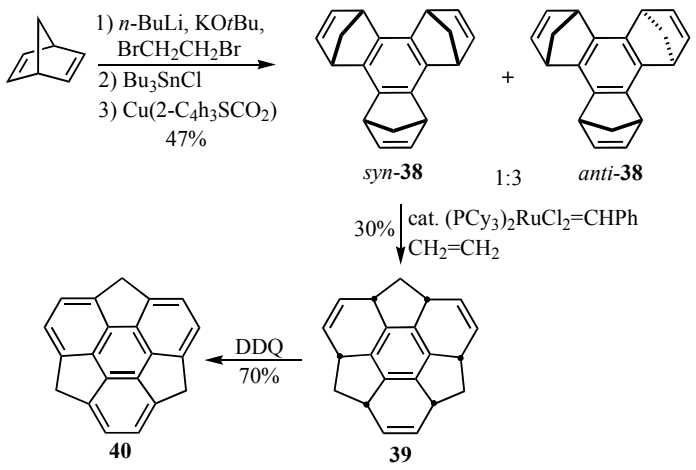

Scheme 1.15 Synthesis of sumanene (**40**)

was used in the next step. The reaction with $Cl_2(PCy_3)_2Ru$=CHPh under an atmospheric pressure of ethylene gives **39** in 30% yield. Finally, synthesis of **40** was completed by oxidation of **39** with DDQ.

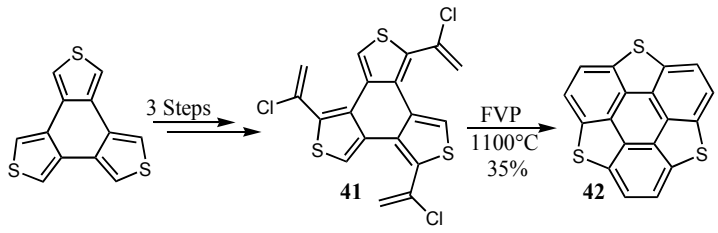

Scheme 1.16 FVP synthesis of triphenylenotrithiophene (**42**)

A sulfur analog of sumanene triphenyleno[1,12-*bcd*:4,5-*b*AcAdA:8,9-*b*BcBdB]-trithiophene (**42**),[130] is the first and only known bowl-shaped heteroaromatic that was successfully synthesized. The synthesis of triphenylenotrithiophene was achieved by Otsubo and co-workers using 1-chlorovinyl substituents as "masked acetylenes" [92b] on the trithiophene **41** (Scheme 1.16). Flash vacuum pyrolysis of **41** at 1000 °C lead to **42** in 35% yield.

1.6.2 Structure and Properties

Variable-temperature NMR studies on sumanene **40** allowed for the measurements of the inversion barrier of **40**. Since the interconversion barrier in **40** was estimated as 19.6 kcal/mol (140 °C), the structure of **40** should be much more rigid than corannulene; bowl depth in **40** was observed as 1.11 Å. X-ray crystal structure analysis of **40** indicates significant bond alternation in the hub six-membered ring to give bond lengths of *r*1a and *r*1b as 1.381 and 1.431 Å. Bond lengths in the flank six-membered ring (*r*1a, *r*2, *r*3a) are similar except for a significantly elongated rim bond (*r*4, Table 1.1).[131]

Table 1.1 Observed and calculated bond lengths of **40**

	bond length (Å)	crystal structure	B3LYP/6-31G
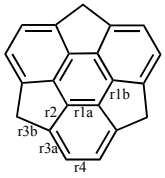	r1a	1.381	1.387
	r1b	1.431	1.433
	r2	1.396	1.399
	r3a	1.398	1.400
	r3b	1.548	1.556
	r4	1.430	1.432

The curvature of **40** was analyzed by POAV and indicates that the six hub carbons are pyramidalized to an extent of 9.0°. Molecular packing in **40** is in a concave-convex fashion and forms a column. The stacking distance between adjacent bowls is approximately 3.86 Å. Each layer of the column is arranged in a staggered fashion with a 3-fold axis (Figure 1.18).

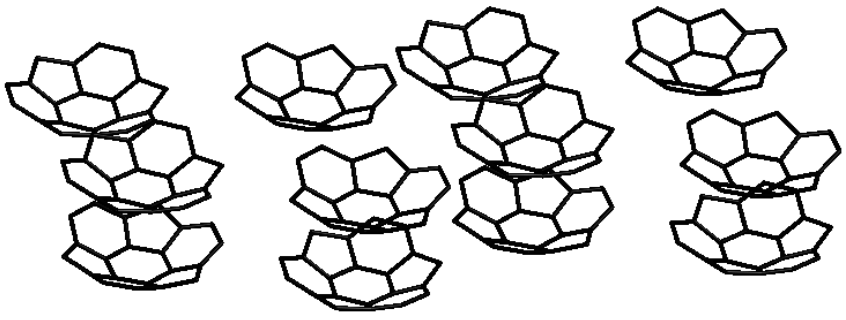

Figure 1.18 Crystal packing of **40**

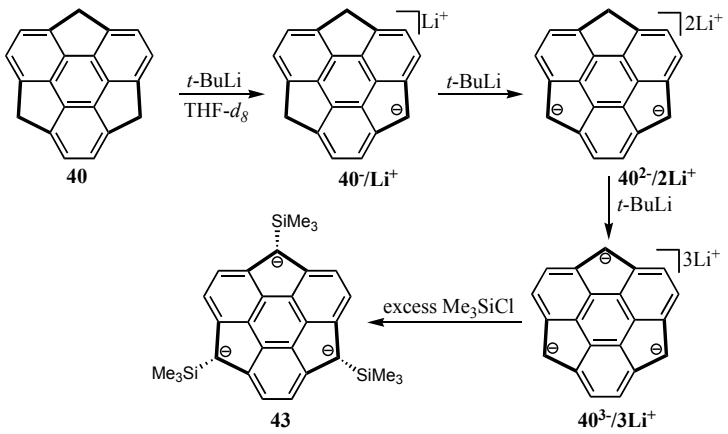

Scheme 1.17 Generation of mono/di/trianions of **40** and preparation of tris(trimethylsilyl)sumanene **43**

Analogues to corannulene, **40** can be reduced to mono-, di-, and trianions in THF-d_8 (Scheme 1.17).[131] When the formation of the trianion was considered upon addition of 3 equivalents of *t*-BuLi, excess Me_3SiCl are introduced to the solution of **40^{3-}/3Li$^+$** to afford the tris(trimethylsilyl) derivative **43** as the sole isomer. Introduction of the trimethylsilyl group proceeds at the *exo* position with perfect selectivity due to the steric demand. Synthesis of the corresponding carbanions allowed functionalize the three benzylic positions of **40** to extend bowl-shaped compounds.

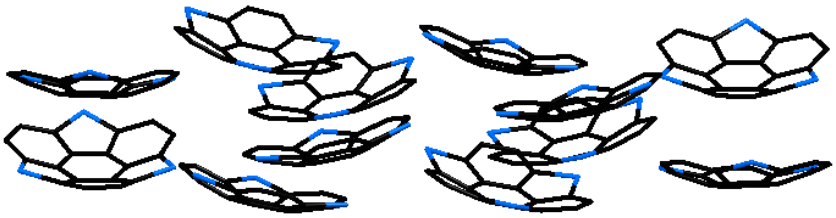

Figure 1.19 Crystal packing of **42**

Expected bowl-shaped molecular structure of **42** was confirmed by X-ray crystallographic analysis and shows bowl depth 0.79 Å,[130] which is somewhat shallow compared to corannulene.[107a] The molecular packing of **42** is in stacked concave-convex fashion, with marked intermolecular S–S contacts (Figure 1.19).

The electronic absorption spectrum of **42** in CH_2Cl_2 shows a long-wavelength

vibrational a-band at $\lambda_{(max)}$ = 368 nm (log e 3.13), and two strong bands centered at 318 (4.42) and 245 nm (4.47). The whole absorption spectrum is similar to that of coronene, supporting isoelectronic structures for both compounds.[132]

1.7 Conclusion

The above section has highlighted several of the key structural motifs of polycyclic aromatic and heteroaromatic hydrocarbons. Naphthalene, quinoline and isoquinoline are the smallest representative of the PAHs, and can be used as building blocks for the larger structures. Our attention in the chemistry of these compounds will be focused in the synthesis of fluoranthene or aza(diaza-)fluoranthene derivatives – key intermediates in the synthesis of heterocorannulenes.

Described in this chapter helicenes, corannulene, sumanenes and fullerenes, represent different families of non-planar PAHs. Investigation of the structures and the properties of these compounds, including unique molecular dynamics, reactivity, as well as interesting electronic properties, and considering the changes, which are taking place in the case of heteroatom substitution, would provide quite useful knowledge for the construction of novel bucky-bowls. Our interest is focused on the development of new synthetic strategies for heterocorannulenes. We will start our investigation with theoretical background of heteroatom-substituted bowl-shaped compounds, which will be discussed in the following chapter.

1.8 References

1. a) Hepworth, J. D.; Waring, D. R.; Waring, M. J. *Aromatic Chemistry*, Wiley-RSC **2003**; b) Katritzky, A. R.; Pozharskii, A. F. *Handbook of Heterocyclic Chemistry*, 2nd ed; Pergamon Press: Oxford **2000**; c) Krygowski, T. M.; Cyranski, M. K. *Aromaticity in Heterocyclic Compounds* (Topics in Heterocyclic Chemistry), Spinger-Verlag, Heidelberg **2009**; d) Balaban, A. T.; Oniciu, D. C.; Katritzky, A. R. *Chem. Rev.* **2004**, *104*, 2777-2812.
2. Harvey, R. G. *Polycyclic Aromatic Hydrocarbons*; Wiley-VCH, Inc.: New York **1997**; Fetzer, J. C. *The Chemistry and Analysis of the Large Polycyclic Aromatic Hydrocarbons*, New York **2000**.
3. Grimmer, G. *Environmental Carcinogens: Polycyclic Aromatic Hydrocarbons*; CRC Press: Boca Raton, Fla. **1983**.
4. a) Monarca, S.; Pasquini, R.; Sforzolini, G. S.; Savino, A.; Viola, V. *Int. Arch. Occup. Environ. Health* **1984**, *54*, 345-354; b) Wang, L-R.; Wang, Y.; Chen, J-W.; Guo, L-H. *Toxicology* **2009**, *262*, 250-257; c) Sese, B. T.; Grant, A.; Reid, B. J. *J. Toxicology Environ. Health* **2009**, *72*, 1168-1180; d) Mahadevan, B.; Lunch, A.; Bravo, C.; Atkin, J.; Steppan, L. B.; Pereira, C.; Kerkvliet, N.; Baird, W. M. *Cancer Letters* **2005**, *227*, 25-32.
5. Larsson, B. K. *J Agric. Food Chem.* **1983**, *31*, 867-873.
6. a) Simoneit, B. R. *Hand Environ. Chem.* **1998**, *3*, 175-221; b) Joa, K.; Panova, E.; Irha, N.; Teinemaa, E.; Lintelmann, J.; Kirso, U. *Oil Shale*, **2009**, *26*, 59-72.
7. Schoket, B. *Mutat. Res.* **1999**, *424*, 143-153.
8. a) Becker, L. *Astrophysics and Space Science Library* **1999**, *236*, 377-398; b) Heymann, D. *Asrophys.* **1997**, *489*, L111-L114.
9. Gutmann, I.; Cyvin, S. J. *Introduction to the Theory of Benzenoid Hydrocarbons*; Spingler-Verlag: Berlin **1989**.
10. a) Fedorov, A.P.; Maslyanskii, G. N.; Mel′nikova, N.P.; Podol′skii, M. A. *Chem. Techn. of Fuels and Oil* **1967**, *3*, 10-13.
11. a) Pisula, W.; Tomovic, Z.; Simpson, C.; Kastler, M.; Pakula T.; Müllen K. *Chem. Mater.* **2005**, *17*, 4296-4303; b) Feng, X.; Wu, J.; Ai, M.; Pisula, W.; Zhi, L.; Rabe, J.; Müllen K. *Angew. Chem. Int. Ed.* **2007**, *46,* 3033-3036; c) Brown, S. P.;

Schnell, I.; Didrich, B.; Müllen K.; Spiess, H. W. *J. Am. Chem. Soc.* **1999**, *121*, 6712; d) Petrova, T. S.; Vij, J. K.; Kocot, A. *Europhys. Lett.* **1998**, *44*, 198-204; Orgasinska, B.; e) Perova, T. S.; Merkel, K.; Kocot, A.; Vij, J. K. *Mater. Sci. Eng.* **1999**, *C8-9*, 283-289.

12. a) Schön, J. H.; Kloc, Ch.; Bucher, E.; Batlogg, *Nature* **2000**, *403*, 408; b) Meyer zu Heringdorf, F. J.; Reuter, M. C.; Tromp, R. M. *Nature* **2001,** *412*, 517; c) Schmitz-Hübsch, A.; Sellam, F.; Staub, R.; Rörker, M.; Fritz, T.; Kübel, C.; Müllen, K.; Leo, K. *Surf. Sci.* **2000**, *445*, 358; d) England, C. D.; Collins, G. E.; Schuerlein, T. J.; Armstrong, N. R. *Langmuir* **1994**, *10*, 2748-2756; e) Keil, M.; Samoir, P.; dos Santos, D. A.; Kugler, T.; Stafström, S.; Brand, J. D.; Müllen, K.; Bredas, J. L.; Rabe, J. P.; Salaneck, W. R. *J. Phys. Chem. B.* **2000**, *104*, 3967-3975; f) Hooks, D. E.; Fritz, T.; Ward, M. D. *Adv. Mater.* **2001**, *13*, 227-241.
13. Schön, J. H.; Kloc, Ch.; Batlogg, B. *Nature* **2000**, *406*, 702.
14. Keil, M.; Samoir, P.; dos Santos, D. A.; Kugler, T.; Stafström, S.; Brand, J. D.; Müllen, K.; Bredas, J. L.; Rabe, J. P.; Salaneck, W. R. *J. Phys. Chem. B.* **2000**, *104*, 3967-3975.
15. a) Hoeben, F. J. M.; Jonkheijm, P.; Meijer, E. W.; Schenning, A. *Chem. Rev.* **2005**, *105*, 1491; b) Wu, J. S.; Pisula, W.; Müllen, K. *Chem. Rev.* **2007**, *107*, 718.
16. Peacocke, A. R. *Heterocyclic Compounds: The Acridines;* New York **1973**.
17. a) Denny, W.A.; Baguley, B. C.; Cain, B. F.; Waring, M. J. *Molecular Aspects of Anticancer Drug Action*; London **1983**, 1-34; b) Denny, W. A. *The Chemistry of Antitumor Agents*, Glasgow **1990**, 1-29.
18. Cain, B. F.; Atwell, G. J.; Denny W. A. *J. Med. Chem.* **1976**, *19*, 772-777.
19. Buckle, D. R.; Cantello, B. C.; Smith, H. H.; Spicer, B. A. *J. Med. Chem.* **1975**, *18*, 726-732.
20. Stotnichi, S. J.; Gilman, C. S.; Steinbaugh, A. B.; Musser, H. J. U. S. Patent 4, **1988**, *748*, 246.
21. Schubert, J.; Wild.; Roeser, K.; Sauter, H.; Pommer, E. H. Ger. *Offen. DE 3*, **1988**, *716*, 512.
22. Bell, R. M.; Ackerman, H. U. S. Patent 4, **1990**, *920*, 128.

23. a) Conner, C. D. *A People's History of Science: Miners, Midwives, and 'Low Mechanicks'*, New York **2005**, 95-96; b) Porter, R. *The Greatest Benefit to Mankind: A Medical History of Humanity,* New York **1998**, 465-466.
24. Kaufman, T. S.; Rúveda, E. A. *Angew. Chem. Int. Ed.* **2005**, *117*, 876-907.
25. a) Baeyer, A. *Ann.* **1866**, *140*, 295; b) Houlihan W. J. *Indoles,* Wiley Interscience, New York **1972**; c) Sundberg, R. J. *Indoles*, San Diego: Academic Press, **1996**; d) Joule, J. A.; Mills, K. *Heterocyclic Chemistry* **2000**, Oxford, UK: Blackwell Science; e) Emmerling, A. *Chem. Ber.* **1869**, *2*, 679; Van Order, R. B.; f) Lindwall, H. G. *Chem. Rev.* **1942**, *30*, 69-96.
26. a) Pollak, N; Dölle C.; Ziegler M. *Biochem. J.* **2007**, *402*, 205-218; b) Belenky, P.; Bogan, K. L.; Brenner, C. *Trends Biochem. Sci.* **2007**, *32*, 12-19.
27. Christie, S. M. H.; Kenner, G. W.; Torr, A. R. N*ature* **1952**, *170*, 924.
28. Newell, L. C. *J. Chem. Ed.* **1931**, *8,* 1493-1522.
29. Erlenmeyer, E. *Ann. Chem. Parm.* **1866**, *137*, 327-359.
30. a) Tadanori, H.; Nakamura, *N. PCT Int. Appl. 9817608*, **1998**; b) Saleh, R.; Wachs, I. E. *US 4831164,* **1989**.
31. Collin, G.; Höke, H.; Greim, H. "*Naphthalene and Hydronaphthalenes*" in Ullmann's Encyclopedia of Industrial Chemistry, **2003**.
32. Abbruzzese, L.; Gozzo, F.; Varese, S.; Rossi, G.; Masoero, M.; Lorusso, S.; Milanese, S-G.; Bonola, P.; Tamburin, G.; Milanese, S-D. US 4058613, **1977**.
33. Ugryumov, O. V. *et al*. RU 2220957, **2004**.
34. Eugene, L. BE 727025, **1969**.
35. Redmore, D. US 4101654, **1978**.
36. a) Anft, B. *J. Chem. Ed.* **1955**, *32*, 566-574; b) Hoogewerff, S.; van Dorp, W. A. *Recl. Trav. Chim.* **1885**, *4*, 285.
37. Weissgerber, R. *Ber. Deut. Chem. Ges.* **1914**, *47*, 3175-3181.
38. Oberkobusch, R. *Brennst. Chem.* **1959**, *40,* 145-151.
39. a) Skraup, Z. H. *Berichte* **1880**, *13*, 2086; b) Manske, R. H. F. *Chem. Rev.* **1942**, *30*, 113.
40. a) Jia, C-S.; Zhang, Z.; Tu, S-J.; Wang, G-W. *Org. Biomol. Chem.* **2006**, *4*, 104-110; b) Cheng, C. C.; Yan, S. J. *Org. React.* **1982**, *28*, 37.

41. a) Combes, A. *Bull. Soc. Chim. Fr.* **1888**, *49*, 89; b) Bergstrom, F. W. *Chem. Rev.* **1944**, *35*, 156.
42. a) Knorr, L. *Ann.* **1886**, *236*, 69; b) Lopez-Alvarado, P.; Avendano, C.; Menendez, J. C. *Synthesis* **1998**, *2*, 186-194.
43. a) Pomeranz, C. *Monatsh. Chem.* **1893**, *14*, 116; b) Fritsch, P. *Ber.* **1893**, *26*, 419; Bobbit, J. M.; Bourgue, A. J. *Heterocycles*, **1987**, *25*, 601-614.
44. a) Bishler, A.; Napieralski, B. *Ber.* **1893**, *26*, 1903; b) Fodor, G.; Gal, J.; Phillips, B. A. *Angew. Chem. Int. Ed.* **1972**, *11*, 919.
45. Pictet, A.; Gams, A. *Ber.* **1910**, *43*, 2384.
46. a) Pictet, A.; Spengler, T. *Chem. Ber.* **1911**, *44*, 2030-2036; b) Maryanoff, B. E.; Zhang, H-C.; Cohen, J. H.; Turchi, I. J.; Maryanoff, C. A. *Chem. Rev.* **2004**, *104*, 1431-1628.
47. a) Bader, R. F. W. *Atoms in Molecules: A Quantum Theory*; Oxford, University Press: New York **1994**; b) Coopens, P. *X-ray Charge Densities and Chemical Bonding*; Oxford, University Press: New York **1997**; c) Abrahams, C.; Robertson, M. J.; White, J. G. *Acta Crystallogr.* **1949**, *2,* 233-235; d) Cruickshank, D. W. J. *Acta Crystallogr.* **1957**, 504-508; e) Ponomarev, V. I.; Filipenko, O. S.; Atovmyan, L. O. *Kristallografiya* **1976**, *21*, 392-394; f) Brock, C. P.; Dunitz, J. D. *Acta Crystallogr.* **1982**, *B38*, 2218-2228; g) Oddershede, J.; Larsen, S. *J. Phys. Chem. A* **2004**, *108,* 1057-1063.
48. Mitsuki, Y.; Tetsuo, H.; Takamasa, T. JP 11209315 A, **1999**.
49. a) Alberto, S. FR 1532866 A, 1968; b) Summers, C. R. US 2804368, **1957**.
50. Zhan, X.; Guin, J. A. *Energy & Fuels* **1994**, *8*, 1384-1393.
51. Davies, J. E.; Bond, A. D. *Acta Cryst.* **2001**, *E57*, o947-o949.
52. a) Gu, H.; Li, X.; Zhang, X. CN 101544601 A, **2009**; b) Li, Q.; Zhang, R.; Zhou, L.; Fu, H.; Chen, H.; Li, X. *Cuihua Xuebao* **2009**, *30*, 242-246; c) Zhu, G.; Pang, K.; Parkin, G. *J. Am. Chem. Soc.* **2008**, *130*, 1564-1565.
53. Bentley, K. W. *The isoquinoline alkaloids*, Amsterdam, **1998**.
54. Hensen, K.; Mayr-Stein, R.; Bolte, M. *Acta Cryst.* **1999**, *C55*, 1565-1567.

55. a) Fujio, K. *Muroran Kogyo Daigaku Kenkyu Hokoku*, **1958**, *3*, 61-80; b) Ray, S. K.; Murty, G. S.; Kulsrestha, G. N.; Shreepathi, R. H.; Lahiri, A. *J. App. Chem.* **1964**, *14*, 129-131.
56. a) Khurana, J. M. *Chemistry of Heterocyclic Compounds*, **2006**, Dehli-110007; b) Bansal, R. K. *Heterocyclic Chemistry,* **1999**, New Delhi-110002; c) Sorrell, T. N. *Organic Chemistry*, **2006**, California.
57. Kisiel, Z.; Desyatyk, O.; Pszczolkowski, L.; Charnley, S. B.; Ehrenfreund, P. *J. Mol. Spectrosc.* **2003**, *217*, 115-122.
58. Martin, R.H. *Angew. Chem., Int. Ed.* **1974**, *13*, 649.
59. Rajca, A.; Miyasaka, M.; *Func. Org. Mat.* **2007**, *15*, 547-581.
60. a) Lovinger, A. J.; Nuckolls, C.; Katz, T. J. *J. Am. Chem. Soc.* **1998**, *120*, 264; b) Nuckolls, C. N.; Katz, T. J.; Verbiest, T.; Van Elshocht, S.; Kuball, H.-G.; Kiesewalter, S.; Lovinger, A. J.; Persoons, A. *J. Am. Chem. Soc.* **1998**, *120*, 8656.
61. Newman, M. S.; Lednicer, D. *J. Am. Chem. Soc.* **1956**, *78*, 4765.
62. Nakagawa, H.; Obata, A.; Yamada, K.; Kawazura, H. *J. Chem. Soc., Perkin Trans.* 2, **1985**, 1899.
63. a) Dai, Y.; Katz, J. *J. Org. Chem.* **1997**, *62*, 1274; b) Nuckolls, C.; Katz, T. J.; Castellanos, L. *J. Am. Chem. Soc.* **1996**, *118*, 1274.
64. a) Lehn, J-M. *Pure Appl. Chem.* **1978**, *50*, 871; b) Alpha, B.; Balzani, V.; Lehn, J-M.; Perathoner, S.; Sabbatini, N. *Angew. Chem., Int. Ed.* **1987**, *26*, 1266.
65. a) Fuchs, W.; Niszel, F. *Ber. Chem. Ges.* **1927**, *60,* 209-212; b) Pischel, I.; Grimme, S.; Kotila, Nieger, M.; Vögtle, F. *Tetrahedron: Asymmetry* **1996**, 7, 109-116; c) Cook, J. W. *J. Chem. Soc.* **1933**, 1952-1957.
66. a) Martin, R. H.; Bayes, M. *Tetrahedron,* **1975**, *31*, 2135-2137; b) Wynberg, H.; Groen, M. B. *J. Am. Chem. Soc.* **1970**, *92*, 6664-6665; c) Wynberg, H. *Acc. Chem. Res.* **1971**, *4*, 65-73; d) Yamada, K.; Ogashiwa, S.; Tanaka, H.; Nakagawa, H.; Kawazura, H. *Chem. Lett.* **1981**, 343-346.
67. Larsen, J.; Bechgaard, K. *Acta Chem. Scand.* **1996**, *50*, 71-76.
68. Phillips, K. E. S; Katz, T. J.; Jockusch, S.; Lovinger, A. J. *J. Am. Chem. Soc.* **2001**, *123,* 11899-11907.

69. Ogawa, Y.; Toyama, M.; Karikomi, M.; Seki, K.; Haga, K.; Uyehara, T. *Terahedron Lett*. **2003***, 44,* 2167-2170.

70. Tanaka, K.; Suzuki, H.; Osuga, H. *J. Org. Chem*. **1997**, *62*, 4465-4470.

71. Sehnal P.; Stara I. G.; Saman D.; Tichy M.; Misek J.; Cvacka J.; Rulisek L.; Chocholousova J.; Vacek J.; Goryl G.; Szymonski M.; Cisarova I.; Stary I. *Proc. Natl. Acad. Sci. USA*, **2009**, *106*, 13169-13174.

72. Jouvenot D.; Glazer E. C.; Tor. Y. *Org. Lett*. **2006**, *8*, 1987-1990.

73. a) Caronna, T.; Sinisi, R.; Catellani, M.; Malpezzi, L.; Meille, S. V.; Mele, A. *Chem. Commun*. **2000**, 1139-1140; b) Caronna, T.; Catellani, M.; Luzzati, S.; Malpezzi, L.; Meille, S.; Mele, A.; Richter, C.; Sinisi, R. *Chem. Mater*. **2001**, *13,* 3906-3914.

74. Groen, M. B.; Schadenberg, H.; Wynberg, H. *J. Org. Chem*. **1971**, *36*, 2797.

75. a) Larsen, J.; Bechgaard, K. *J. Org. Chem*. **1996**, *61*, 1151-1152; b) Fox, J. M.; Katz, T. J. *J. Org. Chem*. **1999**, *64*, 302-305.

76. Miyasaka, M.; Rajca, A.; Pink, M.; Rajca, S. *J. Am. Chem. Soc*. 2005, 127, 13806-13807.

77. a) Tsefrikas, V.; Scott, L. *Chem. Rev*. **2006**, *106*, 4868-4884; b) Wu, Y-T.; Siegel, J. S. *Chem. Rev*. **2006**, *106*, 4843-4867; c) Recent completion of a multikilogram scale process for corannulene (**20**) has been accomplished in our group and will be submitted soon: Butterfield, A.; Gilomen, B.; Siegel, J. Manuscript in preparation.

78. Seiders, J. T.; Baldridge, K. K.; Grube, G. H.; Siegel, J. S. *J. Am. Chem. Soc*. **2001**, *123*, 517-525.

79. a) Miyajima, D.; Tashiro, K.; Araoka, F.; Takezoe, H.; Kim, J.; Kato, K.; Tarata, M.; Aida, T. *J. Am. Chem. Soc*. **2009**, *131*, 44; b) Block, M. A.; Kaiser, C.; Khan, A.; Hecht, S. *Top. Curr. Chem*. **2005**, *245*, 89; c) Sergeyev, S.; Pisola, W.; Geerts, Y. H. *Chem. Soc. Rev*. **2007**, *36*, 1902.

80. Pappo, D.; Mejuch, T.; Reany, O.; Solel, E.; Gurram, M.; Keinan, E. *Org. Lett*. **2009**, *11*, 1063-1066.

81. a) Smith, D. K.; Diederich, F. *Top. Curr. Chem.* **2000**, *210*, 183; b) Dykes, G. M. *J. Chem. Biotechnol.* **2001**, *76*, 903; c) Dykes, G. M.; Smith D. K. *Tetrahedron* **2003**, *59*, 3999.
82. Jackson, E. A.; Steinberg, B. D.; Bancu, M.; Wakamiya, A.; Scott, L. T. *J. Am. Chem. Soc.* **2007**, *129*, 484.
83. Mack, J.; Vogel, P.; Jones, D.; Kaval, N.; Sutton, A. *Org. Biomol. Chem.* **2007**, *5*, 2448.
84. Olson, A. J.; Hu, Y. H. E.; Keinan, E. *Proc. Natl. Acad. Sci. USA* **2007**, *104*, 20731.
85. Seiders, J. T.; Baldridge, K. K.; Siegel, J. S. *Tetrahedron* **2001**, *57*, 3737-3742.
86. a) Kroto, H. W.; Heath, J. R.; O'Brien, S. C.; Curl, R. F.; Smalley, R. E. *Nature* **1985**, *318*, 162; b) Bühl, M.; Hirsch, A. *Chem. Rev.* **2001**, *101*, 1153-1183.
87. a) Tenne, R.; Redlich, M. *Chem. Rev.* **2010**, *39*, 1423-1434; b) Moon, D-G.; Lee, J-Y.; Heo, S-W.; Won, J-U.; Song, H-J.; Song, G-U.; Lee, U-J.; Song, I-S. *KR 2010040695*, **2010**; c) Hwajeong, K.; Minjung, S.; Jiho, P.; Youngkyoo, K. *ChemSusChem* **2010**, *3*, 476-480.
88. Krätschmer, W.; Lamb, L. D.; Fostiropoulos, K.; Huffman, D. R. *Nature* **1990**, *347*, 354-358.
89. a) Hirsch, A. *The Chemistry of the Fullerenes*; G. Thieme: Stuttgart, New York, **1994**; b) Diederich, F.; Thilgen, C. *Science* **1996**, *271*, 317-323.
90. Vostrowsky, O.; Hirsch, A. *Chem. Rev.* **2006**, *106*, 5191-5207.
91. a) Barth, W. E.; Lawton, R. G. *J. Am. Chem. Soc.* **1966**, *88*, 380; b) Barth, W. E.; Lawton, R. G. *J. Am. Chem. Soc.* **1971**, *93*, 1730.
92. a) Scott, L. T.; Hashemi, M. M.; Meyer, D. T.; Warren, H. B. *J. Am. Chem. Soc.* **1997**, *113*, 7082-7084; b) Scott, L. T.; Cheng P-C.; Hashemi, M. M.; Bratcher, M. S.; Meyer, D. T.; Warren, H. B. *J. Am. Chem. Soc.* **1997**, *119*, 10963-10968.
93. a) Seiders, T. J.; Elliott, E. L.; Grube, G. H.; Siegel, J. S. *J. Am. Chem. Soc.* **1999**, *121*, 7804-7813; b) Jones, C. S.; Elliot, E.; Siegel, J. S. *Synlett* **2004**, 187-191.
94. Reisch, H. A.; Bratcher, M. S.; Scott, L. T. *Org. Lett.* **2000**, *2*, 1427.
95. Sygula, A.; Rabideau, P. *J. Am. Chem. Soc.* **1999**, *121*, 6323-6324.
96. Osawa, E. *Kagaku (Chemistry)* **1970**, *25*, 854.

97. a) Iijima, S. *Nature* **1991**, *354*, 56; b) Smith, B. W.; Monthioux, M.; Luzzi, D. E. *Nature* **1998**, *396*, 323.

98. Scott, L. T. *Angew. Chem. Int. Ed. Engl.* **2004**, *43*, 4994.

99. a) Boorum, M. M.; Vasil'ev, Y. V.; Drewello, T.; Scott, L. T. *Science* **2001**, *294*, 828; b) Scott, L. T.; Boorum, M. M.; McMahon, B. J.; Hagen, S.; Mack, J.; Blank, J.; Wegner, H.; de Meijere, A. *Science* **2002**, *295*, 1500.

100. a) *Fullerenes and Related Structures: Topics in Current Chemistry*; Vol. 199, Hirsch, A., Springer, Berlin, **1999**; b) Taylor, R. *Lecture Notes on Fullerene Chemistry: A Handbook for Chemists*; Imperial College, London **1999**.

101. Alekseyev, N. I.; Dyuzhev, G. A. *Carbon* **2003**, *41*, 1343.

102. a) Howard, J. B.; McKinnon, J. T.; Makarovsky, Y.; Lafleur, A. L.: Johnson, M. E. *Nature* **1991**, *352*, 139; b) Goel, A.; Howard, J. B. *Carbon* **2003**, *41*, 1949.

103. Hummelen J. C.; Knight, B.; Pavlovich, J.; Gonzalez, R.; Nuber, B.; Hirsch, A. *Science* **1995**, *269*, 1554-1556.

104. Huber, B.; Hirsch, A. *Chem. Commun.* **1996**, 1421-1422.

105. Kim, K-C.; Hauke, F.; Hirsch, A.; Boyd, P. D. W.; Carter, E.; Armstrong, R. S.; Lay, P. A.; Reed, C. A. *J. Am. Chem. Soc.* **2003**, *125*, 4024.

106. a) Vougioukalakis, G. C.; Orfanopoulos, M. *Tetrahedron Lett.* **2003**, *44*, 8649-8652; b) Keshavarz-K. M.; Gonzalez, R.; Hicks, R. G.; Srdanov, G.; Srdanov, V. I.; Collins, T. G.; Hummelen, J. C.; Bellavia-Lund, C.; Pavlovich, J. *Nature* **1996**, *383*, 147.

107. a) Hanson, J. C.; Nordman, C. E. *Acta. Crystallogr., Sect. B* **1976**, *B32*, 1147. b) Sevryugina. Y.; Rogachev, A. Y.; Jackson, E. A.; Scott, L. T.; Petrukhina, M. A. *J. Org. Chem.* **2006**, *71*, 6615.

108. Fedurco, M.; Olmstead, M. M.; Fawcett, W. R. *Inorg. Chem.* **1995**, *34*, 390.

109. a) Haddon, R. C.; Scott, L. T. *Pure Appl. Chem.* **1986**, *58*, 137; b) Haddon, R. C. *Acc. Chem. Res.* **1988**, *21*, 243; c) Haddon, R. C. *J. Am. Chem. Soc.* **1990**, *112*, 3385; d) Haddon, R. C. *Science* **1993**, *261*, 1545.

110. a) Scott, L. T.; Hashemi, M. M.; Bratcher, M. S. *J. Am. Chem. Soc.* **1992**, *114*, 1920.

111. Benshafrut, R.; Shabtai, E.; Rabinovitz, M.; Scott, L. T. *Eur. J. Org. Chem.* **2000**, 1091.

112. a) Ayalon, A.; Rabinovitz, M.; Cheng, P.; Scott, L. T. *Angew. Chem. Int. Ed. Engl.* **1992**, *31*, 1636 b) Fagan, P. J.; Calabrese, J. C.; Malone, B. *Science* **1991**, *252*, 1160-1161.

113. Ayalon, A.; Sygula, A.; Cheng, P-C.; Rabinovitz, M.; Rabideau, P. W.; Scott, L. T. *Science*, **1994**, *265*, 1065-1067.

114. Haufler, R. E.; Conceicao, J.; Chibante, L. P. F.; Chai, Y.; Byrne, N. E.; Flanagan, S.; Haley, M. M.; O'Brien, S. C.; Pan, C.; Xiao, Z.; Billups, W. E.; Ciufolini, M. A.; Hauge, R. H.; Margrave, J. L.; Wilson, L. J.; Curl, R. F.; Smalley, R. E. *J. Phys. Chem.* **1990**, *94*, 8634.

115. Allemand, P-M.; Koch, A.; Wudl, F.; Rubin, Y.; Diederich, F.; Alvarez, M. M.; Anz, S. J.; Whetten, R. L. *J. Am. Chem. Soc.* **1991**, *113*, 1050.

116. Dubois, D.; Kadish, K. M.; Flanagan, S.; Haufler, R. E.; Chibante, L. P. F.; Wilson, L. J. *J. Am. Chem. Soc.* **1991**, *113*, 4364.

117. Dubois, D.; Kadish, K. M.; Flanagan, S.; Wilson, L. J. *J. Am. Chem. Soc.* **1991**, *113*, 7773.

118. Xie, Q.; Perez-Cordero, E.; Echegoyen, L. *J. Am. Chem. Soc.* **1992**, *114*, 3978.

119. Xie, Q.; Arias, F.; Echegoyen, L. *J. Am. Chem. Soc.* **1993**, *115*, 9818.

120. Grube, G. H.; Elliott, E. L.; Steffens, R. J.; Jones, C. S.; Baldridge, K. K.; Siegel, J. S. *Org. Lett.* **2003**, *5*, 713.

121. Preda, D. V.; Scott, L. T. *Tetrahedron Lett.* **2000**, *41*, 9633.

122. Hirsch, A. *J. Phys. Chem. Solids* **1997**, *58*, 1729.

123. Hammond, G. S.; Kuck, V. J. *Fullerenes: Synthesis, Properties and Chemistry of Large Carbon Clusters*, ACS Symp. Ser., 481, American Chemical Society, Washington DC, **1992**.

124. Birkett, P. R.; Avent, A. G.; Darwish, A. D.; Kroto, H. W.; Taylor, R.; Walton, D. R. *J. Chem. Soc., Chem. Commun.* **1993**, 1230.

125. Reuther, U.; Hirsch, A. *Chem. Commun.* **1998**, 1401.

126. a) Scott, L. T.; Bratcher, M. S.; Hagen, S. *J. Am. Chem. Soc.* **1996**, *118*, 8743.

127. a) Ansems, R. B.; Scott, L. T. *J. Am. Chem. Soc.* **2000**, *122*, 2719-2724; b) Ansems, R. B. M. Ph. D. Dissertation, Boston College, Chestnut Hill MA, **2004**.
128. Forkey, D. M.; Attar, S.; Noll, B. C.; Koerner, R.; Olmstead, M. M.; Balch, A. L. *J. Am. Chem. Soc.* **1997**, *119*, 5766-5767;
129. Sakurai, H.; Daiko, T.; Hirao, T. *Science* **2003**, *301*, 1878.
130. Imamura, K.; Takimiya, K.; Otsubo, T.; Aso, Y. *Chem. Comm.* **1999**, 1859.
131. Sakurai, H.; Daiko, T.; Sakane, H.; Amaya, T.; Hirao, T. *J. Am. Chem. Soc.* **2005**, *127*, 11580.
132. a) Hummel, R. L.; Ruedenberg, K. *J. Phys. Chem.* **1962**, *66*, 2334; b) Gutfreund, H.; Little, W. A. *J. Chem. Phys.* **1969**, *50*, 4468; c) Ohno, K.; Kajiwara, T.; Inokuchi, H. *Bull. Chem. Soc. Jpn.* **1972**, *45*, 996.

Chapter 2. Theoretical Background to Heteroatom-Substituted Bowl-Shaped Compounds

2.1 Introduction

Considerable contributions in molecular modeling and investigation of kinetic and thermodynamic properties of buckybowls were brought by computational chemistry.[1-8] Theoretical calculations on heterofullerenes, containing B, Si, or N atoms predicted these compounds to have novel superconducting, electrical, and redox properties.[9,10] Corannulene, $C_{20}H_{10}$ the 'polar cap' of C_{60} has attracted essential attention because of its bowl - like structure (Figure 2.1), and unique properties such as dipole moment, ionization potential, metal binding *etc*.[11]

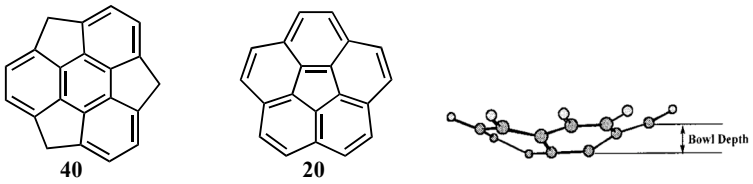

40 **20**

Figure 2.1 Structure of corannulene **20** and sumanene **40**

The inversion dynamic and bowl depth of a series corannulene derivatives have been tested by quartic/quadratic function (Siegel *et al*.) and show excellent correlation with experimental (or calculated) data.[12,13]

2.2 Dynamics

The relationship between the bowl depth and the inversion barrier of buckybowls was tested by introduction of substituents in *peri* (2, 3) positions of **20**.[13] Introduction of bulky groups at adjusted *peri* positions of **20** shows a deflection of the substituent from each other, and resulted in a flattened bowl, with lower inversion barrier. In contrast, introduction of tethering groups would deepen the bowl and accordingly raise the barrier of interconversion (Scheme 2.1). Construction of a cyclopentacorranulene and cyclophane bridge has shown to be successful strategy to lock the bowl structure.[14]

Attempts to understand structural dynamics and its influence on geometry and

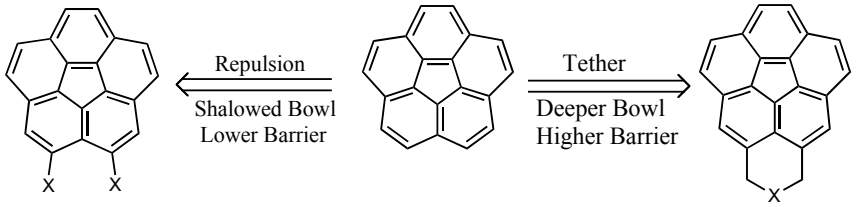

Scheme 2.1 Target molecules for study of bowl depth inversion barrier

curvature by heteroatom substitution on buckybowls was carried out using computational methods and was reported by Priyakumar and Sastry.[15-18] Monosubstituted corannulenes (**44** - **46**) and sumanenes (**47** - **50**), as well as thrisubstituted sumanene (**51**) have been the object of study in efforts to understand the structural and electronic perturbations by heteroatom substitution and their influence on bowl rigidity (Figure 2.2).

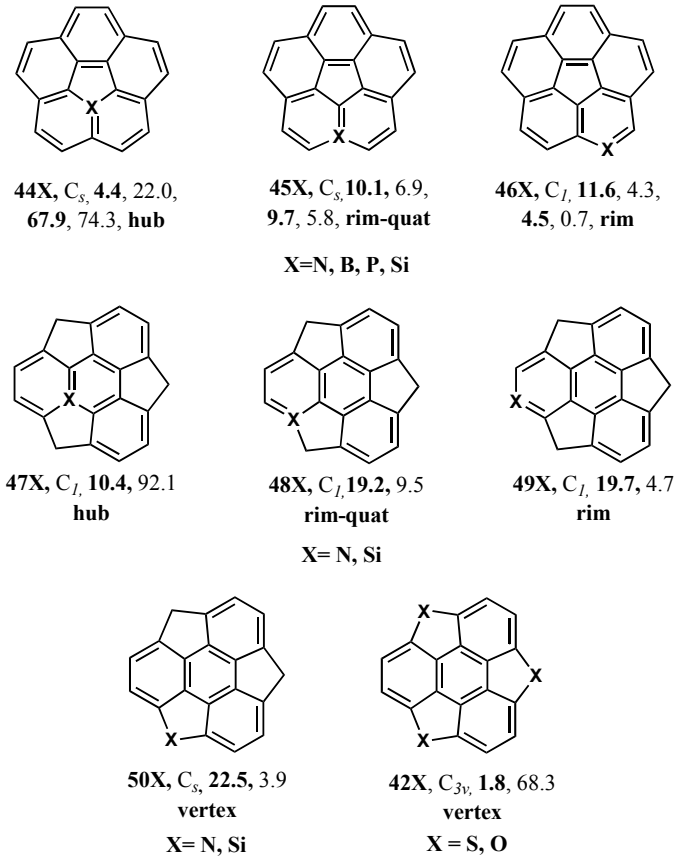

Figure 2.2 The bowl-to-bowl inversion barrier (in kcal/mol) at B3LYP/6-31G* of a variety of heterobuckybowls

Replacement of the skeletal carbon in corannulene **20** and sumanene **40** by isoelectronic substituents (B, P, N and Si) was carried out at four different positions namely hub, rim-quat and rim, and vertex positions in sumanene. According to the calculated data, the bowl-to-bowl inversion barrier of the structural isomers is solely controlled by the location of the heteroatoms. Based on the bond length data, B, P and Si were classified as large substituents and N as a smaller substituent. According to Sastry and Priyakumar: "*Larger heteroatom substituents when compared to C prefer to occupy the rim position and smaller ones prefer the hub position, and this preference seem to be independent of the charge present on the system, as well as the electronegativity of the substituent*."[15a] This assumption was cofirmed by calculated data of the bowl-to-bowl inversion barrier (Figure 2.2).

2.3 Structures and energies

2.3.1 Monosubstituted corannulenes, $C_{19}XH_{10}$ or $C_{19}XH_9$ (X = N, B, P and Si)[16]

Important structural parameters, including total energies of the planar and transition states, as well as bond lengths and pyramidalization angle of hub-substituted corannulenes **44** (Figure 2.5) at the HF/3-21G level are given in Table 2.1. According to this data, substitution of the large atoms at the hub position would increase the strain of the molecule and lead to the structural perturbations, while introduction of smaller atoms such as N, will reduce sterical disturbance of the planar form. The fact that larger substituents at the rim positions make the surface more curved was confirmed by calculation of the pyramidalization angles, which is lower for **44N**$^+$, and is higher for **44B**$^-$, **44P**$^+$ and **44Si.**

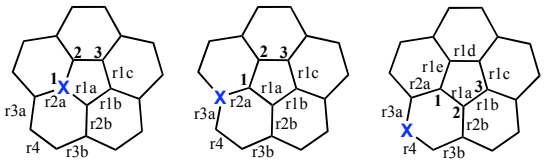

44 hub **45** rim-quat **46** rim

Figure 2.3 The numbering scheme employed in Tables 2.1-2.3 for the monosubstituted corannulenes

Structural parameters of the rim-quat substituted corannulenes **45** are given in Table 2.2. A closer look through Table 2.2 shows similar bond lengths in comparison to that of **20**, and much smaller pyramidalization angle for rim-quat substituted corannulenes. In comparison to the hub-substituted corannulenes **44** there is some small preference for larger atoms to occupy the rim-quat position.

Table 2.1 Selected geometric parameters, total energies at HF/3-21G and B3LYP/6-31G* of the hub substituted corannulenes. Total energies in hartrees, bond lengths in Å and pyramidalization angle (Φ) in degrees.

Parameter	$44N^+$		$44B^-$		$44P^+$		44Si	
	Bowl	Planar	Bowl	Planar	Bowl	Planar	Bowl	Planar
r1a	1.376	1.363	1.513	1.468	1.815	1.641	1.852	1.692
r1b	1.388	1.375	1.427	1.393	1.393	1.391	1.420	1.391
r1c	1.396	1.378	1.445	1.419	1.448	1.422	1.456	1.443
r2a	1.331	1.323	1.457	1.420	1.812	1.606	1.816	1.645
r2b	1.352	1.343	1.369	1.343	1.366	1.339	1.369	1.336
r3a	1.432	1.440	1.448	1.473	1.414	1.534	1.440	1.546
r3b	1.442	1.451	1.463	1.493	1.456	1.525	1.465	1.552
r4	1.374	1.383	1.376	1.402	1.387	1.418	1.374	1.425
Φ	3.8	-	9.3	-	19.8	-	20.7	-
E_{HF}	-775.214	-775.209	-745.804	-745.768	-1059.973	-1059.832	-1008.559	-1008.415
E_{B3LYP}[a]	-784.585	-784.578	-754.917	-754.882	-1071.105	-1070.997	-1019.434	-1019.316

[a]Single point energies of HF/3-21G optimized geometries

Table 2.2 Selected geometric parameters, total energies at HF/3-21G and B3LYP/6-31G* of the corannulenes substituted at rim-quat position. Total energies in hartrees, bond lengths in Å and pyramidalization angle (Φ) in degrees.

Parameter	$45N^+$		$45B^-$		$45P^+$		45Si	
	Bowl	Planar	Bowl	Planar	Bowl	Planar	Bowl	Planar
r1a	1.406	1.387	1.415	1.394	1.412	1.396	1.415	1.398
r1b	1.411	1.386	1.420	1.402	1.416	1.396	1.420	1.405
r1c	1.416	1.391	1.411	1.393	1.411	1.392	1.407	1.392
r2a	1.313	1.296	1.469	1.446	1.707	1.658	1.734	1.716
r2b	1.358	1.341	1.371	1.355	1.369	1.353	1.370	1.357
r3a	1.418	1.433	1.579	1.604	1.821	1.824	1.858	1.882
r3b	1.455	1.474	1.462	1.475	1.453	1.459	1.453	1.461
r4	1.354	1.368	1.368	1.382	1.354	1.370	1.370	1.379
Φ	6.5	-	5.7	-	5.0	-	4.5	-
E_{HF}	-775.190	-775.173	-745.836	-745.823	-1059.997	-1059.983	-1008.631	-1008.622
E_{B3LYP}[a]	-784.560	-784.543	-754.946	-754.935	-1071.128	-1071.113	-1019.498	-1019.488

[a]Single point energies of HF/3-21G optimized geometries

Calculated data for the rim-substituted corannulenes along with the total energies and pyramidalization angles are given in Table 2.3. Analysis of the given parameters shows slight difference in the bond length in comparisson to that of corannu-

Table 2.3 Selected geometric parameters, total energies at HF/3-21G and B3LYP/6-31G* of the corannulenes substituted at the rim position. Total energies in hartrees, bond lengths in Å and pyramidalization angle (Φ) in degrees.

Parameter	46N		46B		46P		46SiH	
	Bowl	Planar	Bowl	Planar	Bowl	Planar	Bowl	Planar
r1a	1.407	1.383	1.419	1.405	1.439	1.422	1.437	1.433
r1b	1.408	1.387	1.407	1.388	1.397	1.398	1.411	1.403
r1c	1.417	1.390	1.414	1.399	1.407	1.389	1.400	1.392
r1d	1.417	1.392	1.408	1.391	1.405	1.388	1.397	1.389
r1e	1.411	1.384	1.420	1.406	1.409	1.402	1.418	1.412
r2a	1.351	1.333	1.372	1.360	1.355	1.358	1.370	1.367
r2b	1.371	1.353	1.382	1.366	1.400	1.369	1.370	1.365
r3a	1.396	1.408	1.581	1.604	1.859	1.799	1.860	1.868
r3b	1.408	1.425	1.422	1.434	1.368	1.414	1.436	1.439
r4	1.343	1.361	1.513	1.527	1.860	1.742	1.778	1.784
Φ	7.0	-	4.7	-	3.7	-	2.0	-
E_{HF}	-775.192	-775.171	-745.832	-745.823	-1060.007	-1059.994	-1008.645	-1008.644
E_{B3LYP}[a]	-784.564	-784.546	-754.950	-754.943	-1071.136	-1071.129	-1019.518	-1019.517

[a]Single point energies of HF/3-21G optimized geometries

lene. Introduction of the small substituent at the rim position of **20** makes the bowl deeper, and in the case of large atoms shallower. **46N** shows maximum changes in the bond length variations and the degree of curvature, which are much smaller in **46B**, and practically absent in **46SiH** and **46P**.

2.3.2 Monosubstituted sumanenes, $C_{20}XH_{12}$ (X = N, Si)[16]

Figure 2.3 depicts various atom centres and bonds in the structure of monosubstituted sumanenes. Skeletal parameters including bond lengths, total energies and pyramidalization angles of rim (**47**), rim-quat (**48**), rim **(49)** and vertex (**50**) monosubstituted sumanenes are given in Table 2.4 and Table 2.5. In a case of monosubstituted sumanenes only the influence of smaller (N) and larger substitutions (Si) was investigated. As it was expected, a more curved network with a large pyramidalization angle was obtained, when Si was substituted at a rim position. However, structures of rim-quat **48Si** and rim **49Si** isomers showed more flattened bowls, and degree of curvature gets reduced in going to the vertex position **50SiH$_2$**. The thermodynamic stability of positional isomers has been shown to increase in the following order: **47Si < 48Si < 49SiH < 50SiH$_2$**. The opposite trends were obtined for the substitution by a smaller atom (N). Most stable structure was formed by the hub substitution **47N$^+$**. The isomer stability decreases going to rim-quat, rim and vertex sub-

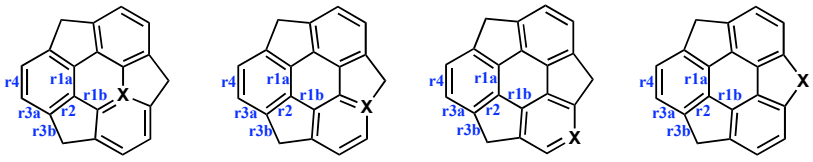

Figure 2.4 Monosubstituted sumanenes at hub (**47**), rim-quat (**48**), rim (**49**) and vertex (**50**) positions

stitutions, in the following order: **47N**$^+$ > **48N**$^+$ > **49N** > **50NH**. Thus, strain factor has the main influence on thermodynamic stabilities of the positional isomers.

Table 2.4 Selected geometric parameters, total energies at HF/3-21G and B3LYP/6-31G* of the sumanenes substituted at the hub **47** and rim-quat **48** positions. Total energies in hartrees, bond lengths in Å and pyramidalization angle (Φ) in degrees.

Parameter	47N$^+$		47Si		48 N$^+$		48Si	
	Bowl	Planar	Bowl	Planar	Bowl	Planar	Bowl	Planar
r1a	1.319	1.310	1.833	1.653	1.363	1.347	1.366	1.353
r1b	1.405	1.378	1.894	1.686	1.415	1.382	1.439	1.413
r2	1.367	1.354	1.884	1.663	1.338	1.314	1.769	1.744
r3a	1.363	1.374	1.348	1.466	1.355	1.374	1.796	1.821
r3b	1.561	1.595	1.555	1.765	1.552	1.611	1.974	2.039
r4	1.438	1.453	1.467	1.508	1.391	1.409	1.428	1.437
Φ	5.1	-	19.7	-	7.1	-	4.8	-
E_{HF}	-814.0033	-813.989	-1047.357	-1047.182	-813.993	-813.963	-1047.428	-1047.414
E_{B3LYP}[a]	-823.8643	-823.848	-1058.721	-1058.574	-823.855	-823.824	-1058.786	-1058.771

[a]Single point energies of HF/3-21G optimized geometries

Table 2.5 Selected geometric parameters, total energies at HF/3-21G and B3LYP/6-31G* of the sumanenes substituted at the rim **49** and vertex **50** positions. Total energies in hartrees, bond lengths in Å and pyramidalization angle (Φ) in degrees.

Parameter	49N		49SiH		50NH		50SiH$_2$	
	Bowl	Planar	Bowl	Planar	Bowl	Planar	Bowl	Planar
r1a	1.366	1.346	1.385	1.379	1.363	1.342	1.370	1.363
r1b	1.432	1.389	1.443	1.426	1.428	1.387	1.457	1.445
r2	1.372	1.348	1.398	1.392	1.376	1.348	1.398	1.390
r3a	1.337	1.356	1.794	1.806	1.373	1.394	1.388	1.396
r3b	1.561	1.624	1.566	1.585	1.554	1.610	1.943	1.965
r4	1.403	1.425	1.828	1.844	1.426	1.449	1.421	1.429
Φ	7.3	-	3.8	-	7.6	-	3.4	-
E_{HF}	-813.991	-813.959	-1047.433	-1047.426	-813.961	-813.924	-1047.480	-1047.474
E_{B3LYP}[a]	-823.853	-823.822	-1058.799	-1058.792	-823.817	-823.781	-1058.840	-1058.833

[a]Single point energies of HF/3-21G optimized geometries

2.3.3 $C_{18}H_6X_3$ (X = CH_2, O and S): sumanenes[16]

Selected structural parameters for the bowl and planar form as well total energies of various sumanenes (X = CH_2, O and S) are given in Table 2.6. According to the calculated data, sumanene **40** possesses a much higher bowl depth than that of corannulene **20**[1,19] and obtained increase in the curvature going from **40** to **42O**. The structure of trithiasumanene **42S** was calculated to be somewhat shallow in comparison to that of corannulene.

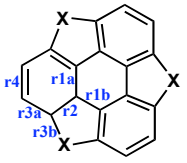

42 vertex

r1a – hub
r1b – hub
r2 – spoke
r3a – flank
r3b – flank
r4 – rim

Figure 2.5 Definition of various bonds in (X = CH_2, O and S): sumanenes

Table 2.6 Selected geometric parameters, total energies at the HF/3-21G and B3LYP/6-31G* levels for sumanenes (**40, 42O, 42S**). Total energies in hartrees, bond lengths in Å and pyramidalization angle (Φ) in degrees. B3LYP/6-31G* optimized value are given in parentheses

Parameter	40		51O		51S	
	Bowl	Planar	Bowl	Planar	Bowl	Planar
r1a	1.364 (1.387)	1.346 (1.366)	1.375 (1.399)	1.330 (1.349)	1.365 (1.391)	1.365 (1.383)
r1b	1.435 (1.433)	1.398 (1.399)	1.433 (1.428)	1.369 (1.369)	1.409 (1.414)	1.409 (1.403)
r2	1.389 (1.399)	1.365 (1.376)	1.373 (1.389)	1.339 (1.351)	1.369 (1.391)	1.369 (1.384)
r3a	1.382 (1.400)	1.403 (1.417)	1.392 (1.409)	1.425 (1.439)	1.390 (1.410)	1.390 (1.414)
r3b	1.567 (1.556)	1.617 (1.597)	1.426 (1.408)	1.495 (1.482)	1.876 (1.813)	1.875 (1.827)
r4	1.426 (1.432)	1.446 (1.455)	1.407 (1.417)	1.460 (1.474)	1.417 (1.419)	1.417 (1.428)
Φ	6.9 (6.7)	-	11.5 (12.5)	-	0.0 (0.3)	-
Bowl dep.	1.122 (1.120)	-	1.424 (1.486)	-	0.001 (0.643)	-
E_{HF}	-797.69900	-797.66986	-904.49414	-904.39310	-1867.98997	-1867.98996
E_{B3LYP}	-807.42523 (-807.43128)	-807.39847 (-807.40445)	-915. 07506 (-915.08203)	-914.96855 (-914.97325)	-1884.10301 (-1884.11528)	-1884.10318 (-1884.11242)

2.4 Structure-inversion barrier relationship

As it was reported by Bürgi and Dunitz, structure-energy correlations can be used for the clarifying the reaction mechanisms.[12b,c,20] The ring inversion study in a series of metallocyclopentenes showed that a quartic function fits the activation energy of ring inversion and the distortion from the planarity.[20] Quartic function was also tested for the

series of corannulene derivatives and shows perfect correlation with experimentally (or computationally) determined inversion barrier and bowl depth.[13]

Siegel *et al*. have shown that bowl inversion relates two symmetry – equivalent minima and the structure – energy expression should fit to a mixed quartic – quadratic potential (eq. 1).[12b-c,13]

$$E = ax^4 - bx^2 \qquad (1)$$

$$\frac{dE}{dx} = 4ax^3 - 2bx = 0 \qquad (2)$$

$$x = 0,\ b = 2a(x_o)^2 \qquad (3)$$

$$\Delta E = E_{x_o} - E_{eq} = a(x_o)^4 - 2a(x_o)^2(x_o)^2 = -ax_o^4 \qquad (4)$$

Correlation between bowl-to-bowl inversion barrier and the bowl depth of all buckybowl derivatives can be fitted to a double well potential shown (Figure 2.6).

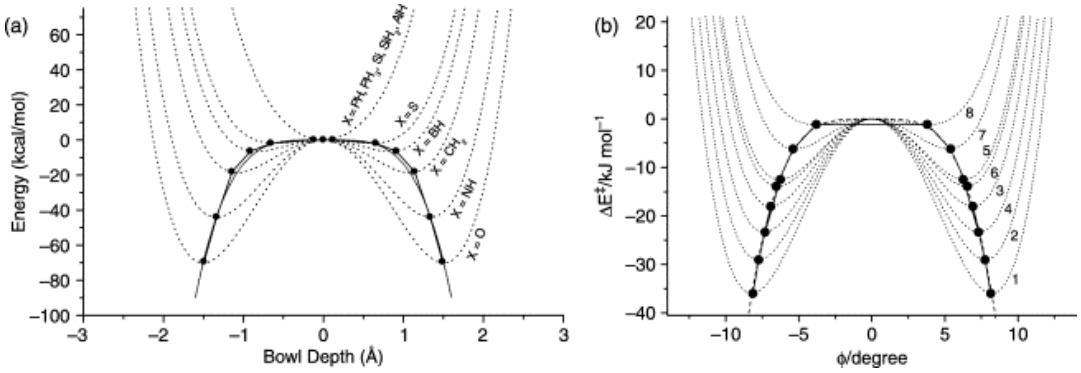

Figure 2.6 Correlation of curvature and energy of the various buckybowl derivatives. (a) For the trisubstituted sumanenes; (b) for the benzoannulated corannulenes

2.5 Conclusion

According to the theoretical calculations on heterobuckybows control on the curvature and bowl-to-bowl inversion barrier of this class of compounds can be achieved by selective heteroatom substitution on **20**. Stability of the positional isomers is controlled by the size of the substituents. Structure – energy correlation for the heterobuckybows perfectly fits to a mixed quartic – quadratic potential.

2.6 References

1. Sastry, G. N.; Jemmis, E. D.; Mehta, G.; Shah, S. R. *J. Chem. Soc., Perkin Trans. 2,* **1993**, 1867.
2. Biedermann, P. U.; Pogodin, S.; Agranat, I. *J. Org. Chem.* **1999**, *64*, 3655.
3. Baldridge, K. K.; Siegel, J. S. *Theor. Chem. Acc.* **1997**, *97*, 67.
4. a) Baldridge, K. K.; Siegel, J. S. *J. Am. Chem. Soc.* **1999**, *121*, 5332; b) Seiders, T. J.; Baldridge, K. K.; Elliott, E. L.; Grube, G. H.; Siegel, J. S. *J. Am. Chem. Soc.* **1999**, *121*, 7439.
5. Martin, J. M. L. *Chem. Phys. Lett.* **1996**, *262*, 97.
6. Sygula, A.; Rabideau, P. W. *Theochem* **1995**, *333*, 215.
7. Schulman, J. M.; Disch, R. L. *J. Comput. Chem.* **1998**, *19*, 189.
8. Dinadayalane, T. C.; Priyakumar, U. D.; Sastry, G. N. *Theochem* **2001**, *543*, 1.
9. a) Chen, Z.; Zhao, X.; Tang, A. *J. Phys. Chem. A* **1999**, *103*, 10961; b) Ray, C.; Pellarin, M.; Lerme, J. L.; Vialle, J. L.; Broyer, M.; Blase, X.; Melinon, P.; Keghelian, P.; Perez, A. *Phys. Rev. Lett.* **1998**, *80*, 5365; c) Hasharoni, K.; Bellavia-Lund, C.; Keshavarz-K, M.; Srdanov, G.; Wudl, F. *J. Am. Chem. Soc.* **1997**, *119*, 11128.
10. a) Billas, I. M. L.; Massobrio, C.; Boero, M.; Parrinello, M.; Branz, W.; Tast, F. M.; Martin, T. P. *J. Chem. Phys.* **1999**, *111*, 6787; b) Chen, Z.; Jiao, H.; Hirsch, A.; Thiel, W. *Chem. Phys. Lett.* **2000**, *329*, 47; c) Chistyakov, A. C.; Stankevich, I. V. *Inorg. Chim. Acta* **1998**, *280*, 219; d) Knupfer, M.; Pichler, T.; Golden, M. S.; Fink, J. *Proc. Electrochem. Soc.* **1998**, *98*, 673.
11. Wu, Y-T, Siegel, J. S. *Chem. Rev.* **2006**, *106*, 4843-4867; Tsefrikas, V. M.; Scott, L. T. *Chem. Rev.* **2006**, *106*, 4868-4884.
12. a) Burgi, H-B.; Dubler-Steudle, K. C. *J. Am. Chem. Soc.* **1988**, *110*, 4953; b) Burgi, H-B.; Dunitz, J. D. *Structure Correlation*; VCH: Weinheim, New York 1994; c) Burgi, H-B. *Acta Crystallogr.* **1998**, *A54*, 873.
13. Seiders, T. J.; Baldridge, K. K.; Grube, G. H.; Siegel, J. S. *J. Am. Chem. Soc.* **2001**, *123*, 517.
14. Seiders, T. J.; Baldrridge, K. K.; Seigel, J. S. *J. Am. Chem. Soc.* **1996**, *118*, 2734.
15. a) Sastry, G. N.; Rao, H. S. P.; Bednarek, P.; Priyakumar, U. D. *Chem. Commun.*

2000, 843; b) Sastry, G. N. *Theochem* **2006**, *771*, 141-147.

16. Sastry, G. N.; Priyakumar, U. D. *J. Chem. Soc., Perkin Trans. 2,* **2001**, 30.
17. a) Priyakumar, U. D.; Sastry, G. N. *Tetrahedron Lett.* **2001**, *42*, 1379; b) Priyakumar, U. D.; Sastry, G. N. *J. Mol. Graphics Mod.* **2001**, *19*, 266.
18. Priyakumar, U. D.; Sastry, G. N. *J. Org. Chem.* **2001**, *66*, 6523-6530.
19. Priyakumar, U. D.; Sastry, G. N. *J. Phys. Chem. A* **2001**, *105*, 4488-4494.
20. a) Burgi, H-B.; Dubler-Steudle, K. C. *J. Am. Chem. Soc.* **1988**, *110*, 4953.

Chapter 3. En Route to the Synthesis of Diazacorannulenes

3.1 Introduction

Corannulene **20**,[1] a bowl-shaped fullerene fragment, has many structural and electronic parallels to C_{60}. Incorporaion of heteroatoms into fullerene architectures manifests special electronic and physical properties.[2] An open question is how this parallel withstands heteroatom substitution into the corannulene scaffold. The heterofullerene $C_{59}N$ is an odd electron species (its stable form is a C–C bonded dimer $(C_{59}N)_2$), and studied extensively, but smaller heterobuckybowls are completely unknown, except theoretical calculations.[3] The first bowl-shaped heteroaromatic that has been successfully synthesized is triphenylenotrithiophene;[4] no nitrogen-substituted aromatic bowl has been prepared to date. We can reasonably expect heteroatom replacement alter the dynamic, electronic and photochemical properties with respect to the parent hydrocarbons. Our primary targets are 1,2-diaza- and 1,3,4,6-tetrazacorannulenes (Figure 3.1). Diazacorannulenes would be interesting objects of study with regard to photophysical, metal binding, and stereodynamic properties. New allotropes of carbon proved to have surprising and distinct properties, information concerning characterization and reactivity of these target molecules will help to refine our views on the nature and function of heteroaromatic compounds.

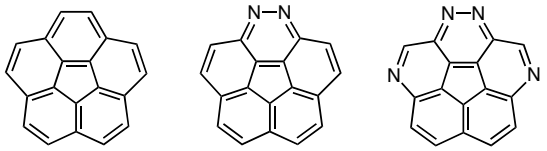

20 **51** **52**

Figure 3.1 Structure of corannulene **20** and 1,2-diaza- and 1,3,4,6-tetrazacorannulenes (**51**, **52**)

Despite longstanding interest to prepare heterobuckybowls, they have eluded chemical synthesis. A first attempt to include nitrogen into the corannulene structure was undertaken by the FVP method using fluoranthene-7,10-dicarbonitrile as a precursor; however the attempted reaction was unsuccsesful.[5] Neither FVP nor palladium-catalyzed intramolecular arylation reactions proved effective in a recent approach to 1,2-diazadibenzo[*d,m*]corannulene from 7,10-bis(2-bromophenyl)-8,9-diazafluoranthene.[6]

3.2 Synthetic Strategies

3.2.1 Progress towards diazafluoranthenes

The initial attempt to synthesize 1,2-diazacorannulene **51** was based on [2 + 4] cycloaddition reactions of 1,2,4,5-tetrazines, with a variety of substituents in the 3-and 6-positions of the heterocycle and acenaphthylene or 3,8-dimethylacenaphthylene (R_1 = H, Me, Scheme 3.1).[7] The use of acenaphthylene as an active dienophile in the inverse electron demand cycloaddition reaction is well known.[8,9] Such chemistry with the sterically encumbered 3,8-dimethylacenaphthylene[10] would lead to 3,4,9,10-tetra-substituted diazafluorantenes. Analogous to the synthesis of corannulene, where tetrasubstituted fluoranthenes act as synthetic precursors, tetrasubstituted diazafluoranthenes are attractive targets as intermediates to diazacorannulene.[6]

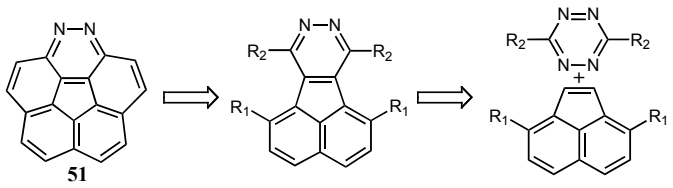

Scheme 3.1 Retrosynthesis of 1,2-diazacorannulene

Towards the synthesis of diazacorannulene, two series of substituted 8,9-diazafluoranthenes (of which **53a** and **59a** were previously reported)[9,11] were synthesized using an inverse electron demand Diels-Alder strategy (Table 3.1). The crystal structure of 17 members of this series have been investigated and compared with theoretical calculations. Starting materials have been taken in a 1:2 ratio of acenaphthylene: tetrazine, where the second molecule of diene serves as an oxidizing agent for the initially formed dihydro intermediate of 8,9-diazafluoranthene (Scheme 3.2). Reactions were often carried out in an autoclave (180 °C, 600 Psi) using *p*-xylene as a solvent; however, in favorable cases, they proceeded at reflux in mesitylene (160 °C), chlorobenzene (120 °C), dichloroethane (80 °C) even dichloromethane (40 °C). Increase of the electron-withdrawing character of the substituent on the 1,2,4,5-tetrazines (*e.g.* pyridyl, 3,5-dimethyl-1*H*-pyrazol-1-yl, CO_2Me *etc.*) increased the reactivity of the diene, which allowed the use of milder reaction conditions or shorter times. Steric and electronic

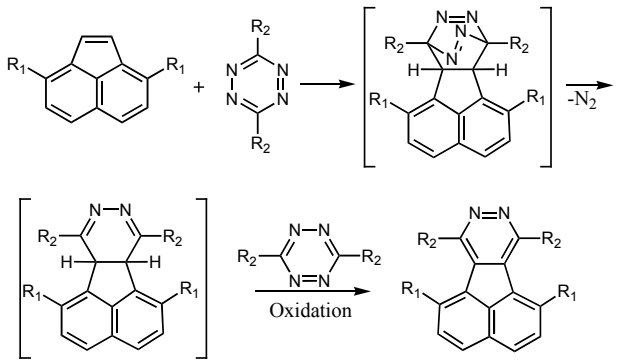

Scheme 3.2 Cycloaddition mechanism

effects influence the reactivity of the dienophile. Higher yields were generally obtained by use of the sterically unencumbered acenaphthylene as a dienophile. The sterically hindered but electronically favored 3,8-dimethylacenaphthylene remained a competent dienophile and provided good yields of the desired products.

Table 3.1 Diazafluoranthene derivatives

R_2	Entry (R_1=H)	Conditions	Time	Yield %	Entry (R_1=Me)	Conditions	Time	Yield %
Ph	**53a**	CH_2Cl_2, reflux	5d	58%	**53b**	*P*-xylene, autoclave, 180 °C	3d	27%
	**54a**	Chlorobenzene, reflux	2d	75%	**54b**	*P*-xylene, autoclave, 180 °C	2d	60%
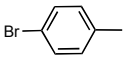	**55a**	Mesitylene, reflux	1d	50%	**55b**	*P*-xylene, autoclave, 180 °C	2d	38%
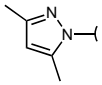	**56a**	CH_2Cl_2, reflux	3d	78%	**56b**	Mesitylene, reflux	1d	85%
	**57a**	DCE, reflux	4d	39%	**57b**	*P*-xylene, autoclave, 180 °C	3d	59%
	**58a**	Chlorobenzene, reflux	2d	73%	**58b**	Chlorobenzene, reflux	1.5d	47%
	**59a**	Chlorobenzene, reflux	12h	60-70%	—	—	—	—
CO_2Me	**60a**	*P*-xylene, autoclave, 180 °C	12h	80-95%	**60b**	CH_2Cl_2, reflux	1d	70%
$CONH_2$	**61a**[a]	DMSO, 100 °C	12h	50%	**61b**[a]	DMSO, 120 °C	1h	95%
CH_3	**62a**	*P*-xylene, autoclave, 180 °C	2d	70-80%	**62b**	*P*-xylene, autoclave, 180 °C	3d	70%
CH_3S	**63a**	*P*-xylene, reflux	1d	75%	**63b**	Mesitylene, reflux	2d	20%
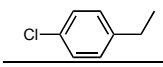	**64a**	*P*-xylene, autoclave, 180 °C	2.5d	30-50%	—	—	—	—

[a] Compound **61a** was obtained as a mixture with 1,4-dihydro-1,2,4,5-tetrazine-3,6-dicarboxamide. The yield of **61a** was determined from the integral intensity ratio in the ^{1}H-NMR spectrum. [b]A cognate of **61a**, **61b**, was prepared using 4,7-di-*tert*-butylacenaphthylene as a dienophile.

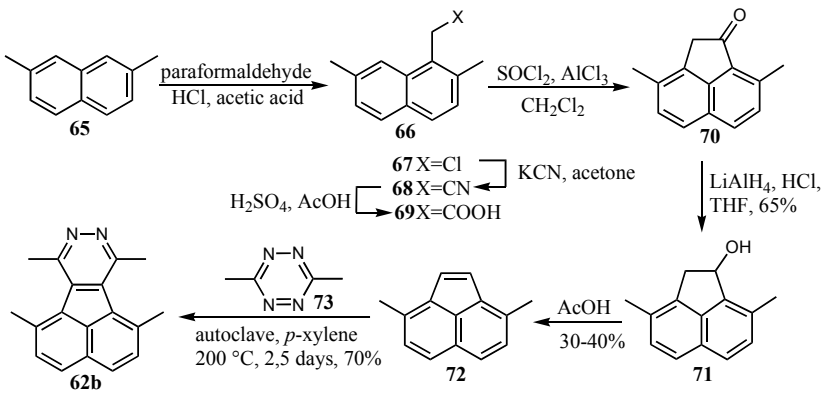

Scheme 3.3 Synthesis of 1,6,7,10-tetramethyl-8,9-diazafluoranthene **62b**

The initial attempt to synthesize 1,2-diazacorannulene **51** was based on the synthesis of the 1,6,7,10-tetramethyl-8,9-diazafluoranthene **62b** by the analogous tetramethylfluoranthene, halogenation, and ring closure.[12] Starting from 2,7-dimethylnaphtalene **65** and via intermediates **66-71**, 3,8-dimethylacenaphthylene **72** was formed in a moderate yield (Scheme 3.3). The Diels-Alder cycloaddition of 3,6-dimethyl-1,2,4,5-tetrazines and 3,8-dimethylacenaphthylene was carried out in an autoclave and led to the formation of desired product in 70% yield. X-Ray crystallographic structure analysis of **62b** has show that 1,6,7,10-tetramethyl-8,9-diazafluoranthene as well as 1,6,7,10-tetramethylfluoranthene[12a] are helically-twisted, strained aromatic molecules (Figure 3.2).

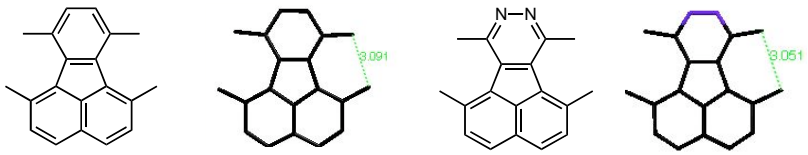

Figure 3.2 X-Ray structure of 1,6,7,10-tetramethylfluoranthene and 1,6,7,10-tetramethyl-8,9-diazafluoranthene

Considering that the dihedral angle in **62b** (0.5° exp., 15.8° calc.) is much lower than in parent hydrocarbons (17.8°), and the proximal C(sp^3) to C(sp^3) distance in **62b** is 3.051Å, and 3.091Å in 1,6,7,10-tetramethylfluoranthene, ring closure reaction in 1,6,7,10-tetramethyl-8,9-diazafluoranthene should proceed easily. However, the attempted photoinduced radical bromination of **62b** with NBS in CCl_4 was unsuccessful (Scheme 3.4).

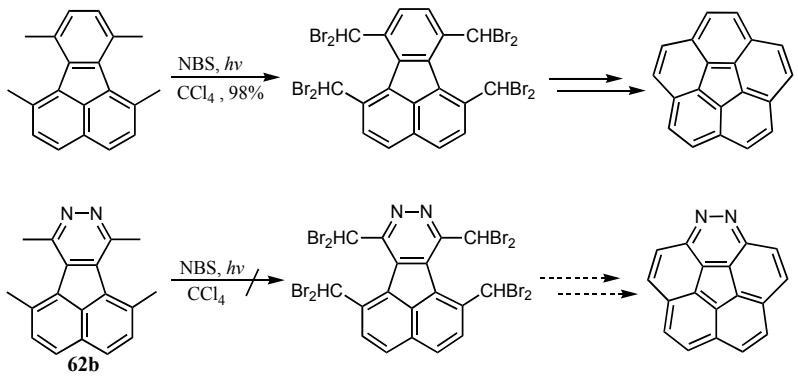

Scheme 3.4 Failed bromination of 1,6,7,10-tetramethyl-8,9-diazafluoranthene **62b**

Another derivative from the series of tetrasubstituted 8,9-diazafluoranthenes, which has been used in the synthesis of 1,2-diazacorannulene is 1,6-dimethyl-8,9-diazafluoranthene-7,10-dimethyl ester **60b** (Scheme 3.5). The initial idea to deprotonate the methyl groups in **60b** with LDA (-78 °C – RT), followed by intramolecular nucleophilic addition to the carbonyl groups, failed; only starting material was recovered after the work up the reaction (Scheme 3.5). Bromination of **60b** with NBS leads to the formation of dimethyl 1,6-bis(bromomethyl)-8,9-diazafluoranthene-7,10-dimethyl ester **74**. However, the use of **74** in intramolecular Barbier coupling, has shown no evidence of the reaction.

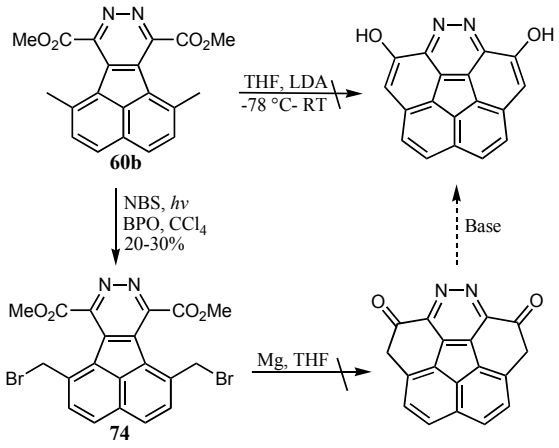

Scheme 3.5 Attempted ring closure reactions

In light of the failure of the palladium catalyzed intramolecular arylation approach to the 1,2-diazacorannulene,[6] which leads to the formation of stable Pd

complexes **75** (Figure 3.3), we decided to use constitutional isomer of initial precursor, compound **76**. The use of **76** would prevent complexation, and intramolecular cyclisation would lead to the formation of desired 1,2-diazadibenzo[*d,m*]corannulene **79** (Scheme 3.6).

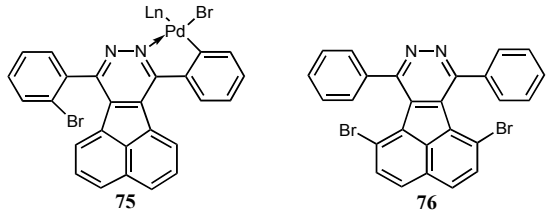

Figure 3.3 Structure of formed complex **75** and 3,8-dibromo-7,10-diphenyl-8,9-diazafluoranthene **76**

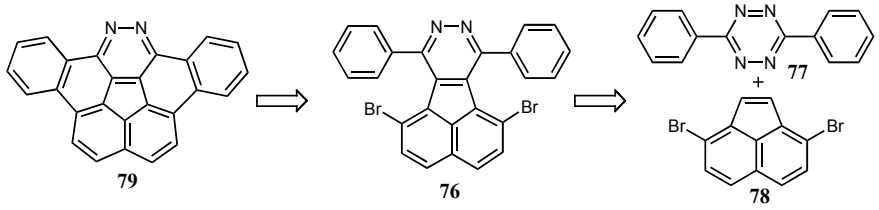

Scheme 3.6 Retrosynthetic approach to the 1,2-diazadibenzo[*d,m*]corannulene **79**

Synthesis of **76** includes commercially available 3,6-diphenyl-1,2,4,5-tetrazine (**77**) and 3,8-dibromoacenaphthylene (**78**). The later was synthesized from known 3,8-dibromoacenaphthylen-1(2*H*)-one **80** in three steps[14] (Scheme 3.7). The use of **78** (which is sterically hindered and electronically disfavored) in [2 + 4] cycloadditions, gave no reaction, even under more drastic conditions; reactions carried out at the melting point of the educts or in an autoclave at 10 kbar gave no detectable products.

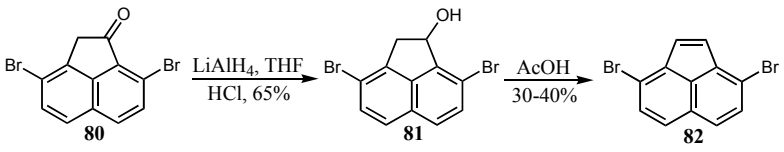

Scheme 3.7 Formation of 3,8-dibromoacenaphthylene

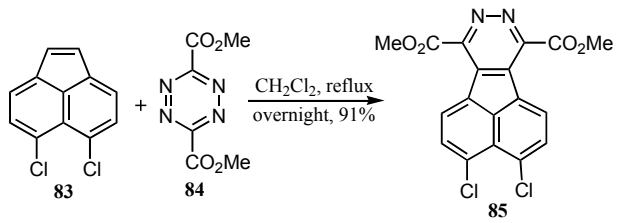

Scheme 3.8 Synthesis of dimethyl 3,4-dichloro-8,9-diazafluoranthene-7,10-dicarboxylate (**85**)

To test the steric and electronic factors, a comparison experiment was run using **82** *vs*. 5,6-dichloroacenaphthylene (**83**) as the dienophile (Scheme 3.10). In **83** the halo groups are situated *para* to the ace-bridge and therefore should not sterically encumber the reactive site. The strong role of steric hindrance becomes clear upon contemplation of the fact that dimethyl-1,2,4,5-tetrazine-3,6-dicarboxylate (**84**) and **83** react in dichloromethane to form dimethyl-3,4-dichloro-8,9-diazafluoranthene-7,10-dicarboxylate (**85**) in 91% yield (Scheme 3.8). However, a mixture of 1,2,4,5-tetrazine-3,6-dicarboxylate and **82** does not react even in *p*-xylene in autoclave at 180 °C and 600 Psi.

3.2.2 Approach to the 1,3,4,6-tetrazacorannulene

The use of palladium-catalyzed C-H activations, nitrene insertion chemistry in the synthesis of nitrogen-containing heterocycles is well known.[15] Recently the Che and Buchwald groups reported successful inter- and intramolecular amidation reaction of a series of substituted 2-arylpyridines, aromatic or aliphatic oximes and 2-phenyl-acetanilides.[16] Based on these results, we decided to examine the nitrene insertion strategy on 8,9-diazafluoranthene-7,10-dicarboxamide (**86a**) and 2,5-di-*tert*-butyl-8,9-diazafluoranthene-7,10-dicarboxamide (**86b**) (Scheme 3.9). However, in a both cases (**86a**, **86b**), the reactions failed, only starting material was recovered.

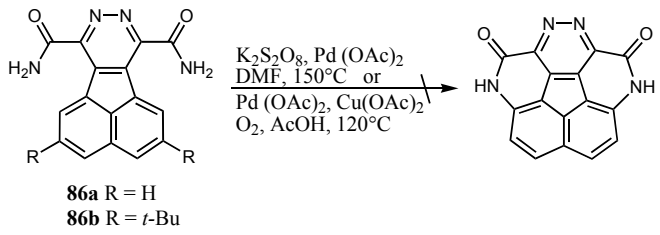

86a R = H
86b R = *t*-Bu

Scheme 3.9 Attempted nitrene insertion reaction

3.3 Structure and Properties

Molecular distortion provides insight to molecular strain. The introduction of substituents into the *peri* and *bay* regions can cause steric overcrowding, and splaying or twisting distortions in the molecule become evident (Figure 3.4).[17] *Peri*-substituted naphthalenes, and 4,5-disubstituted phenanthrenes manifest each of these distortion modes as a function of steric bulk of the substituents. The classic examples of bulky substitution (*tert*-butyl, trimethyl- X, aryl *etc*.) in the *peri* positions of a naphthalene ring,[18] show a deflection of the *peri* groups from each other and an out-of plane C_2 symmetric twisting.[18–21] In the case of phenyl-substituted naphthalenes, steric effects force the phenyl groups into a splayed stacked geometry.[22,23]

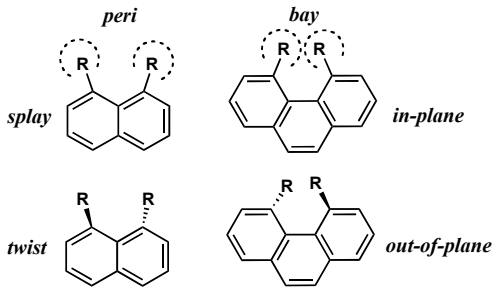

Figure 3.4 *Peri* and *bay* regions and molecular distortions

Newman[24] speculated that the structure of 4,5-dimethylphenanthrene would show displacement of the methyl groups out of the mean plane of the aromatic system due to steric clashing. This assumption was supported by X-ray crystal structures, in which aromatic systems such as 4,5-dimethylphenanthrene demonstrate a helical twist.[25] In fluoranthenes, there are bay-like regions on two sides of the molecule. Symmetrical substitution can lead to two kinds of symmetrical out-of-plane distortions, C_2-twists and C_s-folds (Figure 3.5). The X-ray structure of 1,6,7,10-tetramethylfluoranthene shows a C_2-geometry with a twist of approximately 16°, presumably due to the steric repulsion between the methyl groups.[26] The C_2-twist and C_s-fold options for molecular distortion were evaluated computationally, and the twist was favored by 1-2 kcal/mol. A similar preference for twist distortions are expected for the analogous diazafluoranthene derivatives.

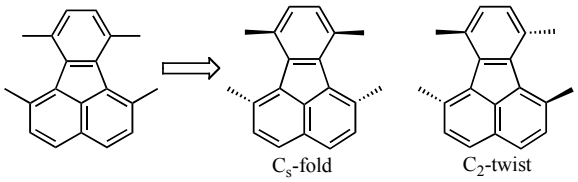

Figure 3.5 Folding and twisting distortion modes of fluoranthene

Table 3.2 Dihedral angle and bay region measurements

Compd.	R_2	Dihedral angle R_1=H exptl [calc][b]	Dihedral angle R_1=CH_3 exptl [calc]	∑Bay angles[a] R_1=H exptl [calc]	∑Bay angles[a] R_1=CH_3 exptl [calc]
53	Ph	6.5(2) [7.6]	14.2 (1) [20.2	517.2(4) [516.3]	522.9(3) [520.7]
54		7.4(2) 8.7(3) 15.9(3) [4.5]	20.9(3) [18.5]	519.1(4), 509.7(4) 517.9(3), 510.0 (3) 512.5(5), 517.3(4) [516.0]	518.0(4) [521.8]
56	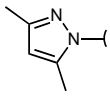	12.0(3) 5.0(1) [3.6]	[17.5]	520.0(4), 511.9(3) 513.3(2), 519.5(2) [515.3]	[519.95]
57		13.6(2) [9.3]	17.0(2) [21.3]	515.5(3) [516.7]	521.6(4) [520.4]
58		[6.0]	13.3(5) [20.7]	[520.7]	523.1(1) 525.0(1) [521.2]
59		3.8(2) [3.4]	[23.9]	517.8(3) [515.1]	[525.3]
60	CO_2Me	1.0(2) 4.4(2) [1.4]	10.4(2) [12.9]	515.8(3), 515.4(3) 516.2(3), 516.8(4) [515.6]	521.6(4) [518.5]
61	$CONH_2$	[0]	2.4(4) 6.7(4) [16.1]	515.9(5), 514.2(5) 516.6(5), 515.8(5) [516.6]	[520.0]
62	CH_3	2.2(3) [0]	0.6(2), [15.6]	513.5(3) 512.4(5) [514.1]	524.2(4) 524.9(4) [521.4]
63	CH_3S	3.0(2) [0]	17.9(2) [15.6]	509.9(3), [511.8]	517.7(4) 521.2(3) [520.3]
64	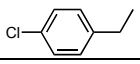	5.3(2)	—	513.8(4), 513.7(3)	—
Average[c]		5.8 [3.6]	13.5, [18.2]	515.0, [515.8]	521.8, [520.9]

[a]Sum of α, β, γ and δ (see Figure xx). [b]M06-2X/cc-pVDZ. [c]Diazafluoranthene ref. calcd α, β, γ and δ = 514.3°

The crystal structures of **53**(**a**/**b**), **54**(**a**/**b**), **56a**, **57**(**a**/**b**), **58b**, **59a**, **60**(**a**/**b**), **61b**, **62**(**a**/**b**), **63**(**a**/**b**), and **64**(**a**) have been determined, 17 structures in all. From the crystallographic data obtained, the dihedral angle between the best-planes-of-fit through

atoms C7/N/N/C10 of the pyridazyl ring and atoms C2/C3/C4/C5 of the naphthyl ring (Figure 3.6) was determined. In addition, the bay region bond angles α, β, γ and δ for each side of the molecule were measured and summed (Figure 3.5). The same parameters were determined from coordinates obtained by quantum mechanical computations (Table 3.2).

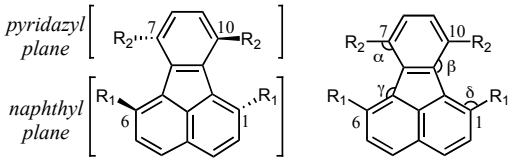

Figure 3.6 Distortion parameters for diazafluoranthenes: left) pyridazyl/naphthyl dihedral; right) bay angles α, β, γ and δ

A reasonable reference compound is the parent diazafluoranthene ($R_1 = R_2 = H$). Here the molecule is flat (dihedral angle = 0°) and the sum of bay angles is calculated to be 514.3°. On average, replacement of R_2 by a carbon atom based functional group (not tertiary) yields a molecule with a slight twist (exptl 5.8°, calcd [3.6°]) and essentially no splaying as confirmed by the sum of the bay angles (exptl 515.0°, calcd [515.8°]). The same R_2 substitution when R_1 = Me leads to a more substantial twist (exptl 13.5°, calcd [18.2°]) and some evidence for splaying (exptl 521.8° calcd [520.9°]). It would appear that the out-of-plane twisting is a softer distortion mode than the in-plane splaying mode. At higher twisting angles, the mode becomes stiffer and the splaying mode sets in to accommodate the steric encroaching of substituents across the bay region. An exception to this steric bulk model is 1,6,7,10-tetramethyl-8,9-diazafluoranthene (**62b**) for which the crystallographic model exhibits a greater twist of the molecule for the dimethyl compound **62a** (R_1 = H; 2.2(3)°) than for **62b** (R_1 = Me; 0.6(2)°). Although the experimental diffraction data for **62b** models well as a planar form, the H···H distances between adjacent methyl groups from 2.04–2.16 Å, and some of the methyl C-atoms have quite elongated atomic displacement ellipsoids perpendicular to the molecular plane. Computations on **62b** predict a twist angle of 15.6° and, as mentioned above, computation and X-ray structures of the hydrocarbon analog, tetramethylfluoranthene,

display twists between 15–20°. Thus, the X-ray structure of **62b** must either reflect an unresolved disorder or a substantial packing effect on the molecular conformation. A packing effect would arise from a trade of higher strain energy as a planar form in return for better packing energy. Computations on the planar form predict only a 1.2 kcal/mol difference from the twisted ground state. Such an energy difference would be within the bounds of packing effects.

3.3.1 Computational Methods

The conformational analyses of the molecules described in this study were carried out with the Gaussian 03[27] software package, using density functional methods. In particular, the M06-2X[28] functional together with Dunning's correlation consistent basis set, cc-pVDZ,[29] a [3s2p1d] was employed. Full geometry optimizations were performed and uniquely characterized *via* second derivative (Hessian) analysis to determine the number of imaginary frequencies (0 = minima; 1 = transition state). Analysis of dihedral and bay region angles was carried out using QMView[30] and PLATON.[31]

3.4 Conclusion

The initial attempts to synthesize 1,2-diazacorannulene was based on [2 + 4] cycloaddition reaction of 3,6-disubstituted 1,2,4,5-tetrazines and acenaphthylenes or 3,8-dimethylacenaphthylenes. Two series of substituted 8,9-diazafluoranthenes were synthesized and X-ray crystallographic structural analyses have been determined for eighteen derivatives and compared to theoretical calculations. Increase of the electron-withdrawing demand of the substituent in *s*-tetrazines increases the yield of desired diazafluoranthenes. Steric hindrance in the *ortho* positions of the dienophile can be tolerated if the substituents are methyl groups. The structure of these molecules show a helical twist due to steric interactions across the bay region. The dihedral and sum of bay region angles correlate with the degree of bay region steric congestion. Methods for ring closure remains an active, developing problem.

3.5 Future work

The failure of 1,6,7,10-tetramethyl-8,9-diazafluoranthene (**62b**, (Scheme 3.4) undergo radical bromination, drove us forward to use monosubstituted fluoranthenes. Benzylic bromination of heteroaromatic compounds (including 2-methylpyridines, polymethylpyrimidines and oligopyridines) using *N*-bromosuccinimide is well known.[32] Azafluoranthenes can be easily prepared using Diels-Alder reaction of 3,6-disubstituted-1,2,4-triazines and 3,8-disubstituted acenaphthylenes (Scheme 3.10). Once a suitable 1,6,7,10-tetrakis(bromomethyl)-8-azafluoranthene **89** is available, the next steps will focus on ring closure reaction, which could be achieved according Rabideau methodology for the synthesis of parent corannulene.[33]

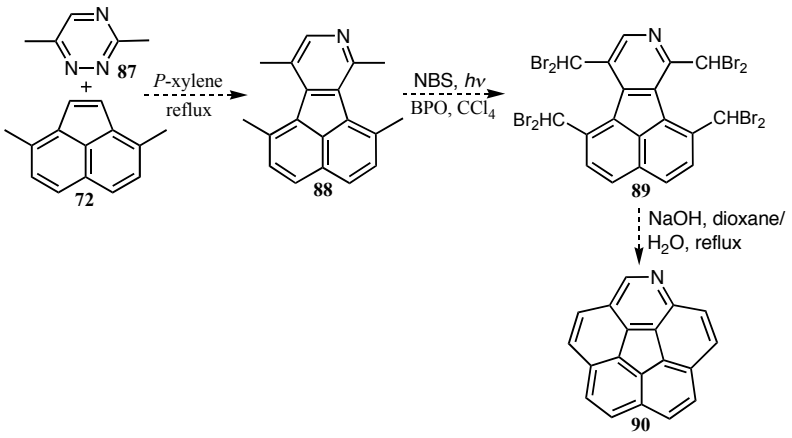

Scheme 3. 10 Approach to the azacorannulene **90**

As a fundamental subunit of many polycyclic heteroaromatics, quinoline and isoquinoline can be also used as a precursor for the construction of azacorannulene. Synthesis of azacorannulene will be started from dimethyl quinoline or isoquinoline, both known materials. Similar to the synthesis of corannulene from naphthalene, azacorannulene from quinolines requires selective ring construction toward the analogous tetramethyl "azafluoranthene", halogenation and ring closure (Scheme 3.11).

Construction of quinoline derivative **93** will be started from *p*-toluidine **91** and ethyl 3-formylbuturate **92**. [34] The employed method is based on the procedure of Conrad and Limpach [35,36] for the formation of 4-hydroxyquinoline derivatives from anilines and

β-keto esters. Quinoline-4-ol **93** can be easily converted to the corresponding 4-halo-quinolines **94** via treatment with PBr_3/DMF.[37] Metalation of **94** and followed quench with paraformaldehyde will contribute the formation of primary alcohol **95**.[38] Chlorination of **95** and followed displacement by cyanide, hydrolysis to the carboxylic acid, and cyclization by way of the acid chloride would support the formation of **99**.[39] Diketone functionalization can be achieved via oxidation of **99** with selenium dioxide in dioxane/water. Double Knoevenagel condensation of **99** with 3-pentanone in methanolic potassium hydroxide, and further Diels-Alder reaction with norbornadiene will afford 1,6,7,10-tetramethyl-4-azafluoranthene **101**. Bromination of **101** and followed ring closure will complete the synthesis of azacorannulene **90**.

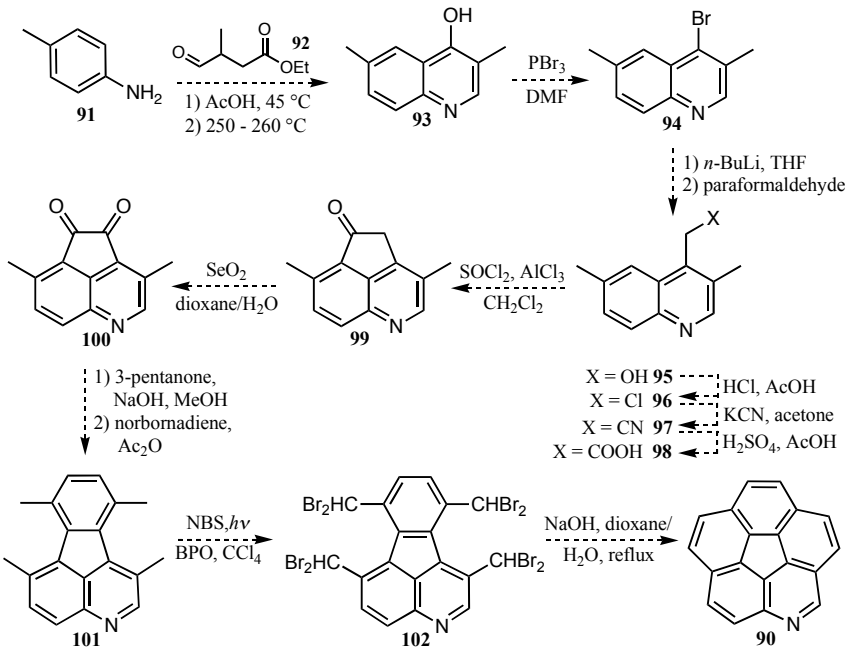

Scheme 3.11 Approach to the azacorannulene via quinoline derivatives

Direct functionalization of 3,6-dimethylisoquinoline **103** (Scheme 3.12) can be achieved via boron-activated enamine **104**, which could be prepared by the reduction of **101** with sodium triethylborohydride.[40,41] Next step, formation of 3,6-dimethyl-isoquinoline-4-acetic acid **105** is described in the literature,[41] and can be accomplished by the reaction of **104** with ethyl glyoxalate. Having 2-(3,6-dimethylisoquinolin-4-yl)acetic acid **105** in the hand, construction of azacorannulene will be carried out according the

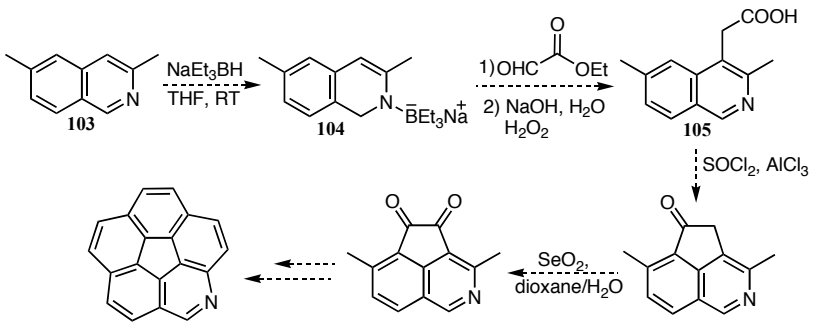

Scheme 3.12 Synthesis of azacorannulene via isoquinoline derivatives

standard procedure for the synthesis of corannulene.[39]

3.6 Experimental Section

3.6.1 General information

All reactions were carried out under nitrogen (except for compound **3**). Solvents were used as purchased (p.a. grade) without further purification. 3,6-Disubstituted-1,2,4,5-tetrazines were synthesized according literature procedures. Commercially available acenaphthylene was also used as purchased without further purification. Melting points were determined using a heating microscope from Cristoffel Labor- and Betriebstechnik and are uncorrected. Infrared spectra were recorded on a Perkin-Elmer Spectrum One FT-IR spectrometer. Compounds were measured as KBr pellets. Absorption bands are given in wavenumbers (cm^{-1}), and the intensities are characterized as follows: *s* = strong (0 – 33% transmission), *m* = medium (34 – 66% transmission), *w* = weak (67 – 100% transmission). ^{1}H- and ^{13}C-NMR spectra were recorded on Bruker Avance 300 (300 MHz), Bruker ARX 300 (75 MHz), Bruker Avance 400 (400 MHz), Bruker Avance 500 (500 MHz), Bruker DRX-500 (500 MHz) and Bruker DRX – 600 (600 MHz) spectrometers, with the solvent as the internal standard. Data are reported as follows: chemical shift in ppm, multiplicity (*s* = singlet, *d* = doublet, *t* = triplet, *m* = multiplet, *dd* = doublet of doublets, *dt* = doublet of triplet, *etc*.), coupling constant ^{n}J in Hz, integration and interpretation. The atom numbering used for compounds **54a** and **59a**

is shown in Figure 3.7. Mass spectra (MS) were obtained from Finnigan MAT95 instrument. Analytical thin layer chromatography (TLC) was performed with Macherey-Nagel POLYGRAM SIL N-HR/UV254 and POLYGRAM ALOX N/UV_{254}, visualization by an ultraviolet (UV) lamp (l = 254 nm and l = 366 nm). Column chromatography was carried out on silica gel (Merck 60 0.040 – 0.063 mm) or deactivated (5% water) aluminium oxide (Sigma-Aldrich type 507C, 150 mesh).

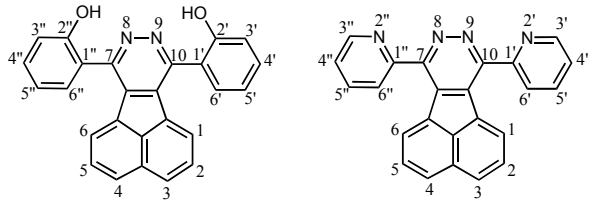

Figure 3.7 Atom numbering of diazafluoranthene derivatives

HPLC analysis were performed with Spherisorb-NH_2, 3μm, 4.6×100 mm analytical column. The purity of the compounds was determined by integration of peak areas on an HPLC chromatogram.

3.6.2 Chemical abstract nomenclature (graciously provided by Dr. Volkan Kisakürek)

7,10-Diphenylacenaphtho[1,2-*d*]pyridazine (**53a**), 1,6-dimethyl-7,10-diphenyl-acenaphtho[1,2-*d*]pyridazine (**53b**), 2,2′-acenaphtho-[1,2-*d*]pyridazine-7,10-diyldiphenol (**54a**), 2,2′-(1,6-dimethylacenaphtho[1,2-*d*]pyridazine-7,10-diyl)diphenol (**54b**), 7,10-bis-(4-bromophenyl)acenaphtho[1,2-*d*]pyridazine (**55a**), 7,10-bis(4-bromophenyl)1,6-di-methylacenaphtho[1,2-*d*]pyridazine (**55b**), 7,10-bis(3,5-dimethyl-1*H*-pyrazol-1-yl)ace-naphtho[1,2-*d*]pyridazine (**56a**), 7,10-bis(3,5-dimethyl-1*H*-pyrazol-1-yl)-1,6-dimethyl-acenaphtho[1,2-*d*]pyridazine (**56b**), 7,10-di(thiophen-2-yl)acenaphtho[1,2-*d*]pyridazine (**57a**), 1,6-dimethyl-7,10-di(thiophen-2-yl)acenaphtho[1,2-*d*]pyridazine (**57b**), 7,10-di-(furan-2-yl)acenaphtho[1,2-*d*]pyridazine (**58a**), 7,10-di(furan-2-yl)-1,6-dimethylace-naphtho[1,2-*d*]pyridazine (**58b**), 7,10-di(pyridin-2-yl)acenaphtho[1,2-*d*]pyridazine (**59a**), dimethyl acenaphtho[1,2-*d*]pyridazine-7,10-dicarboxylate (**60a**), dimethyl 1,6-dimethyl-acenaphtho[1,2-*d*]pyridazine-7,10-dicarboxylate (**60b**), acenaphtho[1,2-*d*]pyridazine-

7,10-dicarboxamide (**61a**), 2,5-di-*tert*-butylacenaphtho[1,2-*d*]pyridazine-7,10-dicarboxamide (**61b**), 7,10-dimethylacenaphtho[1,2-*d*]pyridazine (**62a**), 1,6,7,10-tetramethylacenaphtho[1,2-*d*]pyridazine (**62b**), 7,10-bis(methylsulfanyl) acenaphtho[1,2-*d*]pyridazine (**63a**), 1,6-dimethyl-7,10-bis(methylsulfanyl)acenaphtho[1,2-*d*]pyridazine (**63b**), 7,10-bis(4-chlorobenzyl)acenaphtho[1,2-*d*]pyridazine (**64a**).

3.6.3 Synthetic Procedures

7,10-Diphenyl-8,9-diazafluoranthene (53a)

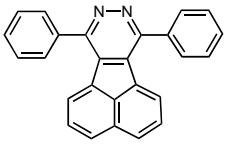

A mixture of 3,6-diphenyl-1,2,4,5-tetrazine[42] (0.310 g, 1.32 mmol) and acenaphthylene (0.10 g, 0.66 mmol) in CH_2Cl_2 (10 mL) was stirred at reflux for 5 d. The solvent was evaporated, the residue was purified by column chromatography (silica gel, hexane, hexane/acetone 1:5) to yield a yellow solid (0.18 g, 58%). IR (KBr): 3057*s*, 3035*m*, 3010*m*, 2863*w*, 2239*w*, 1962*w*, 1904*w*, 1602*w*, 1580*w*, 1552*m*, 1534*m*, 1485*m*, 1440*m*, 1419*s*, 1382*s*, 1355*m*, 1342*m*, 1312*m*, 1231*m*, 1177*m*, 1158*m*, 1121*m*, 1087*s*, 1072*s*, 1016*m*, 1001*m*, 986*m*, 928*m*, 919*w*, 857*w*, 829*s*, 783*s*, 769*s*, 750*s*, 730*w*, 705*s*, 674*m*, 640*m*, 622*m*, 610*m*, 566*w*, 530*w*, 520*m*, 495*w*; ^{1}H-NMR (400 MHz, $CDCl_3$) δ 8.04 (d, ^{3}J = 8.0 Hz, 1H), 8.0-7.97 (m, 2H, Ph), 7.84 (d, 1H, ^{3}J = 7.2 Hz), 7.68-7.63 (m, 3H, Ph), 7.59 (dd, 1H, ^{3}J = 7.2, 8.0 Hz); ^{13}C-NMR (500 MHz, $CDCl_3$) δ 156.4, 137.2, 134.5, 132.8, 132.1, 130.8, 130.1, 130.0, 129.6, 129.0, 128.5, 127.0; MS (EI) *m*/*z* (%): 356 (M^+, 100), 326 (57), 163 (28%); mp 312 °C decomp; HPLC (A:B = 17:3), A = 2% (*i*-Pr)$_2$NEt in hexane, B = 2,5% MeOH + 2% (*i*-Pr)$_2$NEt in CH_2Cl_2, 99.6 %, k′ = 5.43; Uv-Vis (CH_3Cl), λ_{max}= 243, 269, 325, 371 nm.

1,6-Dimethyl-7,10-diphenyl-8,9-diazafluoranthene (53b)

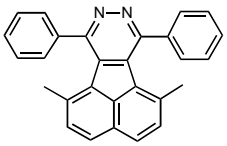

A mixture of 3,6-diphenyl-1,2,4,5-tetrazine (0.050 g, 0.28 mmol) and 2,7-dimethylacenaphthylene (0.13 g, 0.56 mmol) in *p*-xylene (5 mL) was stirred at 180 °C in an autoclave (600 Psi) for 3 d. The solvent was evaporated, the residue was purified by column chromatography (silica gel, hexane/acetone 5:1→1:5) to yield a yellow solid (0.03 g, 27%). IR (KBr): 3056*m*, 3025*m*, 3006*m*, 2924*m*, 2241*w*, 1971*w*, 1944*w*, 1879*w*, 1769*w*, 1611*m*, 1570*w*, 1530*w*,

1501*m*, 1487*s*, 1444*s*, 1408*s*, 1379*s*, 1354*m*, 1335*s*, 1304*w*, 1258*w*, 1205*m*, 1173*w*, 1161*m*, 1110*m*, 1091*s*, 1072*m*, 1059*s*, 1028*m*, 1013*m*, 985*w*, 950*w*, 916*m*, 848*s*, 800*m*, 775*m*, 757*s*, 696*s*, 679*m*, 640*w*, 599*w*, 541*m*, 532*m*, 484*w*; ^{1}H-NMR (500 MHz, $CDCl_3$) δ 7.90 (d, 1H, ^{3}J = 8.4 Hz), 7.78-7.81 (m, 2H, Ph), 7.52-7.53 (m, 3H, Ph), 7.37 (d, 1H, ^{3}J = 8.4 Hz), 1.95 (s, 3H, CH_3); ^{13}C-NMR (500 MHz, $CDCl_3$) δ 155.5, 140.5, 139.0, 135.6, 133.2, 132.2, 130.4, 130.0, 129.9, 129.2, 128.9, 126.8 22.9; MS (EI) *m*/*z* (%): 384 (M^+, 100), 356 (40), 341 (24%); mp 335 °C decomp; HPLC (A:B = 17:3), A = 2% (*i*-Pr)$_2$NEt in hexane, B = 2.5% MeOH + 2% (*i*-Pr)$_2$NEt in CH_2Cl_2 98.9 %, k′ = 7.82; Uv-Vis (CH_3Cl), λ_{max}= 254, 340, 383 nm.

7,10-Bis(2-hydroxyphenyl)-8,9-diazafluoranthene (54a)

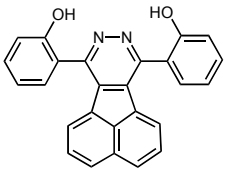

A mixture of 3,6-bis(2-hydroxyphenyl)-1,2,4,5-tetrazine[43] (0.18 g, 0.68 mmol) and acenaphthylene (0.050 g, 0.33 mmol) in chlorobenzene (10 mL) was stirred at reflux for 2 d. The solvent was evaporated, the residue was purified by column chromatography (silica gel, hexane/acetone 7:1) to yield a yellow solid (0.1 g, 75%). IR (KBr): 3065*m* (br., OH), 1940*w*, 1740*w*, 1618*s*, 1580*s*, 1517*m*, 1487*s*, 1463*m*, 1449*m*, 1416*s*, 1379*s*, 1355*s*, 1298*s*, 1253*s*, 1236*m*, 1213*m*, 1178*m*, 1125*w*, 1088*m*, 1038*m*, 953*w*, 838*w*, 825*s*, 778*s*, 764*s*, 725*m*, 665*m*, 615*w*, 599*w*, 574*w*, 503*w*, 486*w*, 464*w*, 451*w*; ^{1}H-NMR (300 MHz, $CDCl_3$) δ 10.87 (s, br, 1H, OH), 8.34 (d, 1H, ^{3}J = 7.2 Hz), 8.12 (d, 1H, ^{3}J = 8.4 Hz), 8.05 (dd, 1H, ^{4}J = 1.8, ^{3}J = 7.8 Hz, H-C (6′, 6″)), 7.67 (dd, 1H, ^{3}J = 7.5, 8.1 Hz), 7.52 (ddd, 1H, ^{4}J = 1.5, ^{3}J = 7.2, 8.4 Hz, H-C (4′, 4″)), 7.29 (dd, 1H, ^{4}J = 1.2, ^{3}J = 8.4 Hz, H-C (3′, 3″)), 7.13 (td, 1H, ^{4}J = 1.2, ^{3}J = 7.5, ^{3}J = 8.4 Hz, H-C (5′, 5″)); ^{13}C-NMR (400 MHz, $CDCl_3$) δ 157.3, 155.9, 135.4, 132.6, 132.2, 131.9, 131.5, 130.9, 130.2, 128.4, 127.5, 119.6, 119.5, 118.7; mp 233 °C decomp; MS (EI) *m*/*z* (%): 388 (M^+, 100%); HPLC (A:B:C = 1:5:4) A = 2% (*i*-Pr)$_2$NEt in hexane, B = 2% (*i*-Pr)$_2$NEt in ethyl acetate, C = 2% (*i*-Pr)$_2$NEt in MeOH, 99.0 %, k′ = 3.08; Uv-Vis (CH_2Cl_2), λ_{max}= 243, 271, 333 nm.

7,10-Bis(2-hydroxyphenyl)-1,6-dimethyl-8,9-diazafluoranthene (54b)

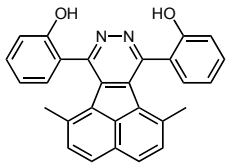

A mixture of 3,6-bis(2-hydroxyphenyl)-1,2,4,5-tetrazine (0.15 g, 0.56 mmol) and 2,7-dimethylacenaphthylene (0.050 g, 0.28 mmol) in *p*-xylene (5 mL) was stirred at 180 °C in an autoclave (600 Psi) for 2 d. The solvent was evaporated, the residue was purified by column chromatography (silica gel, hexane/ethyl acetate 10:1→ 5:1) to yield a yellow solid (0.12 g, 60%). IR (KBr): 3523*m* and 3281*m* (br., OH), 3049*m*, 2961*m*, 2922*m*, 2852*m*, 1728*w*, 1700*w*, 1614*s*, 1576*s*, 1517*m*, 1485*s*, 1460*s*, 1413*s*, 1375*s*, 1341*s*, 1293*s*, 1236*s*, 1209*s*, 1178*s*, 1153*s*, 1091*s*, 1061*s*, 1036*s*, 951*w*, 849*m*, 837*s*, 897*m*, 787*s*, 748*s*, 701*w*, 666*w*, 657*m*, 605*m*, 533*m*, 501*w*, 440*w*; ^{1}H-NMR (300 MHz, CD_2Cl_2) δ 10.53 (s, br., 1H, OH), 8.01 (d, 1H, ^{3}J = 8.4 Hz), 7.47 (d, 1H, ^{3}J = 8.1 Hz), 7.37-7.42 (m, 2H), 7.21 (d, 1H, ^{3}J = 7.8 Hz), 6.93 (dd, 1H, ^{3}J = 7.5, ^{3}J = 7.2 Hz), 2.19 (s, 3H); ^{13}C-NMR (400 MHz, $CDCl_3$) δ 156.2, 154.6, 139.9, 137.0, 133.1, 132.1, 131.6, 130.7, 130.6, 130.0, 126.7, 122.9, 120.2, 118.4, 23.7; MS (EI) *m*/*z* (%): 416 (M^+, 34), 399 (100%); mp 325-330 °C decomp; HPLC (A:B:C = 1:5:4), A = 2% (*i*-Pr)$_2$NEt in hexane, B = 2% (*i*-Pr)$_2$NEt in ethyl acetate, C = 2% (*i*Pr)$_2$NEt in MeOH, 98.0 %, k′ = 2.71; Uv-Vis (CH_2Cl_2), λ_{max}= 261, 340 nm.

7,10-Bis(4-bromophenyl)-8,9-diazafluoranthene (55a)

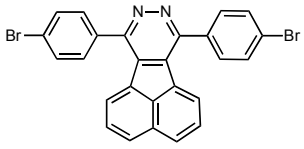

A mixture of 3,6-bis(4-bromophenyl)-1,2,4,5-tetrazine[44] (0.10 g, 0.66 mmol) and acenaphthylene (0.10 g, 1.32 mmol) in mesitylene (10 mL) was stirred at reflux for 1 d. The reaction was cooled to the room temperature, the yellow precipitate was filtered, stirred for 1.5 h in CH_2Cl_2 to dissolve the rest of the starting materials, filtered off, and dried *in vacuo*, yielding (0.17 g, 50%) of a yellow solid. IR (KBr): 3056*m*, 3010*m*, 2229*w*, 1924*w*, 1862*w*, 1590*s*, 1527*w*, 1479*s*, 1457*w*, 1435*w*, 1419*s*, 1396*s*, 1378*s*, 1353*m*, 1334*s*, 1297*m*, 1233*m*, 1178*w*, 1117*m*, 1103*m*, 1086*s*, 1071*s*, 1009*s*, 985*m*, 948*m*, 835*s*, 812*m*, 784*s*, 746*m*, 728*s*, 674*m*, 651*m*, 631*w*, 590*w*, 568*w*, 527*s*, 514*m*, 503*w*, 461*m*, 451*m*, 415*w*; ^{1}H-NMR (400 MHz, $CDCl_3$) δ 8.08 (d, 1H, ^{3}J = 8.0 Hz), 7.87-7.89 (m, 3H), 7.80 (d, 2H, ^{3}J = 8.4 Hz), 7.64 (dd, 1H, ^{3}J = 8.4, 8.4 Hz); ^{13}C-NMR (600 MHz, $CDCl_3$) δ 155.5, 136.4, 134.1, 132.5, 132.3, 132.0, 131.3, 131.0, 130.2, 128.5, 126.8, 124.4; MS

(EI) *m/z* (%): 514 (M^+, 100), 486 (18), 405 (18), 326 (73), 243 (M^{2+},13), 163, (41), 149, (10%); mp 356 °C decomp; HPLC (A:B:C = 5:10:0.5), A = 2% (*i*-Pr)$_2$NEt in hexane, B = 2% (*i*-Pr)$_2$NEt in acetone, C = 2% (*i*-Pr)$_2$NEt in MeOH, 97.2 %, k′= 4.39; Uv-Vis (CH_2Cl_2), λ_{max}= 244, 325, 372 nm.

7,10-Bis (4 -bromophenyl)-1,6-dimethyl-8,9-diazafluoranthene (55b)

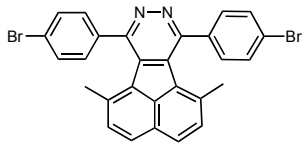

A mixture of 2,7-dimethylacenaphthylene (0.05 g, 0.28 mmol) and 3,6-bis(4-bromophenyl)-1,2,4,5-tetrazine (0.22 g, 0.56 mmol) in *p*-xylene (5 mL) was stirred in an autoclave (600 Psi) at 180 °C for 2 d. The solvent was evaporated, the residue was washed thoroughly with acetone and dried *in vacuo* to yield a light yellow solid (0.05 g, 33%). IR (KBr): 3055*w*, 2995*w*, 2956*w*, 2916*w*, 2236*w*, 1970*w*, 1899*w*, 1638*m*, 1608*m*, 1595*s*, 1563*m*, 1503 1479*s*, 1446*s*, 1412*s*, 1391*s*, 1374*s*, 1347*m*, 1331*s*, 1318*m*, 1293*w*, 1206*m*, 1183*m*, 1154*s*, 1108*s*, 1066*s*, 1030*m*, 1007*s*, 854*s*, 834*s*, 811*m*, 795*m*, 740*m*, 726*m*, 678*m*, 626*m*, 546*m*, 534*m*, 445*m*; ^{1}H-NMR (300 MHz, $CDCl_3$) δ 7.93 (d, 1H, ^{3}J = 8.1 Hz), 7.68 (s, 4H, 4-bromophenyl), 7.40 (d, 1H, ^{3}J = 8.1 Hz), 2.03 (s, 3H, CH_3); ^{13}C-NMR (400 MHz, $CDCl_3$) δ 154.5, 139.4, 138.9, 135.5, 133.2, 132.2, 132.15, 131.5, 130.3, 130.0, 126.9, 123.8, 23.3; MS (EI) *m/z* (%): 542 (M^+, 100), 514 (42), 420 (46), 353 (26), 276 (22), 169 (M^{2+}, 43%); mp 310 °C decomp; HPLC (A:B:C = 84:15:1), A = 2% (*i*-Pr)$_2$NEt in hexane, B = 2% (*i*-Pr)$_2$NEt in ethyl acetate, C = 2% (*i*-Pr)$_2$NEt in MeOH, 98.3 %, k′ = 5.42; Uv-Vis (CH_2Cl_2), λ_{max}= 256, 307, 339, 380 nm.

7,10-Bis(3,5-dimethyl-1*H*-pyrazol-1-yl)-8,9-diazafluoranthene (56a)

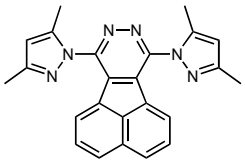

A mixture of 3,6-bis(3,5-dimethyl-1*H*-pyrazol-1-yl)-1,2,4,5-tetrazine[45] (0.18 g, 0.66 mmol) and acenaphthylene (0.05 g, 0.33 mmol) in dichloromethane (10 mL) was stirred at reflux for 3 d. The solvent was evaporated, the residue was purified by column chromatography (silica gel, hexane/ethyl acetate, 5:1) to yield a light yellow solid (0.1 g, 78%. IR (KBr): 3055*w*, 2978*w*, 2921*m*, 2856*w*, 1560*s*, 1537*m*, 1488*w*, 1466*m*, 1439*m*, 1419*s*, 1284*w*, 1264*w*, 1231*w*, 1184*w*, 1146*w*, 1091*m*, 1043*m*, 1022*m*, 988*w*, 968*m*, 823*m*, 770*s*, 760*s*, 746*m*, 698*w*, 676*w*, 632*w*, 571*w*, 502*w*; ^{1}H-NMR (400 MHz, $CDCl_3$) δ 8.12 (dd, 1H, ^{4}J = 0.4,

^{3}J= 8.0 Hz), 8.01 (dd, 1H, ^{4}J = 0.4, ^{3}J = 7.6 Hz), 7.71 (dd, 1H, ^{3}J = 7.2, 8.0 Hz), 6.23 (s, 1H, pyrazol), 2.47 (s, 3H, CH_3), 2.45 (s, 3H, CH_3); ^{13}C-NMR (400 MHz, $CDCl_3$) δ 151.1, 151.0, 142.5, 134.6, 132.3, 131.6, 130.9, 129.8, 129.4, 128.8, 108.3, 14.0, 12.5; MS (EI) *m*/*z* (%): 392 (M^+, 74), 391 (M^+ – 1, 100), 393 (M^+ + 1, 19%); mp 203 °C decomp; HPLC (A:B = 4:1), A = 2% (*i*-Pr)$_2$NEt in hexane, B = 2% (*i*-Pr)$_2$NEt in ethyl acetate, 99.4 %, k′ = 6.27; Uv-Vis (CH_2Cl_2), λ_{max}= 245, 268, 327, 372 nm.

7,10-Bis(3,5-dimethyl-1*H*-pyrazol-1-yl)-1,6-dimethyl-8,9-diazafluoranthene (56b)

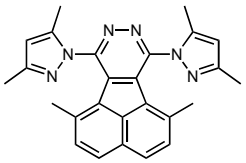

A mixture of 3,6-bis(3,5-dimethyl-1*H*-pyrazol-1-yl)-1,2,4,5-tetrazine (0.15 g, 0.56 mmol) and 2,7-dimethylacenaphthylene (0.05 g, 0.28 mmol) in mesitylene (8 mL) was stirred at reflux for 1 d. The mixture was cooled to the room temperature, the precipitate was filtered, washed thoroughly with acetone and dried *in vacuo* to yield a yellow solid (0.1 g 85%); IR (KBr): 3014*w*, 2961*w*, 2925*m*, 2860*w*, 1614*w*, 1554*s*, 1505*s*, 1462*s*, 1414*s*, 1398*s*, 1375*s*, 1348*m*, 1274*w*, 1202*m*, 1195*m*, 1157*w*, 1139*w*, 1102*s*, 1071*m*, 1034*m*, 1023*m*, 977*w*, 859*s*, 811*w*, 798*m*, 788*s*, 773*m*, 743*m*, 693*w*, 655*w*, 615*w*, 606*w*, 540*w*, 506*w*, 438*w*; ^{1}H-NMR (500 MHz, $CDCl_3$) δ 7.94 (d, 1H, ^{3}J = 8.0 Hz), 7.43 (d, 1H, ^{3}J = 8.0 Hz), 6.17 (s, 1H, pyrazol), 2.51 (s, 3H, CH_3), 2.31 (s, 3H, CH_3), 2.06 (s, 3H, CH_3); ^{13}C-NMR (500 MHz, $CDCl_3$) δ 150.9, 150.7, 143.1, 141.8, 135.8, 133.9, 132.3, 131.4, 128.0, 127.0, 108.3, 20.2, 13.9, 12.2; (600 MHz, CD_2Cl_2) δ 150.6, 150.6, 142.8, 141.7, 135.3, 133.2, 132.2, 131.2, 127.7, 126.7, 107.8, 19.7, 13.4, 11.7; MS (EI) *m*/*z* (%): 420 (M^+, 11), 405 (100), 195 (7%); mp 350 °C decomp; HPLC (A:B:C = 89:10:1), A = 2% (*i*-Pr)$_2$NEt in hexane, B = 2% (*i*-Pr)$_2$NEt in acetone, C = 2% (*i*-Pr)$_2$NEt in MeOH, 96.7 % , k′ = 6.98; Uv-Vis (CH_2Cl_2), λ_{max}= 252, 347, 382 nm.

7,10-Di(thiophen-2-yl)-8,9-diazafluoranthene (57a)

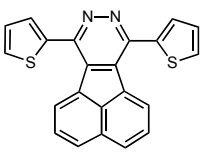

A mixture of 3,6-di(thiophen-2-yl)-1,2,4,5-tetrazine[46] (0.32 g, 1.32 mmol) and acenaphthylene (0.10 g, 0.66 mmol) in 1,2-dichloro-ethane (10 mL) was stirred at reflux for 4 d. The yellow precipitate was filtered, washed thoroughly with methanol and dried *in vacuo*, yielding (0.095 g, 39%); IR (KBr): 3102*s* (br), 3058*s*, 2582*m* (br), 1811*w*, 1695*w*, 1630*m*, 1607*m*, 1579*m*,

1554*m*, 1506*w*, 1485*m*, 1458*m*, 1418*s*, 1379*s*, 1333*s*, 1311*s*, 1221*m*, 1187*m*, 1111*s*, 990*w*, 928*w*, 852*s*, 826*s*, 785*m*, 775*s*, 741*m*, 698*s*, 669*w*, 618*s*, 518*w*, 501*w*; ^{1}H-NMR (400 MHz, $CDCl_3$) δ 8.35 (d, 1H, ^{3}J = 7.2 Hz), 8.11 (d, 1H, ^{3}J = 8.0 Hz), 7.87 (dd, 1H, ^{4}J = 1.2, ^{3}J = 3.6 Hz), 7.70 (dd, 1H, ^{3}J = 7.2, ^{3}J = 8.0 Hz), 7.67 (dd, 1H, ^{3}J= 5.2, ^{4}J = 1.2 Hz), 7.33 (dd, 1H, ^{3}J = 3.6, ^{3}J = 5.2 Hz); ^{13}C-NMR (400 MHz, $CDCl_3$) δ 150.6, 139.2, 134.1, 132.5, 132.0, 131.1, 130.3, 129.1, 129.0, 128.5, 127.5, 126.9; MS (EI) *m*/*z* (%): 368 (M^+, 100), 340 (62), 295 (24), 248 (14), 170 (11%); mp 220 °C decomp; HPLC (A:B = 17:3), A = 2% (*i*-Pr)$_2$NEt in hexane, B = 2,5% MeOH + 2% (*i*-Pr)$_2$NEt in CH_2Cl_2, 99.0 %, k′ = 7.98; Uv-Vis ($CHCl_3$), λ_{max}= 246, 283, 320 nm.

7,10-Di(thiophen-2-yl)-1,6-dimethyl-8,9-diazafluoranthene (57b)

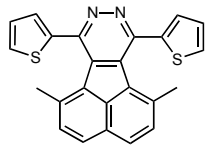

A mixture of 2,7-dimethylacenaphthylene (0.05 g, 0.28 mmol) and 3,6-di(thiophen-2-yl)-1,2,4,5-tetrazine (0.14 g, 0.56 mmol) in *p*-xylene (5 mL) was stirred at 180 °C in an autoclave (600 Psi) for 3 d. The solvent was evaporated, the residue was purified by column chromatography (silica gel, hexane/ethyl acetate 5:1, hexane/acetone 5:1) to yield a yellow solid (0.065 g, 59%). IR (KBr): 3107*w*, 3022*w*, 3004*w*, 2913*w*, 2250*w*, 1788*w*, 1612*m*, 1573*w*, 1550*w*, 1498*m*, 1443*m*, 1404*s*, 1375*s*, 1332*s*, 1315*m*, 1220*w*, 1202*m*, 1174*w*, 1155*w*, 1094*m*, 1055*m*, 1039*m*, 987*w*, 974*w*, 900*w*, 853*s*, 832*m*, 798*w*, 769*m*, 693*s*, 637*w*, 606*w*, 541*w*; ^{1}H-NMR (400 MHz, $CDCl_3$) δ 7.93 (d, 1H, ^{3}J = 8.4 Hz), 7.55 (dd, 1H, ^{4}J = 1.0, ^{3}J = 5.2 Hz), 7.43 (d, 1H, ^{3}J = 8.4 Hz), 7.30 (dd, 1H, ^{4}J = 1.0, ^{3}J = 3.6 Hz), 7.17 (dd, 1H, ^{3}J = 3.6, 5.2 Hz), 2.21 (s, 3H, CH_3); ^{13}C-NMR (500 MHz, $CDCl_3$) δ 149.4, 140.3, 139.9, 136.6, 133.4, 132.2, 130.5, 130.0, 129.8, 128.9, 127.6, 126.7, 23.0; MS (EI) *m*/*z* (%): 396 (M^+, 100), 368 (41), 353 (40), 319 (18%); mp 260 °C decomp; HPLC (A:B = 17:3), A = 2% (*i*-Pr)$_2$NEt in hexane, B = 2,5% MeOH + 2% (*i*-Pr)$_2$NEt in CH_2Cl_2, 95.7 %, k′ = 7.69; Uv-Vis ($CHCl_3$), λ_{max}= 258, 284, 329, 400 nm.

7,10-Di(furan-2-yl)-8,9-diazafluoranthene (58a)

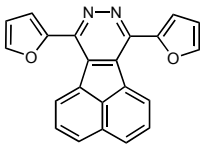

A mixture of acenaphthylene (0.05 g, 0.33 mmol) and 3,6-di(furan-2-yl)-1,2,4,5-tetrazine[47] (0.14 g, 0.66 mmol) in chlorobenzene (10 mL) was stirred at reflux for 2 d. The solvent was evaporated, the residue was purified by column chromatography (aluminium oxide, hexane). Yield (0.08 g, 73%) of a yellow solid. IR (KBr): 3138*w*, 3059*w*, 2924*m*, 2853*w*, 1599*m*, 1529*w*, 1490*m*, 1476*s*, 1421*s*, 1398*s*, 1323*s*, 1217*m*, 1181*w*, 1161*m*, 1129*s*, 1104*w*, 1071*w*, 1055*m*, 1012*s*, 888*s*, 827*s*, 810*s*, 773*s*, 728*s*, 628*w*, 592*m*; ^{1}H-NMR (400 MHz, $CDCl_3$) δ 8.80 (d, 1H, ^{3}J =7.2 Hz), 8.29 (d, 1H, ^{3}J = 8.4 Hz), 8.11 (dd, 1H, ^{4}J = 0.6, ^{3}J = 1.8 Hz, furyl), 7.89 (dd, 1H, ^{3}J = 7.8, 7.8. Hz), 7.50 (dd, 1H, ^{4}J = 1.0, ^{3}J = 3.4 Hz, furyl), 6.89 (dd, 1H, ^{3}J = 1.8, 3.4 Hz, furyl); ^{13}C-NMR (400 MHz, acetone-d_6) δ 153.0, 146.9, 145.4, 133.0, 132.82, 132.8, 131.8, 131.0, 129.6, 129.3, 113.4, 113.2; MS (EI) *m*/*z* (%): 336 (M^+, 100), 308 (21), 279 (80), 250 (51%); mp 150 °C; HPLC (A:B:C = 79:20:1), A = 2% (*i*-Pr)$_2$NEt in hexane, B = 2% (*i*-Pr)$_2$NEt in ethyl acetate, C = 2% (*i*-Pr)$_2$NEt in MeOH, 99.9 %, k′ = 8.01; Uv-Vis ($CHCl_3$), λ_{max}= 245, 291, 340 nm.

7,10-Di(furan-2-yl)-1,6-dimethyl-8,9-diazafluoranthene (58b)

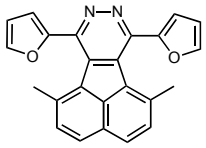

A mixture of 2,7-dimethylacenaphthylene (0.050 g, 0.28 mmol) and 3,6-di(furan-2-yl)-1,2,4,5-tetrazine (0.12 g, 0.56 mmol) in chlorobenzene (10 mL) was stirred at reflux for 1.5 d. The solvent was evaporated, the residue was purified by column chromatography (aluminium oxide, hexane). Yield (0.047 g, 47%) of a yellow solid. IR (KBr): 3105*m*, 3062*m*, 3026*m*, 3008*m*, 2972*m*, 2933*m*, 2879*w*, 2247*w*, 1979*w*, 1954*w*, 1741*w*, 1608*s*, 1573*m*, 1523*w*, 1503*m*, 1479*m*, 1450*s*, 1410*s*, 1380*s*, 1335*s*, 1256*w*, 1218*m*, 1208*s*, 1159*s*, 1110*w*, 1095*s*, 1070*s*, 1037*m*, 1012*s*, 908*s*, 885*m*, 856*s*, 827*m*, 799*w*, 780*m*, 736*s*, 727*s*, 666*w*, 596*s*, 543*m*, 468*w*; ^{1}H-NMR (300 MHz, $CDCl_3$) δ 7.91 (d, 1H, ^{3}J = 8.1 Hz), 7.63 (dd, 1H, ^{4}J = 0.9, ^{3}J =1.8 Hz, furyl), 7.42 (d, 1H, ^{3}J = 8.1 Hz), 7.16 (dd, 1H, ^{4}J = 0.9, ^{3}J = 3.3 Hz, furyl), 6.67 (dd, 1H, ^{3}J = 1.8, ^{3}J = 3.3 Hz, furyl), 2.29 (s, 3H, CH_3); ^{13}C-NMR (500 MHz, $CDCl_3$) δ 152.3, 146.8, 144.2, 140.0, 135.9, 133.5, 131.9, 130.4, 129.5, 126.8, 112.9, 111.9, 20.1; MS (EI) *m*/*z* (%): 364 (M^+, 100), 336 (25), 307 (32), 293 (17), 263 (24%); mp 170 °C

decomp; HPLC (A:B:C= 79:20:1) A = 2% (i-Pr)$_2$NEt in hexane, B = 2% (i-Pr)$_2$NEt in ethyl acetate, C = 2% (i-Pr)$_2$NEt in MeOH, 99.9 %, k′ = 6.91; Uv-Vis ($CHCl_3$), λ_{max}= 259, 328, 406 nm.

7,10-Di(pyridin-2-yl)-8,9-diazafluoranthene (59a)

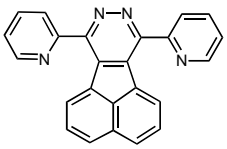

A mixture of acenaphthylene (0.50 g, 3.3 mmol) and 3,6-di(pyridin-2-yl)-1,2,4,5-tetrazine[48] (1.55 g, 6.6 mmol) in chlorobenzene (25 mL) was stirred at reflux overnight. The solvent was evaporated, the residue was purified by column chromatography (silica gel, hexane/ethyl acetate, 15:1–5:1) to yield a yellow solid (0.8 g, 68%). IR (KBr): 3091*m*, 3057*m*, 3011*m*, 2937*w*, 2255*w*, 1951*w*, 1896*w*, 1847*w*, 1586*s*, 1569*s*, 1548*m*, 1533*m*, 1476*m*, 1429*s*, 1419*s*, 1381*s*, 1356*m*, 1342*s*, 1294*m*, 1244*m*, 1232*m*, 1150*m*, 1109*m*, 1090*s*, 1045*m*, 1001*m*, 991*s*, 961*m*, 827*s*, 802*s*, 784*s*, 774*s*, 751*s*, 674*m*, 649*m*, 630*m*, 617*m*, 608*m*, 568*w*, 533*w*, 521*w*, 448*w*, 404*m*; ^{1}H-NMR (300 MHz, $CDCl_3$) δ 8.94 (ddd, 2H, ^{3}J = 4.8, ^{4}J = 1.8, ^{5}J = 0.9 Hz, H-C (6′, 6″)), 8.42 (d, 2H, ^{3}J = 7.2 Hz), 8.36 (dt, 2H, ^{3}J =7.8, ^{4}J = 0.9 Hz, H-C (3′, 3″)), 8.07 (d, ^{3}J = 8.1 Hz, 2H), 8.04 (td, 2H, ^{3}J = 7.8, ^{4}J = 1.8 Hz, H-C (5′, 5″)), 7.67 (dd, 2H, ^{3}J = 7.5, ^{3}J = 8.1Hz), 7.56 (ddd, 2H, ^{3}J = 7.5, ^{3}J = 4.8, ^{4}J = 1.2 Hz, H-C (4′, 4″)); ^{13}C-NMR (400 MHz, $CDCl_3$) δ 156.5, 155.3, 149.0, 137.6, 135.6, 132.8, 132.6, 130.9, 129.9, 129.3, 128.3, 125.3, 124.7; MS (EI) *m*/*z* (%): 358 (M^+, 100), 357 (M^+ – 1, 84), 329 (33), 280 (22%); mp 305 °C decomp; HPLC (A:B:C= 29:10:1), A = 2% (i-Pr)$_2$NEt in hexane, B = 2,5% MeOH + 2% (i-Pr)$_2$NEt in CH_2Cl_2, C = 2% (i-Pr)$_2$NEt in MeOH, 99.9 %, k′ = 2.75; Uv-Vis (CH_2Cl_2), λ_{max}= 243, 273, 325, 368 nm.

Dimethyl 8,9-diazafluoranthene-7,10-dicarboxylate (60a)

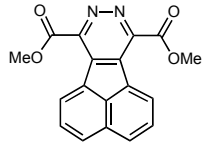

A mixture of acenaphthylene (0.10 g, 0.66 mmol) and dimethyl 1,2,4,5-tetrazine-3,6-dicarboxylate[49] (0.260 g, 1.32 mmol) in chlorobenzene (10 mL) was stirred at reflux overnight. The solvent was evaporated, the residue was purified by column chromatography (silica gel, hexane/ethyl acetate 10:1→5:1→ethyl acetate) to yield a yellow solid (0.17 g, 80%). IR (KBr): 3125*w*, 3103*w*, 3051*m*, 3008*m*, 2949*m*, 2845*m*, 1976*w*, 1885*w*, 1775*w*, 1726*s* (C=O), 1601*m*,

1523*w*, 1488*w*, 1458*w*, 1434*s*, 1421*s*, 1367*m*, 1336*s*, 1277*s*, 1235*s*, 1217*s*, 1187*m*, 1146*s*, 1090*m*, 1042*s*, 996*m*, 970*m*, 935*m*, 835*s*, 789*s*, 776*s*, 753*m*, 626*m*, 570*w*, 505*w*, 450*w*; ^{1}H-NMR (500 MHz, $CDCl_3$) δ 8.91 (d, 1H, ^{3}J = 7.0 Hz), 8.19 (d, 1H, ^{3}J= 8.0 Hz), 7.83 (dd, 1H, ^{3}J = 7.5, 8.0 Hz), 4.24 (s, 3H, CH_3); ^{13}C-NMR (500 MHz, $CDCl_3$) δ 166.0, 148.0, 136.8, 133.1, 132.2, 130.8, 130.0, 129.97, 128.9, 53.7; MS (EI) *m*/*z* (%): 320 (M^+, 14), 262 (33), 203 (100%); mp 215 °C; HPLC (A:B = 4:1), A = 2% (*i*-Pr)$_2$NEt in hexane, B = 2,5% MeOH + 2% (*i*-Pr)$_2$NEt in CH_2Cl_2, 99.9 %, k′ = 4.69; Uv-Vis (CH_2Cl_2), λ_{max}= 241, 301, 359 nm.

Dimethyl 1,6-dimethyl-8,9-diazafluoranthene-7,10-dicarboxylate (60b)

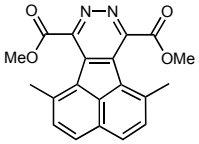

A mixture of 2,7-dimethylacenaphthylene (0.050 g, 0.28 mmol) and dimethyl 1,2,4,5-tetrazine-3,6-dicarboxylate (0.11 g, 0.56 mmol) in dichloromethane (10 mL) was stirred at reflux for 1 d. The solvent was evaporated, the residue was purified by column chromatography (aluminium oxide, hexane/ethyl acetate 10:1→hexane/acetone 3:2), to yield a yellow solid (0.07 g, 70%). IR (KBr): 3007*w*, 2949*m*, 2258*w*, 1987*w*, 1960*w*, 1724*s* (C=O), 1614*m*, 1577*m*, 1503*m*, 1449*m*, 1434*s*, 1412*s*, 1375*s*, 1344*s*, 1282*s*, 1209*s*, 1193*m*, 1161*s*, 1045*s*, 961*w*, 857*s*, 834*m*, 815*m*, 800*w*, 753*m*, 675*w*, 638*w*, 603*w*, 542*w*, 535*w*, 425*w*; ^{1}H-NMR (300 MHz, $CDCl_3$) δ 7.98 (d, 1H, ^{3}J = 8.1 Hz), 7.51 (d, 1H, ^{3}J = 8.1 Hz), 4.17 (s, 3H, CH_3), 2.75 (s, 3H, CH_3); ^{13}C-NMR (400 MHz, $CDCl_3$) δ 167.6, 150.2, 140.7, 133.9, 133.4, 132.2, 131.6, 128.0, 127.0, 53.8, 22.8; MS (EI) *m*/*z* (%): 349 (M^+ + 1, 20), 348 (M^+, 99), 333 (100), 290 (70), 231 (54), 202 (28%); mp 225 °C; HPLC (A:B= 4:1), A = 2% (*i*-Pr)$_2$NEt in hexane, B = 2,5% MeOH + 2% (*i*-Pr)$_2$NEt in CH_2Cl_2, 99.9 %, k′ = 5.67; Uv-Vis (CH_2Cl_2), λ_{max}= 244, 290, 334, 370 nm.

8,9-Diazafluoranthene-7,10-dicarboxamide (61a)

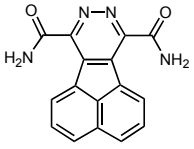

A mixture of acenaphthylene (0.10 g, 0.66 mmol) and 1,2,4,5-tetrazine-3,6-dicarboxamide[50] (0.22 g, 1.32 mmol) in DMSO (10 mL) was heated to 120 °C for 1 h. After 20 min of stirring the mixture turned yellow, then light brown. The reaction was stirred at 100 °C for an additional 10 h, and cooled to room temperature. The orange precipitate was

filtered off, washed with methanol and dried *in vacuo*. The ^{1}H-NMR (DMSO-d_6) spectrum has shown mixture of dimethyl-8,9-diazafluoranthene-7,10-dicarboxamide and 1,4-dihydro-1,2,4,5-tetrazine-3,6-dicarboxamide. Attempts to separate **61a** from tetrazine derivative using column chromatography or crystallization was unsuccessful. ^{1}H-NMR (500 MHz, DMSO-d_6) δ 9.04 (d, 1H, ^{3}J = 7.0 Hz), 8.69 (s, 1H, NH_2), 8.39 (d, 1H, ^{3}J = 8.5 Hz), 8.24 (s, 1H, NH_2), 7.96 (dd, 1H, ^{3}J = 7.0, 8.5 Hz); MS (EI) *m*/*z* (%): 290 (M^+, 26), 203 (M^+- 2$CONH_2$, 31%).

2,5-Di- *tert* -butyl -8,9-diazafluoranthene-7,10-dicarboxamide (61b)

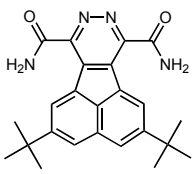

A mixture of 3,6-di-*tert*-butylacenaphthylene (0.20 g, 0.76 mmol) and 1,2,4,5-tetrazine-3,6-dicarboxamide (0.250 g, 1.52 mmol) in DMSO was stirred at 120 °C for 1 h. After 10 min stirring the mixture became clear. The reaction was stirred an additional 10 h at 100 °C. The solvent was evaporated, the residue was purified by column chromatography (aluminium oxide, acetone/methanol 5:1) to yield a light yellow solid (0.29 g, 95%). IR (KBr): 3299*s* (br), 2961*s*, 2870*m*, 1676*s* (br), 1651*s*, 1596*s* (br), 1478*s*, 1441*s*, 1396*s*, 1370*s*, 1309*s*, 1258*m*, 1231*s*, 1213*m*, 1179*m*, 1149*m*, 1121*m*, 1102*m*, 1050*m*, 1024*w*, 931*w*, 899*m*, 828*w*, 802*m*, 752*m*, 636*m*, 585*m* (br), 535*m*; ^{1}H-NMR (300 MHz, DMSO-d_6) δ 9.24 (s, 1H), 8.68 (s, 1H, NH_2), 8.34 (s, 1H), 8.24 (s, 1H, NH_2), 1.48 (s, 9H); ^{13}C-NMR (300 MHz, DMSO-d_6) δ 167.0, 151.5, 150.5, 135.4, 129.6, 129.3, 129.0, 128.8, 127.2, 35.6, 31.4; MS (EI) *m*/*z* (%): 402 (M^+, 11), 387 (100), 299 (10%); mp 325 °C decom; HPLC (A:B:C = 27:12:11), A = 2% (*i*-Pr)$_2$NEt in hexane, B = 2,5% MeOH + 2% (*i*-Pr)$_2$NEt in CH_2Cl_2, C = 2% (*i*-Pr)$_2$NEt in MeOH, 99.2 %, k′ = 4.81; Uv-Vis ($CHCl_3$), λ_{max}= 245, 313, 387 nm.

7,10-Dimethyl-8,9-diazafluoranthene (62a)

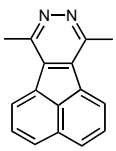

A mixture of 3,6-dimethyl-1,2,4,5-tetrazine[51] (0.070 g, 0.658 mmol) and acenaphthylene (0.05 g, 0.329 mmol) in *p*-xylene (5 mL) was stirred at 180 °C in an autoclave (600 Psi) for 2 d. The solvent was evaporated, the residue was purified by column chromatography (silica gel, hexane/acetone 5:1) to yield a yellow solid (0.4 g, 88%). IR (KBr): 3054*m*, 2922*m*, 2853*m*, 2178*w*, 1928*w*, 1727*w*,

1598*w*, 1564*m*, 1549*m*, 1483*m*, 1423*s*, 1397*s*, 1367*m*, 1290*w*, 1251*m*, 1222*m*, 1183*s*, 1139*m*, 1093*m*, 1074*m*, 1030*m*, 826*s*, 775*s*, 749*m*, 632*m*, 565*w*, 551*w*; ^{1}H-NMR (400 MHz, $CDCl_3$) δ 8.15 (d, 1H, ^{3}J = 7.2 Hz) 8.06 (d, 1H, ^{3}J = 8.0 Hz), 7.76 (dd, 1H, ^{3}J = 7.2, 8.0 Hz), 3.11 (s, 3H, CH_3); ^{13}C-NMR (500 MHz, $CDCl_3$) δ 153.8, 133.9, 133.8, 131.4, 130.1, 130.0, 128.7, 126.4, 21.2; MS (EI) *m*/*z* (%): 232 (M^+, 100), 203 (58), 189 (15), 101 (16%); mp 290 °C; HPLC (A:B = 4:1), A = 2% (*i*-Pr)$_2$NEt in hexane, B = 2,5% MeOH + 2% (*i*-Pr)$_2$NEt in CH_2Cl_2, 99.2 %, k′ = 7.9; Uv-Vis (CH_2Cl_2), λ_{max}= 240, 259, 279, 320, 350 nm.

1,6,7,10-Tetramethyl-8,9-diazafluoranthene (62b)

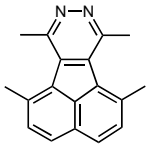

A mixture of 3,6-dimethyl-1,2,4,5-tetrazine (0.120 g, 1.12 mmol) and 2,7-dimethylacenaphthylene (0.1 g, 0.56 mmol) in *p*-xylene (5 mL) was stirred at 180 °C in an autoclave (600 Psi) for 3 d. The solvent was evaporated, the residue was purified by column chromatography (silica gel, hexane/ester 5:1, hexane/acetone 3:2) to yield a yellow solid (0.1 g, 70%). IR (KBr): 3061*m*, 3037*m*, 3021*m*, 3004*m*, 2926*m*, 2858*m*, 2270*w*, 1978*w*, 1609*s*, 1565*w*, 1531*w*, 1503*s*, 1456*s*, 1431*s*, 1409*s*, 1387*s*, 1375*s*, 1333*m*, 1244*w*, 1227*w*, 1197*s*, 1176*w*, 1158*m*, 1138*w*, 1086*m*, 1051*m*, 1032*m*, 846*s*, 827*w*, 798*s*, 774*m*, 636*w*, 535*m*, 463*w*; ^{1}H-NMR (500 MHz, $CDCl_3$) δ 7.90 (d, 1H, ^{3}J = 8.0 Hz), 7.49 (d, 1H, ^{3}J = 8.5 MHz), 3.20 (s, 3H, CH_3), 3.02 (s, 3H, CH_3); ^{13}C-NMR (500 MHz, $CDCl_3$) 151.8, 137.4, 136.0, 133.0, 132.6, 131.2, 130.1, 127.1, 25.8, 25.3; MS (EI) *m*/*z* (%): 260 (M^+, 100), 217 (32), 202 (36%); mp 210 °C decomp; HPLC (A:B = 4:1), A = 2% (*i*-Pr)$_2$NEt in hexane, B = 2,5% MeOH + 2% (*i*-Pr)$_2$NEt in CH_2Cl_2, 98.0 % , k′ = 7.07; Uv-Vis (CH_2Cl_2), λ_{max}= 246, 336, 368 nm.

7,10-Bis(methylthio)-8,9-diazafluoranthene (63a)

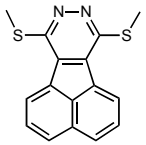

A mixture of acenaphthylene (0.050 g, 0.33 mmol) and 3,6-bis(methylthio)-1,2,4,5-tetrazine[52] (0.11 g, 0.66 mmol) in *p*-xylene (10 mL) was stirred at reflux for 1 d. The solvent was evaporated, the residue was purified by column chromatography (aluminium oxide, hexane/ethyl acetate 20:1 → 10:1) to yield a yellow solid (0.07 g, 75%). IR (KBr): 2923*s*, 2853*s*, 1727*m*, 1590*m*,

1529*w*, 1491*s*, 1413*s*, 1346*m*, 1282*s*, 1165*m*, 1141*m*, 1074*s*, 1040*s*, 983*m*, 828*s*, 796*m*, 776*s*, 695*w*, 570*w*; ^{1}H-NMR(400 MHz, $CDCl_3$) δ 8.36 (d, 1H, ^{3}J = 7.2 Hz), 8.02 (d, 1H, ^{3}J = 8.0 Hz), 7.73 (dd, 1H, ^{3}J = 7.2, 8.0 Hz), 2.95 (s, 3H, CH_3); ^{13}C-NMR (400 MHz, $CDCl_3$) δ 154.6, 132.5, 132.3, 130.6, 130.4, 129.5, 128.5, 128.1, 13.2; MS (EI) *m*/*z* (%): 296 (M^+, 100), 249 (21), 238 (52), 203 (24), 119 (37%); mp 165 °C; HPLC (A:B = 99:1), A = 2% (*i*-Pr)$_2$NEt in hexane, B = 2% (*i*-Pr)$_2$NEt in ethyl acetate, 99.9 %, k′ = 5.63; Uv-Vis (CH_2Cl_2), λ_{max}= 246, 271, 329, 348, 420 nm.

1,6-Dimethyl-7,10-bis(methylthio)-8,9-diazafluoranthene (63b)

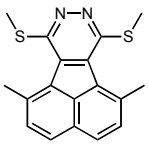

A mixture of 2,7-dimethylacenaphthylene (0.10 g, 0.56 mmol) and 3,6-bis(methylthio)-1,2,4,5-tetrazine (0.20 g, 0.11 mmol) in mesitylene (10 mL) was stirred at reflux for 2 d. The solvent was evaporated, the residue was purified by column chromatography (aluminium oxide, hexane → hexane/ethyl acetate 10:1) to yield a yellow solid (0.037 g, 20%). IR (KBr): 2955*s*, 2920*s*, 2853*s*, 1717*w*, 1612*m*, 1505*m*, 1488*m*, 1460*s*, 1444*s*, 1411*s*, 1370*s*, 1334*m*, 1304*m*, 1278*s*, 1212*s*, 1185*s*, 1158*m*, 1084*m*, 1033*s*, 981*s*, 899*w*, 846*s*, 806*m*, 794*s*, 778*m*, 725*w*, 632*m*, 612*m*, 536*m*; ^{1}H-NMR (400 MHz, $CDCl_3$) δ 7.87 (d, 1H, ^{3}J = 8.0 Hz), 7.46 (d, 1H, ^{3}J = 8.0 Hz), 3.19 (s, 3H, CH_3), 2.84 (s, 3H, CH_3); ^{13}C-NMR (400 MHz, $CDCl_3$) δ 153.0, 139.0, 134.2, 132.5, 132.2, 130.4, 130.1, 126.6, 26.5, 15.2; MS (EI) *m*/*z* (%): 324 (M^+, 30), 309 (100), 265 (24), 231 (18%); mp 165 °C decomp; HPLC (A:B = 99:1), A = 2% (*i*-Pr)$_2$NEt in hexane, B = 2% (*i*-Pr)$_2$NEt in ethyl acetate, 99.9 %, k′ = 6.97; Uv-Vis ($CHCl_3$), λ_{max}= 259, 337, 352, 434 nm.

7,10-Bis(4-chlorobenzyl)-8,9-diazafluoranthene (64a)

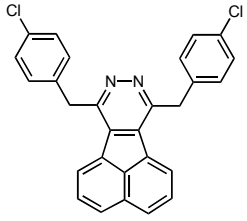

A mixture of acenaphthylene (0.050 g, 0.33 mmol) and 3,6-bis(4-chlorobenzyl)-1,2,4,5-tetrazine[53] (0.22 g, 0.66 mmol) in *p*-xylene was stirred in an autoclave at 180 °C (600 Psi) for 2.5 d. The solvent was evaporated, the residue was purified by column chromatography (silica gel, hexane/ethyl acetate 5:1, hexane/acetone 1:5) to yield a beige solid (0.082 g, 55%). IR (KBr): 3045*m*, 3010*m*,

2928*w*, 2205*w*, 1898*w*, 1595*w*, 1562*w*, 1540*m*, 1490*s*, 1460*m*, 1420*s*, 1381*s*, 1356*m*, 1320*w*, 1268*w*, 1225*w*, 1192*m*, 1143*m*, 1103*s*, 1089*s*, 1052*s*, 1015*s*, 990*w*, 955*w*, 926*w*, 860*m*, 828*s*, 796*s*, 779*s*, 722*m*, 684*w*, 628*w*, 609*w*, 589*w*, 562*w*, 553*m*, 500*m*, 482*m*, 411*w*; ^{1}HNMR (400 MHz, $CDCl_3$) δ 8.12 (d, 1H, ^{3}J = 7.2 Hz), 8.07 (d, 1H, ^{3}J = 8.1Hz), 7.72 (dd, ^{3}J = 7.2, 8.2 Hz), 7.30 (d, 2H, ^{3}J = 8.6 Hz), 7.24 (d, 2H, ^{3}J = 8.6 Hz), 4.91 (s, 2H, CH_2); ^{13}C-NMR (400 MHz, DMSO-d_6, t = 120 °C) δ 154.5, 136.5, 132.9, 131.5, 130.6, 130.3, 129.8, 129.7, 129.1, 128.0, 127.7, 126.3, 38.2; MS (EI) *m*/*z* (%): 451 (M^+ - 2, 100), 453 (M^+, 77), 416 (11), 276 (8%); mp 255 °C decomp; HPLC (A:B:C = 79:20:1), A = 2% (*i*-Pr)$_2$NEt in hexane, B = 2% (*i*-Pr)$_2$NEt in acetone, C = 2% (*i*-Pr)$_2$NEt in MeOH, 99.6 %, k′ = 4.09; Uv-Vis ($CHCl_3$), λ_{max}= 307, 322, 356 nm.

3,8-Dibromo-1-acenaphthenol (81)

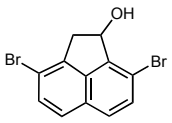

To a dry three-necked 100 mL round-bottom flask, equipped with a condenser, N_2 inlet and a stir bar, dry THF (28 mL) and 3,8-dibromo-1-acenaphthenone (1.6 g, 4.9 mmol) were added. The mixture was cooled in an acetone/ice bath and $LiAlH_4$ (0.28 g, 7.3 mmol) was added in small portions with stirring. After stirring at RT overnight and 24 h at reflux, the mixture was hydrolyzed (28 mL of 1 N HCl was added dropwise) with ice cooling, concentrated to about one-half its volume, extracted with CH_2Cl_2 (3 × 50 mL) and dried with $MgSO_4$. The solvent was evaporated, the residue was purified by column chromatography (silica gel, hexane) to yield a white solid (1.1 g, 65%). IR (KBr): 3377*s* (br. OH), 3083*w*, 3038*w*, 2925*w*, 2667*w*, 1898*w*, 1607*m*, 1581*m*, 1479*s*, 1443*w*, 1405*m*, 1346*w*, 1287*m*, 1272*m*, 1227*w*, 1217*m*, 1189*m*, 1168*w*, 1115*m*, 1103*m*, 1084*s*, 1025*s*, 996*w*, 976*m*, 898*s*, 868*w*, 837*s*, 824*s*, 779*m*, 682*w*, 605*w*, 574*w*, 527*m*, 493*w*; ^{1}H-NMR (500 MHz, $CDCl_3$) d 7.59 (d, 1H, ^{3}J = 8.5 Hz), 7.57 (d, 1H, ^{3}J = 3.5 Hz), 7.55 (d, 1H, ^{3}J = 4.0 Hz), 7.50 (d, 1H, ^{3}J = 9.0 Hz), 5.73 (ddd, 1H, ^{3}J = 2.0, ^{3}J = 4.0, ^{3}J = 7.0 Hz), 3.70 (ddd, 1H, ^{4}J = 0.5, ^{3}J = 7.1, ^{2}J = 18.5 Hz), 3.26 (ddd, 1H, ^{4}J = 0.5, ^{3}J = 2.0, ^{2}J = 18.5 Hz), 2.65 (d, 1H, OH, ^{3}J = 4.0 Hz); ^{13}C-NMR (500 MHz, $CDCl_3$) d 144.7, 141.8, 139.2, 131.9, 131.6, 129.0, 127.4, 125.3, 116.2, 115.7, 74.0, 42.0; MS (EI) *m*/*z* (%): 328 (M^+, 79), 310 (22), 247 (42), 230 (27), 168 (100), 150 (22), 139 (69%); mp 129 °C; Uv-Vis (CH_2Cl_2), λ_{max}= 242, 262, 291 nm.

3,8-Dibromoacenaphthylene (82)

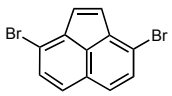

3,8-Dibromo-1-acenaphthenol (0.50 g, 1.5 mmol) was stirred at reflux in acetic acid (32 mL) for 3 d. The mixture was diluted with water (30 mL), extracted with CH_2Cl_2 and dried with $MgSO_4$. The solvent was evaporated, the residue was purified by column chromatography (silica gel, hexane) to yield a yellow solid (0.21 g, 44%). IR (KBr): 2922*w*, 2852*w*, 1886*w*, 1814*w*, 1632*w*, 1601*s*, 1472*w*, 1462*m*, 1439*m*, 1420*m*, 1409*m*, 1356*w*, 1301*w*, 1261*w*, 1196*w*, 1149*m*, 1124*w*, 1106*w*, 1078*s*, 954*w*, 899*m*, 871*s*, 823*s*, 723*s*, 707*m*, 523*m*, 507*w*, 494*w*; ^{1}H-NMR (500 MHz, $CDCl_3$) δ 7.58 (d, 1H, ^{3}J = 9.0 Hz), 7.55 (d, 1H, ^{3}J = 8.5 Hz), 7.07 (s, 1H); ^{13}C-NMR (500 MHz, $CDCl_3$) δ 140.3, 131.8, 130.7, 129.3, 129.2, 125.9, 121.2; MS (EI) *m*/*z* (%): 310 (M^+, 100), 308 (M^+ - 2, 52), 229 (29), 150 (71), 75 (33%); mp 103 °C; HPLC (2% (*i*-Pr)$_2$NEt in hexane), 99.9 %, k′ = 2.87; Uv-Vis (CH_2Cl_2), λ_{max}= 246, 335, 348 nm.

Dimethyl 3,4-dichloro-8,9-diazafluoranthene-7,10-dicarboxylate (85)

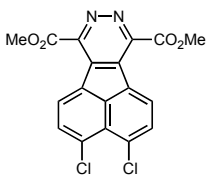

A mixture of 5,6-dichloroacenaphthylene (0.10 g, 0.45 mmol) and dimethyl 1,2,4,5-tetrazine-3,6-dicarboxylate (0.18 g, 0.9 mmol) was refluxed in CH_2Cl_2 overnight. The solvent was evaporated the residue was washed thoroughly with methanol and dried *in vacuo*. Yield 0.16 g (91%) of a yellow solid. IR (KBr): 3119*w*, 3075*w*, 3007*w*, 2956*w*, 1933*w*, 1732*s* (C=O), 1589*w*, 1567*s*, 1437*s*, 1413*s*, 1377*s*, 1339*m*, 1324*m*, 1284*s*, 1201*s*, 1149*s*, 1101*m*, 1088*s*, 1055*s*, 964*m*, 946*w*, 863*w*, 845*s*, 819*m*, 802*m*, 781*m*, 661*w*, 578*w*, 554*w*, 513*w*; ^{1}H-NMR (500 MHz, $CDCl_3$) δ 8.86 (d, 1H, ^{3}J = 7.5 Hz), 7.89 (d, 1H, ^{3}J = 8.0 Hz), 4.23 (s, 3H, CH_3); ^{13}C-NMR (500 MHz, DMSO-d_6, t = 120 °C) δ 164.4, 146.9, 134.3, 134.0, 133.2, 132.0, 129.7, 128.7, 123.7, 52.6; MS (EI) *m*/*z* (%): 388 (M^+, 14), 330 (41), 271 (100), 237 (8%); mp 233 °C decomp; HPLC (A:B:C = 79:20:1), A = 2% (*i*-Pr)$_2$NEt in hexane, B = 2% (*i*-Pr)$_2$NEt in ethyl acetate, C = 2% (*i*-Pr)$_2$NEt in MeOH, 99.4 %, k′ = 7.92; Uv-Vis (CH_2Cl_2), λ_{max}= 253, 307, 381 nm.

Dimethyl 1,6-bis(bromomethyl)-8,9-diazafluoranthene-7,10-dicarboxylate (74)

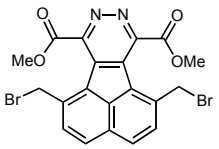

A mixture of dimethyl 1,6-dimethyl-8,9-diazafluoranthene-7,10-dicarboxylate (0.10 g, 0.29 mmol), *N*-bromosuccinimide (NBS) (0.10 g, 0.58 mmol) and dibenzoyl peroxide (BPO) (0.014 g, 0.058 mmol) in 20 mL of CCl_4 was irradiated with incandescent light and refluxed for 12 h. The solvent was evaporated, the residue was purified by column chromatography (silica gel, hexane/acetone, 4:1) to yield a yellow solid (0.044 g, 30%). IR (KBr): 3066*w*, 3020*w*, 2953*m*, 2848*w*, 1732*s*, 1609*m*, 1575*w*, 1519*w*, 1505*w*, 1439*s*, 1416*s*, 1374*w*, 1334*s*, 1278*s*, 1201*s*, 1159*s*, 1101*m*, 1039*s*, 1023*m*, 955*m*, 929*w*, 868*w*, 853*m*, 834*w*, 817*m*, 805*w*, 767*w*, 751*m*, 658*m*, 636*w*, 526*w*; ^{1}H-NMR (500 MHz, $CDCl_3$) δ 8.11 (d, 1H, ^{3}J = 8.0Hz), 7.81 (d, 1H, ^{3}J = 8.5Hz), 4.95 (s, 2H), 4.26 (s, 3H); ^{13}C-NMR (500 MHz, $CDCl_3$) δ 167.5, 150.1, 140.0, 134.7, 133.7, 132.5, 132.2, 129.4, 129.0, 54. 4, 32.4; MS (EI) *m*/*z* (%): 506 (M^+, 4.1), 427 (4.0), 348 (8.51), 333.0 (8.7), 290.0 (6.3), 230 (7.4), 94 (93), 44 (100%); mp 195 °C decomp; Uv-Vis (CH_2Cl_2), λ_{max}= 260, 342, 377 nm.

3.7 Crystal Data

All X-ray crystal structure determination measurements were made on a *Nonius-KappaCCD* area-detector diffractometer[54] using graphite monochromated Mo *K*a radiation (l = 0.71073 Å) and an *Oxford Cryosystems Cryostream 700* cooler.

Compound 53a, **CCDC 710133**. (Obtained from acetone): $C_{26}H_{16}N_2$, M = 356.43, space group: $C2/c$ (monoclinic), a = 22.513(2) Å, b = 9.9474(8) Å, c = 7.9414(6) Å, β = 103.717(5)°, V =1727.7(2) Å^3, Z = 4, μ(Mo $K\alpha$) = 0.0806 mm^{-1}, Dx = 1.370 g cm^{-3}, $2\theta_{(max}$ = 50°, T = 160 K, 10175 measured reflections, 1531 independent reflections, 996 reflections with $I > 2\sigma(I)$, refinement on F^2 with SHELXL97,[55] 129 parameters, $R(F)$ [$I > 2\sigma(I)$ reflections] = 0.0524, $wR(F^2)$ [all data] = 0.1445, goodness of fit = 1.047, $\Delta\varrho_{max}$ = 0.37 eÅ^{-3}. The molecule possesses crystallographic C_2 symmetry.

Compound 53b, **CCDC 710122**. (Obtained from CH_2Cl_2): $C_{28}H_{20}N_2$, M = 384.48, space group: $C2/c$ (monoclinic), a = 21.7712(6) Å, b =9.9895(3) Å, c = 9.2316(3) Å, β = 104.664(2)°, V =1942.3(1) Å^3, Z = 4, μ(Mo $K\alpha$) = 0.0769 mm^{-1}, Dx = 1.315 g cm^{-3}, $2\theta_{(max)}$

= 60°, T = 160 K, 29059 measured reflections, 2827 independent reflections, 2042 reflections with $I > 2\sigma(I)$, refinement on F^2 with SHELXL97, 138 parameters, $R(F)$ [$I > 2\sigma(I)$reflections] = 0.0609, $wR(F^2)$ [all data] = 0.1688, goodness of fit = 1.033, $\Delta\varrho_{max}$ = 0.41 eÅ^{-3}. The molecule has crystallographic C_2 symmetry.

Compound 54a·0.25CH_2Cl_2, CCDC 710125. (Obtained from CH_2Cl_2): $C_{26.25}H_{16.50}C_{l0.50}N_2O_2$, M = 409.66, space group: Pn (monoclinic), a = 7.4781(1) Å, b = 22.6399(3) Å, c = 23.8830(3) Å, β = 97.0449(7)°, V = 4012.95(9) Å^3, Z = 8, μ(Mo $K\alpha$) = 0.150 mm^{-1}, Dx = 1.356 g cm-3, $2\theta_{(max)}$ = 55°, T = 160 K, 86266 measured reflections, 17993 independent reflections, 14245 reflections with $I > 2\sigma(I)$, refinement on F^2 with SHELXL97, 1132 parameters, $R(F)$ [$I > 2\sigma(I)$ reflections] = 0.0563, $wR(F^2)$ [all data] = 0.1380, goodness of fit = 1.074, $\Delta\varrho_{max}$ = 0.45 eÅ^{-3}. The asymmetric unit contains four molecules of the polycyclic compound and one molecule of CH_2Cl_2. The atomic coordinates of the model were tested carefully for a relationship from a higher symmetry space group using the program *PLATON*,[56] but none could be found.

Compound 54b·2$CHCl_3$, CCDC 710124. (Obtained from $CHCl_3$): $C_{30}H_{22}C_{l6}N_2O_2$, M = 655.23, space group: $C2/c$ (monoclinic), a = 14.6105(4) Å, b = 18.4987(4) Å, c = 11.5185(3) Å, β = 110.070(1)°, V = 2924.1(1) Å^3, Z = 4, μ(Mo $K\alpha$) = 0.619 mm^{-1}, Dx = 1.488 g cm^{-3}, $2\theta_{(max)}$ = 60°, T = 160K, 38403 measured reflections, 4282 independent reflections, 2786 reflections with $I > 2\sigma(I)$, refinement on F^2 with SHELXL97, 188 parameters, $R(F)$ [$I > 2\sigma(I)$ reflections] = 0.0563, $wR(F^2)$ [all data] = 0.1608, goodness of fit = 1.033, $\Delta\varrho_{max}$ = 0.51 eÅ^{-3}. The asymmetric unit contains one half of the polycyclic molecule, which sits across a C_2 axis, plus one molecule of $CHCl_3$.

Compound 56a, **CCDC 710126**. (Obtained from acetone): $C_{24}H_{20}N_6$, M = 392.46, space group: $P2_1/n$ (monoclinic), a = 11.4681(2) Å, b = 8.0005(1) Å, c = 20.8185(4) Å, β = 94.471(1)°, V = 1904.30(5) Å^3, Z = 4, μ(Mo $K\alpha$) = 0.0853 mm^{-1}, Dx = 1.369 g cm^{-3}, $2\theta_{(max)}$ = 60°, T = 160 K, 52686 measured reflections, 5570 independent reflections, 4014 reflections with $I > 2\sigma(I)$, refinement on F^2 with SHELXL97, 276 parameters, $R(F)$ [$I > 2\sigma(I)$ reflections] = 0.0509,$wR(F^2)$ [all data] = 0.1330, goodness of fit = 1.040, $\Delta\varrho_{max}$ = 0.33 eÅ^{-3}.

Compound 57a, **CCDC 710131**. (Obtained from CH_2Cl_2): $C_{22}H_{12}N_2S_2$, M = 368.47, space group: *Pbcn* (orthorhombic), a = 21.4777(6) Å, b = 10.0334(3) Å, c = 7.5250(3) Å, V = 1621.60(9) Å^3, Z = 4, μ(Mo $K\alpha$) = 0.336 mm^{-1}, Dx = 1.509 g cm^{-3}, $2\theta_{(max)}$ = 60°, T = 160 K, 24334 measured reflections, 2364 independent reflections, 1861 reflections with $I > 2\sigma(I)$, refinement on F^2 with SHELXL97, 119 parameters, $R(F)$ [$I > 2\sigma(I)$ reflections] = 0.0503, $wR(F^2)$ [all data] = 0.1365, goodness of fit = 1.039, $\Delta\varrho_{max}$ = 0.42 eÅ^{-3}. The molecule possesses crystallographic C_2 symmetry about an axis through the middle of the N–N bond and the centre of the molecule.

Compound 57b, **CCDC 710130**. (Obtained from CH_2Cl_2): $C_{24}H_{16}N_2S_2$, M = 396.52, space group: $C2/c$ (monoclinic), a = 8.8710(2) Å, b = 10.0494(2) Å, c = 21.2597(5) Å, β = 102.122(2)°, V = 1853.00(7) Å^3, Z = 4, μ(Mo $K\alpha$) = 0.300 mm^{-1}, Dx = 1.421 g cm^{-3}, $2\theta_{(max)}$ = 55°, T = 160 K, 16306 measured reflections, 2108 independent reflections, 1655 reflections with $I > 2\sigma(I)$, refinement on F^2 with SHELXL97, 166 parameters, $R(F)$ [$I > 2\sigma(I)$ reflections] = 0.0552, $wR(F^2)$ [all data] = 0.1484, goodness of fit = 1.088, $\Delta\varrho_{max}$ = 0.34 eÅ^{-3}. The molecule has crystallographic C_2 symmetry. The heterocyclic five-membered ring is disordered through an approximately 180° rotation of the ring about its bond to the polycyclic system. Two sets of overlapping positions were defined for the unsubstituted atoms of the heterocyclic five-membered ring and the site occupation factor of the major conformation of these groups refined to 0.767(3). Similarity restraintswere applied to the chemically equivalent bond lengths and angles involving all disordered atoms, while neighbouring atoms within and between each conformation of the disordered ring were restrained to have similar atomic displacement parameters.

Compound 58b, **CCDC 713715**. (Obtained from acetone): $C_{24}H_{16}N_2O_2$, M = 364.40, space group: $P2_1/c$ (monoclinic), a = 8.3569(5) Å, b = 9.9526(6) Å, c = 21.8278(9) Å, β = 100.864(4)°, V = 1782.9(2) Å ^{3}, Z = 4, μ(Mo $K\alpha$) = 0.0875 mm^{-1}, Dx = 1.357 g cm^{-3}, $2\theta_{(max)}$ = 50°, T = 160 K, 21964 measured reflections, 3189 independent reflections, 1544 reflections with $I > 2\sigma$ (I), refinement on F^2 with SHELXL97, 257 parameters, $R(F)$ [$I > 2\sigma(I)$ reflections] = 0.0565, $wR(F^2)$ [all data] = 0.1775, goodness of fit = 1.046, $\Delta\varrho_{max}$ = 0.18 eÅ^{-3}. The crystals are twinned by a two-fold rotation about [201]. The twin volume fraction of the major twin component is 0.247(2). There is some suggestion that the

structure should belong to a higher symmetry space group (*C2/c*), however, attempts to refine the structure in this higher symmetry space group gave inferior results and many systematic absence violations. The current model refuses to converge with the displacement parameters of the two central C atoms, C(4) and C(14), "hunting" around some mean value. It is thought that this is a consequence of matrix correlations brought about by the pseudo-symmetry.

Compound 59a, **CCDC 710129**. (Obtained from CH_2Cl_2): $C_{24}H_{14}N_4$, M = 358.40, space group: *Pbcn* (orthorhombic), a = 21.4230(5) Å, b = 10.0153(3) Å, c = 7.9227(3) Å, V = 1699.88(9) Å^3, Z = 4, μ(Mo $K\alpha$) = 0.0854 mm^{-1}, Dx = 1.400 g cm-3, $2\theta_{(max)}$ = 60°, T = 160K, 39180 measured reflections, 2479 independent reflections, 1785 reflections with $I > 2\sigma(I)$, refinement on F^2 with SHELXL97, 128 parameters, $R(F)$ [$I > 2\sigma(I)$ reflections] = 0.0698, $wR(F^2)$ [all data] = 0.1879, goodness of fit = 1.062, $\Delta\varrho_{max}$ = 0.53 eÅ^{-3}. The molecule possesses crystallographic C_2 symmetry about an axis through the middle of the N–N bond and the centre of the molecule.

Compound 60a, **CCDC 710135**. (Obtained from hexane/acetone): $C_{18}H_{12}N_2O_4$, M = 320.30, space group: $P2_1$ (monoclinic), a = 9.9472(2) Å, b = 13.2994(2) Å, c = 11.5775(2) Å, β =114.6580(8)°, V = 1391.95(4) Å^3, Z = 4, μ(Mo $K\alpha$) = 0.110mm^{-1}, Dx = 1.528 g cm^{-3}, $2\theta_{(max)}$ = 60°, T = 160 K, 39027 measured reflections, 4226 independent reflections, 3767 reflections with $I > 2\sigma(I)$, refinement on F^2 with SHELXL97, 438 parameters, $R(F)$ [$I > 2\sigma(I)$ reflections] = 0.0434, $wR(F^2)$ [all data] = 0.1187, goodness of fit = 1.085, $\Delta\varrho_{max}$ = 0.46 eÅ^{-3}. There are two symmetry-independent molecules in the asymmetric unit. The atomic coordinates of the two molecules were tested carefully for a relationship from a higher symmetry space group using the program *PLATON*, but none could be found.

Compound 60b, **CCDC 710134**. (Obtained from CH_2Cl_2): $C_{20}H_{16}N_2O_4$, M = 348.36, space group: $C222_1$ (orthorhombic), a = 8.3958(2) Å, b = 9.9699(2) Å, c = 19.624(5) Å, V = 1391.95(4) Å^3, Z = 4, μ(Mo $K\alpha$) = 0.0995 mm^{-1}, Dx = 1.408 g cm^{-3}, $2\theta_{(max)}$ = 60°, T = 160 K, 12353 measured reflections, 1086 independent reflections, 1000 reflections with $I > 2\sigma(I)$, refinement on F^2 with SHELXL97, 122 parameters, $R(F)$ [$I > 2\ \sigma(I)$ reflections]

= 0.0448, $wR(F^2)$ [all data] = 0.1135, goodness of fit = 1.161, $\Delta\varrho_{max}$ = 0.23 eÅ^{-3}. The molecule exhibits crystallographic C_2 symmetry.

Compound 61b·0.5CH3OH, **CCDC 710123**. (Obtained from MeOH): $C_{24.5}H_{28}N_4O_{2.5}$, M = 418.51, space group: $P2/c$ (monoclinic), a = 15.7180(7) Å, b = 13.3493(6) Å, c = 23.922(1) Å, β = 92.478(2)°, V = 5014.7(4) Å^3, Z = 8, μ(Mo $K\alpha$) = 0.0732 mm^{-1}, Dx = 1.109 g cm^{-3}, $2\theta_{(max)}$ = 50°, T =160 K, 49418 measured reflections, 8767 independent reflections, 5315 reflections with $I > 2\ \sigma(I)$, refinement on F^2 with SHELXL97, 553 parameters, $R(F)$ [$I > 2\sigma(I)$ reflections] = 0.0.0933, $wR(F2)$ [all data] = 0.2758, goodness of fit = 1.053, $\Delta\varrho_{max}$ = 0.44 eÅ^{-3}. The asymmetric unit contains two molecules of the polycyclic compound and one disordered molecule of MeOH. Attempts to model the solvent molecule were unsuccessful. Therefore the *SQUEEZE*[57] routine of the program *PLATON* was employed. This procedure, which allows the disordered solvent molecule to be omitted entirely from the subsequent refinement model, gave improved refinement results and there were no significant peaks of residual electron density to be found in the voids of the structure. When the solvent molecule is omitted from the model, each unit cell contains two cavities of 566 Å^3. The electron count in each cavity was calculated to be approximately 34 e. As the crystals grew from a MeOH solution, it is assumed the cavities contain MeOH molecules. Allowing for two molecules of MeOH per cavity yields 36 e and this estimate was used in the subsequent calculation of the empirical formula, formula weight, density, linear absorption coefficient and $F(000)$. As a consequence, the ratio of polycyclic molecules to solvent molecules is 2:1.

Compound 62a, **CCDC 710132**. (Obtained from $CDCl_3$): $C_{16}H_{12}N_2$, M = 232.28, space group: $C2/c$ (monoclinic), a = 15.681(1) Å, b =10.8157(9) Å, c = 15.085(1) Å, β = 118.174(4)°, V = 2255.3(3) Å^3, Z = 8, μ(Mo $K\alpha$) = 0.0818 mm^{-1}, Dx = 1.368 g cm^{-3}, $2\theta_{(max)}$ = 50°, T = 160 K, 16289 measured reflections, 1999 independent reflections, 1251 reflections with $I > 2\sigma(I)$, refinement on F^2 with SHELXL97, 165 parameters, $R(F)$ [$I > 2\ \sigma\ (I)$ reflections] = 0.0608,$wR(F^2)$ [all data] = 0.1785, goodness of fit = 1.015, $\Delta\varrho_{max}$ = 0.27 eÅ^{-3}.

Compound 62b·0.5CH$_3$CN, **CCDC 710121**. (Obtained from hexane/ acetonitrile):

$C_{19}H1_{7.5}N_{2.5}$, M = 280.86, space group: *Fddd* (orthorhombic), a = 13.9453(4) Å, b = 25.7283(5) Å, c = 31.5668(7) Å, V = 11325.8(5) Å^3, Z = 32, μ(Mo $K\alpha$)= 0.0786 mm^{-1}, Dx = 1.318 g cm^{-3}, $2\theta_{(max)}$ = 50°, T = 260 K, 36810 measured reflections, 2505 independent reflections, 1612 with $I > 2\sigma(I)$, refinement on F^2 with SHELXL97, 214 parameters, $R(F)$ [$I > 2\sigma(I)$ reflections] = 0.0559, $wR(F^2)$ [all data] = 0.1748, goodness of fit = 1.014, $\Delta\varrho_{max}$ = 0.23 eÅ^{-3}. The unit cell contains eight cavities of 105 Å^3 that are occupied by highly disordered solvent molecules. The *SQUEEZE* routine of the *PLATON* program did not produce any improvement in the refinement results, so was not employed, but the electron count per unit cell of 431 e is roughly consistent with two MeCN molecules per cavity, or 0.5 MeCN molecules per polycyclic molecule in the structure. A logical arrangement of atoms in the cavities could not be defined, so the detected residual electron density peaks were assigned arbitrarily to partial occupancy C-atoms and this approximation led to acceptable refinement results for the organic molecule of interest.

Compound 63a, **CCDC 710128**. (Obtained from CH_2Cl_2): $C_{16}H_{12}N_2S_2$, M = 296.40, space group: $P2_1/m$ (monoclinic), a = 5.2259(1) Å, b =18.3970(5) Å, c = 7.1404(2) Å, β = 109.441(2)°, V = 647.33(3) Å^3, Z = 2, μ(Mo $K\alpha$) = 0.400 mm^{-1}, Dx = 1.521 g cm^{-3}, $2\theta_{(max)}$ = 55°, T = 160 K, 14381 measured reflections, 1538 independent reflections, 1273 reflections with $I > 2\sigma(I)$, refinement on F^2 with SHELXL97, 95 parameters, $R(F)$ [$I > 2\sigma(I)$ reflections] = 0.0420, $wR(F^2)$ [all data] = 0.1104, goodness of fit = 1.054, $\Delta\varrho_{max}$ = 0.40 eÅ^{-3}. The molecule possesses crystallographic mirror symmetry about a plane perpendicular to the molecular plane.

Compound 63b, **CCDC 710120**. (Obtained from CH_2Cl_2): $C_{18}H_{16}N_2S_2$, M = 324.46, space group: $P\bar{1}$(triclinic), a = 7.5950(1) Å, b = 10.1858(2) Å, c = 10.5743(2) Å, α = 105.965(1)°, β = 105.306(1)°, γ = 95.0213(9)°, V = 747.20(2) Å^3, Z = 2, μ(Mo $K\alpha$) = 0.353 mm^{-1}, Dx = 1.442 g cm^{-3}, $2\theta_{(max)}$ = 60°, T = 160 K, 21179 measured reflections, 4352 independent reflections, 3454 reflections with $I > 2\sigma(I)$, refinement on F^2 with SHELXL97, 203 parameters, $R(F)$ [$I > 2\sigma(I)$ reflections] = 0.0563, $wR(F^2)$ [all data] = 0.1515, goodness of fit = 1.037, $\Delta\varrho_{max}$ = 0.58 eÅ^{-3}.

Compound 64a, **CCDC 710127**. (Obtained from CH_2Cl_2): $C_{28}H_{18}C_{l2}N_2$, M = 453.37, space group: $P\bar{1}$ (triclinic), a = 9.5615(2) Å, b =9.9958(3) Å, c=12.9420(3) Å, a =

85.621(1)◦, b = 72.671(1)°, g = 62.302(1)°, V = 1042.65(5) Å^3, Z = 2, μ(Mo $K\alpha$) = 0.331 mm^{-1}, Dx = 1.444 g cm^{-3}, $2\theta_{(max)}$ = 60°, T = 160 K, 26889 measured reflections, 6052 independent reflections, 4975 reflections with $I > 2\sigma(I)$, refinement on F^2 with SHELXL97, 289 parameters, $R(F)$ [$I>2\sigma(I)$ reflections] = 0.0742, $wR(F^2)$ [all data] = 0.2015, goodness of fit = 1.085, $\Delta\varrho_{max}$ = 0.80 eÅ^{-3}.

Compound 82, **CCDC 713714**. (Obtained from CH_2Cl_2): $C_{12}H_6Br_2$, M =309.99, space group: $P2_1/c$ (monoclinic), a = 7.8327(2) Å, b =19.1058(4) Å, c = 6.8699(2) Å, b = 105.770(1) Å, V = 989.39(4) Å^3, Z = 4, μ(Mo $K\alpha$) = 8.167 mm^{-1}, Dx = 2.081 g cm^{-3}, $2\theta_{(max)}$ = 60°, T = 160 K, 22044 measured reflections, 2893 independent reflections, 2315 reflections with $I > 2\sigma(I)$, refinement on F^2 with SHELXL97, 128 parameters, $R(F)$ [$I >2\sigma(I)$ reflections] = 0.0402, $wR(F^2)$ [all data] = 0.1004, goodness of fit = 1.086, $\Delta\varrho_{max}$ = 0.89 eÅ^{-3}.

3.8 References

1. a) Tsefrikas, V.; Scott, L. *Chem. Rev.* **2006**, *106*, 4868-4884; b) Wu, Y-T.; Siegel, J. S. *Chem. Rev.* **2006**, *106*, 4843-4867.
2. Vostrowsky, O.; Hirsch, A. *Chem. Rev.* **2006**, *106*, 5191-5207.
3. a) Sastry, G. N. *Theochem* **2006**, *771*, 141-147; b) Sastry, G. N.; Rao, H. S. P.; Bednarek, P.; Priyakumar, U. D. *Chem. Commun.* **2000**, 843.
4. Bratcher M. S. Dissertation, Boston College, Chestnut Hill MA, **1996**.
5. Scott, L. T. *Angew. Chem.* **2004**, *116*, 5102-5116.
6. Tsefrikas, V. M.; Arns, S.; Merner, P. M.; Warford, C. C.; Merner, B. L.; Scott, L. T.; Bodwell, G. *Org. Lett.* **2006**, *8*, 5195-5198.
7. Rahanyan, N.; Linden, A.; Baldridge, K. K.; Siegel, J. S. *Org. Biomol. Chem.* **2009**, *7*, 2082-2092.
8. a) Schönberg, A.; Latif, N. *J. Chem. Soc.* **1952**, 446; *b*) Tucker, H. *J. Chem. Soc.* **1958**, 1462; *c*) Morrison, D. *J. Org. Chem.* **1960**, *25*, 1665.
9. *a*) For a previous synthesis of **53a**, see: Sasaki, T.; Kanematsu K.; Hiramatsu, T. *J. Chem. Soc., Perkin Trans. 1* **1974**, *11*, 1213; *b*) For synthesis of the related bromophenyl derivative, see ref. 6.
10. *a*) Wittig, G.; Reppe H.; Eicher, T. *Liebings Ann. Chem.* **1961**, *643*, 47; *b*) Belliard P.; Marechal, E. *Bull. Chem. Soc. France* **1972**, *11*, 4255.
11. For a previous synthesis of **59a,** see: *a*) Pozharskii, A.; Ozeryanskii, V. *Russ. Chem. Bull.* **2003**, *52*, 218; b) Ghedini, M.; Neve, F.; Bruno, M. *Inorg. Chim. Acta* **1988**, *143*, 89.
12. a) Borchard, A.; Hardcastle, K.; Gantzel, P.; Siegel, J. S. *Tetrahedron Lett.* **1999**, *121*, 7804-7813; b) Seiders, T. J.; Elliot, E. L.; Grube, G. H.; Siegel, J. S. *J. Am. Chem. Soc.* **1999**, *121*, 7804-7813.
13. Reisch, H. A.; Bratcher, M. S.; Scott, L. *Org. Lett.* **2000**, *2*, 1427.
14. Zimmermann, K.; Haenel, M. *Synlett* **1997**, *5*, 609-611.
15. Collet, F.; Dodd, R. H.; Dauban, P. *Chem. Comm.* **2009**, 5061.
16. a) Tsang, W. C. P.; Zheng, N.; Buchwald, S. L. *J. Am. Chem. Soc.* **2005**, *127*, 14560-14561; b) Thu, H-Y.; Yu, W-Y.; Che, C-M. *J. Am. Chem. Soc.* **2006**, *128*, 9048.

17. a) Kashino, S.; Zacharias, D.; Peck, R.; Glusker, J.; Bhatt, T.; Coombs, M. *Cancer Res*. **1986**, *46*, 1817; *b*) Weis, L.; Rummel, A.; Masten, S.; Trosko, J.; Upham, B. *Env*. *Health Persp*. **1998**, *106*, 17; *c*) Troche, K. S.; Braga, S. F.; Coluci, V. R.; Galvao, D. S. *Int*. *J*. *Quantum Chem*. **2005**, *103*, 718; *d*) Prout, K.; Smith, A.; Daub, G.; Zacharias, D.; Glusker, J. *Carcinogenesis*, **1992**, *13*, 1775.
18. Cozzi, F.; Sjöstrand, U.; Mislow, K. *J*. *Organomet*. *Chem*. **1979**, *174*, C1.
19. a) Blount, J.; Cozzi, F.; Damewood, J.; Iroff, L.; Sjöstrand, U.; Mislow, K.; *J*. *Am*. *Chem*. *Soc*. **1980**, *102*, 99; b) Wolf, C.; Ghebremariam, B. *Tetrahedron: Asymmetry*, **2002**, *13*, 1153; *c*) Wolf, C.; Ghebremariam, B. *Synthesis*, **2002**, *6*, 749; d) Imashiro, F.; Takegoshi, K.; Saika, A.; Taira, Z.; Asahi, Y. *J*. *Am*. *Chem*. *Soc*. **1985**, *107*, 2341.
20. a) Franck, R.; Leser, E. *J*. *Am*. *Chem*. *Soc*, **1969**, *91*, 1577; b) Franck, F.; Leser, E. *J*. *Org*. *Chem*. **1970**, *35*, 3932; *c*) Anderson, J.; Franck, R.; Mandella, W. *J*. *Am*. *Chem*. *Soc*. **1972**, *94*, 4608; d) Handal, J.; White, J.; Franck, R.; Yuh, Y.; Allinger, N. *J*. *Am*. *Chem*. *Soc*. **1979***, 101,* 5654.
21. Seyferth, D.; Vick, S. *J*. *Organomet*. *Chem*. **1977***, 141,* 173.
22. *a*) Clough, R.; Roberts, J. *J*. *Am*. *Chem*. *Soc*. **1976**, *98*, 1018; b) Evrard, P.; Piret, P.; van Meerssche, M. *Acta Crystallogr*. *Sect*. *B* **1972**, *28*, 497; c) Ogilvie, R. Ph.D Thesis, Massachusetts Institute of Technology, **1971**; *d*) Clough, R.; Marsh, W.; Roberts, J. *J*. *Org*. *Chem*. **1976**, *41*, 3603.
23. Cozzi, F.; Cinquini, M.; Annunziata, R.; Dwyer, T.; Siegel, J. S. *J*. *Am*. *Chem*. *Soc*. **1992**, *114*, 5729.
24. Neuman, M. *J*. *Am*. *Chem*. *Soc*. **1940**, *62*, 2295.
25. *a*) Armstrong, R.; Ammon, H.; Darnow, J. *J*. *Am*. *Chem*. *Soc*. **1987**, *109,* 2077; b) Newman, M.; Hussey, A. *J*. *Am*. *Chem*. *Soc*. **1947**, *69*, 3023; *c*) Kitaigorodsky, A.; Dashevsky, V. *Tetrahedron*, **1968**, *24*, 5917.
26. Borchardt, A.; Hardcastle, K.; Gantzel, P.; Siegel, J. *Tetrahedron Lett*. **1993***, 34,* 273.
27. *Gaussian 03, Revision A.6*, Gaussian, Inc., Wallingford CA, **1998**.
28. Zhao, Y.; Truhlar, D. *Theor*. *Chem*. *Acccts*. **2008**, *120*, 215.
29. Dunning, T. *J*. *Chem*. *Phys*. **1989**, *90*, 1007.

30. Baldridge, K.; Greenberg, J. *Mol. Graphics*, **1995**, *13*, 63.
31. Spek, A.; *PLATON, Program for the Analysis of Molecular Geometry*, University of Utrecht, The Netherlands **2007**.
32. a) Strekowski, L.; Wydra, R. L.; Janda, L.; Harden, D. *J. Org. Chem.* **1991**, *56*, 5610-5614; b) Bedel, S.; Ulrich, G.; Picard, C. *Tetrahedron Lett.* **2002**, *43*, 1697-1700; c) Laval, S. G.; Tu, S-M.; Jiang, D.; Robinson, C. L.; Scott, R.; Golding, B. T. *Synthesis* **2009**, *11*, 1807-1810.
33. Sygula, A.; Rabideau, P. W. *J. Am. Chem. Soc.* **2000**, *122,* 6323-6324.
34. Steck, E. A.; Hallock, L. L.; Holland, A. J. *J. Am. Chem. Soc.* **1946**, *68,* 129-132.
35. Conrand, M.; Limpach, L. *Ber.* **1887**, *20*, 944.
36. a) Manske, R. H. *Chem. Rev.* **1942**, *30*, 113; b) Reitsema, R. H. *Chem. Rev.* **1948**, *43*, 43.
37. Margolis, B.; Long, K. A.; Laird, D. L. T.; Ruble, J. C.; Pulley, S. R. *J. Org. Chem.* **2007**, *72*, 2232-2235.
38. Schaap, A.; Brandsma, L.; Arens, J. F. *Recueil des Travaux Chimiques des Pays-Bas* **1965**, *84*, 1200-1202.
39. Seiders, T. J.; Elliott, E. L.; Grube, G. H.; Siegel, J. S. *J. Am. Chem. Soc.* **1999**, *121*, 7804-7813.
40. Minter, D. E.; Re, M. A. *J. Org. Chem.* **1988**, *53*, 2653-2655.
41. Arnold, N. J. et al. *Bioorg. Med. Chem. Lett.* **2002**, *12*, 1973.
42. a) Francis, J. E.; Gorczyca, L. A.; Mazzenga, G. C.; Meckler, H. *Tetrahedron Lett.* **1987**, *28*, 5133; b) Haddadin, M. J.; Ghazvini Zadeh, E. H. *Tetrahedron Lett.* **2010**, *51*, 1654-1656.
43. Patra, S.; Sarkar, B.; Maji, S.; Fiedler, J.; Urbanos, F. A.; Jimenez-Aparicio, R.; Kaim, W.; Lahiri, G. K. *Chem. Eur. J.* **2006**, *12*, 489-498.
44. a) Suen, Y. F.; Hope, H.; Nantz, M. H.; H, M. J.; Kurth, M. J. *J. Org. Chem.* **2005**, *70*, 8468-8471; b) Robins, L. I.; Carpenter, R. D.; Fettinger, J. C.; Haddadin, M. J.; Tinti, D. S.; Kurth, M. J. *J. Org. Chem.* **2006**, *71*, 2480-2485.
45. Nhu, D.; Duffy, S.; Avery, V. M.; Hughes, A.; Baell, J. B. *Bioorg. Med. Chem. Lett.* **2010**, *20*, 4496-4498.

46. a) Wu, C-Y.; Chen, Y.; Jing, S. Y.; Lee, C-S.; Dinda, J.; Hwang, W-S. *Polyhedron* **2006**, *25*, 3053-3065; b) Audebert, P.; Sadki, S.; Miomandre, F.; Clavier, G.; Claude V. M.; Saoud, M.; Hapiot, P. *New J. Chem.* **2004**, *28*, 387-392.
47. Tsiulin, P. A.; Sosnina, V. V.; Krasovskaya, G. G.; Kofanov, E. R. *Izvestiya Vysshikh Uchebnykh Zavedenii, Khimiya i Khimicheskaya Tekhnologiya* **2008**, *51*, 13-15.
48. a) Suen, Y. F.; Hope, H.; Nantz, M. H.; Haddadin, M. J.; Kurth, M. J. *J. Org. Chem.* **2005**, *70*, 8468-8471; b) Bakkali, H. *et al. Eur. J. Org. Chem.* **2008**, *12*, 2156-2166.
49. Boger, D. L.; Coleman, R. S.; Panek, J. S.; Huber, F. X.; Sauer, J. *J. Org. Chem.* **1985**, *50*, 5377-5379.
50. Curtius, T.; Darapsky, A.; Muller, E. *Ber. Deutsch. Chem. Ges.* **1907**, *39*, 3410-3437.
51. a) Skorianetz, W.; Kovats, E. *Helvetica Chim. Acta* **1971**, *54*, 1922-39; b) Carboni, R. A.; Lindsey, R. V. *J. Am. Chem. Soc.* **1959**, *81*, 4342-4346.
52. a) Sandström, J. *Acta Chem. Scand.* **1961**, *15*, 1575-1582; b) Dobrov, A.; Arion, V. B.; Shova, S.; Roller, A.; Rentschler, E.; Keppler, B. K. *Eur. J. Inorg. Chem.* **2008**, *26*, 4140-4145.
53. Rao, G-W.; Hu, W-X. Bioorg. *Med. Chem. Lett.* **2006**, *16*, 3702-3705.
54. Hooft, R. *Kappa CCD Collect Software*, Nonius BV, Delft, The Netherlands **1999**.
55. Sheldrick, G. M. *Acta Crystallogr. Sect. A* **2008**, *64*, 112.
56. Spek, A. *PLATON, Program for the Analysis of Molecular Geometry*, University of Utrecht, The Netherlands, **2007**.
57. von der Sluis, P.; Spek, A. *Acta Crystallogr.* **1990**, *A46*, 194.

Chapter 4. Progress towards Thiacorannulenes

4.1 Targets and retrosynthetic analysis

In the previous chapter, various synthetic routes to the nitrogen-substituted corannulenes were discussed. The following section will be dedicated to sulfur-containing heterocorannulenes, with 1,6-dithiacorannulenes (**106**, **107**) as synthetic targets (Figure 4.1). Intriguing molecular architectures of these compounds, possessing bowl-like structures, make these molecules highly attractive targets of study with regard to physicochemical and stereodynamic properties. Dithiacorannulenes as well as triphenylenotrithiophene **42** (first non-planar heteroaromatic), could form a basis for novel organic conductors.[1,2]

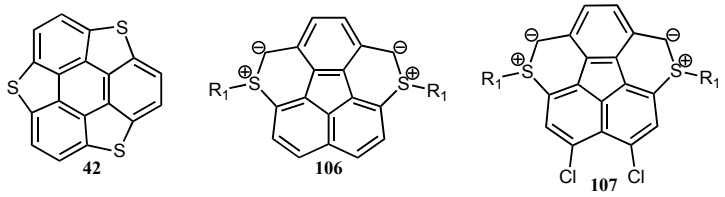

Figure 4.1 Structure of triphenylenotrithiophene **42** and target 1,6-dithiacorannulenes (**106**, **107**)

The retrosynthetic pathway to **106**, **107** proceeds via construction 1,6-dithia-1,2,5,6-tetrahydrocorannulenes (**108**, **109** Scheme 4.1). Opening the six-membered rings across the bay region in the fluoranthene skeleton of **108** and **109** reveals the corresponding thiols, which have been synthesize from **110**, **111** via displacement of benzylic bromines by thioacetate groups. Construction of a fluoranthene framework was accomplished according to classical methods, described in literature.[3]

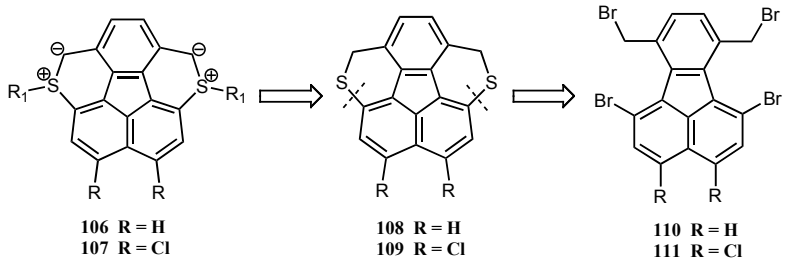

Scheme 4.1 Retrosynthesis of 1,6-disubstituted corannulenes

4.2 Synthesis

Synthetic routes to the 1,6-dithiacorannulenes proceed via construction of 1,6-dibromo-7,10-bis(bromomethyl)fluoranthene (**110)** and 1,6-dibromo-7,10-bis(bromomethyl)-3,4-dichlorofluoranthene (**111**), key intermediates in this synthesis (Scheme 4.2). These compounds were synthesized via condensation of corresponding acenaphthaquinones (**112, 113**) with 3-pentanone in methanolic potassium hydroxide to construct the cyclopentadienone intermediate.[3] The cyclopentadienone, generated in acetic anhydride was then trapped by a Diels-Alder reaction with norbornadiene. A cascade of retrocycloadditions followed to release cyclopentadiene and carbon monoxide afforded fluoranthenes **114**, **115**. Further bromination of **114**, **115** with *N*-bromosuccinimide (NBS) under irradiation with light formed **110** and **111**. Introduction of sulfur atoms was carried out via replacement of benzylic bromines in **110**, **111** by thioacetate groups, and followed intramolecular Cu-catalyzed nucleophilic substitution gave **108**, **109** in a moderate yield (Scheme 4.2).[4]

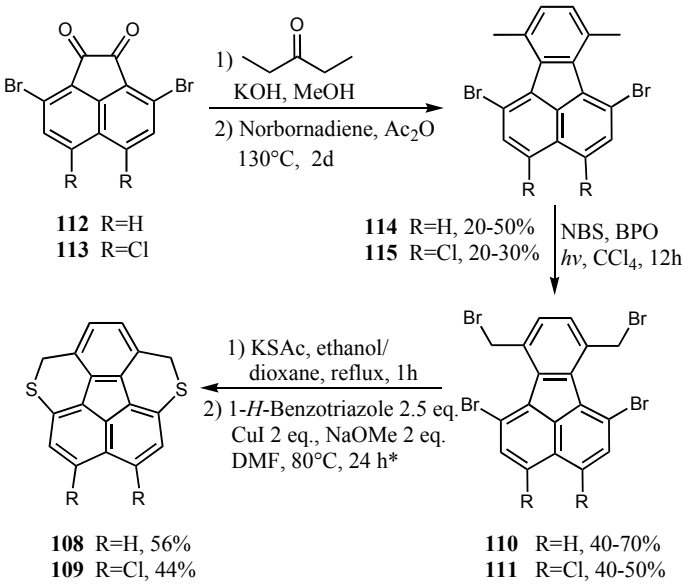

Scheme 4.2 Synthesis of 1,6-dithia-1,2,5,6-tetrahydrocorannulenes

Attempts to close the ring in **110**, **111** in one step by displacement of the bromines with sodium sulfide failed. Only formation of an insoluble material was

detected. The same undesired results were achieved when the reaction took place stepwise. The first step, introduction of thioacetate groups was carried out in a refluxing ethanol/dioxane solution (1h) yielding 84-90% and 99% of the corresponding thiols. However, the following attempted ring closure reaction with sodium methoxide in methanol gave the same insoluble product.

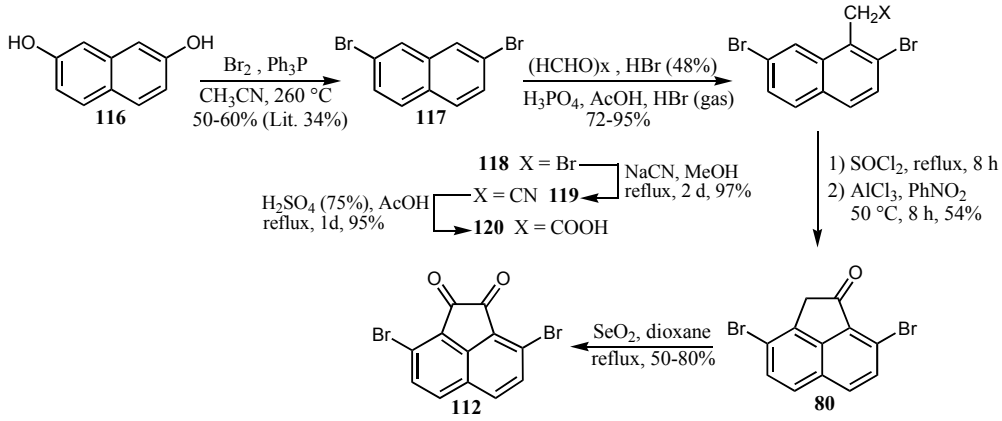

Scheme 4.3 Synthesis of 3,8-dibromoacenaphthaquinone **112**

Synthesis of diketones **112**, **113** is known and was previously reported. The former comes from 2,7-dihydroxynaphthalene in 6 steps (Scheme 4.3),[5] whereas the latter from acenaphthene in 3 steps (Scheme 4.4).[3]

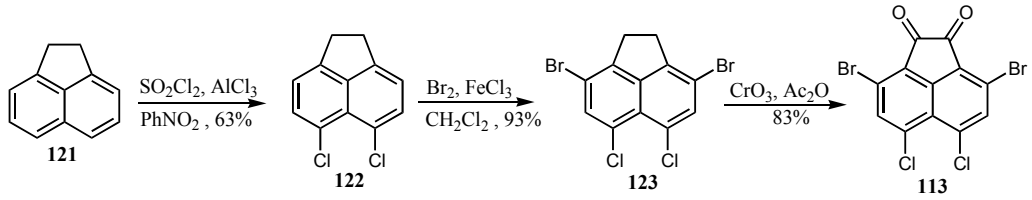

Scheme 4.4 Synthesis of 5,6-dichloro-3,8-dibromoacenaphthaquinone **113**

To probe the reactivity of the bromine atoms on the acenaphthylene ring in **110**, **111** 1,6-dibromo-7,10-dimethylfluoranthene **114** has been used as a model compound (Scheme 4.5). Reactions of **114** with six different substrates have shown modest to excellent yields of desired products. In the case of the copper-catalyzed amidation reaction[6] (**124g**), only monosubstitution followed by concomitant reduction of the second

bromine was observed; 7,10-dimethylfluoranthene was formed as a by-product. The yield of the desired product in **124f** is only 4-9% and 25% of monosubstitution (**124f'**). In contrast to the **124f**-**g** the reaction of **114** with sodium azide and three different thiols occur easily using milder reaction conditions.

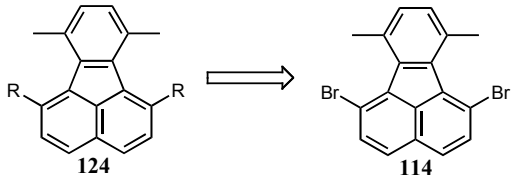

124 **114**

124a R= PhS, 99%
124b R= BnS, 85%
124c R= *i*-C_3H_7S, 97%
124d R=N_3, 65%
124f R=SCN 4-9%, 25% monosubst. (**124f'**)
124g R=NHCOPh 11-18% monosubst.*

Scheme 4.5 Reactivity of 1,6-dibromo-7,10-dimethylfluoranthene **114**
*Only monosubstitution followed by concomitant reduction of the second bromine was observed

Nucleophilic substitution of the benzylic bromines in **111** with different groups produced **125a-f (**Scheme 4.6), attractive intermediates for the synthesis of heterocorannulenes. Reduction of **125f** to the diamine followed by Pd catalyzed aromatic amination reaction would be an alternative way towards the aim of preparing 1,6-diazacorannulene.

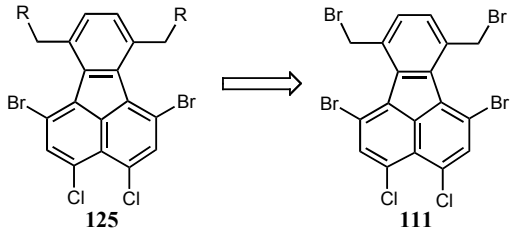

125 **111**

125a* R=SAc, 84-90%
125b R=SAc, 99%
125c R=SCN, 45%
125d R=SeCN, 77%
125f R=N_3, 35%

Scheme 4.6 Reactivity of 1,6-dibromo-7,10-bis(bromomethyl)-3,4-dichlorofluoranthene
*Compound **125a** was synthesized from 1,6-dibromo-7,10-bis(bromomethyl)fluoranthene

4.3 Structures and properties

The structures of 1,6-dithia-1,2,5,6-tetrahydrocorannulenes (**108)** and 1,6-diaza-1,2,5,6-tetrahydrocorannulenes (**126)** are similar to 1,2,5,6-tetrahydrocorannulene (**127)**

(Figure 4.1). Compound **127** was isolated as a by-product in the high-temperature corannulene synthesis.[7] In the ground-state bowl conformation of **127**, the geminal hydrogens are diastereotopic with an exo/endo relationship. Thus, variable-temperature NMR studies allows for measurement of the barrier to bowl inversion. Thus for **127,** the measured value was previously reported as 6.6 kcal/mol[7] and as presented in this work, calculated data is 6.6 kcal/mol. Calculated value for **108** and **126** are 3.4 kcal/mol and 16.9 kcal/mol.

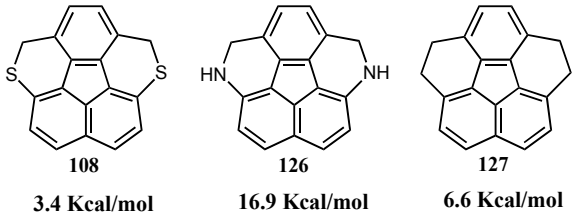

Figure 4.2 Inversion barrier in 1,6-dithia-1,2,5,6-tetrahydrocorannulene **108** and related compounds

Theoretical calculations of relative energies for the possible structural conformations of **108**, **109** and **106**, **107** (Figure 4.3) are presented in Figure 4.4. Calculated data shows that 1,6-dithia-1,2,5,6-tetrahydrocorannulenes have the lowest energy conformation of these structures (with either R = Cl or R = H). In the conformation of **106** with R = R_1= H, the *trans* relationship of two hydrogens is energetically preferable (by 32.3 kcal/mol with **107** R = Cl, and 32.7 kcal/mol with **106** R= H). The R groups (Cl or H) in this case does not seem to have a great effect.

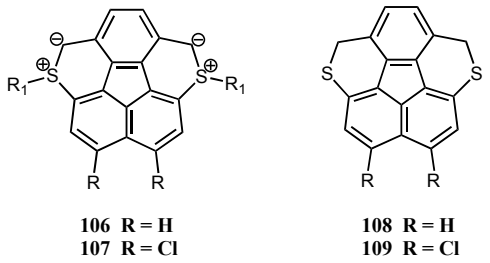

Figure 4.3 Structures of 1,6-dithiacorannulenes **106**, **107** and 1,6-dithia-1,2,5,6-tetrahydrocorannulenes **108**, **109**

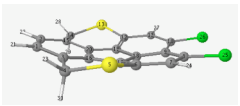

109 R = Cl
S-CH_2
0.0 kcal/mol

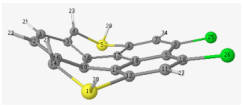

107 R = Cl, R_1= H
$^{+}$SH-CH^{-} - *cis*
107.6 kcal/mol

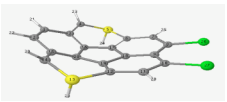

107 R = Cl, R_1 = H
$^{+}$SH-CH^{-} - *trans*
138.3 kcal/mol

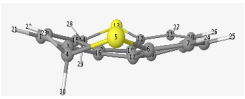

108 R = H
S-CH_2
0.0 kcal/mol

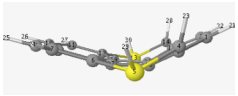

106 R = R_1 = H
$^{+}$SH-CH^{-} - *cis*
138.0 kcal/mol

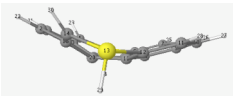

106 R = R_1 = H
$^{+}$SH-CH^{-} - *trans*
106.8 kcal/mol

Figure 4.4 M06-2X/TZVP Relative Energies for possible conformations of structures **107** – **109**

The electronic absorption spectra of 1,6-dithia-1,2,5,6-tetrahydrocorannulene **108** and 8,9-dichloro-1,6-dithia-1,2,5,6-tetrahydrocorannulene **109** in CH_2Cl_2 (Figure 4.5) show a long-wavelength vibration α-band at λ_{max}= 400 nm (ε = 7.6) for **108** and λ_{max}= 404 nm (ε = 4.8) for **109**. Two additional bands are centered at λ_{max}= 285 nm (12.6), λ_{max}= 252 nm (20.8) (**108**), and λ_{max}= 290 nm (8.8), λ_{max}= 257 nm (14.4) (**109**). The entire spectra for both compounds look similar with an exception of an additional *p*-band in **108** at λ_{max}= 318 nm (ε = 4.9).

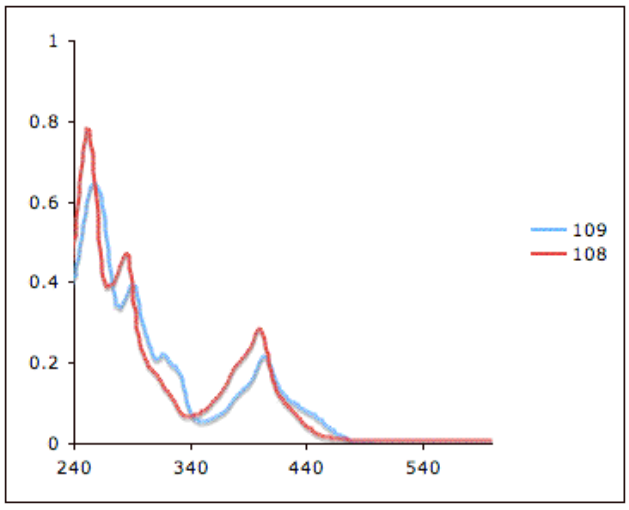

Figure 4.5 The electronic absoption spectra of 1,6-dithia-1,2,5,6-tetrahydrocorannulene **108** and 8,9-dichloro-1,6-dithia-1,2,5,6-tetrahydrocorannulene **109**

4.4 Computational methods

The conformational analyses of the molecular systems described in this study were carried out with a special module of Gaussian 03[8] software package provided by D. Truhlar,[9] enabling the use of the M06-2X[10] DFT functional. The triple-z basis set, TZVP basis set,[11,12] was employed for all computations. Full geometry optimizations were performed and uniquely characterized via second derivatives (Hessian) analysis to determine the number of imaginary frequencies (0 = minima; 1 = transition state). Structural and property analysis was carried out using QMView[13] and WebMO.[14]

4.5 Future work

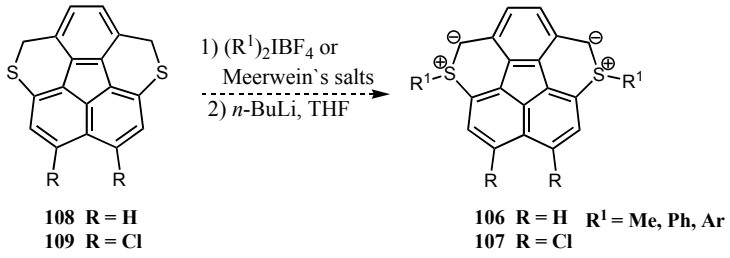

Scheme 4.7 Synthetic route to the sulfur ylides

Full aromatization of **108, 109** (via construction of sulfur ylides) will be required to complete the synthesis of desired 1,6-dithiacorannulenes (**106**, **107**). Ylide functionalization can be achieved by reaction **108, 109** with Meerwein salts[15] or diphenyliodonium tetrafluoroborate, and further deprotonation with a strong base, usually an alkyllithium reagent (Scheme 4.7).[16]

4.6 Conclusion

In this work, the synthetic route to the 1,6-disubstituted heterocorannulenes has been investigated. 1,6-dithia-1,2,5,6-tetrahydrocorannulene and 1,6-dithia-8,9-dichloro-1,2,5,6-tetrahydrocorannulene have been synthesized in moderate yield using intramolecular copper-catalyzed C-S coupling reactions. Full aromatization of **108, 109** could be observed by synthesis of sulfur ylids (**106**, **107**). Studies on the scope of these reactions are currently underway in our laboratory. Relative energy calculations for possible conformations of **106**-**109** have shown structures **108, 109** to be energetically preferable.

4.7 Experimental Section

1,6-dithia-1,2,5,6-tetrahydrocorannulene (108)

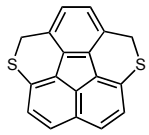

A mixture of 1,6-dibromo-7,10-bis(bromomethyl)fluoranthene (0.05 g, 0.09 mmol), and potassium thioacetate (0.021 g, 0.183 mmol) in DMF (4 mL) was stirred at -20 °C for 1 h and then allowed to warm to room temperature. This mixture was added to a Cu / benzothiazole complex in DMF (1 mL), previously prepared in a flame-dried separate reaction vessel by stirring CuI (0.035 g, 0.183 mmol) and 1H-benzothiazole (0.022 g, 0.183 mmol) at room temperature for 10 min. This reaction was stirred for 30 min, and sodium methoxide (0.01 g, 0.183 mmol) was added. The mixture was heated to 80 °C and stirred for 1 d. The solvent was evaporated, the residue was purified by column chromatography (silica gel, hexane) to yield of yellow solid (0.015 g, 56%). IR (KBr): 3051*w*, 2961*m*, 2924*m*, 2904*m*, 2853*m*, 1888*w*, 1681*w*, 1623*w*, 1605*s*, 1456*m*, 1423*s*, 1411*s*, 1395*m*, 1261*s*, 1214*m*, 1135*s*, 1123*s*, 1093*s*, 1021*s*, 939*m*, 883*m*, 822*s*, 801*s*, 777*m*, 770*m*, 747*m*, 672*m*, 650*s*, 608*m*, 571*m*, 544*w*, 527*w*, 489*w*, 472*w*, 444*m*; ^{1}H-NMR (500 MHz, DMSO-d_6) δ 7.74 (d, 1H, ^{3}J = 8.5 Hz), 7.24 (d, 1H, ^{3}J = 8.5 Hz), 7.18 (s, 1H), 4.72 (s, 2H); ^{13}C-NMR (400 MHz, DMSO-d_6) δ 133.8, 133.7, 132.4, 131.1, 129.9, 127.3, 127.1, 123.0, 120.1, 32.8; MS (EI) m/z (%): 290.1 (M^+, 100), 244.1 (26), 144.0 ($(M-2H)^{2+}$, 28%); HRMS (EI) [M-2H fragment] calcd. for $C_{18}H_8S_2$: 288.0067; found: 288.0065; mp 200 °C decomp.

S-(6-bromo-2*H*-fluoreno[1,9,8-*cdef*]thiochromen-5-yl)-methyl ethanethioate (108′)

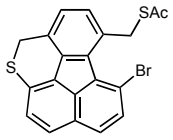

IR (KBr): 3338*w*, 3004*w*, 2918*m*, 2850*m*, 1888*w*, 1676*s*, 1629*s*, 1559*m*, 1467*m*, 1433*m*, 1421*m*, 1413*m*, 1353*m*, 1332*m*, 1259*w*, 1224*w*, 1197*w*, 1136*s*, 1108*m*, 1086*s*, 1028*m*, 996*m*, 965*m*, 922*m*, 885*w*, 830*s*, 811*m*, 785*m*, 756*w*, 721*w*, 640*m*, 633*m*, 580*w*, 533*m*, 521*w*, 489*w*; ^{1}H-NMR (600 MHz, DMSO-d_6) δ 7.84 (d, 1H, ^{3}J = 8.4 Hz), 7.82 (d, 1H, ^{3}J = 9.0 Hz), 7.73 (d, 1H, ^{3}J = 8.4 Hz), 7.43 (d, 1H, ^{3}J = 8.4 Hz), 7.32 (d, 1H, ^{3}J = 7.8 Hz), 7.22 (d, 1H, ^{3}J = 7.8 Hz), 4.88 (s, 2H), 4.65 (s, 2H), 2.33 (s, 3H); ^{13}C-NMR (600 MHz, DMSO-d_6) δ 194.5, 135.4, 135.2, 133.5, 133.4, 132.8, 132.4, 132.2, 130.9, 129.6, 128.7, 127.5, 127.2, 126.1, 124.9, 123.4, 118.9, 34.5, 30.3; MS (EI) m/z (%): 414.1 (M^+, 42), 339.0 (100), 323.0 (9), 289.1 (17), 258.1

(57), 245.1 (16%); HRMS (EI) calcd. for $C_{20}H_{13}BrOS_2$: 411.9591; found: 411.9595; mp 150 °C decomp.

8,9-dichloro-1,6-dithia-1,2,5,6-tetrahydrocorannulene (109)

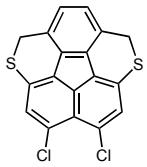

A mixture of CuI (0.05 g, 0.26 mmol) and 1H-benzothiazole (0.031 g, 0.26 mmol) in DMSO (5 mL) were stirred for 10 min at room temperature in a flame-dried two-neck flask. *S*,*S*'-(1,6-dibromo-3,4-dichloro-fluoranthene-7,10-diyl)bis(methylene)diethanethiolate (0.078 g, 0.13 mmol) was added as a solution in DMSO (20 mL) and the mixture was stirred an additional 20 min. Sodium methoxide (0.028 g, 0.52 mmol) was added and the reaction was stirred at 80 °C over night, cooled to room temperature, diluted with water (50 mL), and extracted with dichloromethane. The organic phase was separated, dried with magnesium sulfate, and evaporated to yield of yellow solid, which was purified by column chromatography (silica gel, hexane), yielding 0.02g, 44%. IR (KBr): 3068*m*, 2957*s*, 2924*s*, 2853*s*, 1728*s*, 1688*s*, 1569*s*, 1460*s*, 1411*s*, 1377*m*, 1349*m*, 1262*s*, 1183*s*, 1122*s*, 1067*s*, 964*m*, 865*m*, 801*s*, 747*m*, 697*w*, 684*w*, 652*w*, 626*w*, 588*w*, 561*w*, 479*w*; ^{1}H-NMR (400 MHz, $CDCl_3$) δ 7.18 (s, 1H), 7.03 (s, 1H), 4.59 (s, 2H); ^{13}C-NMR (400 MHz, $CDCl_3$) δ134.9, 134.2, 133.1, 132.6, 129.8, 127.3, 125.5, 122.0, 120.5, 33.8; MS (EI) m/z (%): 357.9 (M^+, 100), 321.9 (8), 312.9 (14), 276.9 (10), 243.0 (7), 178.9 ($(M-2H)^{2+}$,9%); HRMS (EI) calcd. for $C_{18}H_8Cl_2S_2$: 357.9444; found: 357.9427; mp 274 °C.

1,6-dibromo-7,10-bis(bromomethyl)fluoranthene (110)

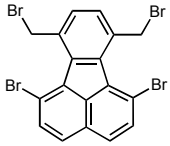

A mixture of 1,6-dibromo-7,10-dimethylfluoranthene (0.5 g, 1.29 mmol), N-bromosuccinimide (NBS) (0.46 g, 2.58 mmol) and dibenzoyl peroxide (BPO) 0.03 g, 0.13 mmol) in CCl_4 (25 mL) was irradiated with incandenscent light and refluxed for 12 h. The solvent was evaporated, the residue was purified by column chromatography (silica gel, hexane) to yield of yellow solid (0.32 g, 46%). IR (KBr): 3062*m*, 2958*w*, 2924*w*, 2106*w*, 1896*w*, 1733*w*, 1641*w*, 1593*s*, 1559*w*, 1472*s*, 1442*w*, 1425*m*, 1410*s*, 1337*m*, 1251*w*, 1204*m*, 1190*w*, 1145*s*, 1105*m*, 1184*s*, 954*w*, 895*w*, 834*s*, 782*s*, 746*m*, 701*m*, 685*m*, 679*s*, 658*m*, 639*s*, 619*m*, 607*s*, 567*w*, 553*m*, 527*s*, 506*w*, 478*w*, 440*w*; ^{1}H-NMR (400 MHz, $CDCl_3$) δ 7.82 (d, 1H, ^{3}J = 8.8 Hz),

7.67 (d, 1H, ^{3}J = 8.8 Hz), 7.62 (s, 1H), 5.35 (s, 2H); ^{13}C-NMR (400 MHz, $CDCl_3$) δ 137.6, 136.6, 135.4, 134.8, 133.6, 133.0, 128.8, 127.5, 118.5, 35.8; MS (EI) m/z (%): 545,7 (M^+, 11), 464.8 (93), 385.8 (85), 306 (11), 226 (100), 113 (84 %); HRMS (EI) [M-H fragment] calcd. for $C_{18}H_9Br$: 540.7438; found: 540.7426; mp 163-165 °C.

1,6-dibromo-7,10-bis(bromomethyl)-3,4-dichlorofluoranthene (111)

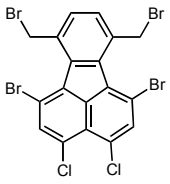

A mixture of 1,6-dibromo-3,4-dichloro-7,10-dimethylfluoranthene (1.5 g, 3.28 mmol), N-bromosuccinimide (NBS) (1.17 g, 6.57 mmol) and azobisisobutyronitrile (AIBN) (0.05 g, 0.33 mmol) in benzene (50mL) was refluxed for 8 h. The solvent was evaporated, the residue was purified by column chromatography (silica gel, hexane) to yield of yellow solid (0.3g, 43%). IR (KBr): 3046*m*, 3023*w*, 2955*m*, 2923*s*, 2852*m*, 1898*w*, 1761*w*, 1714*w*, 1636*w*, 1569*s*, 1557*s*, 1457*s*, 1426*m*, 1396*s*, 1342*m*, 1300*w*, 1245*m*, 1209*m*, 1195*m*, 1119*s*, 1038*s*, 1009*s*, 893*m*, 884*s*, 858*s*, 844*m*, 814*m*, 790*m*, 774*m*, 707*m*, 688*m*, 679*m*, 662*w*, 627*s*, 556*m*, 522*s*, 503*w*, 488*w*, 474*m*; ^{1}H-NMR (500 MHz, $CDCl_3$) δ 7.92 (s, 1H), 7.62 (s, 1H), 5.23 (s, 2H); ^{13}C-NMR (400 MHz, $CDCl_3$) δ 138.4, 137.1, 136.6, 135.3, 133.5, 133.2, 132.2, 123.1, 118.0, 35.1; MS (EI) m/z (%): 613,7 (M^+, 11), 578.7 (6), 490.8 (11), 453.9 (64), 409.9 (6) 340 (17), 224 (31%); HRMS (EI) calcd. for $C_{18}H_8Br_4Cl_2$: 609.6737; found: 609.6733; mp 220-223 °C.

1,6-dibromo-7,10-dimethylfluoranthene (114)

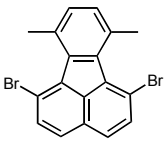

A 20% solution of potassium hydroxide in methanol (10 mL) was added to a solution of 3,8-dibromoacenaphthequinone (2 g, 6 mmol) and 3-penthanone (1 mL) in methanol (50 mL). The solution was stirred at ambient temperature for 1.5 h, diluted with water (50 mL), and neutralized with 10% aqueous hydrochloric acid solution. The precipitate formed was collected by filtration, washed with water, dried and transferred in to 20 mL sealable reaction vessel. 2,5-norbornadiene (3 mL) and acetic anhydride (6 mL) were added and the vessel was sealed and placed in an oil bath at 130 °C for 1.5 d. The mixture was cooled to ambient temperature, diluted with dichloromethane (30 mL), neutralized slowly with 10% aqueous sodium hydroxide and extracted 3 times with water (30 mL). The organic layers

was dried with magnesium sulfate, filtered and evaporated to yield a dark brown solid, which was purified by column chromatography (silica gel, hexane) to yield a yellow crystalline product (1.1 g, 47%). IR (KBr): 3059*w*, 2959*m*, 2923*m*, 2860*m*, 1885*w*, 1717*w*, 1659*w*, 1592*s*, 1553*m*, 1494*w*, 1469*s*, 1454*s*, 1408*s*, 1379*m*, 1332*m*, 1285*m*, 1256*w*, 1218*w*, 1199*m*, 1181*w*, 1148*m*, 1103*m*, 1083*s*, 1051*m*, 1033*m*, 1017*m*, 986*s*, 954*m*, 890*m*, 830*s*, 806*s*, 781*m*, 743*w*, 651*w*, 634*m*, 618*m*, 563*w*, 541*m*, 503*w*, 486*w*; ^{1}H-NMR (500 MHz, $CDCl_3$) δ 7.75 (d, 1H, ^{3}J = 8.5 Hz), 7.56 (d, 1H, ^{3}J = 8.5 Hz), 7.17 (s, 1H), 2.92 (s, 3H, CH_3); ^{13}C-NMR (400 MHz, $CDCl_3$) δ 138.2, 137.0, 136.8, 134.8, 132.7, 131.5, 127.7, 127.4, 116.9, 26.3; MS (EI) m/z (%): 388 (M^+, 100), 309 (12), 226 (47), 213 (13), 200 (7), 113 (54 %); HRMS (EI) calcd. for $C_{18}H_{12}Br_2$: 385.9306; found: 385.9300; mp 190 °C.

1,6-bis(phenylthio)-7,10-dimethylfluoranthene (125a)

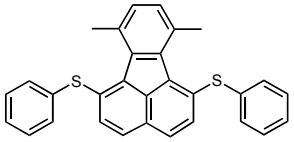

A solution of thiophenol (0.053 mL, 0.52 mmol) in 1,3-dimethyl-2-imidazolidinone (DMEU) was added to the NaH, previously washed with dry cyclohexane. The mixture was stirred at room temperature for 30 min and 1,6-dibromo-7,10-dimethylfluoranthene was added. The reaction was stirred an additional 4 h at RT and 30 min at 100 °C, diluted with water, acidified with HCl, extracted with CH_2Cl_2 and dried with $MgSO_4$. The solvent was evaporated, the residue was purified by column chromatography (silica gel, hexane) to yield of yellow oil (0.057 g, 99%). IR (KBr): 3053*m*, 2956*m*, 2919*s*, 2849*m*, 1943*w*, 1879*w*, 1733*w*, 1580*s*, 1542*m*, 1493*m*, 1474*s*, 1439*s*, 1409*s*, 1386*m*, 1333*m*, 1286*m*, 1258*m*, 1231*m*, 1204*m*, 1177*m*, 1148*m*, 1098*s*, 1082*s*, 1050*m*, 1022*s*, 995*s*, 955*m*, 923*m*, 831*s*, 804*s*, 738*s*, 689*s*, 623*w*, 572*m*, 545*m*, 499*w*, 475*m*, 440*w*; ^{1}H-NMR (400 MHz, CD_2Cl_2) δ 7.56 (d, 1H, ^{3}J=8.4 Hz), 7.39 (d, 1H, ^{3}J=8.4 Hz), 7.33-7.23 (m, 5H), 7.13 (s, 1H), 2.9 (s, 3H); ^{13}C-NMR (400 MHz, CD_2Cl_2) δ 139.2, 138.1, 137.4, 134.9, 133.9, 132.3, 131.8, 131.4, 130.6, 129.8, 128.0, 127.6, 127.3, 25.8; MS (EI) m/z (%): 446.0 (M^+, 100), 431.0 (6), 338.0 (8), 322.0 (8), 259.0 (14), 245.0 (7), 226.0 (11%); HRMS (EI) calcd. for $C_{30}H_{22}S_2$: 446.1163; found 446.1159.

1,6-bis(phenylmethylthio)-7,10-dimethylfluoranthene (125b)

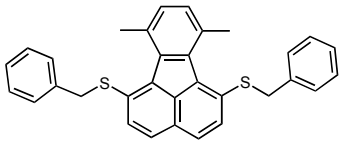

A mixture of 1,6-dibromo-7,10-dimethylfluoranthene (0.05 g, 0.13 mmol) and sodium benzylthiolate (0.08 g, 0.55 mmol) in dry DMF was stirred for 4 h. The red solution was poured into 50 mL of water, acidified with HCl and extracted with dichloromethane. The organic layer were separated and dried with magnesium sulfate. The solvent was evaporated, the residue was purified by column chromatography (silica gel, hexane:ethyl acetate 40 : 1) to yield a yellow oil (0.052 g, 85%). IR (KBr): 3082*w*, 3028*s*, 3004*m*, 2986*m*, 2962*m*, 2927*s*, 2853*m*, 2734*w*, 1939*w*, 1870*w*, 1790*w*, 1734*w*, 1590*s*, 1537*w*, 1494*s*, 1478*s*, 1452*s*, 1408*m*, 1379*m*, 1339*w*, 1287*w*, 1231*w*, 1199*m*, 1156*m*, 1097*s*, 1067*m*, 1053*m*, 1035*m*, 1021*m*, 997*m*, 950*w*, 910*w*, 825*s*, 799*s*, 785*w*, 773*m*, 703*s*, 692*s*, 663*m*, 622*w*, 574w, 544*m*, 502*w*, 479*m*; ^{1}H-NMR (500 MHz, $CDCl_3$) δ 7.62 (d, 1H, ^{3}J = 8.5 Hz), 7.59 (d, 1H, ^{3}J = 8.5 Hz), 7.20-7.18 (m, 5H), 7.14 (s, 1H), 4.09 (s, 2H), 2.86 (s, 3H); ^{13}C-NMR (500 MHz, $CDCl_3$) δ 138.9, 137.6, 137.2, 136.9, 134.5, 131.64, 131.62, 131.1, 129.1, 128.6, 127.6, 127.4, 127.0, 126.4, 40.7, 25.4; MS (EI) m/z (%): 474.0 (M^+, 100), 384.0 (9), 350.0 (6), 290.9 (61), 260.0 (65), 245.0 (26), 213.0 (7), 91.0 (94%); HRMS (EI) calcd. for $C_{32}H_{26}S_2$: 474.1476; found: 474.1474.

1,6-bis(isopropylthio)-7,10-dimethylfluoranthene (125c)

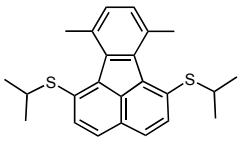

A mixture of 1,6-dibromo-7,10-dimethylfluoranthene (0.05 g, 0.13 mmol) and sodium isopropylthiolate (0.1 g, 1 mmol) in 3 mL of DMF was stirred at room temperature for 3 h. The solvent was evaporated, the residue was purified by column chromatography (silica gel, hexane:ethyl acetate 15:1) to yield of yellow oil, which crystallized on standing (0.095 g, 97%). IR (KBr): 3046*w*, 2977*s*, 2958*s*, 2921*s*, 2859*s*, 1897*w*, 1734*w*, 1670*w*, 1590*s*, 1474*s*, 1439*s*, 1409*s*, 1379*s*, 1317*m*, 1286*m*, 1247*s*, 1209*m*, 1151*s*, 1113*m*, 1092*s*, 1043*s*, 1018*m*, 996*m*, 952*w*, 927*m*, 834*s*, 814*m*, 800*s*, 774*w*, 742*m*, 679*w*, 639*w*, 623*w*, 570*w*, 558*s*, 545*m*, 495*w*, 432*w*; ^{1}H-NMR (400 MHz, acetone-d_6) δ 7.81 (d, 1H, ^{3}J = 8.4 Hz), 7.74 (d, 1H, ^{3}J = 8.4 Hz), 7.18 (s, 1H), 3.55-3.45 (m, 1H), 2.86 (s, 3H), 1.17 (s, 3H), 1.16 (s, 3H); ^{13}C-NMR (500 MHz, CD_2Cl_2) δ 139.3, 137.9, 134.9, 133.3, 131.92, 131.9, 131.6, 127.5,

126.6, 39.9, 25.9, 23.3; MS (EI) m/z (%): 378.0 (M^+, 100), 336.0 (21), 294.0 (33), 260.0 (65); 245.0 (32), 226.0 (7%); HRMS (EI) calcd. for $C_{24}H_{26}S_2$: 378.1476; found 378.1472; mp 99 °C.

1,6-diazido-7,10-dimethylfluoranthene (125d)

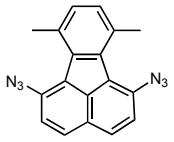

A mixture of 1,6-dibromo-7,10-dimethylfluoranthene (0.1 g, 0.08 mmol) and sodium azide (0.07 g, 1.1mmol) in DMF (5 mL) was stirred at 100 °C for 3 h. The solvent was evaporated, the residue was purified by column chromatography (silica gel, hexane) to yield of brown solid (0.053 g, 65%). IR (KBr): 3028*w*, 2977*w*, 2930*m*, 2859*w*, 2437*m*, 2291*w*, 2104*s*, 1710*w*, 1612*s*, 1502*m*, 1490*s*, 1454*m*, 1423*m*, 1362*w*, 1303*s*, 1157*s*, 1033*m*, 1008*w*, 819*s*, 805*m*, 788*w*, 671*m*, 644*w*, 543*w*; ^{1}H-NMR (500 MHz, CD_2Cl_2) δ 7.81 (d, 1H, ^{3}J = 8.5 Hz), 7.38 (d, 1H, ^{3}J = 8.5 Hz), 7.07 (s, 1H), 2.92 (s, 3H); ^{13}C-NMR (500 MHz, $CDCl_3$) δ 136.8, 135.8, 133.5, 132.1, 132.0, 128.8, 126.2, 124.8, 119.5, 25.8; MS (EI) m/z (%): 255.0 (M^+-2N_2, 100), 238.0 (6); 227.0 (20), 201.0 (8%); HRMS (EI) calcd. for $C_{18}H_{12}N_6$: 312.1123; found 312.1142; mp 164 °C.

7,10-dimethyl-1,6-dithiocyanatofluoranthene (125f)

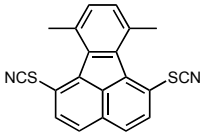

A mixture of 1,6-dibromo-7,10-dimethylfluoranthene (0.03 g, 0.26 mmol) and potassium thiocyanate (0.03 g, 0.31mmol) in DMF (1 mL) was refluxed for 2 d. The solvent was evaporated, the residue was purified by column chromatography (silica gel, hexane : ethyl acetate 30 : 1) to yield two products (1 mg , 4% desired product and 7 mg , 25% of monosubstitution), conversation 57%. IR (KBr): 2956*s*, 2923*s*, 2853*s*, 2152*m*, 1998*w*, 1726*m*, 1636*m*, 1595*m*, 1548*m*, 1464*s*, 1450*s*, 1417*m*, 1371*m*, 1341*m*, 1093*s* (br.), 992*s*, 827*m*, 801*m*, 744*w*, 546*w*, 473*m*; ^{1}H-NMR (500 MHz, $CDCl_3$) δ 7.91 (d, 1H, ^{3}J = 8.5 Hz), 7.86 (d, 1H, ^{3}J = 8.5 Hz), 7.21 (s, 1H), 2.81 (s, 3H); ^{13}C-NMR (500 MHz, $CDCl_3$) δ 138.7, 137.8, 135.1, 133.5, 132.4, 131.4, 129.4, 128.7, 118.5, 110.5, 25.3; MS (EI) m/z (%): 344.1 (M^+, 100), 316.1 (55), 302.0 (24), 284.1 (20), 258.1 (32), 226.1 (22%); HRMS (EI) calcd. for $C_{20}H_{12}N_2S_2$: 344.0442; found 344.0442; mp 200 °C.

1-bromo-7,10-dimethyl-6-thiocyanatofluoranthene (125f′)

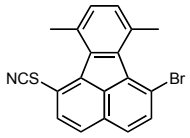

IR (KBr): 2958*w*, 2926*m*, 2856*w*, 2155*w*, 1633*w*, 1593*w*, 1551*w*, 1465*m*, 1447*m*, 1413*m*, 1375*m*, 1088*s* (br), 991*m*, 826*m*, 809*m*, 745*w*, 622*w*, 547*w*, 468*s*; ^{1}H-NMR (500 MHz, $CDCl_3$) δ 7.87 (d, 1H, ^{3}J = 8.5 Hz), 7.82 (d, 1H, ^{3}J = 8.5 Hz), 7.80 (d, 1H, ^{3}J = 8.5 Hz), 7.61 (d, 1H, ^{3}J = 8.5 Hz), 7.19 (s, 2H), 2.93 (s, 3H), 2.80 (s, 3H); ^{13}C-NMR (500 MHz, $CDCl_3$) δ 138.6, 138.3, 137.5, 137.45, 136.2, 136.0, 133.63, 132.6, 132.2, 131.3, 130.7, 128.5, 128.47, 127.9, 117.7, 117.5, 110.9, 26.4, 25.3; MS (EI) m/z (%): 366.9 (M^+, 100), 338.9 (41), 324.9 (20), 287.0 (11), 259.0 (32), 226.0 (46%); HRMS (EI); calcd. for $C_{19}H_{12}BrNS$: 364.9874; found 364.9868; mp 220 °C decomp.

***N*-(7,10-dimethylfluoranthen-1-yl)benzamide (125g)**

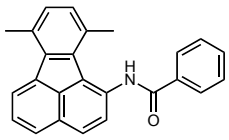

A Schlenk tube was charged with CuI (0.0025 g, 0.013 mmol), 1,6-dibromo-7,10-dimethylfluoranthene (0.05 g, 0.13 mmol), benzamide (0.038 g, 0.31 mmol), K_2CO_3 (0.072g, 0.52 mmol), briefly evacuated and backfilled with argon. *N,N′*-Dimethylendiamine and toluene were added under argon. The tube was sealed with a teflon valve and the reaction mixture was stirred at 110 °C for 16 h, and cooled to room temperature. The solvent was evaporated, the residue was purified by column chromatography (silica gel, hexane:ethyl acetate 10:1, hexane:acetone 5:1) to yield of yellow-green solid (0.01 g, 18% monosubstitution, 7,10-dimethylfluoranthene was formed as a by-product 6%). IR (KBr): 3256*s*, 3037*w*, 2958*m*, 2925*m*, 2860*w*, 1650*s*, 1602*m*, 1580*m*, 1515*s*, 1490*s*, 1454*m*, 1421*s*, 1373*m*, 1345*m*, 1300*m*, 1280*s*, 1201*w*, 1180*w*, 1141*w*, 1073*w*, 1044*w*, 1029*w*, 900*w*, 830*s*, 806*s*, 752*m*, 713*s*, 690*m*, 649*w*, 578*w*, 541*m*, 515*w*; ^{1}H-NMR (500 MHz, DMSO-d_6) δ 10.78 (s, 1H, NH), 8.14 (d, 1H, ^{3}J = 7.0 Hz), 8.13 (d, 2H, ^{3}J = 6.5 Hz), 8.0 (d, 1H, ^{3}J = 8.5 Hz), 7.97 (d, 1H, ^{3}J = 8.0 Hz), 7.73 (dd, 1H, ^{3}J = 8.0, 7.0 Hz), 7.67-7.63 (m, 2H), 7.58 (dd, 2H, ^{3}J = 7.5, 7.0), 7.16 (d, 1H, ^{3}J = 7.5 Hz), 7.06 (d, 1H, ^{3}J = 7.5 Hz), 2.74 (s, 3H), 2.55 (s, 3H); ^{13}C-NMR (400 MHz, DMSO-d_6) δ 165.2, 137.1, 136.8, 136.3, 133.9, 132.8, 132.4, 131.9, 131.7, 131.2, 131.1, 130.9, 130.2, 130.18, 128.6, 127.9, 127.7, 127.6, 127.57, 126.0, 123.2, 23.0, 20.4; MS (EI) m/z (%): 349.4 (M^+, 72), 244.3 (100), 215.2 (11), 202.2 (6),

105.1 (70%); HRMS (EI) calcd. for $C_{25}H_{19}NO$: 349.1467; found: 349.1464; mp 254 °C decomp.

_S_,_S_'-(1,6-dibromofluoranthene-7,10-diyl)bis(methylene)diethanethioate (126a)

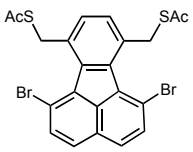

A mixture of 1,6-dibromo-7,10-bis(bromomethyl)fluoranthene (0.05 g, 0.092 mmol) and potassium thioacetate (0.021 g, 0.18 mmol) was refluxed in ethanol/dioxane solution for 1 h. The solvent was evaporated, the residue was washed with methanol and dried to yield of yellow solid (0.041 g, 84%). IR (KBr): 3067*w*, 2921*w*, 1922*w*, 1681*s*, 1595*w*, 1562*w*, 1473*m*, 1417*m*, 1349*m*, 1238*w*, 1141*s*, 1106*m*, 1085*s*, 1015*w*, 988*m*, 957*m*, 893*w*, 880*w*, 830*m*, 783*m*, 709*w*, 663*w*, 631*m*, 618*m*, 549*w*, 521*w*; ^{1}H-NMR (400 MHz, $CDCl_3$) δ 7.78 (d, 1H, ^{3}J = 8.8 Hz), 7.62 (d, 1H, ^{3}J = 8.4 Hz), 7.39 (s, 1H), 4.91 (s, 2H), 2.34 (s, 3H); ^{13}C-NMR (400 MHz, $CDCl_3$) δ 195.6, 138.0, 136.7, 135.9, 134.8, 133.2, 132.2, 128.4, 127.5, 118.0, 35.5, 30.5; MS (EI) m/z (%): 535.9 (M^+, 0.57), 460.9 (9), 416.9 (10), 385.9 (14), 337 (100), 323 (9), 258.1 (29), 226.1 (29%); HRMS (EI) calcd. for $C_{22}H_{16}Br_2O_2S_2$: 533.8958; found: 533.8958; mp 116-119 °C.

_S_,_S_'-(1,6-dibromo-3,4-dichlorofluoranthene-7,10-diyl)bis(methylene)diethanethioate (126b)

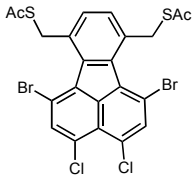

To a solution of ethanol/dioxane (100/50 mL) was added 1,6-dibromo-7,10-bis(bromomethyl)-3,4-dichlorofluoranthene (0.1 g, 0.16 mmol) and potassium thioacetate (0.037 g, 0.32 mmol). The mixture was stirred at reflux for 1 h and cooled to room temperature. The solvent was evaporated, the residue was washed with ethanol and dried to yield of yellow solid (0.097 g, 99%). IR (KBr): 3349*w*, 3077*w*, 3012*w*, 2917*w*, 1688*s*, 1587*w*, 1568*m*, 1558*m*, 1487*w*, 1461*m*, 1428*m*, 1396*m*, 1342*m*, 1246*w*, 1220*w*, 1122*s*, 1103*m*, 1038*m*, 1009*m*, 960*m*, 877*m*, 844*w*, 826*w*, 706*w*, 664*w*, 627*m*, 589*w*, 558*w*; ^{1}H-NMR (500 MHz, $CDCl_3$) δ 7.87 (s, 1H), 7.38 (s, 1H), 4.79 (s, 2H), 2.33 (s, 3H); ^{13}C-NMR (500 MHz, $CDCl_3$) δ 195.3, 138.4, 137.1, 137.0, 135.8, 133.1, 132.5, 131.6, 123.0, 117.5, 35.3, 30.5; MS (EI) m/z (%): 605.8 (M^+, 0.73), 559.7 (0.81), 528.8 (8), 486.7 (16), 453.8 (11), 406.8 (100), 360.9 (6), 325.9 (13), 290 (10%); HRMS (ESI) calcd. for $C_{22}H_{14}Br_2Cl_2NaO_2S_2$: 624.8077; found: 624.8068; mp 200-203 °C.

1,6-dibromo-3,4-dichloro-7,10-bis(thiocyanatomethyl)fluoranthene (126c)

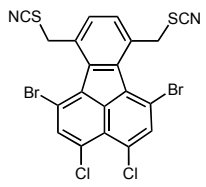

To a degassed solution of ethanol/dioxane (50/25 mL) were added 1,6-dibromo-7,10-bis(bromomethyl)-3,4-dichlorofluoranthene (0.05 g, 0.08 mmol) and potassium thiocyanate (0.037 g, 0.32 mmol). The mixture was stirred at reflux for 2 h and cooled to room temperature. The solvent was evaporated, the residue was purified by column chromatography (silica gel, hexane : ethyl acetate 15:1) to yield of yellow solid (0.033 g, 45%). IR (KBr): 3071*m*, 2924*s*, 2853*s*, 2145*s*, 1730*m*, 1691*m*, 1559*s*, 1463*m*, 1430*m*, 1412*m*, 1392*s*, 1344*m*, 1267*m*, 1244*m*, 1222*m*, 1122*s*, 1074*m*, 1041*s*, 1007*s*, 872*m*, 844*m*, 823*m*, 792*w*, 739*w*, 715*w*, 702*w*, 683*m*, 642*w*, 546*w*, 484*w*; ^{1}H-NMR (500 MHz, $CDCl_3$) δ 7.95 (s, 1H), 7.60 (s, 1H), 5.0 (s, 2H); ^{13}C-NMR (500 MHz, $CDCl_3$) δ 138.6, 137.7, 137.3, 134.8, 132.9, 132.6, 131.5, 123.3, 118.3, 112.0, 40.5; MS (EI) m/z (%): 569.8 (M^+, 2.3), 534.8 (37), 511.9 (45), 468.9 (19), 453.9 (72), 419.9 (20), 376.0 (28), 340.0 (19), 294 (28%); HRMS (EI) [M - SCN fragment] calcd. for $C_{19}H_8Br_2Cl_2NS$: 509.8121; found: 509.8123; mp 128-130 °C.

1,6-dibromo-3,4-dichloro-7,10-bis(selenocyanatomethyl)fluoranthene (126d)

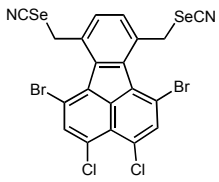

To a solution of ethanol/dioxane (50/25 mL) were added potassium selenocyanate (0.037 g, 0.326 mmol) and 1,6-dibromo-7,10-bis-(bromomethyl)-3,4-dichlorofluoranthene (0.05 g, 0.163 mmol). The mixture was refluxed for 1 h then allowed to cool to room temperature. The solvent was evaporated, the residue was washed with methanol and dried, to yield of yellow solid (0.85 g, 77%). IR (KBr): 3071*m*, 2924*w*, 2851*w*, 2142*s*, 2068*w*, 1902*w*, 1688*w*, 1632*w*, 1560*s*, 1489*w*, 1461*m*, 1430*m*, 1391*s*, 1363*m*, 1345*s*, 1299*w*, 1243*m*, 1204*m*, 1188*m*, 1117*s*, 1037*s*, 1007*s*, 870*m*, 842*m*, 820*m*, 791*w*, 709*m*, 673*m*, 630*m*, 606*w*, 558*w*, 520*m*, 474*w*; ^{1}H-NMR (400 MHz, $CDCl_3$) δ 7.95 (s, 1H), 7.60 (s, 1H), 5.05 (s, 2H); ^{13}C-NMR (400 MHz, $CDCl_3$) δ 138.8, 137.32, 137.3, 135.0, 133.2, 133.0, 132.8, 123.4, 118.1, 102.4, 35.4; MS (EI) m/z (%): 613.4 (M - 2CN, 1), 534.5 (17), 469.6 (7), 453.6 (100), 440.6 (16), 373.7 (21); HRMS (ESI) calcd. for $C_{20}H_8Br_2Cl_2N_2NaSe_2$: 686.6659; found: 686.6642; mp 174-175 °C.

7,10-bis(azidomethyl)-1,6-dibromo-3,4-dichlorofluoranthene (126f)

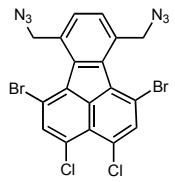

To a degassed solution of ethanol/THF (100/50 mL) was added 1,6-dibromo-7,10-bis(bromomethyl)-3,4-dichlorofluoranthene (0.1 g, 0.16 mmol) and sodium azide (0.022 g, 0.34 mmol). The mixture was stirred at reflux for 1 h and cooled to room temperature. The solvent was evaporated, the residue was purified by column chromatography (silica gel, hexane:ethyl acetate 30:1) to yield of yellow solid (0.03 g, 34%). IR (KBr): 3394*w*, 3072*w*, 2962*m*, 2925*m*, 2853*w*, 2104*s*, 1730*w*, 1627*w*, 1561*m*, 1460*w*, 1435*w*, 1395*m*, 1351*w*, 1292*m*, 1261*s*, 1242*m*, 1098*s*, 1047*s*, 938*w*, 867*m*, 846*w*, 800*s*, 706*w*, 659*w*, 491*w*; ^{1}H-NMR (400 MHz, $CDCl_3$) δ 7.92 (s, 1H), 7.57 (s, 1H), 5.09 (s, 2H); ^{13}C-NMR (400 MHz, $CDCl_3$) δ 138.3, 137.1, 137.0, 135.4, 132.2, 131.6, 131.0, 123.0, 118.0, 55.8; MS (EI) m/z (%): 537.9 (M^+, 12), 495.9 (33), 467.9 (24), 440.9 (46), 402.9 (35), 388.9 (100), 375.9 (36), 354.0 (18), 322.0 (44), 295.0 (55%); HRMS (EI) calcd. for $C_{18}H_8Br_2Cl_2N_6$: 535.8554; found: 535.8507; mp 130-132 °C.

4.8 Crystal data

All X-ray crystal structure determination measurements were made on a *NoniusKappaCCD* area-detector diffractometer[17] using graphite monochromated Mo *K*a radiation (*l* = 0.71073A˚) and an *Oxford Cryosystems Cryostream 700* cooler.

1,6-dibromo-7,10-bis(bromomethyl)fluoranthene (110). (Obtained from hexane/ EtOAc): $C_{18}H_{10}Br_4$, M = 545.89, space group: $Cmc2_1$ (orthorhombic), a = 20.3086(7) Å, b =14.1050(5) Å, c = 5.5138(2) Å, V = 1579.4(1) Å^3, Z = 4, μ(Mo $K\alpha$) = 10.215 mm^{-1}, Dx = 2.295 g cm^{-3}, $2\theta_{(max)}$ = 55°. T = 160 K, 13062 measured reflections, 1845 independent reflections, 1699 reflections with $I > 2s$ (I), refinement on F^2 with SHELXL97,[18] 104 parameters, $R(F)$ [$I > 2\ s\ (I)$ reflections] = 0.0331, $wR(F^2)$ [all data] = 0.0850, goodness of fit = 1.040, $\Delta\rho_{max}$ = 0.89 Å^{-3}.

1,6-bis(isopropylthio)-7,10-dimethylfluoranthene (125c). (Obtained from hexane/ Et_2O): $C_{24}H_{26}S_2$, M = 378.59, space group: $C2/c$ (monoclinic), a = 9.8579(2) Å, b

=120230(2) Å, c = 17.7565(4) Å, V = 4004.7(1) Å^3, Z = 8, μ(Mo $K\alpha$) = 0.271 mm^{-1}, Dx = 1.256 g cm^{-3}, $2\theta_{(max)}$ = 55°. T = 160 K, 53883 measured reflections, 4573 independent reflections, 3461 reflections with $I > 2s$ (I), refinement on F^2 with SHELXL97, 241 parameters, $R(F)$ [$I > 2s$ (I) reflections] = 0.0384, $wR(F^2)$ [all data] = 0.1050, goodness of fit = 1.020, $\Delta\rho_{max}$ = 0.27 e Å^3.

***S*,*S*'-(1,6-dibromo-3,4-dichlorofluoranthene-7,10-diyl)bis(methylene)diethanethioate (126b)**. Obtained from hexane: $C_{22}H_{14}Br_2Cl_2O_2S_2$, M = 605.18, space group: *Pbca* (orthorhombic), a = 7.5997(1) Å, b =20.5777(3) Å, c = 25.6079(4) Å, β = 93.443(1), V = 2100.73(7) Å^3, Z = 4, μ(Mo $K\alpha$) = 4.342 mm^{-1}, Dx = 1.913 g cm^{-3}, $2\theta_{(max)}$ = 60°. T = 160 K, 29743 measured reflections, 3059 independent reflections, 2535 reflections with $I > 2s$ (I), refinement on F^2 with SHELXL97, 138 parameters, $R(F)$ [$I > 2s$ (I) reflections] = 0.0592, $wR(F^2)$ [all data] = 0.1622, goodness of fit = 1.051, $\Delta\rho_{max}$ = 1.21 e Å^{-3}.

4.9 References

1. Imamura, K.; Takimiya, K.; Aso, Y.; Otsubo, T. *Chem. Commun.* **1999**, 1859.
2. a) Otsubo, T. *Synlett* **1997**, 544; b) Caronna, T.; Sinisi, R.; Catellani, M.; Malpezzi, L.; Meille, S. V.; Mele, A. *Chem. Commun.* **2000**, 1139.
3. Seiders, T. J.; Elliott, E. L.; Grube, G. H.; Siegel, J. S. *J. Am. Chem. Soc.* **1999**, *121*, 7804-7813.
4. a) Verma, A. K.; Singh. J.; Chaudhary, R. *Tetrahedron Lett.* **2007**, *48*, 7199-7202; b) Sperotto, E.; Van Klink, G. P. M.; De Vries, J. G.; Van Koten, G. *J. Org. Chem.* **2008**, *73*, 5625-5628.
5. Zimmerman, K.; Haenel, M. *Synlett* **1997**, *5*, 609-611.
6. Klapars, A.; Huang, X.; Buchwald, S. *J. Am. Chem. Soc.* **2002**, *124*, 7421-7428.
7. Borchard, A.; Fuchicello, A.; Kilway, K. V.; Baldridge, K. K.; Siegel, J. S. *J. Am. Chem. Soc.* **1992**, *114*, 1921-1923.
8. *Gaussian 03*, Revision D.01, Gaussian, Inc.: Wallingford CA **2005**.
9. Minnesota Supercomputer Center, g03/mn.
10. Zhao, Y.; Truhlar, D. *Theor. Chem. Acc.* **2008**, *120,* 215.
11. Schaefer, A.; Horn, H.; Ahlrichs, R. *J. Chem. Phys.* **1992**, *97*, 2571.
12. Schaefer, A.; Huber, C.; Ahlrichs, R. *J. Chem. Phys.* **1994**, *100*, 5829.
13. Baldridge, K.; Greenberg, J. *Mol. Graphics* **1995**, *13*, 63.
14. http://www.webmo.net
15. Olah, G. A.; Doggweiler, H.; Felber, J. D. *J. Org. Chem.* **1984**, *49*, 2112-2116.
16. a) Oki, M.; Yamada, Y. *Bull. Chem. Soc. Jpn.* **1988**, *61*, 1181-1184; b) *Tetrahedron Lett.* **1981**, 22, 3629-3632; c) Hodgson, D. M.; Fleming, M. J.; Stanway. S. J. *Org. Lett.* **2005**, *7*, 3295-3298.
17. Hooft, R. *Kappa CCD Collect Software*, Nonius BV, Delft. The Netherlands **1999**.
18. Sheldrick, G. M. SHELXL97 *Acta Crystallogr. Sect A* **2008**, *64*, 112-122.

Chapter 5. Prospect for Heteroatom-Substituted Corannulenes

5.1 Introduction

The key intermediates for the synthesis of the heterocorannulenes are tetrasubstituted fluoranthenes and related diazafluoranthenes.[1,2] Such compounds are typically prepared via Diels-Alder reactions of cyclopentadienones with norbornadiene, or double Knoevenagel condensations of acenaphthenequinones with disubstituted dienes (Scheme 5.1). The use of acetylene derivatives in Diels-Alder cycloadditions allows the synthesis of fluoranthenes with substitution in the 8 and/or 9 positions.[3] A synthetic approach to the 1,2-diazacorannulenes proceeds via [2+4] cycloaddition reactions of 3,6-disubstituted 1,2,4,5-tetrazines and acenaphthylenes, resulting in the formation of 8,9-diazafluoranthene derivatives.[2] Synthesis and properties of these compounds have been extensively studied in Chapter 3. This chapter will examine several routes to novel 1,6-heterocorannulenes.

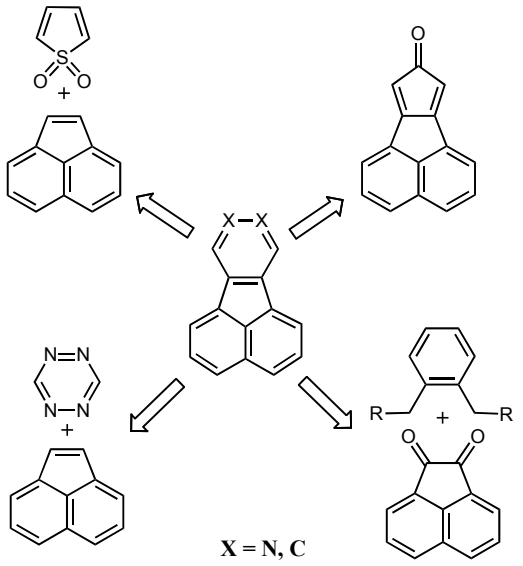

Scheme 5.1. Retrosynthetic routes to the fluoranthenes

Retrosynthetic analysis to the 1,6-disubstituted corannulenes provides construction of two types (***a***, ***b***) fluoranthene derivatives (Scheme 5.2). Synthesis of these intermediates and possible routes to the ring closure reaction will be presented below.

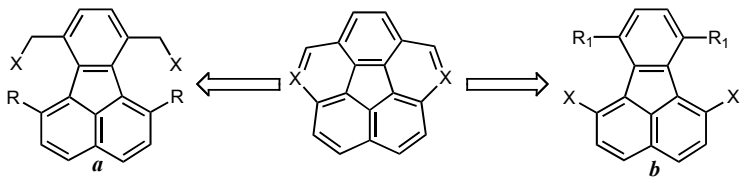

Scheme 5.2 Retrosynthetic approaches to the 1,6-heterocorannulenes

5.2 Synthesis via intramolecular nucleophilic substitution

Previously mentioned 1,6-dibromo-7,10-bis(bromomethyl)fluoranthene (**110**) and 1,6-dibromo-7,10-bis(bromomethyl)-3,4-dichlorofluoranthene (**111**) belong to the *a*-type structures (Scheme 5.2). Derivatization of **111** via nucleophilic displacement of the benzylic bromines produces **125c-f** (Scheme 5.3), attractive intermediates for the synthesis of heterocorannulenes. Thus, generation of the selenide or thiolate anions, necessary for intramolecular nucleophilic substitution in **125c-d**, can be accomplished by reaction with $NaBH_4$.[4] Reduction of azide groups in **125f** to the diamine and followed Buchwald-Hartwig chemistry[5] would support ring closure reaction toward the aim of preparing 1,6-diazacorannulene.

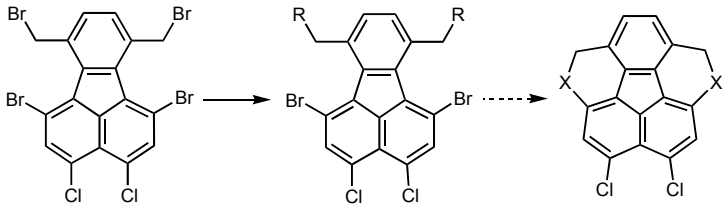

Scheme 5.3 Synthetic approach to the heterocorannulenes via **125c-d**

5.3 Nitrene insertion chemistry

The C-H insertion reaction of nitrenes is a potentially useful way of functionalizing an unactivated C-H bond, converting hydrocarbons into amine derivatives. Notable achievements in catalytic C-H bond amidation have been reached by

using Ru, Rh, Pd and Cu catalysts.[6-8] According to the reports by Che,[6b-e] Dubois,[7] and others,[6a,8] these catalytic systems involve reactive metalimido/nitrene species, which undergo insertion to C-H bonds. Among the diverse synthetic methods, intramolecular annulation of nitrene intermediates proved to be an efficient approach for the preparation of N-heterocycles. A synthetic route to the 1,6-diazacorannulenes via of 7,10-dimethylfluoranthene is described in Scheme 5.4. Synthesis of 7,10-dimethylfluoranthene was carried out via classical methods for the construction of fluoranthenes[9] and produces **129** as light-yellow crystals. Bromination of **129** with NBS and further derivatization would lead to formation of **131**, **132**. In the case of **131**, nitrene insertion chemistry will be supported by thermolysis or irradiation.[10] Ring closure in **132** could be achieved via Pd mediated nitrene cyclisations.

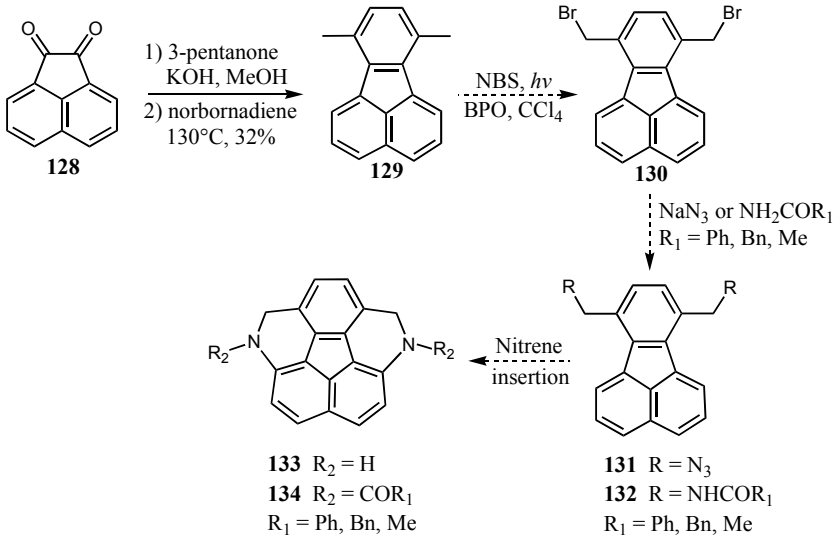

Scheme 5.4 Synthesis of heterocorannulenes via nitrene insertion chemistry

[2+4] cycloadditions of 2,5-disubstituted cyclic sulfones with acenaphtylenes is an elegant way for construction of valuable fluoranthenes (Scheme 5.5),[11] initial building blocks in heterocorannulene synthesis. Primary investigation of these reactions was carried out in our laboratory, using 2,5-dibromothiophene-1,1-dioxide **135** as a diene. Reactions were accomplished in refluxing toluene, resulting in moderate to excellent yields of desired products (Scheme 5.6). Initial bromination of methyl groups in **138** and further derivatization could open a new window to the 1,4-heterocorannulene. In the case

of R = Me, R_1= NO_2 and R = H, R_1 = CN, $CONR_2$ (cyano and nitro groups can be converted into the amides)[11] nitrene insertion chemistry can be used as a ring closure strategy.

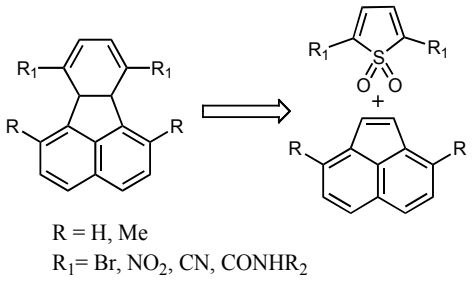

Scheme 5.5 Retrosynthesis of fluoranthene derivatives via Diels-Alder reaction

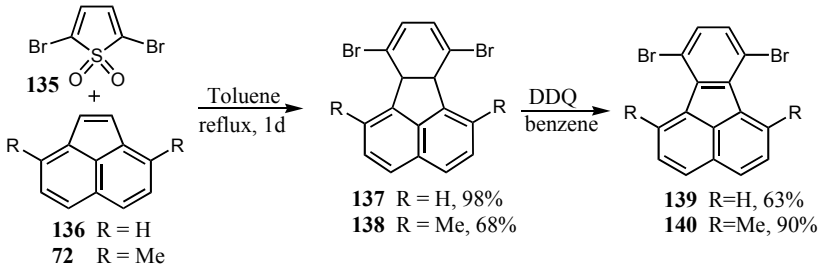

Scheme 5.6 Synthesis of fluoranthenes via cyclic sulfones

Previously reported (Chapter 4) 1,6-diazido-7,10-dimethylfluoranthene **124d** (Scheme 5.7) belongs to the *b*-type structures (Scheme 5.2). Similar to the **131**, **124d** can be also involved in nitrene insertion chemistry.

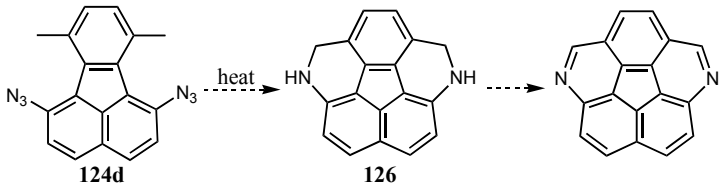

Scheme 5.7 The use diazide **124d** in nitrene insertion chemistry

Another synthetic approach to the fluoranthene nucleus, containing cyano- or amide groups involves ortho disubstituted benzene rings, containing activated benzylic

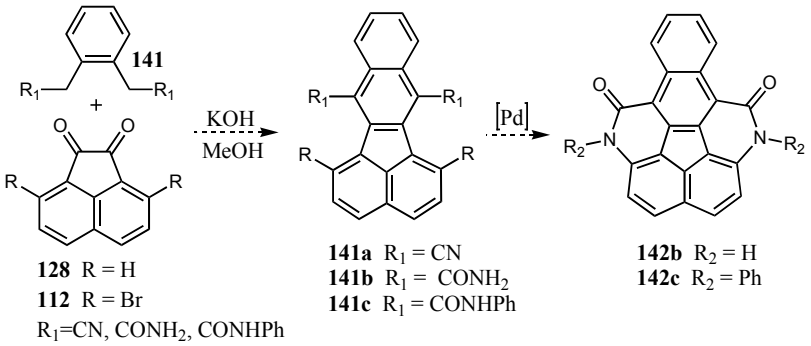

Scheme 5.8 Synthesis of fluoranthene derivatives via Knoevenagel condensation

substituents in the Knoevenagel condensation. This method allows the synthesis of corresponding benz[*k*]fluoranthenes in one step from quinones (Scheme 5.8). Synthesis of 7,12-dicyano-benz[*k*]fluoranthene (**141a** R = H) and benz[*k*]fluoranthene-7,12-dicarboxamide (**141b**, R = H) is known and was previously reported.[12] Compounds **141b,c** can be converted to the corresponding diazacorannulene precursors **142b-c** using Pd mediated intramolecular cyclization reaction. In a case of compound **141a**, preliminary reduction of the cyano groups to the diamine **142a** will be required towards the aim of preparing diazacorannulene **143** (Scheme 5.9).

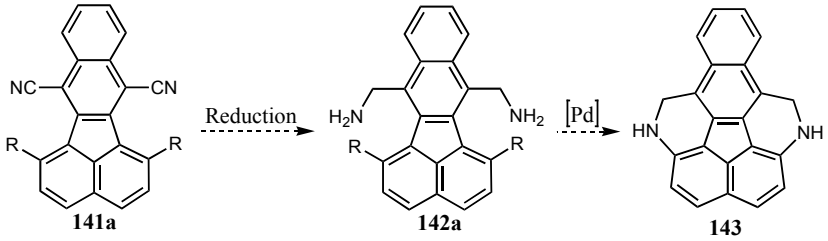

Scheme 5.9 Approach to the diazacorannulene **143** via 7,12-dicyanobenz[*k*]fluoranthenes

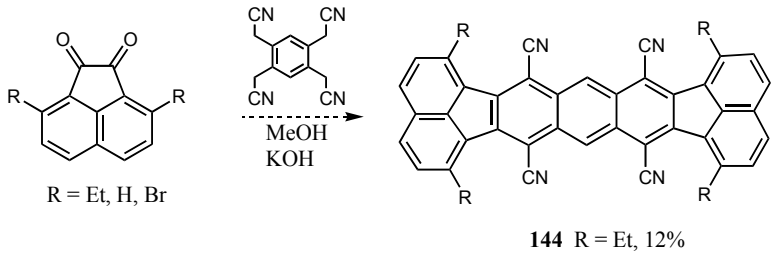

Scheme 5.10 Synthesis of tetracyano derivatives **144**

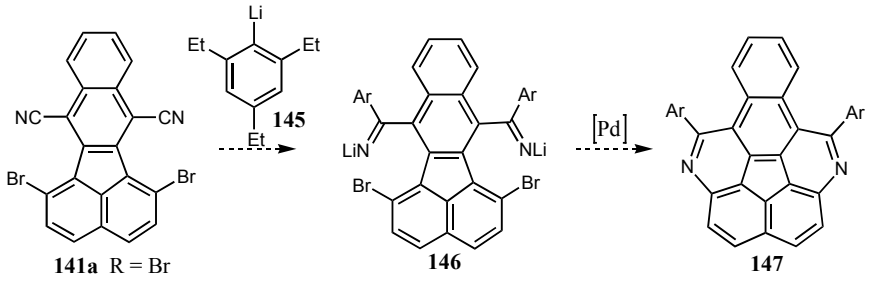

Scheme 5.11 Synthesis of diimine salts via organomettallic reagent

Nitriles **141a** (R = Br) and **144** (R = Br) would also react with strong nucleophiles, such as organometallic reagents,[14] to give anionic imine salts, which could undergo Pd mediated coupling reaction to form **147**and **119** respectively (Scheme 5.11 and 5.12).

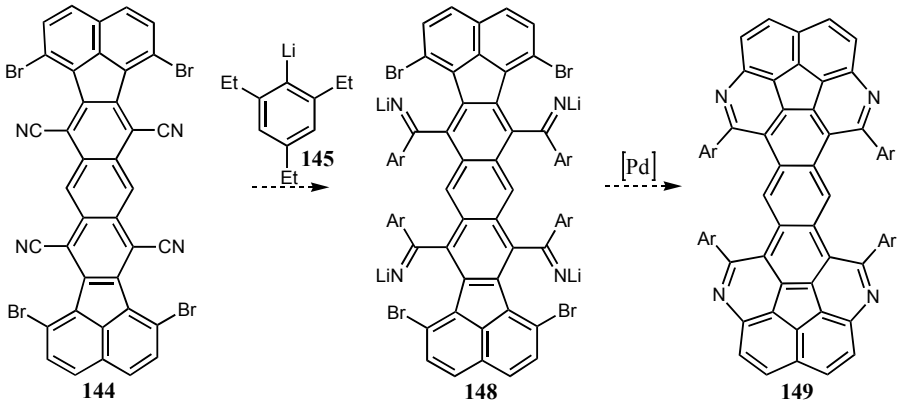

Scheme 5.12 Synthesis of tetraimine salts via organometallic reagent

5.4 Hofmann-Löffler-Freytag approach to the 1,6-heterocorannulenes

The Hofmann-Löffler-Freytag reaction[15,16] provides a convenient and useful method for the intramolecular C-H amination chemistry, resulting the formation of a new C-N bonds. The first step of the reaction is a rearrangement, with the halogen migrating from the nitrogen to 4 or 5 position of the alkyl group. It is possible to isolate the resulting haloamine salts, but usually this is not done, and the second step, ring closure,

takes place. The reactions are induced by heat or irradiation. The mechanism is of a free-radical type, with the main step involving an internal hydrogen abstraction.[17]

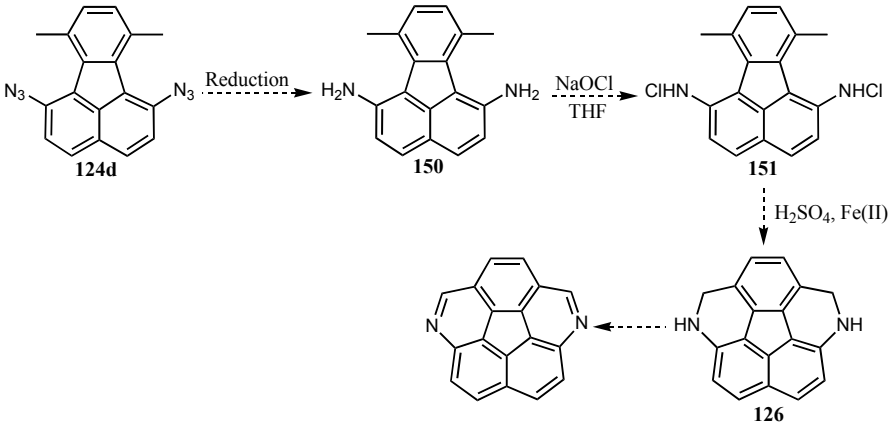

Scheme 5.13 Hofmann-Löffler-Freytag path to the heterocorannulene

Conversion of azide groups in **124d** to the diamine **150** and followed chlorination by the Hofmann-Löffler-Freytag strategy can be successfully used in the synthesis of 1,6-diazacorannulenes (Scheme 5.13).

5.5 Summary

Chapter 3 and 4 of this thesis describe different synthetic pathways to the heterosubstituted corannulenes. Significant progress toward the synthesis of dithiacorannulene, and important intermediates in the case of diazacorannulenes has been achieved, and synthetic routes to these compounds are not exhausted. This chapter provides new synthetic pathways to the novel heterocorannulenes, based on nitrene insertion chemistry, Pd catalyzed intramolecular cyclisation reaction and Hofmann-Löffler-Freitag chemistry.

5.6 Experimental Section

7,10-Dimethylfluoranthene (129)

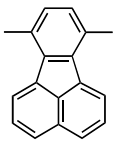

A 20% solution of potassium hydroxide in methanol (10 mL) was added to a solution of acenaphthenequinone (**128**) (2.76 g, 15.2 mmol) and 3-heptanone (10 mL) in methanol (25 mL). The solution was stirred at ambient temperature for 1 h, diluted with water (50 mL), and extracted with dichloromethane (50 mL). The organic layer was washed once with 10% aqueous hydrochloric acid (10 mL) and three times with water (25 mL), dried with magnesium sulfate, filtered, and evaporated. The solid product was transferred to a 100 mL sealable reaction vessel and 2,5-norbornadiene (10 mL) and acetic anhydride (20 mL) were added. The vessel was sealed and placed in an oil bath at 130 °C for 3 d. The reaction was cooled to ambient temperature, diluted with water and extracted with dichloromethane (100 mL). The organic layer was dried with magnesium sulfate, filtered, and evaporated to yield a yellow solid, which was purified by column chromatography on silica gel with hexane as the eluent to yield a light yellow crystals (1.1 g, 32% 2 steps). mp 213-214 °C; IR (KBr): 3040*m*, 3009*w*, 2968*w*, 2919*w*, 2855*w*, 1921*w*, 1872*w*, 1799*w*, 1505*w*, 1478*m*, 1451*m*, 1435*m*, 1424*m*, 1379*m*, 1258*w*, 1220*w*, 1183*w*, 1147*w*, 1137*w*, 1031*m*, 823*m*, 801*s*, 771*s*, 636*w*, 540*m*; ^{1}H-NMR (300 MHz, $CDCl_3$) δ 8.01 (d, ^{3}J = 6.9 Hz, 1H), 7.86 (d, ^{3}J = 8.1 Hz, 1H), 7.66 (dd, ^{3}J = 6.9, 6.9 Hz, 1H), 7.11 (s, 1H), 2.77 (s, 3H); ^{13}C-NMR (75 MHz, $CDCl_3$) δ 138.0, 137.5, 132.7, 132.1, 130.0, 129.9, 128.1, 126.4, 123.2, 20.6; MS (EI) *m*/*z* (%): 230 (M^+, 100), 215 (49), 202 (8%).

7,10-Dibromo-6*b*,10*a*-dihydrofluoranthene (137)

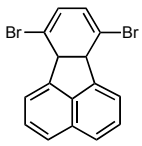

Mixture of 2,5-dibromothiophene 1,1-dioxide (**135**) (0.27 g, 0.99mmol) and acenaphthylene (**136**) (0.15 g, 0.99 mmol) in 10 mL of toluene was refluxed for 1 d. The solvent was evaporated, the residue was purified by column chromatography (silica gel, hexane/ethyl acetate 5:1) to yield of white solid (0.35 g, 98%). mp 133-134 °C; IR (KBr): 3060*w*, 2877*w*, 1642*m*, 1588*m*, 1494*m*, 1415*w*, 1367*m*, 1328*w*, 1318*w*, 1264*m*, 1224*w*, 1188*w*, 1169*w*, 1098*w*, 1075*w*, 1020*m*, 997*m*, 952*m*, 831*m*, 820s, 776*s*, 704*w*, 692*w*, 640*w*, 552*m*, 535*m*, 495*m*, 486*m*, 456*w*, 432*w*; ^{1}H-NMR

(500 MHz, $CDCl_3$) δ 7.89 (d, ^3J = 7.0 Hz, 1H), 7.73 (d, ^3J = 8.0 Hz, 1H), 7.54 (dd, ^3J = 7.5, 8.0 Hz, 1H), 6.09 (s, 1H), 4.86 (s, 1H); ^{13}C-NMR (400 MHz, $CDCl_3$) δ 143.5, 137.0, 131.7, 128.0, 125.2, 124.7, 124.1, 121.4, 53.3; MS (EI) *m/z* (%): 362 (M^+, 13), 282 (4), 202 (100%).

7,10-Dibromo-1,6-dimethyl-6b,10a-dihydrofluoranthene (138)

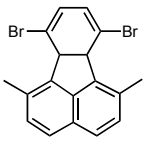

Mixture of 2,5-dibromothiophene 1,1-dioxide (**135**) (0.15 g, 0.56 mmol) and 3,8-dimethylacenaphthylene (**72**) (0.1 g, 0.56 mmol) in 10 mL of toluene was refluxed for 1 d. The solvent was evaporated, the residue was purified by column chromatography (silica gel, hexane/ethyl acetate 6:1) to yield of yellow solid (0.15g, 68%). mp 200-201 °C; IR (KBr): 3054*m*, 2920*s*, 2895*m*, 2852*m*, 1761*w*, 1742*w*, 1630*m*, 1590*m*, 1502*m*, 1437*m*, 1415*m*, 1381*m*, 1324*m*, 1312*w*, 1272*w*, 1264*m*, 1229*m*, 1173*m*, 1111*w*, 1067*m*, 1024*s*, 1006*s*, 948*s*, 908*m*, 883*w*, 839*s*, 820*s*, 798*s*, 709*m*, 696*w*, 674*m*, 603*w*, 569*w*, 537*w*, 514*s*, 477*m*, 468*m*, 448*m*; ^{1}H-NMR (400 MHz, $CDCl_3$) δ 7.57 (d, ^3J = 8.4 Hz, 1H), 7.26 (d, ^3J = 8.0 Hz, 1H), 6.24 (s, 1H), 4.61 (s, 1H), 2,64 (s, 3H); ^{13}C-NMR (400 MHz, $CDCl_3$) δ 138.3, 137.8, 131.5, 130.9, 128.1, 127.2, 125.4, 124.2, 54.1, 21.0; MS (EI) *m/z* (%): 390 (M^+, 19), 230 (100), 215 (27%).

7,10-Dibromofluoranthene (139)

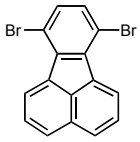

Mixture of 7,10-dibromo-6*b*,10*a*-dihydrofluoranthene (**137**) (0.35 g, 0.92 mmol) and DDQ (0.44 g, 1.94 mmol) in 5 mL of benzene was refluxed for 1 d. The solvent was evaporated, the residue was purified by column chromatography (silica gel, hexane) to yield of white solid. mp 222 - 224 °C; IR (KBr): 3055*w*, 2922*w*, 1931*w*, 1865*w*, 1817*w*, 1591*w*, 1486*w*, 1471*w*, 1430*s*, 1368*m*, 1345*m*, 1281*m*, 1225*m*, 1182*w*, 1104*s*, 1045*m*, 1027*m*, 970*m*, 823*s*, 790*m*, 770*s*, 594*w*, 527*m*; ^{1}H-NMR (400 MHz, $CDCl_3$); δ 8.71 (d, ^3J = 7.6 Hz, 1H), 7.98 (d, ^3J = 8.0 Hz, 1H), 7.74 (dd, ^3J = 7.2, 8.0 Hz, 1H), 7.4 (s, 1H); ^{13}C-NMR (400 MHz, $CDCl_3$) δ 139.9, 135. 2, 132.8, 132.6, 129.9, 128.4, 128.0, 124.8, 117.5; MS (EI) *m/z* (%): 360 (M^+, 100), 281 (8), 200 (15), 180 (15 %).

7,10-Dibromo-1,6-dimethylfluoranthene (140)

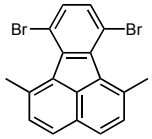

Mixture of 7,10-dibromo-1,6-dimethyl-6*b*,10*a*-dihydrofluoranthene (0.08 g, 0.21 mmol) and DDQ (0.093 g, 0.41 mmol) in 5 mL of benzene was refluxed for 1 d. The solvent was evaporated, the residue was purified by column chromatography (silica gel, hexane/ethyl acetate 20:1) to yield of yellow solid. mp 165 °C ; IR (KBr): 3088*w*, 3040*w*, 2963*m*, 2924*m*, 2854*w*, 1867*w*, 1722*w*, 1607*m*, 1503*w*, 1436*m*, 1410*m*, 1373*m*, 1312*m*, 1264*m*, 1221*w*, 1199*m*, 1182*m*, 1118*s*, 1051*w*, 1028*m*, 1001*m*, 972*m*, 834*s*, 794*s*, 748*m*, 695*w*, 654*w*, 620*w*, 581*w*, 531*w*, 515*m*; ^{1}H-NMR (400 MHz, $CDCl_3$) δ 7.78 (d, ^{3}J = 8.4 Hz, 1H), 7.43 (s, 1H), 7.42 (d, ^{3}J = 8.0 Hz, 1H), 3.04 (s, 3H); ^{13}C-NMR (400 MHz, $CDCl_3$) δ 142.8, 135.1, 134.0, 133.5, 132.6, 132.2, 127.9, 126.6, 115.2, 27.6; MS (EI) *m*/*z* (%): 388 (M^+, 100), 373 (23), 309 (19), 226 (49 %).

5.7 Crystal data

7,10-Dimethylfluoranthene (129). (Obtained from CH_2Cl_2): $C_{18}H_{14}$, M = 230.31, space group: *Cc* (monoclinic), a = 18.7089(7) Å, b = 11.4440(6) Å, c = 11.4191(5) Å, β = 102.259(3)°, V =2389.1(2) Å^3, Z = 8, μ(Mo $K\alpha$) = 0.0722 mm^{-1}, D_x = 1.280 g cm^{-3}, $2\theta_{(max}$ = 50°, T = 253(1) K, 16361 measured reflections, 2102 independent reflections, 1591 reflections with $I > 2\sigma(I)$, refinement on F^2 with SHELXL97, 659 parameters, $R(F)$ [$I > 2\sigma(I)$ reflections] = 0.0524, $wR(F^2)$ [all data] = 0.1593, goodness of fit = 1.046, $\Delta\rho_{max}$ = 0.17 eÅ^{-3}. The molecule possesses crystallographic C_2 symmetry.

7,10-Dibromo-1,6-dimethylfluoranthene (140). (Obtained from acetone): $C_{18}H_{12}Br_2$, M = 388.1, space group: $P2_1/c$ (monoclinic), a = 10.2031(2) Å, b = 10.9090(2) Å, c = 13.8476(5) Å, β = 110.7661(9)°, V = 1441.19(5) Å^3, Z = 4, μ(Mo $K\alpha$) = 5.627 mm^{-1}, D_x = 1.789 g cm^{-3}, $2\theta_{(max)}$ = 55°, T = 160(1) K, 33329 measured reflections, 3293 independent reflections, 2639 reflections with $I > 2\sigma(I)$, refinement on F^2 with SHELXL97, 184 parameters, $R(F)$ [$I > 2\sigma(I)$ reflections] = 0.1069, $wR(F^2)$ [all data] = 0.1069, goodness of fit = 1.057, $\Delta\rho_{max}$ = 0.78 eÅ^{-3}.

5.8 References

1. a) Wu, Y-T.; Siegel, J. S. *Chem. Rev.* **2006**, *106*, 4843-4867; b) Tsefrikas, V. M.; Scott, L. T. *Chem. Rev.* **2006**, *106*, 4868-4884.
2. Rahanyan, N.; Linden, A.; Baldridge, K. K.; Siegel, J. S. *Org. Biomol. Chem.* **2009**, *7*, 2082.
3. Sygula, A.; Karlen, S. D.; Sygula, R.; Rabideau, P. W. *Org. Lett.* **2002**, *4*, 3135-3137.
4. Seiders, J. T.; Baldridge, K. K.; Siegel, J. S. *Tetrahedron* **2001**, *57*, 3737-3742.
5. a) Wolfe, J. P.; Buchwald, S. L. *Org. Synth.* **2004**, *10*, 423; b) Paul, F.; Patt, J.; Hartwig, J. F. *J. Am. Chem. Soc.* **1994**, *116*, 5969-5970.
6. a) Müller, P.; Fruit, C. *Chem. Rev.* **2003**, *103*, 2905; b) Thu, H-Y.; Yu, W-Y.; Che, C-M. *J. Am. Chem. Soc.* **2006**, *128*, 9048; c) Leung, S. K-Y.; Tsui, W-M.; Huang, J-S.; Che, C-M.; Liang, J-L.; Zhu, N. *J. Am. Chem. Soc.* **2005**, *127*, 16629; d) Liang, J-L.; Huang, J-S.; Yu, X-Q.; Zhu, N.; Che, C-M. *Chem. Eur. J.* **2002**, *8*, 1563; e) Liang, J-L.; Yuan, S-X.; Huang, J-L.; Yu, W-Y.; Che, C-M. *Angew. Chem., Int. Ed.* **2002**, *41*, 3465; f) Au, S-M.; Huang, J-S.; Yu, W-Y.; Fung, W-H.; Che, C-M. *J. Am. Chem. Soc.* **1999**, *121*, 9120-9132.
7. a) Espino, C. G.; Fiori, K. W.; Kim, M.; Du Bois, J. *J. Am. Chem. Soc.* **2004**, *126*, 15378; b) Guthikonda, K.; Du Bois, J. *J. Am. Chem. Soc.* **2002**, *124*, 13672; c) Espino, C. G.; Wehn, P. M.; Chow, J.; Du Bois, J. *J. Am. Chem. Soc.* **2001**, *123*, 6935; d) Espino, C. G.; Du Bois, J. *Angew. Chem., Int. Ed.* **2001**, *40*, 598.
8. a) Davies, H. M. L.; Long, M. S. *Angew. Chem., Int. Ed.* ***2005****, 44,* 3518; b) Tsang, P. W. C.; Zheng, N.; Buchwald, S. L. *J. Am. Chem. Soc.* **2005**, *127*, 14560-14561.
9. a) Seiders, T. J.; Elliott, E. L.; Grube, G. H.; Siegel, J. S. *J. Am. Chem. Soc.* **1999**, *123*, 7804-7813; b) Borchardt, A.; Fuchicello, A.; Kilway, K.V.; Baldridge, K. K.; Siegel, J. S. *J. Am. Chem. Soc.* **1992**, *114*, 1921-1923.
10. a) Pudlo, M.; Csanyli, D.; Moreau, F.; Hajos, G.; Riedl, Z.; Sapi, J. *Tetrahedron* **2007**, *63*, 10320-10329; b) Alonso, R.; Campos, P. J.; Garcia, B.; Rodriguez, M. *Org. Lett.* **2006**, *8*, 3521-3523.

11. Miyamoto, H.; Yui, K.; Aso, Y.; Otsubo, T.; Ogura, F. *Tetrahedron Lett*. **1986**, *27*, 2011-2014.
12. Orchin, M.; Reggel, L. *J. Am. Chem. Soc*. **1951**, *73*, 436-442.
13. Elliot, E. L. Ph.D Thesis, University of California, San Diego **2003**.
14. Pattison, I.; Wade, K.; Wyatt, B. K. *J. Chem. Soc*. (A) **1968**, 837-842.
15. a) Hofmann, A. W. *Ber. Dtsch. Chem. Ges*. **1883**, *16*, 558–560; b) Löffler, K.; Freytag, C. *Ber. Dtsch. Chem. Ges*. **1909**, 42, 3427; c) Stella, L. *Angew. Chem., Int. Ed. Engl*. ***1983****, 22,* 337; d) Sosnovsky, G.; Rawlinson, D. J. *Adv. Free-Radical Chem*., **1972**, *4*, 203; see pp. 249-259; e) Deno, N. C. *Methods Free-Radical Chem*. **1972**, *3*, 135-143.
16. Schmitz, E.; Murawski, D. *Chem. Ber*. **1966**, *99*, 1493.
17. Wawzonek, S.; Thelan, P. J. *J. Am. Chem. Soc*. **1950**, *72*, 2118.

Chapter 6. Grid-Type Metal Ion Architectures

6.1 Introduction

Metallosupramolecular chemistry, the chemistry of metal ion ligand association, is one of the most fascinating areas of research, providing direct access to complex architectures, which are of great interest for chemistry and biology.[1-3] Numerous metal-based supramolecular architectures have been synthesized using transition metal coordination chemistry.[4] Metal ion – ligand directed complexation can lead to the formation of multimetallic arrays with novel redox, optical, magnetic, and other properties.[4e] The main class of such molecular aggregations can be presented by helicates,[2,5] cages,[6] rotaxanes[7] and grids.[8,9]

The design of grid-like systems requires orthogonal arrangements of the ligands at each metal center for the purpose of forming two-dimensional coordination networks with regularly arrayed ligands and metal ions. The structure of the ligands involved in the construction of grids usually contains bidentate or tridentate binding subunits; coordination geometry around the metal ions can be best described as tetrahedral or octahedral (Figure 6.1).

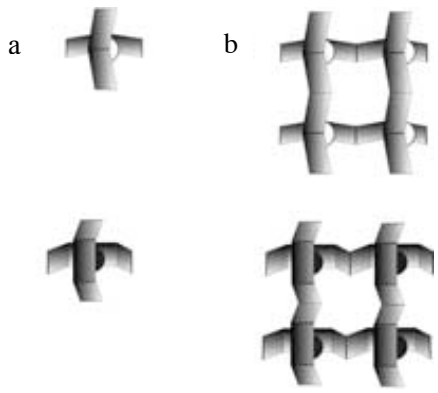

Figure 6.1 Perpendicular arrangement of the ligand L about a metal center M. Coordination geometry of the metal ions: o tetrahedral, ● octahedral.

Some of the ligands used for the construction of grids, are listed in Figure 6.2. The most common ligands contain nitrogen atoms (bipyridine or terpyridine ligands), but ligands containing sulfur and oxo-bridging subunits are also known.[10]

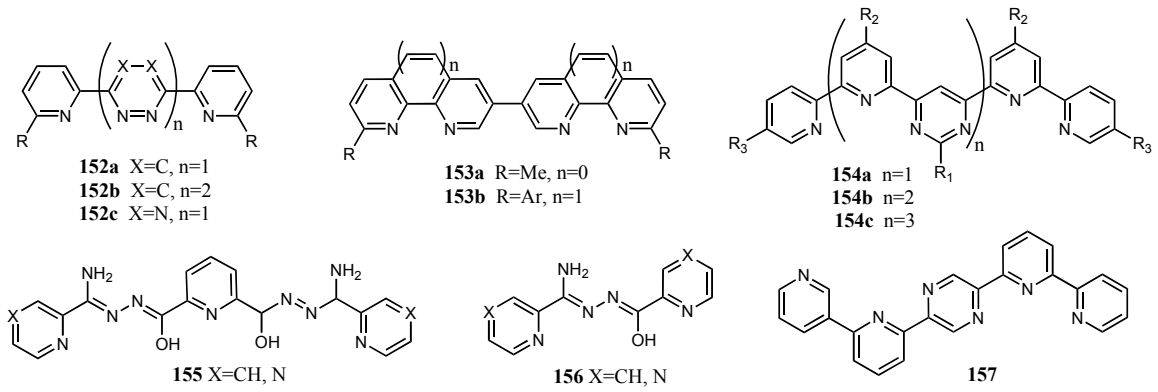

Figure 6.2 Ligands employed in the grid-type complexation

6.2 Grid-Type Metal Ion Arrays

6.2.1. [2 x 2] Metal Ion Arrays

The formation of first [2 x 2] metal grid was reported in 1992 by Osborn *et al*. and involved four *ditopic* ligands **152a**, arranged in tetrahedral coordination geometry around four metal ions (Scheme 6.1).[11a] The formation of both Cu^{I}_{4} and Ag^{I}_{4} ion arrays proceed spontaneously when equimolar amounts of 3,6-di(pyridine-2-yl)-pyridazine (**152a**) and Cu^{I} or Ag^{I} salts were mixed.[11]

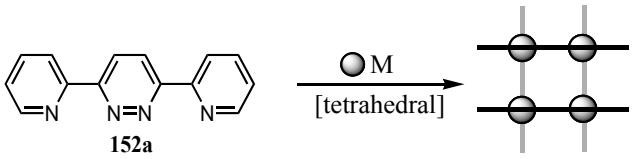

Scheme 6.1 Schematic representation of the constrution of [2x2] grid-type metalloarray $[M^{I}_{4}(\mathbf{L})_{4}]^{4+}$

Brown crystals of $[Cu^{I}_{4}(\mathbf{152a})_{4}]^{4+}$ complex were obtained from a mixture of methanol/acetone/ethanol and reveals a distorted rhombus with the four metal ions (Figure 6.3a). The coordination environment around each metal is distorted tetrahedral. The average Cu^{I}-N and Ag^{I}–N distances are about 2.0 Å and 3.0 Å, respectively, whereas the Cu^{I}–Cu^{I} distance is 3.57 Å and the Cu^{I}–Cu^{I}–Cu^{I} angles are approximately 79° and 101°.

Unlike the complexation of **152a** with copper, the reaction of **152a** with Ag^{I} does not always endows with [2 x 2] grid-type architecture. The reaction of one equivalent of $Ag(O_3SCF_3)$ with **152a** in $MeNO_2$ gave a pale yellow solution from which a yellow solid of the stoichiometry $[Ag(\mathbf{152a})_2O_3SCF_3]$ was isolated.[12] The nature of $[Ag^{I}(\mathbf{152a})_2][O_3SCF_3]$ was clarified by X-ray crystallographic structure analysis (Figure 6.3b). The coordination geometry about the silver ion is square planar, with *cisoid*-coordinated bipyridine motif; the non-coordinated pyridine ring of **152a** ligands are *transoid*.

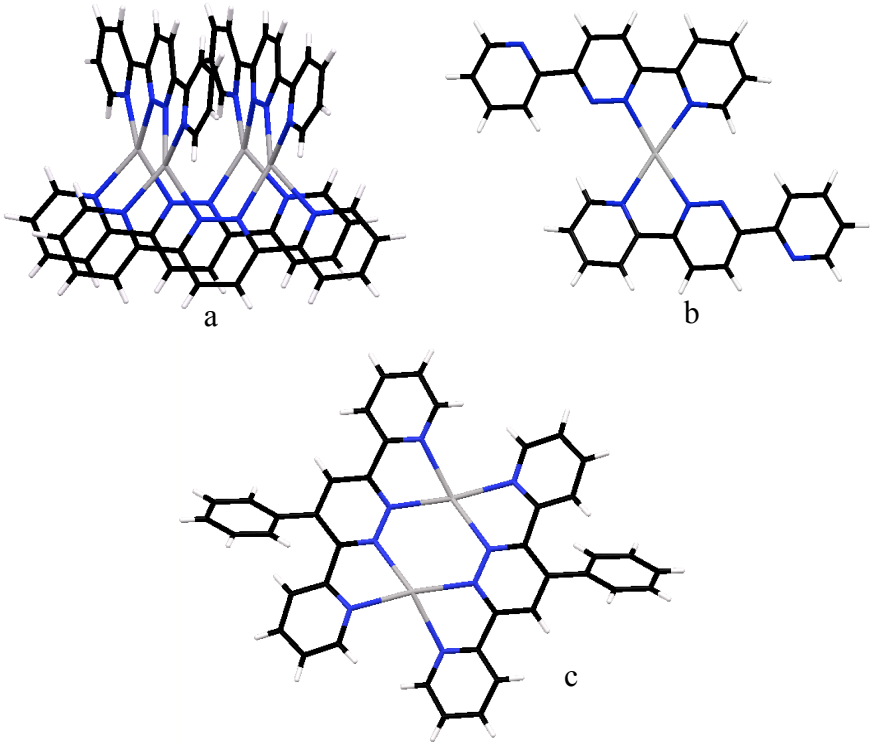

Figure 6.3 Crystal structure of a)$[Cu^{I}_4(\mathbf{152a})_4][O_3SCF_3]$, b)$[Ag^{I}(\mathbf{152a})_2][O_3SCF_3]$ and c)$[Ag^{I}_2(\mathbf{152a'})_2][BF_4]_2$

The reaction of equimolar amount of phenyl-substituted ligand **152a'** and $AgBF_4$ in CH_3NO_2 resulted in the formation of planar dimeric complex $[Ag^{I}_2(\mathbf{152a'})_2][BF_4]_2$, where the two ligands of **152a'** were arranged in a *trans* configuration about the dinuclear silver core. The phenyl groups are twisted, with respect to the pyridazine, to which they are bonded with a torsion angle of 58°. The solid-state structure of the cation present in $[Ag^{I}_2(\mathbf{152a'})_2][BF_4]_2$ is presented in Figure 6.3c.

152a' R=Ph
152a R=TMS

Figure 6.4 Molecular representation of structures **152a'** and **152a″**

Introduction of bulky substituents (such as TMS) on the 4-position of the pyridazine would lead to a helically twisted structure, with out of plane pyridyl rings (Figure 6.4).[13] The reaction of **152a″** with $AgBF_4$ in acetonitrile in a 1:1 stoichiometry proceeded smoothly to give $[Ag^{I}_5(\mathbf{152a''})_4][BF_4]_5$ complex. Yellow crystals were obtained from the mixture diethyl ether/acetonitrile and the structure was best described as a tetrahedron of four silver atoms with a fifth silver at the centre (Figure 6.5).

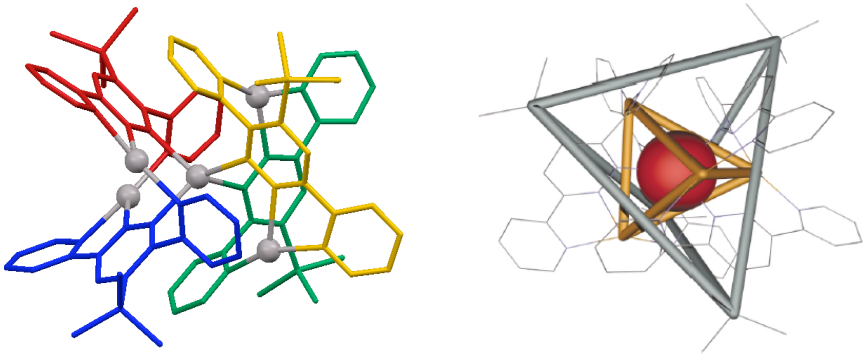

Figure 6.5 Crystal structure of pentanuclear centered tetrahedral complex of $[Ag^{I}_5(\mathbf{152a''})_4][BF_4]_5$[13]

The reaction of **152a** and **152c** with the AgX salts (X= $[PF_6]^-$, $[AsF_6]^-$, $[SbF_6]^-$ and $[BF_6]^-$) afforded comlexes of different structural motifs.[14] Treatment of **152a** with AgX produces the grid-type structures $[Ag^{I}_4(\mathbf{152a})_4][X]_4$, regardless of anion present. Reactions of **152c** with the same salts lead to the polymeric complex $\{[Ag^{I}(\mathbf{152c})][PF_6]\}_\infty$, dinuclear compounds $[Ag^{I}_2(\mathbf{152c})_2(CH_3CN)_2][PF_6]_2$ and $[Ag^{I}_2(\mathbf{152c})_2(CH_3CN)_2][SbF_6]_2$ (Figure 6.6a, b), as well as the propeller-type species $[Ag^{I}_2(\mathbf{152c})_3][AsF_6]_2$ and $[Ag^{I}_2(\mathbf{152c})_3][SbF_6]_2$ (Figure 6.6 c, d).

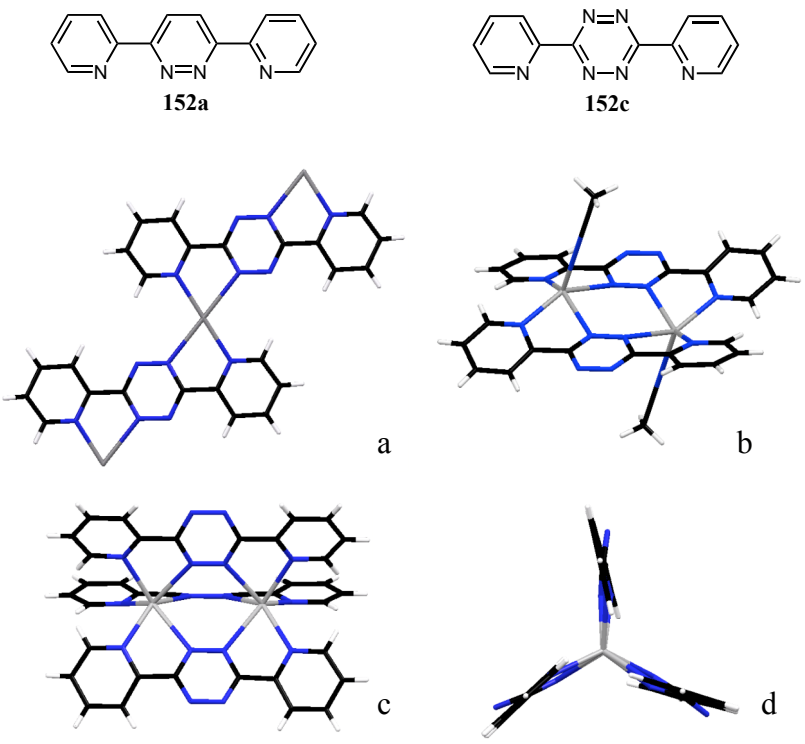

Figure 6.6 a) Crystal structure of polymeric complex $\{[Ag^{I}$ (**152c**)$][PF_6]\}_{\infty}$, b) dinuclear compound $[Ag^{I}_2$(**152c**)$_2(CH_3CN)_2][\ X]_2$, X=PF_6, SbF_6, c) side view and d) top view of propeller-type species $[Ag^{I}_2$(**152c**)$_3][X]_2$, X=PF_6, AsF_6

In the dinuclear cationic unit of $[Ag^{I}_2$(**152c**)$_2(CH_3CN)_2]^{+}$, each molecule of **152c** is bis-chelating to two Ag^{I} ions and is in the *syn* orientation. The coordination geometry around each Ag^{I} ion is a square-pyramidal with the two additional acetonitrile molecules positioned on opposite sides of the dinuclear structure. The cationic unit of the C_{3v} symmetrical $[Ag^{I}_2$(**152c**$)_3]^{+}$ consists of two Ag^{I} ions, each coordinated to six nitrogen atoms from three **152c** ligand moieties in a trigonal prismatic arrangement.

The formation of an unusual [2 x 2] metal ion array deviating from the general M_4L_4 stoichiometry was obtained by the Siegel group, when stoichiometric amount of bis(phenanthroline) based ligand **153b** and CuI were mixed.[15] In addition to the expected $[Cu^{I}_4$(**153b**$)_4]^{4+}$ scaffold, two additional, uncoordinated ligands **153b** were sandwiched as a results of multiple CH-N and π-π interactions (Scheme 6.2).

A number of first- and second-row transition metal ions (e.g. Mn^{II}, Co^{II}, Fe^{II}, Ni^{II}, Cu^{II}, Zn^{II}, Cd^{II}) as well as main group metal ions (e.g. Pb^{II}) have been involved in the construction of grids, with octahedrally arrangement ligand systems, containing terpyri-

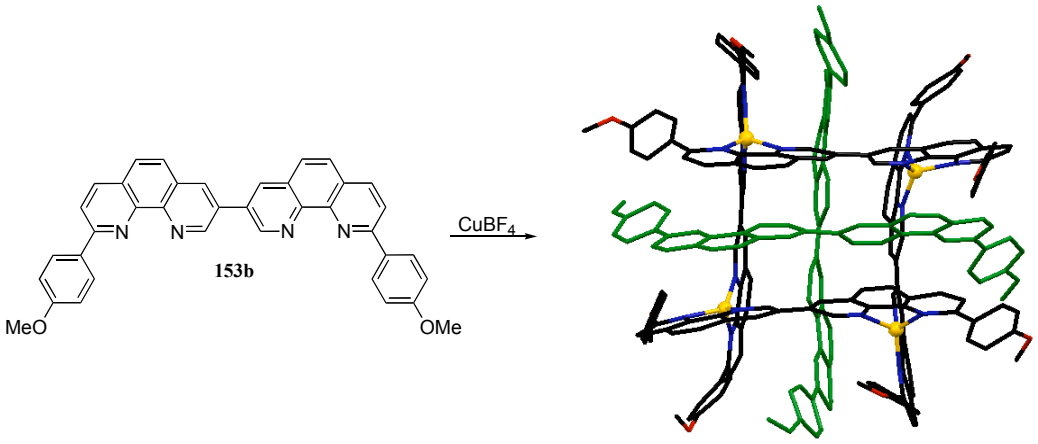

Scheme 6.2 Formation of [3 x 3] grid $[Cu^{I}_{4}(\mathbf{153b})_{6}]^{4+}$

dine-like coordination sites.[16-20]

The ability to use different transition metals in the complexation process with ligand systems such as **154a** (Figure 6.7) gives access to a wide variety of optical, electrochemical, photophysical, and magnetic properties.[21-23] Furthermore, these properties can be modulated by the use of the different substituents R_1, R_2 and R_3.

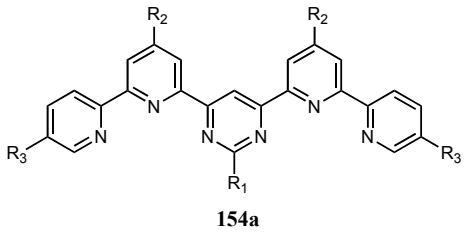

Figure 6.7 Structure of **154a**

Another type of grids results from the controlled introduction of different metal ions into the same structure. Metal ions can be introduced selectively at specific locations of the grid array. Such complexes are of great interest because of their crossover properties, resulting from the presence of different metal ions in the same architecture. The formation of the mixed ion [2 x 2] grid structures were obtained by a homochiral assembly of the ligands, containing R or S "corners" (Scheme 6.3).[24] The resulting grid is achiral in the homometallic case and chiral in the heterobimetallic case.

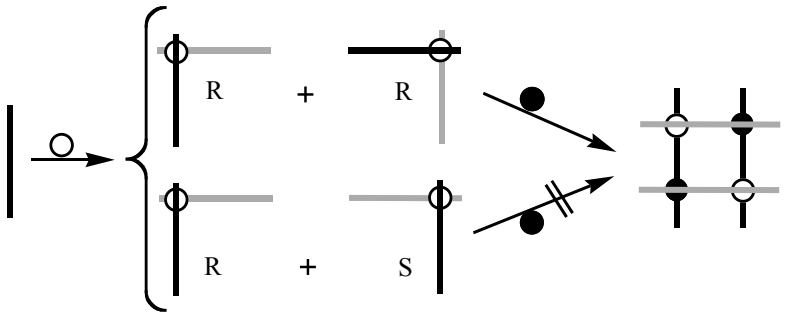

Scheme 6.3 Molecular association of a chiral heterobimetallic [2 x 2] grid from two cornerlike homochiral precursors (R + R) or (S + S) [24]

The use of two different metal ions in the construction [2 x 2] grids leads to the formation of *anti* or *syn* topoisomers. Usually it is not possible to predict which topoisomer is going to be generated. Formation of the *anti* topoisomer, with diagonally located identical metal ions was obtained selectively from the reaction two terpyridine-type ligands (e.g. **154a**) with Ru^{II} or Os^{II} (strongly coordinating metals, and lead to $[M^{II}(\mathbf{154a})_2]$). Filling two other vacant sites with a second metal ion $M^{II\prime}$ of lower coordinative binding strength lead to a heterometallic [2 x 2] complex. Formation of C_2-symmetric array (e.g. $[M^{II}{}_2M^{II\prime}{}_2(\mathbf{154a})_4]$ (Figure 6.8) was achieved by the combination of homochiral fragments.[24]

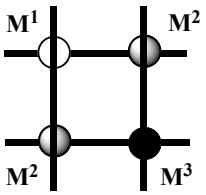

1) $M^1=M^3=Ru^{II}$ $M^2=Fe^{II}$
2) $M^1=M^3=Ru^{II}$ $M^2=Co^{II}$
3) $M^1=M^3=Os^{II}$ $M^2=Fe^{II}$
4) $M^1=M^3=Os^{II}$ $M^2=Ni^{II}$
5) $M^1=Ru^{II}$ $M^2=Fe^{II}$ $M^3=Os^{II}$

Figure 6.8 Introduction of different metals in the grid-like architecture

Such methodology, based on increasing coordinative lability of different metal ions allows one to synthesize complexes containing three different metal ions. Thus, a complex containing Fe^{II}, Ru^{II} and Os^{II} ions was detected by addition of Fe^{II} ions to the solution, containing an equimolar amount of $[Ru^{II}(\mathbf{154a})_2]$ and $[Os^{II}(\mathbf{154a})_2]$ species. Formation of grid-like architecture with three different metal ions was determined by FAB-MS and ^{1}H-NMR spectroscopy.[24]

6.2.2 [3 x 3] Metal Ion Arrays

The reaction of six molar equivalents of the tritopic ligand **152b** with nine molar equivalents of silver (I) salts resulted in a quantitative formation of the first [3 x 3] grid, $[Ag^{I}_{9}(\mathbf{152b})_{6}][OTf]_{9}$ (Scheme 6.4).[8] The whole structure is deviating from the rectangular geometry, forming a trapezoid with Ag-Ag-Ag angles of about 73° and 107°.

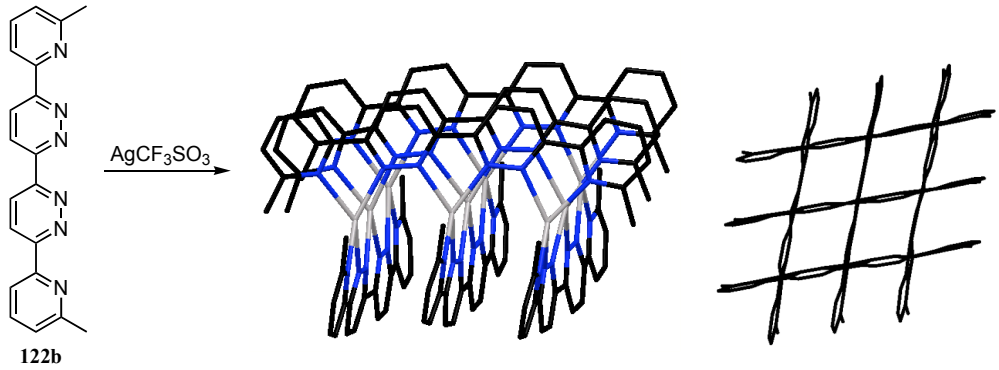

Scheme 6.4 [3 x 3] grid-type structure of $[Ag^{I}_{9}(\mathbf{152b})_{6}]^{9+}$

The reaction of tritopic ligand **154b** with a number of octahedrally coordinating metal ions give incomplete metal ion arrays.[25a] Formation of [3 x 3] grid-like species were detected by electrospray mass spectrometry in solution from the reaction of **154b** with large metal ions, such as Pb^{II} or Hg^{II}.[25b] Such assembling behavior of **154b** can be explained by the structural features of the ligand, binding subunit of which possessing the pinching on coordination with metal ions.[25c] Therefore, the use of Pb^{II} or Hg^{II}, which are ascribed as a large ions, would bring less pinching in the system, resulting in a less strained grid architecture. The formation of [3 x 3] grids was also detected by use of polytopic ligands **155** with Mn^{II}, Cu^{II}, Zn^{II}, Ni^{II}, Co^{II}, and Fe^{III} metal salts.[26,27]

6.2.3 [4 x 4] Metal Ion Arrays

The reaction of eight equivalents of the tridentate ligand **154c** and sixteen equivalents of Pb^{II} salts resulted in the quantitative formation of the largest [4 x 4] square grid reported to date $[Pb^{II}_{16}(\mathbf{154c})_{8}][OTf]_{32}$.[17,19] This complexation process included 24

components and leads to the formation of 96 new coordination bonds in a single operation.

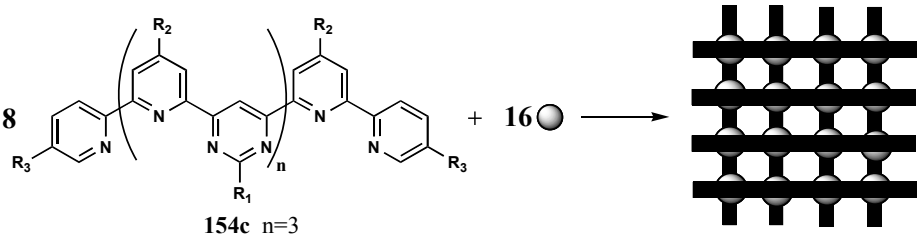

Scheme 6.5 Formation of [4 x 4] grid structure of $[Pb^{II}_{16}(\mathbf{154c})_8]$ framework[17,19]

Yellow crystals of [4 x 4]Pb_{16} array were obtained from an acetonitrile/ benzene/isopropyl ether mixture and consists of 8 **154c** ligands, 16 Pb^{II} ions, 16 triflate counterions, and 8 water molecules. According to the X-ray analysis, each Pb^{II} atom is coordinated by two ligands **154c**, ordered in a perpendicular arrangement. The whole complex is presented by disposed sets of four outer and four inner ligands, forming a set of four [2 x 2] subgrids (Scheme 6.5). Face-to-face stacking arrangements of the four inner ligands shows π–π stacking overlap between the aromatic groups with average stacking distance of 3.62 Å. The coordination geometry around each Pb^{II} atoms is best described as distorted octahedral, with an average Pb-Pb distance of 6.3 Å and average inner angles of 89.5°.

6.2.4 Rectangular [n x m] Metal Ion Arrays with (n ≠ m)

Complexation of two ligands having different number of coordination sites can lead to a mixed homo- and heteroleptic rectangular grids, as seen in the reaction of the di- and tritopic ligands **152a** and **152b** with $AgCF_3SO_4$.[28a] The reaction of two different ligands with metal salt in a 3:2:6 stoichiometric ratio resulted in a formation of [2 x 3] grid as the major compound (90%), together with minor amounts of a [2 x 2] and a [3 x 3] grid (8% and 2%, respectively, Scheme 6.6).

Such selectivity could be explained by the fact that there is lower stability in the metal-ligand coordination bonds of a [3 x 3] grid. The formation of a [2 x 3] grid was

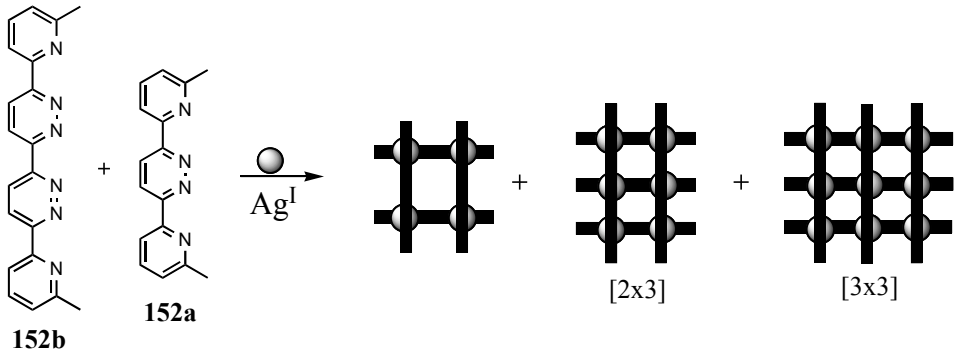

Scheme 6.6 Synthesis of a [2 x 3] array from three ditopic ligands **152a**, two tritopic ligands **152b** and six Ag^{I} metal ions.[28]

confirmed by X-ray crystal structure analysis. The crystal consist of $[Ag_6(\mathbf{152a})_3(\mathbf{152b})_2]^{6+}$ ions, triflate anions, as well as solvent and water molecules. The silver ions presented in the [2 x 3] grid are on a rhombohedrally distorted rectangular matrix.[28] Rectangular [2 x 2] M^{II} complexes can be also formed by using ligands of type **156** with different bridging groups.[27a,28b,29]

6.3 Mechanistic Features of the Complexation Process

Mechanistic investigations of the complexation processes were carried out in solution and the solid-state, using different grid-like structures. For the purpose of identifying the nature of the species formed during the assembling of different grid-type structures, complexation reactions of the bis(bipyridine)-based ligand **153a** with Cu^{I} ions were investigated. During this investigation three major species were indicated: a double-helical architecture, a triangular complex, and square [2 x 2] grid complexes (Scheme 6.7). The same results were obtained for ligand systems **157** with Zn^{II} ions, which shows the presence of triangular and tetranuclear reaction products.[30]

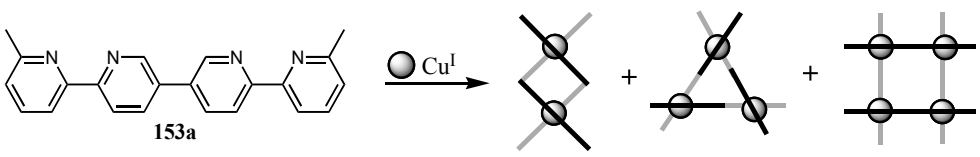

Scheme 6.7 Formation of a mixture of the double-helical, triangular, and square [2 x 2] grid complexes from **153a** and CuI ions[30]

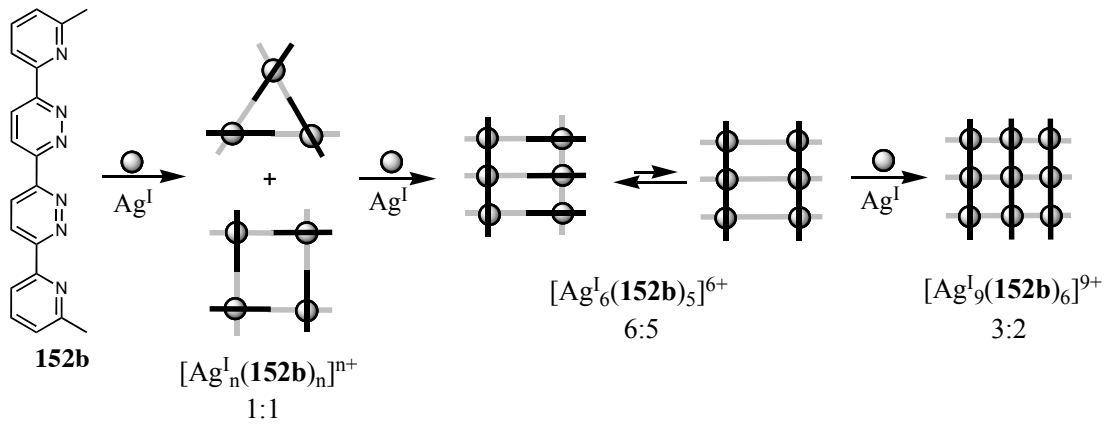

Scheme 6.8 Complexation pathway for the [3 x 3] array[31] $[Ag^{I}_{9}(\mathbf{152b})_{6}]^{9+}$

Formation of the [3 x 3] $[Ag^{I}_{9}(\mathbf{152b})_{6}]^{9+}$ metal ion array was monitored by NMR spectroscopy, and shows the formation of number intermediates.[31] Several unidentified species were observed until Ag^{I}/(**152b**) ≈ 1:1 ratio was reached. This ratio shows the presence of two main complexes of $[Ag^{I}_{n}(\mathbf{152b})_{n}]^{n+}$ with *transoid* arrangement of ligands. The mixture containing ≈ 6:5 stochiometric amounts of Ag^{I}/(**152b**) shows the presence of $[Ag^{I}_{6}(\mathbf{152b})_{5}]^{6+}$ species, with three ligands in *transoid* form and two ligands arranged in *cisoid* form. Additional equivalents of AgI ions lead to the $[Ag^{I}_{9}(\mathbf{152b})_{6}]^{9+}$ grid, formation of which goes through a $[Ag^{I}_{6}(\mathbf{152b})_{5}]^{6+}$ species with all ligands in the *cisoid* form (Scheme 6.8).

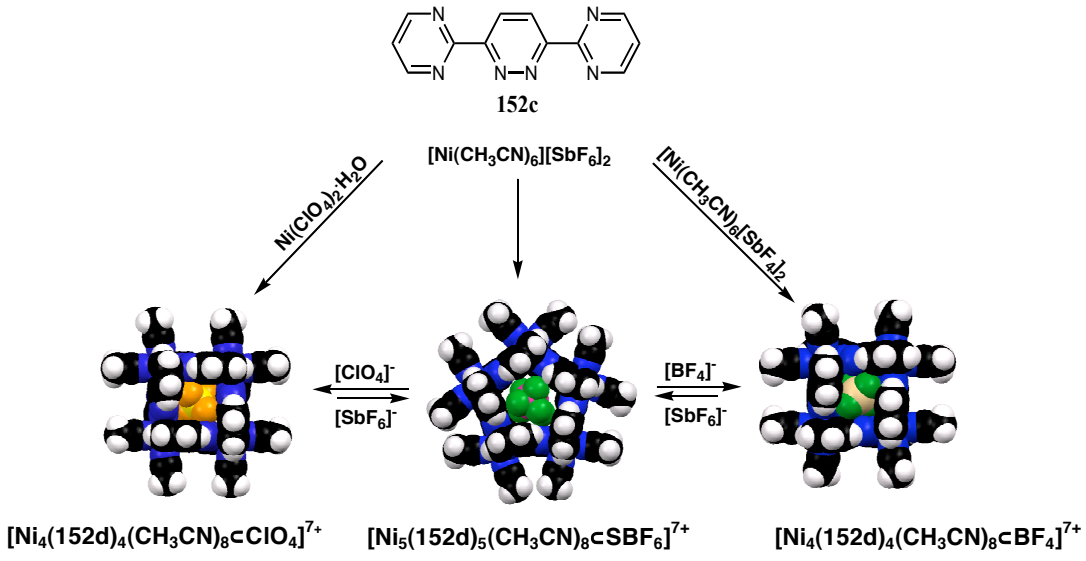

Scheme 6.9 Templating effect of the anions BF_4^- (ClO_4^-) and SbF_6^- on the formation of metallosupramolecular nanoarchitectures with the ligand **152d**

The templating effect of the anions in the construction of metallosupramolecular structures was investigated by Dunbar group.[32] The reaction of Ni^{II} or Zn^{II} ions with ligand **152c** in the presence of tetrahedral $[BF_4]^-$ or $[ClO_4]^-$ anions form [2 x 2] grid-like complexes (Scheme 6.9). The coordination geometry around each metal ion is octahedral, and included two ligands coordinated in a bis-chelating fashion, and two acetonitrile and/or water molecules. However, the reaction of **152c** with Ni^{II} salts, containing large counterion such as $[SbF_6]^-$, favors exclusive formation of a molecular pentagon,[33] which is less stable than a molecular square, and can be easily converted in to the [2 x 2] grid by addition of excess $[BF_4]^-$, $[ClO_4]^-$, and $[I]^-$ anions. Heating and longer reaction time in the presence of excess $[SbF_6]^-$ ions allows partial convertion of the Ni^{II} square in to the less stable pentagon.

6.4 Conclusion

Transition metal coordination chemistry allows one to synthesize grid-type complexes, comprising of a two-dimensional network and consisting from a metal ions and organic ligands, connected in orthogonal arrangement. Above discussed are synthesis and mechanistic features of the complexation processes, which lead to the formation of [2 x 2], [3 x 3], [4 x 4], rectangular [n x m] and multicomponent (containing different metal ions) grids. Unique optical, electrochemical, and magnetic properties of these structures have potential importance for nanothechnology, particularly in the area of information storage and processing. The ability to synthesize molecular grids, containing of different metal ions in a particular arrangement, allows design of new materials with specific electrochemical, photochemical and magnetic properties.

6.5 References

1. Leininger, S.; Olenyuk, B.; Stang, P. J. *Chem. Rev.* **2000**, *100*, 853.
2. Lehn, J-M. *Supramolecular Chemistry: Concepts and Perspectives*; VCH: Weinheim **1995**.
3. Steed, J. W.; Atwood, J. L. *Supramolecular Chemistry*; John Wiley: New York **2001**.
4. a) Davis, A. V.; Raymond, K. N. *J. Am. Chem. Soc.* **2005**, *127*, 7912; b) Mukherjee, P. S.; Min, K. S.; Arif, A. M.; Stang, P. J. *Inorg. Chem.* **2004**, *43*, 6345; c) Atwood, J. L.; Barbour, L. J.; Dalgarno, S. J.; Hardie, M. J.; Raston, C. L.; Webb, H. R. *J. Am. Chem. Soc.* **2004**, *126*, 13170; d) Uppadine, L. H.; Lehn, J-M. *Angew. Chem., Int. Ed.* **2004**, *43*, 240; e) Ruben, M.; Rojo, J.; Romero-Salguero, F. J.; Uppadine, L. H.; Lehn, J-M. *Angew. Chem., Int. Ed.* **2004**, *43*, 3644; f) Sun, S-S.; Stern, C. L.; Nguyen, S-B. T.; Hupp, J. T. *J. Am. Chem. Soc.* **2004**, *126*, 6314; g) Kryschenko. Y. K.; Seidel, S. R.; Muddiman, D. C.; Nepomuceno, A. I.; Stang, P. J. *J. Am. Chem. Soc.* **2003**, *125*, 9647.
5. Constable, E. C. *Tetrahedron* **1992**, *48*, 10013; Potts, K. T.; Keshavarz-K, M.; Tham, F. S.; Abruna, H. D.; Arana, C. *Inorg. Chem.* **1993**, *32*, 4436.
6. a) Baxter, P. N. W.; Lehn, J-M.; De Cian, A.; Fischer, J. *Angew. Chem.* **1993**, *105*, 92; *Angew. Chem. Int. Ed. Engl.* **1993**, *32*, 69; b) Fujita, M.; Nagao, S.; Ogura, K. *J. Am. Chem. Soc.* **1995**, *117*, 1649.
7. Sleiman, H.; Baxter, P. N. W.; Lehn, J-M.; Rissanen, K. *J. Chem. Soc. Chem. Commun.* **1995**, 715.
8. Baxter, P. N. W.; Lehn, J-M.; Fischer, J.; Youinou, M-T. *Angew. Chem.* **1994**, *106*, 2432; *Angew. Chem. Int. Ed. Engl.* **1994**, *33*, 2284.
9. Youinou, M-T.; Rahmouni, N.; Fischer, J.; Osborn, J. A. *Angew. Chem.* **1992**, *104*, 771; *Angew. Chem. Int. Ed. Engl.* **1992**, *31*, 133.
10. Manoj, E.; Kupur, P.; Fun, H-K.; Punnoose, A. *Polyhedron* **2007**, *26*, 4451-4462.
11. a) Youinou, M. T.; Rahmouni, N.; Fischer, J.; Osborn, J. A. *Angew. Chem.* **1992**, *104*, 771-773; *Angew. Chem. Int. Ed. Engl.* **1992**, *31*, 733-735; b) Baxter, P. N. W.; Lehn, J-M.; Kneisel, B. O.; Fenske, D. *Chem. Commun.* **1997**, 2231-2232.
12. Constable, E. C.; Housecroft, C. E.; Kariuki, B. M.; Neuburger, M.; Smith, C. B.

Aust. J. Chem. **2003**, *56*, 653-655.

13. Constable, E. C.; Housecroft, C. E.; Neuburger, M.; Reymann, S.; Schaffner, S. *Chem. Commun.* **2004**, 1056-1057.
14. Schottel, B. L.; Chifotides, H. T.; Shatruk, M.; Chouai, A.; Perez, L. M.; Bacsa, J.; Dunbar, K. *J. Am. Chem. Soc.* **2006**, *128*, 5895.
15. Toyota, S.; Woods, C. R.; Benaglia, M.; Haldimann, R.; Wärnmark, K.; Hardcastle, K.; Siegel, J. S. *Angew. Chem.* **2001**, *113*, 773-776; *Angew. Chem. Int. Ed.* **2001**, *40*, 751-754.
16. a) Rojo, J.; Romero-Salguero, F. J.; Lehn, J-M.; Baum, G.; Fenske, D. *Eur. J. Inorg. Chem.* **1999**, 1421-1428; b) Patroniak, V.; Baxter, P. N. W.; Lehn, J-M.; Kubicki, M.; Nissinen, M.; Rissanen, K.; *Eur. J. Inorg. Chem.* **2003**, 4001-4009.
17. Barbiou, M.; Lehn, J-M. *J. Am. Chem. Soc.* **2003**, *125*, 10257-10265.
18. Hanan, G. S. PhD thesis, Universitè Louis Pasteur, Strasbourg, **1995**.
19. Garcia, A. M.; Romero-Salguero, F. J.; Bassani, D.; Lehn, J-M.; Baum, G.; Fenske, D. *Chem. Eur. J.* **1999**, *5*, 1803-1808.
20. a) Hausmann, J.; Jameson, G. B.; Brooker, S. *Chem. Commun.* **2003**, 2992-2993; b) Cati, D. S.; Ribas, J.; Ribas-Arino, J.; Stoeckli- Evans, H. *Inorg. Chem.* **2004**, *43*, 1021-1030.
21. a) Ruben, M.; Breuning, E.; Gisselbrecht, J.-P.; Lehn, J.-M. *Angew. Chem.* **2000**, *112*, 4312-4315; *Angew. Chem. Int. Ed.* **2000**, *39*, 4139-4142; b) Ruben, M.; Breuning, E.; Barboiu, M.; Gisselbrecht, J.-P.; Lehn, J.-M. *Chem. Eur. J.* **2003**, *9*, 291-299; Bassani, D. M.; Lehn, J.-M.; Serroni, S.; Puntoriero, F.; Campagna, S. *Chem. Eur. J.* **2003**, *9*, 5936-5946.
22. Breuning, E.; Ruben, M.; Lehn, J.-M.; Renz, F.; Garcia, Y.; Ksenofontov, V.; Gütlich, P.; Wegelius, E.; Rissanen, K.; *Angew. Chem.* **2000**, *112*, 2563-2566; *Angew. Chem. Int. Ed.* **2000**, *39*, 2504-2507.
23. Semenov, A.; Spatz, J. P.; Müller, M.; Lehn, J.-M.; Sell, B.; Schubert, D.; Weidl, C. H.; Schubert, U. S. *Angew. Chem.* **1999**, *111*, 2701-2705; *Angew. Chem. Int. Ed.* **1999**, *38*, 2547-2550.
24. a) Bassani, D. M.; Lehn, J-M.; Fromm, K.; Fenske, D. *Angew. Chem.* **1998**, *110*, 2534-2537; *Angew. Chem. Int. Ed.* **1998**, *37*, 2364-2367.

25. a) Breuning, E.; Hanan, G. S.; Romero-Salguero, F. J.; Garcia, A. M.; Baxter, P. N. W.; Lehn, J-M.; Wegelius, E.; Rissanen, K.; Nierengarten, H.; van Dorsselaer, A. *Chem. Eur. J.* **2002**, *8*, 3458-3466; b) Nierengarten, H.; Leize, E.; Breuning, E.; Garcia, A.; Romero-Salguero, F.; Rojo, J.; Lehn, J-M.; van Dorsselaer, A. *J. Mass Spectrom.* **2002**, *37*, 56-62; c) Hanan, G. S.; Arana, C. R.; Lehn, J-M.; Baum, G.; Fenske, D. *Chem. Eur. J.* **1996**, *2*, 1292-1299.

26. a) Maverick, A. W.; Klavetter, F. E. *Inorg. Chem.* **1984**, *23*, 4129-4135; b) Köhler, R.; Kirmse, B.; Richter, R.; Sieler, J.; Hoyer, E.; Beyer, L. *Z. Anorg. Allg. Chem.* **1986**, *537*, 133-144.

27. a) Mathews, C. J.; Avery, K.; Xu, Z.; Thompson, K. L.; Zhao, L.; Miller, D. O.; Biradha, K.; Poirier, K.; Zaworotko, M. J.; Wilson, C.; Goeta, A. E.; Howard, J. A. K. *Inorg. Chem.* **1999**, *38*, 5266-5281; b) Zhao, L.; Matthews, C. J.; Thompson, L. K.; Heath, S. L. *Chem. Commun.* **2000**, 265-266; c) Zhao, L.; Xu, Z, Thompson, L. K.; Miller, D. O. *Polyhedron* **2001**, *20*, 1359-1364.

28. a) Baxter, P. N. W.; Lehn, J-M.; Baum, G.; Fenske, D. *Angew. Chem.* **1997**, *109*, 2067-2070; *Angew. Chem. Int. Ed. Engl.* **1997**, *36*, 1978-1981; b) Schmittel, M.; Kalsani, V.; Fenske, D.; Wiegrefe, A. *Chem. Commun.* **2004**, 490-491.

29. Thompson, L. K. *et al. J. Solid State Chem.* **2001**, *159*, 308-320.

30. Bark, T.; Düggeli, H.; Stoeckli-Evans, von Zelevsky, A. *Angew. Chem.* **2001**, *113*, 2924-2927; *Angew. Chem. Int. Ed.* **2001**, *40*, 2848-2850.

31. a) Marquis, A.; Kintzinger, J-P.; Graff, R.; Baxter, P. N. W.; Lehn, J-M. *Angew. Chem.* **2002**, *114*, 2884-2888; *Angew. Chem. Int. Ed.* **2002**, *41*, 2760-2764; b) Marquis, A.; Kintzinger, J-P.; Graff, R.; Baxter, P. N. W.; Lehn, J-M. *Angew. Chem.* **2002**, *114*, 3888; *Angew. Chem. Int. Ed.* **2002**, *41*, 3738.

32. a) Campos-Fernandez, C. S.; Clerac, R.; Dunbar, K. R. *Angew. Chem.* **1999**, *111*, 3685-3688; *Angew. Chem. Int. Ed. Engl.* **1999**, *38*, 3477-3479; b) Bu, X-H.; Morishita, H.; Tanaka, K.; Biradha, K.; Furusho, S.; Shionoya, M. *Chem. Commun.* **2000**, 971-972.

33. Campos-Fernandez, C. S.; Clerac, R.; Koomen, J. M.; Russell, D. H.; Dunbar, K. R. *J. Am. Chem. Soc.* **2001**, *123*, 773-774.

Chapter 7. Synthesis and Study of Silver (I) and Copper (I) Complexes of Diazafluoranthene Derivatives

7.1 Introduction

Transition metal coordination chemistry provides a powerful methodology for the construction of a various metallosupramolecular architectures. Grid-like complexes are of particular interest due to their intriguing physicochemical and electronic properties.[1,2] Construction of such metal complexes is a subject of study of many research groups and is in an active development stage.[3-5] Special design of the initial ligand systems and selection of appropriate metal salts are the main requirement for the successful synthesis of grids.

In the current work, complexation reactions of 7,10-disubstituted 8,9-diazafluoranthene derivatives **158-160** (Figure 7.1) with $[Cu(CH_3CN)_4][PF_6]$ and three different silver salts Ag[X], (X = $[PF_6]^-$, $[SbF_6]^-$, $[CB_{11}HCl_{11}]^-$) have been investigated. Synthesis of diazafluoranthene derivatives were carried out by [2 + 4] cycloaddition reactions of 4,7-di-*tert*-butylacenaphthylene and 3,6-disubstituted 1,2,4,5-tetrazines.[6] The reaction of 7,10-disubstituted diazafluoranthene derivatives with silver (I) salts Ag[X] afforded complexes of four different leitmotifs. An expected grid-like architecture was isolated by the reaction of 2,5-di-*tert*-butyl-7,10-di-(pyrimidin-2-yl)-8,9-diazafluoranthene **159** with $[Cu(CH_3CN)_4][PF_6]$.

7.2 Ligand design

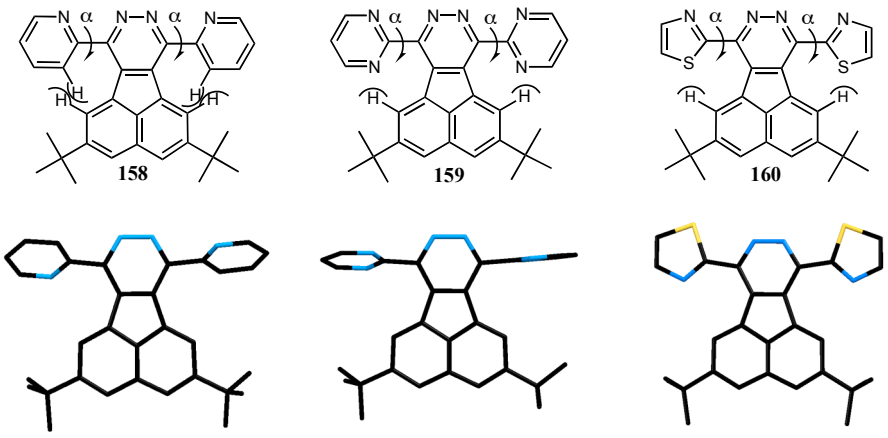

Figure 7.1 Structures of diazafluoranthene derivatives, involved in the complexation reactions

Considering that the formation of grid-type architectures is favored by a planar geometry of the initial ligand system, we first examined the structure of ligands **158-160** (Figure 7.1). In the case of compound **158** steric repulsion between hydrogen atoms in pyridyl and acenaphtylene rings would force pyridyl ring out of the pyridazine plane, leading to $\alpha > 0°$. Therefore, compound **158** was not anticipated to form grid-type complexes. On the other hand, reduced steric *H*–heterocycle interactions in **159** and **160** make these ligands attractive for [2 x 2] molecular association.

7.3 NMR and Mass spectrometry data

The reaction of stoichiometric amounts of 2,5-di-*tert*-butyl-7,10-di(pyridin-2-yl)-8,9-diazafluoranthene **158** with $[Cu(CH_3CN)_4][PF_6]$ in acetone-d_6 and three different silver salts Ag[X] in acetonitrile-d_3 or dichloromethane-d_2 affords complexes of three structural motifs (Scheme 7.1). ^{1}H-NMR spectra of these reactions indicated quantitative conversion of all ligands to the corresponding complexes.

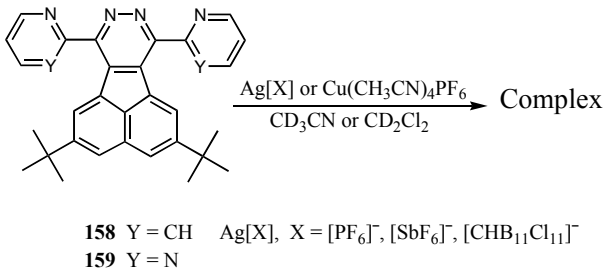

Scheme 7.1 Synthesis of silver (I) and copper (I) complexes of **158**, **159**

ESI MS data of copper (I) complexes exhibits the highest *m/z* ion signal at 1476.4, ascribed to $[Cu(\mathbf{158})_3+H]^+$, and ion signals at *m/z* 534.5, 574.5, 769.3, 1004.0 and 1211.7, which correspond to $[Cu_2(\mathbf{158})_2]^{2+}$, $[Cu(\mathbf{158})+CH_3CN]^+$, $[Cu_2(\mathbf{158})_3]^{2+}$, $[Cu(\mathbf{158})_2]^+$, $[Cu_2(\mathbf{158})_2PF_6]^+$ respectively (Figure 7.2). The mass spectra of the silver (I) complexes showed a similar peak distribution with the exception of ion signals at *m/z* 733.9 in the case of X = $CHB_{11}Cl_{11}$, which corresponds to $[Ag_3(\mathbf{158})_4]^{3+}$, and *m/z* 578.2, which was assigned to the parent ion $[Ag_2(\mathbf{158})_2]^{2+}$ (X = PF_6, SbF_6, Figure 7.3). The experimental and theoretical isotopic distribution patterns correlated well. Ion signals

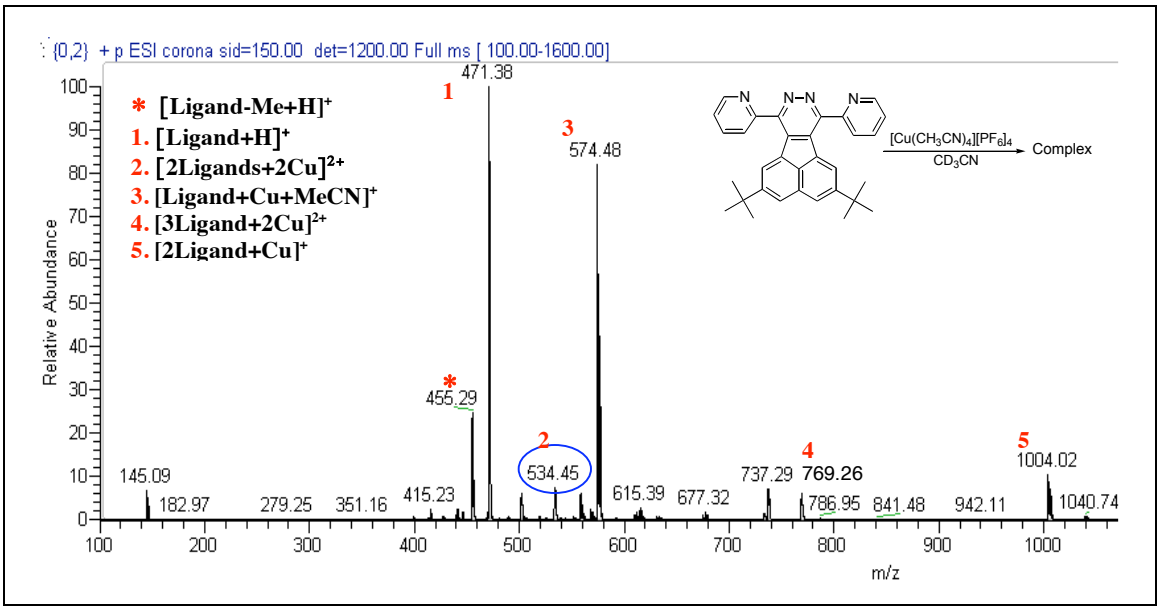

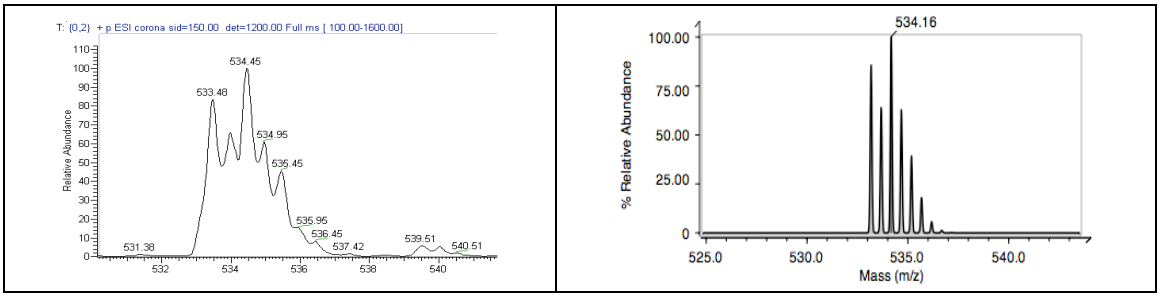

Exp.	533.48	533.98	534.45	534.95	535.45	535.95	536.45	537.42
Calc.*	533.19	533.73	534.16	534.71	535.19	535.68	536.19	537.18

*for $[C_{64}H_{60}Cu_2N_8]^{2+}$

Figure 7.2 MS-Spectrum of $[Cu_x(\mathbf{158})_x][PF_6]_x$ complex and experimental and theoretical isotopic distribution pattern of ion signal m/z 534.45

were also observed for $[Ag(\mathbf{158})+MeCN]^+$, $[Ag_2(\mathbf{158})_3]^{2+}$ and $[Ag(\mathbf{158})_2]^+$ at *m/z* 618.4, 813.3 and 1049.7 respectively, and $[Ag(\mathbf{158})_2PF_6]^+$, $[Ag(\mathbf{158})_2SbF_6]^+$ at *m/z* 1301.4, 1391.3.

^{1}H-NMR spectra of the reaction of 2,5-di-*tert*-butyl-7,10-di-(pyrimidin-2-yl)-8,9-diazafluoranthene (**159**) with $[Cu(CH_3CN)_4][PF_6]$ and $AgPF_6$ (or $AgSbF_6$) have shown quantitative conversion of **159** to the corresponding metal complexes. The ESI MS data of silver (I) complexes in acetonitrile-d_3 exhibit a peak at *m/z* 620.5 with appropriate isotopic distributions, that corresponds to $[Ag_2(\mathbf{159})_2]^{2+}$. Other signals were observed at *m/z* 816.5 and 1054.0, corresponding to $[Ag_2(\mathbf{159})_3]^{2+}$ and $[Ag(\mathbf{159})_2]^+$ respec-

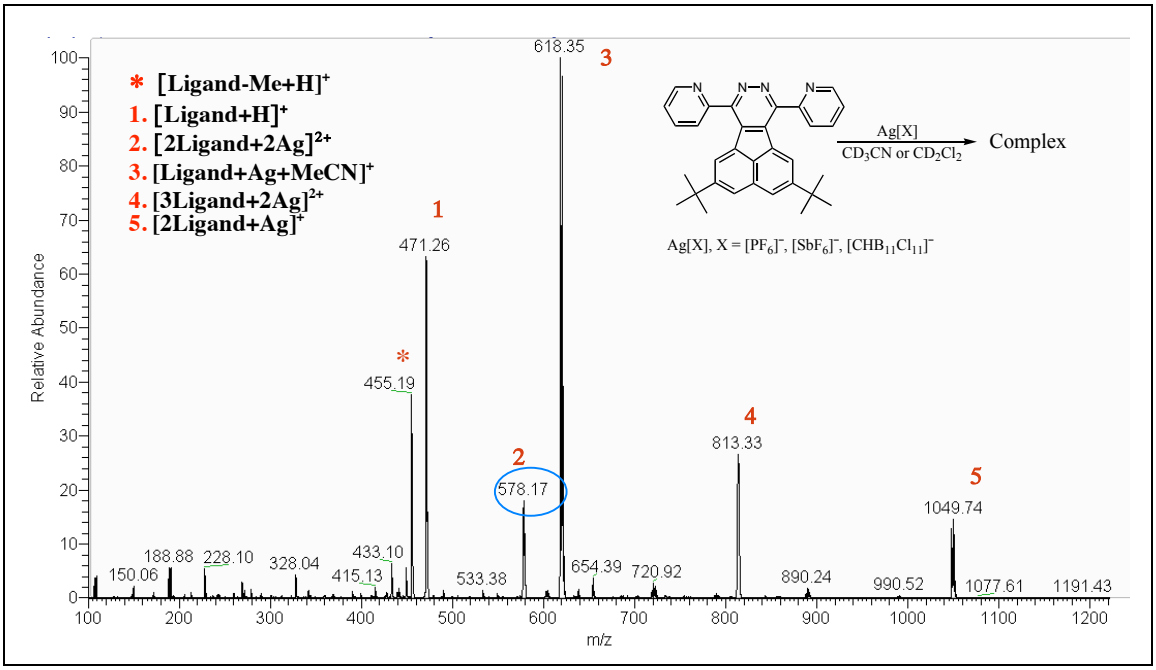

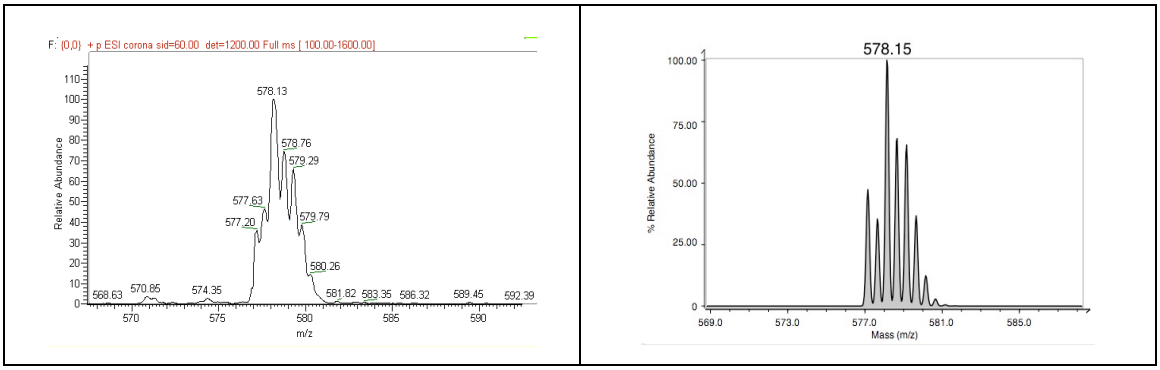

Exp.	577.20	577.63	578.13	578.76	579.29	579.79	580.26
Calc.*	577.15	577.65	578.15	578.66	579.15	579.66	580.16

*for $[C_{64}H_{60}Ag_2N_8]^{2+}$

Figure 7.3 MS-Spectrum of $[Ag_x(\mathbf{158})_x][Y]_x$, Y = $[PF_6]^-$, $[SbF_6]^-$. The experimental and theoretical isotopic distribution pattern of ion signal m/z 578.1

tively, and *m/z* 1305.6 and 1397.8, which correspond to the ion clusters $[Ag_2(\mathbf{159})_2PF_6]^+$ and $[Ag_2(\mathbf{159})_2SbF_6]^+$. A dark red solution was obtained from the reaction of **159** with equimolar amounts of $[Cu(CH_3CN)_4][PF_6]$ in acetone-d_6. The MS data of the this solution contains ion signals for the species $[Cu_2(\mathbf{159})_2]^{2+}$, $[Cu_2(\mathbf{159})_3]^{2+}$, $[Cu(\mathbf{159})_2]^+$ at *m/z* 536.5,

772.5 and 1008.0 respectively (Figure 7.4). Similarly to the complexes of **158** (X = PF_6, SbF_6), there was no evidence for tetranuclear species in solution.

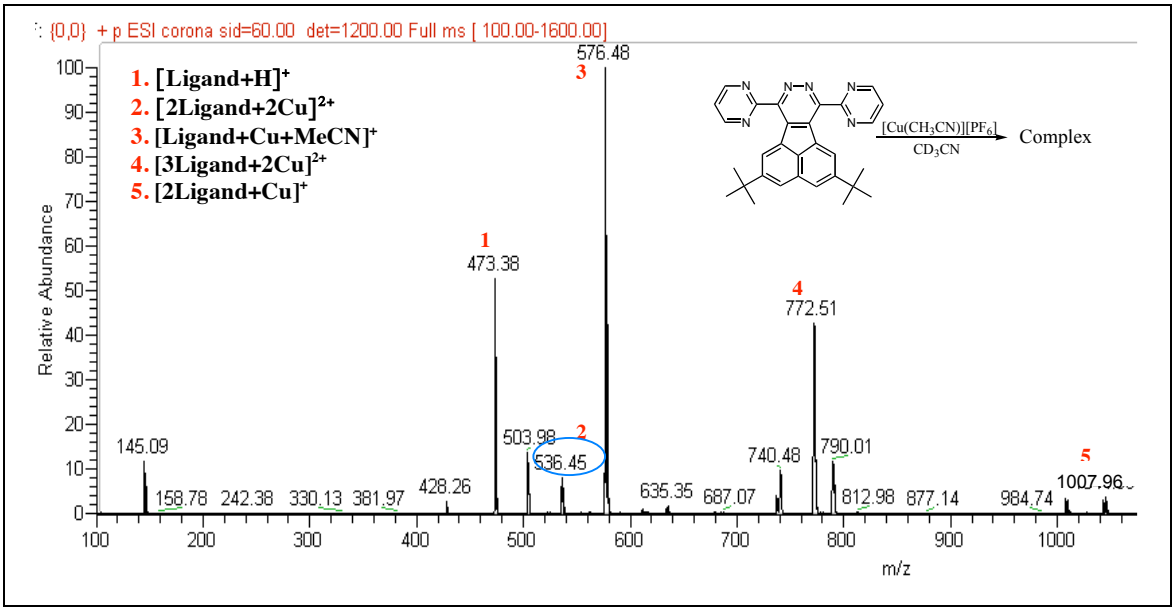

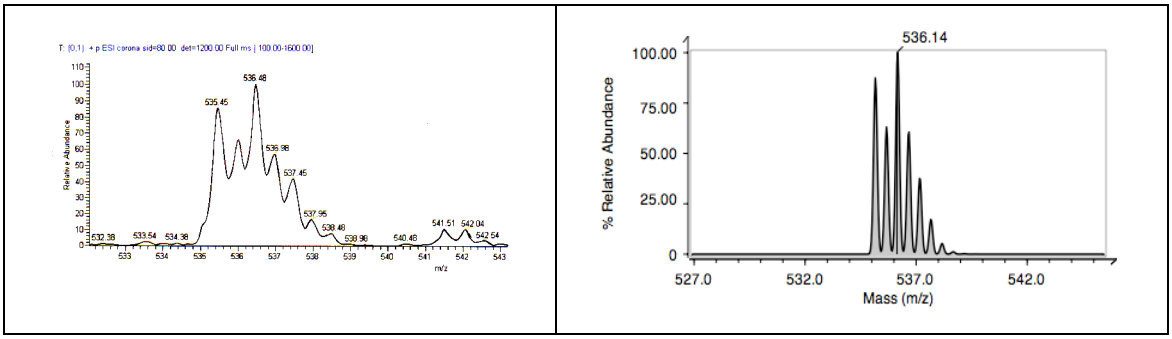

Exp.	535.45	536.01	536.48	536.98	537.45	537.98	538.51
Calc.*	535.17	535.71	536.14	536.73	537.22	537.70	538.19

*for $[C_{60}H_{56}Cu_2N_{12}]^{2+}$

Figure 7.4 MS-Spectrum of $[Cu_x(\mathbf{159})_x][PF_6]_x$ complex and experimental and theoretical isotopic distribution pattern of ion signal m/z 536.48

The reaction of 2,5-di-*tert*-butyl-7,10-di(thiazol-2-yl)-8,9-diazafluoranthene (**160**) with one equivalent of $[Cu(CH_3CN)_4][PF_6]$ in acetone-d_6 or equimolar amount of AgPF (or $AgSbF_6$) in nitromethane-d_3 proceeded smoothly to give dark red and yellow solutions respectively (Scheme 7.2). ^{1}H-NMR spectra of these solutions showed a single ligand environment. The MS data of the copper (I) complex have shown the existence of

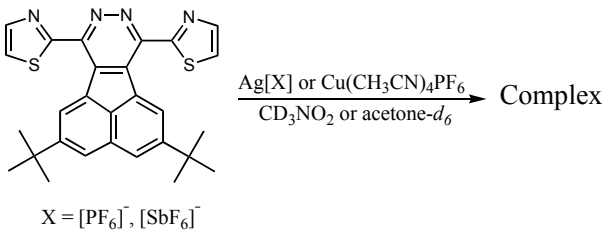

Scheme 7.2 Synthesis of silver (I) and copper (I) complexes of **160**

ion signal for the species $[Cu(\mathbf{160})+MeCN]^+$, $[Cu_3(\mathbf{160})_4]^{3+}$, $[Cu(\mathbf{160})_2+H]^+$, $[Cu_2(\mathbf{160})_2PF_6]^+$, $[Cu(\mathbf{160})_3]^+$, at *m/z* 586.4, 709.3, 1027.9, 1237.6 and 1511.3. In the case of silver (I) complexes, the highest *m/z* ion signal at 1556.8 was ascribed to $[Ag(\mathbf{160})_3]^+$. Ion signals were also obtained at *m/z* 632.3 and 1073.5, which corresponded to $[Ag(\mathbf{160})+MeCN+H]^+$ and $[Ag(\mathbf{160})_2]^+$ respectively, and *m/z* 1325.2 and 1417.7 corresponding to $[Ag_2(\mathbf{160})_2PF_6]^+$ and $[Ag_2(\mathbf{160})_2SbF_6]^+$.

7.4 Structures

According to our prediction, a [2 x 2] grid-like architecture was formed from the reaction of copper (I) salts with ligand **159**. Single crystals were obtained from an acetone/ methanol mixture and X-ray structure determination indicated the formation of a $[Cu_4(\mathbf{159})_4][PF_6]_4 \cdot 2.17H_2O$ complex (Figure 7.5, 7.6). The asymmetric unit contains two tetranuclear cations, eight PF_6^- anions; four sites fully occupied by water molecules and one site approximately one-third occupied by a water molecule. Due to the lower symmetry of the structure, there are four different Cu···Cu separations in the range 3.373-3.456 Å. Each Cu^I ion is coordinated with two different ligands **159** in a distorted tetrahedral geometry, and the Cu-N (pyridazine) and Cu-N (pyrimidine) distances are in the range of 1.980-2.047 Å and 2.021-2.056 Å respectively.

The reaction of the sterically hindered ligand **158** with one equivalent of $[Cu(CH_3CN)_4][PF_6]$ in acetone resulted in the formation of a dark red solution, from which crystals of tetrameric complex $[Cu_4(\mathbf{158})_4][PF_6]_4 \cdot 8C_3H_6O$ were obtained from the mixture acetone/pentane. The asymmetric unit contains one tetranuclear Cu-complex cation, four PF_6^- anions and an estimated eight acetone molecules, some of which are highly disordered. The solid-state structure of the cationic unit $[Cu_4(\mathbf{158})_4]^{4+}$ is presented

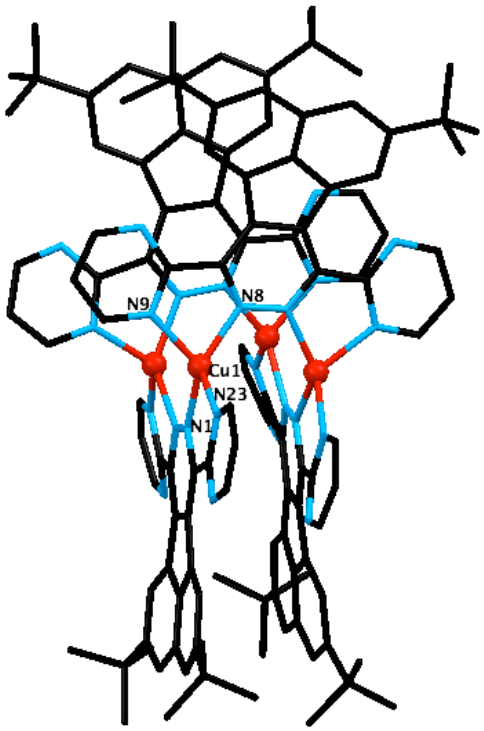

Figure 7.5 [2 x 2] grid-type structure of the cationic unit of $[Cu_4(\mathbf{159})_4]^{4+}$ present in $[Cu_4(\mathbf{159})_4][PF_6]_4$ (hydrogen atoms and counter ions have been omitted for clarity). Selected bond distances (Å) and angles (°): Cu1—N1 1.980(5), Cu1—N23 2.024(5), Cu1—N8 1.995(5), Cu1—N9 2.021(5), N1—Cu1—N23 79.9(2), N8—Cu1—N23 121.1(2), N9—Cu1—N8 80.5(2), N9—Cu1—N1 127.4 (2)

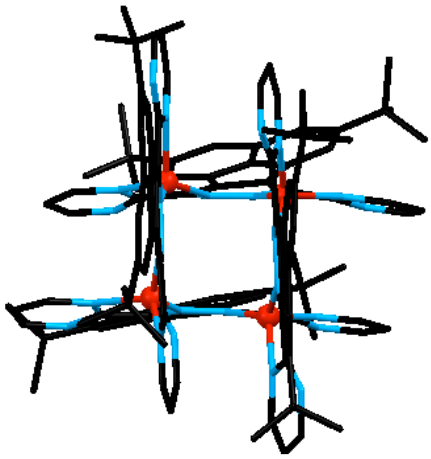

Figure 7.6 Top view of grid-type structure of $[Cu_4(\mathbf{159})_4][PF_6]_4$ (hydrogen atoms and counter ions have been omitted for clarity)

in Figure 7.7. In the cation, each Cu atom is coordinated by three different ligands in a distorted tetrahedral geometry, and the Cu-N (pyridazine) and Cu-N (pyridine) distances

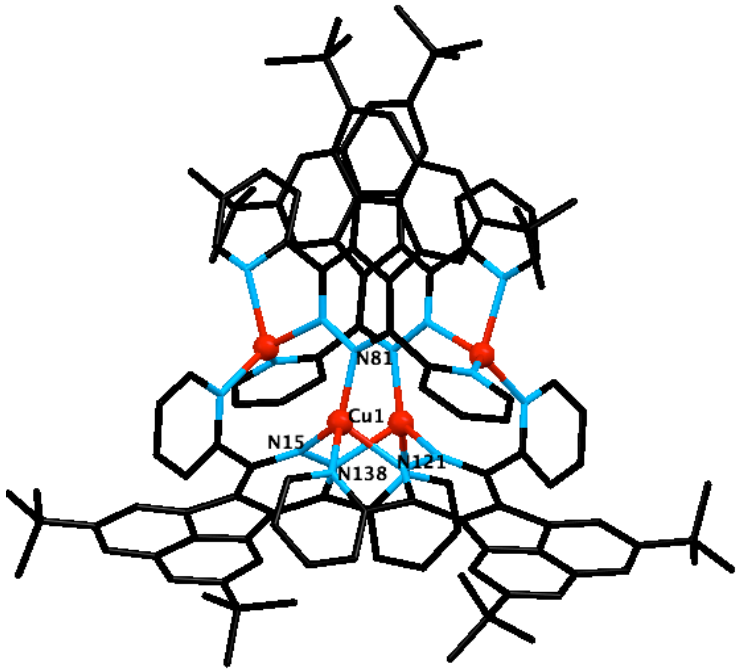

Figure 7.7 The solid state structure of the $[Cu_4(\mathbf{158})_4]^{2+}$ cation present in $[Cu_4(\mathbf{158})_4][PF_6]_4{\cdot}8C_3H_6O$ complex (hydrogen atoms, counter ions and solvent molecules have been omitted for clarity). Selected bond distances (Å) and angles (°): Cu1—N15 2.075(4), Cu1—N81 1.953(4), Cu1—N121 2.075(4), Cu1—N138 2.046(4), N15—Cu1—N138 107.5(2), N138—Cu1—N121 79.5(2), N121—Cu1—N15 94.3(2), N121—Cu1—N81 115.0(2)

are in the range of 1.940-2.089 Å and 2.013-2.120 Å respectively. Attempts to isolate crystals of the product from the reaction of $[Cu(CH_3CN)_4][PF_6]$ with **160** were unsuccessful.

The reactions of 7,10-disubstituted diazafluoranthene derivatives with silver salts Ag[X], (X = $[PF_6]^-$, $[SbF_6]^-$ and $[CB_{11}HCl_{11}]^-$) afforded complexes of three different leitmotifs. The use of 2,5-di-*tert*-butyl-7,10-di(pyridin-2-yl)-8,9-diazafluoranthene (**158**) as a ligand and $[Ag][CHB_{11}Cl_{11}]$ as the silver salt led to the formation of a dimeric complex $[Ag_2(\mathbf{158})_2][CHB_{11}Cl_{11}]_2{\cdot}4C_6H_4Cl_2{\cdot}CH_2Cl_2$, which was obtained from dichloromethane/dichlorobenzene/hexane (Figure 7.8). In this structure each molecule of **158** is bis-chelating to two Ag^I ions and is in the *syn* orientation, resulting in the formation of dinuclear cations $[Ag_2(\mathbf{158})_2]^{2+}$, (the Ag···Ag separation is 3.884 Å). The coordination geometry about each silver atom is best described as square-planar. The asymmetric unit contains two cationic pieces of $[Ag_2(\mathbf{158})_2]^{2+}$which are ordered in wave-type packing fashion. The use of silver salts with smaller anions $[PF_6]^-$, $[SbF_6]^-$ and the

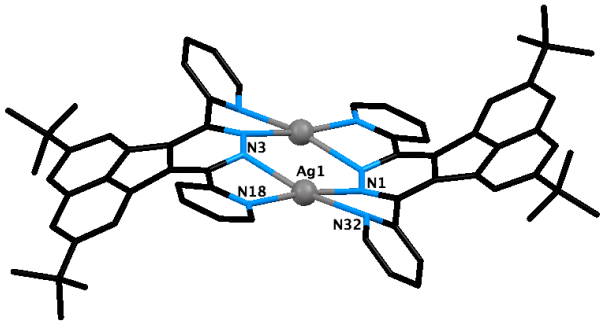

Figure 7.8 The solid state structure of the $[Ag_2(\mathbf{158})_2]^{2+}$ cation present in $[Ag_2(\mathbf{158})_2][CHB_{11}Cl_{11}]_2$ complex (hydrogen atoms, $[CHB_{11}Cl_{11}]^-$ ions and solvent molecules have been omitted for clarity). Selected bond distances (Å) and angles (°): Ag1—N1 2.240(2), Ag1—N2 2.478(2), Ag1—N18 2.254(2), Ag1—N32 2.602(2), N1—Ag1—N2 115.10(5), N1—Ag1—N32 72.55(5), N2—Ag1—N18 72.55(5), N32—Ag1—N32 103.24(5)

system acetonitrile/benzene/hexane for crystallization leads to isostructural tetrameric complexes $[Ag_4(\mathbf{158})_4][PF_6]_4$ and $[Ag_4(\mathbf{158})_4][SbF_6]_4$ that do not exhibit a grid-type architecture (Figure 7.9). In the cation, two ligands coordinate two Ag-atoms in a bidentate mode, while the other two ligands each coordinate all four Ag-atoms. As a result, each Ag-atom is coordinated by three different ligands and have found to adopt distorted tetrahedral geometry. Four silver atoms, are in a vertex positions of a quadrangle, with side distances of 5.062 and 3.876 Å.

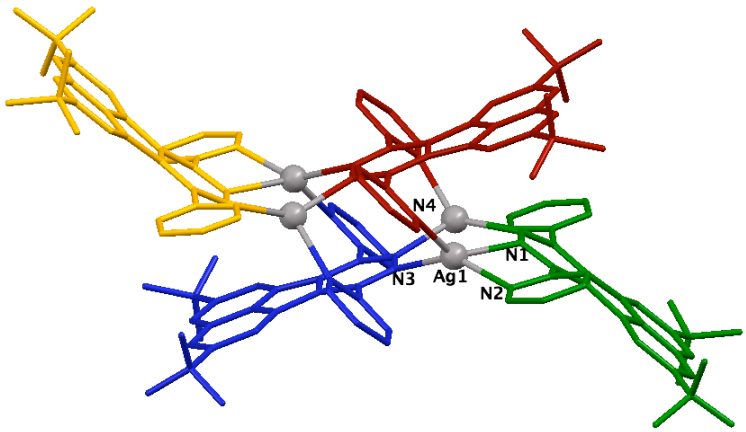

Figure 7.9 Crystal structure of tetrameric cation $[Ag_4(\mathbf{158})_4]^{4+}$ present in $[Ag_4(\mathbf{158})_4][PF_6]_4$ or $[Ag_4(\mathbf{158})_4][SbF_6]_4$ complexes (hydrogen atoms, counter ions and solvent molecules have been omitted for clarity). Selected bond distances (Å) and angles (°): Ag1—N3 2.343 (2), Ag1—N1 2.363(2), Ag1—N3 2.343(2), Ag1—N1 2.363(2), N1—Ag1—N2 72.17(8), N2—Ag1—N3 141.07(9), N3—Ag1—N4 102.67(8), N4—Ag1—N2 99.41(8)

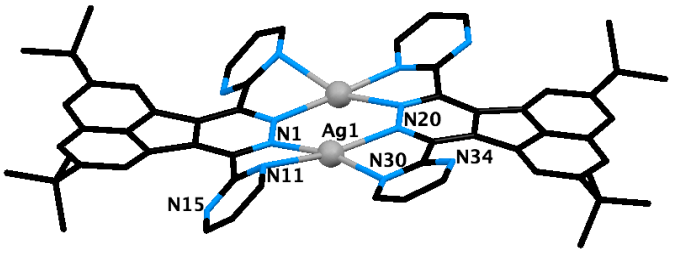

Figure 7.10 The solid state structure of the $[Ag_2(\mathbf{159})_2]^{2+}$ cation present in $[Ag_2(\mathbf{159})_2][PF_6]_2$ complex (hydrogen atoms, solvent molecules and $[PF_6]^-$ ions have been omitted for clarity). Selected bond distances (Å) and angles (°): Ag1—N1 2.362(3), Ag1—N2 2.329(3), Ag1—N7 2.601(3), Ag1—N8 2.265(3), N1—Ag1—N7 99.7(1), N1—Ag1—N2 69.7(1), N2—Ag1—N8 124.0(1), N8—Ag1—N7 69.5(1)

2,5-di-*tert*-butyl-7,10-di-(pyrimidin-2-yl)-8,9-diazafluoranthene (**159**) affords crystals of dimeric complexes with $AgPF_6$ and $AgSbF_6$. Compounds $[Ag_2(\mathbf{159})_2][PF_6]_2$ and $[Ag_2(\mathbf{159})_2][SbF_6]_2$ are isomorphous, and in both cases, the cation consists of two Ag^I ions (Ag···Ag separations are 3.543 and 3.529 Å respectively), each coordinated by four nitrogen atoms from two ligands in a square-planar arrangement (Figure 7.10). The asymmetric unit of $[Ag_2(\mathbf{159})_2][X]_2$ contains half of a dinuclear cation, which sits across a mirror plane perpendicular to the Ag···Ag axis and two disordered anions. The whole structure of $[Ag_2(\mathbf{159})_2]^{2+}$ looks similar to that which was obtained for $[Ag_2(\mathbf{158})_2]^{2+}$; however, the dimeric complex of **159** is flatter, as a result of absence of steric H-H repulsion across the bay region in the ligand.

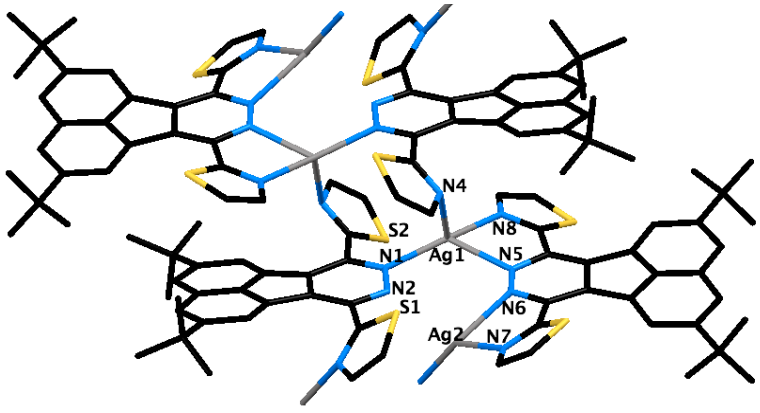

Figure 7.11 Crystal structure of polymeric cation $[Ag_2(\mathbf{160})_2]^{2+}$ present in $([Ag_2(\mathbf{160})_2]^{2+})_n \cdot 2nPF_6 \cdot nC_3H_6O$ complex (hydrogen atoms, counter ions and solvent molecules have been omitted for clarity). Selected bond distances (Å) and angles (°): Ag1—N1 2.247(7), Ag1—N8 2.258(7), Ag1—N4 2.506(8), Ag1—N5 2.348(7), Ag2—N2 2.720(7), Ag2—N6 2.371(7), Ag2—N7 2.285(7), N1—Ag1—N4 87.1(3), N4—Ag1—N8 70.7(3), N4—Ag1—N5 94.0(3), N7—Ag2—N6 70.5(3)

A single crystal of $([Ag_2(\mathbf{160})_2]^{2+})_n \cdot 2nPF_6$ was obtained from acetone/benzene/hexane. The cation $[Ag_2(\mathbf{160})_2]^{2+}$ forms a one-dimensional polymeric ribbon (Figure 7.11). The asymmetric unit contains two silver cations, two ligands, two $[PF_6]^-$ anions and one acetone molecule. Each silver atoms is coordinated by four N-atoms from three different ligands, resulting in the formation of distorted tetrahedral geometry, (although one Ag–N bond is quite long at 2.721(7) Å and each silver cation also has one very weak interaction with an S-atom (Ag–S = 3.162(3) and 3.292(3) Å).

Based on the NMR and MS data from the reaction of **160** with $AgSbF_6$ we can assume the formation of the same polymeric structure. Attempts to isolate crystals of this complex were so far unsuccessful.

7.5 Conclusion

In summary, we have investigated complexation reactions of 7,10-disubstituted diazafluoranthene derivatives with three different silver salts and $[Cu(CH_3CN)_4][PF_6]$. The expected [2 x 2] grid-like molecular association was obtained from the reaction of 2,5-di-*tert*-butyl-7,10-di-(pyrimidin-2-yl)-8,9-diazafluoranthene (**159**) with $[Cu(CH_3CN)_4][PF_6]$. In a case of sterically-hindered ligand 2,5-di-*tert*-butyl-7,10-di(pyridin-2-yl)-8,9-diazafluoranthene (**158**) tetrameric complex $[Cu_4(\mathbf{158})_4][PF_6]_4$ with butterfly geometry was obtained from the solvent system acetone/pentane. The reaction of **158** with Ag[X] salts afforded complexes of two structural motifs . The use of relatively small anions, namely $[PF_6]^-$ and $[SbF_6]^-$, leads to the formation of tetranuclear complexes $[Ag_4(\mathbf{158})_4][X]_4$, differing from grid-type structures, whereas the larger anion $[CHB_{11}Cl_{11}]^-$ favors the formation of a wave-type dimeric structure. 2,5-di-*tert*-butyl-7,10-di-(pyrimidin-2-yl)-8,9-diazafluoranthene (**159**) and 2,5-di-*tert*-butyl-7,10-di-(thiazol-2yl)-8,9-diazafluoranthene (**160**), which are less hindered in terms of *H*–heterocycle repulsion, afford crystals of dinuclear and polymeric complexes with $AgPF_6$ and $AgSbF_6$.

7.6 Experimental

7.6.1 General information

All solvents were used as purchased (p.a. grade) without further purification. Commercially available chemicals were used as purchased without further purification. Melting points were determined using a heating microscope from Christoffel Labor and Betriebstechnik and are uncorrected. Infrared spectra were recorded on a Perkin-Elmer Spectrum One FT-IR spectrometer. Compounds were measured as KBr pellets. Absorption bands are given in wave-numbers (cm^{-1}), and the intensities are characterized as follows: *s* = strong (0 - 33% transmission), *m* = medium (34 - 66% transmission), *w* = weak (67 - 100% transmission). ^{1}H- and ^{13}C-NMR spectra were recorded on Bruker Avance 400 (400 MHz), Bruker Avance 500 (500 MHz), Bruker DRX-500 (500 MHz) and Bruker DRX-600 (600 MHz) spectrometers, with the solvent as the internal standard. Data are reported as follows: chemical shift in ppm, multiplicity (*s* = singlet, *d* = doublet, *m* = multiplet, *dd* = doublet of doublets, *dt* = doublet of triplet, *etc*.), coupling constant ^{n}J in Hz, integration and interpretation. Mass spectra (MS) were obtained from Finnigan MAT95 instrument. Analytical thin layer chromatography (TLC) was performed with Macherey-Nagel POLYGRAM SIL N-HR/UV_{254} and POLYGRAM ALOX N/UV_{254}, visualization by an ultraviolet (UV) lamp (λ = 254 nm and λ = 366 nm). Column chromatography was carried out on silica gel (Merck 60 0.040 - 0.063 mm).

Complexation reactions were carried out using stoichiometric amounts of metal salts and diazafluoranthene ligands. ^{1}H-NMR of these reactions indicated full conversion to the silver and copper complexes of **158**, **159** and **160**.

7.6.2 Synthetic procedures

2,5-Di-*tert*-butyl-7,10-di(pyridin-2-yl)-8,9-diazafluoranthene (158).

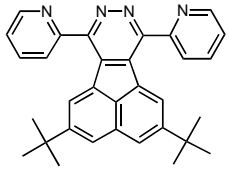

Mixture of 3,6-di(pyridin-2-yl)-1,2,4,5-tetrazine (0.36 g, 1.52 mmol) and 4,7-di-*tert*-butylacenaphthylene (0.2 g 0.76 mmol) in *p*-xylene (10 mL) was refluxed for 1.5 d. The solvent was evaporated, the residue was purified by column chromatography (silica gel, hexane/ethyl acetate 10:1) to yield of yellow crystals 0.3 g, 84%. IR (KBr): 3064*m*,

2961*s*, 2904*s*, 2886*s*, 1624*w*, 1587*s*, 1566*s*, 1552*w*, 1538*m*, 1475*s*, 1443*s*, 1434*s*, 1393*m*, 1369*s*, 1325*s*, 1290*m*, 1244*m*, 1224*m*, 1210*m*, 1155*m*, 1116*m*, 1093*s*, 1084*s*, 1041*m*, 1022*w*, 925*m*, 894*m*, 822*w*, 800*m*, 787*s*, 749*s*, 684*m*, 664*m*, 638*m*, 614*m*, 591*w*, 569*w*, 406*w*; ^{1}H-NMR (500 MHz, CD_3CN) δ 8.96 (ddd, 1H, ^{3}J = 4.8, ^{4}J = 2.0, ^{5}J = 1.2 Hz), 8.59 (d, 1H, ^{4}J = 1.6 Hz), 8.32 (dt, 1H, ^{3}J = 8.0, ^{4}J = 1.2), 8.13 (d, 1H, ^{4}J = 1.2 Hz), 8.10 (td, 1H, ^{3}J = 7.6, ^{4}J = 1.6 Hz), 7.64 (ddd, 1H, ^{3}J = 6.0, ^{3}J = 4.8, ^{5}J = 1.2 Hz), 1.43 (s, 9H); ^{13}C-NMR (400 MHz, CD_3CN), δ 157.2, 156.0, 152.3, 149.5, 138.2, 136.1, 132.3, 130.1, 130.0, 128.2, 126.9, 125.5, 125.4, 36.5, 31.8; MS (EI) m/z (%): 470.2 (M^+, 100), 455.2 (M^+-Me, 69), 439.2 (22), 414.2 (47%); HRMS (EI) calcd. for $C_{32}H_{30}N_4$: 470.2470; found: 470.2459; mp. 290 °C.

$[Ag_2(158)_2][CHB_{11}Cl_{11}]_2$. Mixture of 2,5-di-*tert*-butyl-7,10-di(pyridin-2-yl)-8,9-diaza-fluoranthene (**158)** (0.019 g, 0.04 mmol) and $AgCHB_{11}Cl_{11}$ (0.025 g, 0,04 mmol) in CD_3CN (1mL) was stirred at RT over night. ^{1}H-NMR (400 MHz, CD_2Cl_2) δ 8.67 (s, 1H), 8.23 (s, 2H), 8.05 (s, 1H), 7.90 (s, 1H), 7.56 (s, 1H), 1.39 (s, 9H); ^{13}C-NMR (400 MHz, CD_2Cl_2) δ 154.2, 153.3, 152.9, 151.9, 138.3, 137.2, 130.3, 129.9, 129.7, 129.2, 127.1, 127.0, 126.8, 36.3, 31.9; MS (EI) m/z (%): 1049.7 ($[Ag(C_{32}H_{30}N_4)_2]^+$, 2.5), 734.0 ($[Ag_3(C_{32}H_{30}N_4)_4]^{3+}$, 24), 620.3 ($[Ag(C_{32}H_{30}N_4)+CH_3CN]^+$, 17), 471.3 ($[(C_{32}H_{30}N_4)+H]^+$, 100%).

$[Ag_4(158)_4][PF_6]_4$. Mixture of 2,5-di-*tert*-butyl-7,10-di(pyridin-2-yl)-8,9-diazafluoran-thene (**158**) (0.03 g, 0.064 mmol) and $AgPF_6$ (0.016 g, 0.064 mmol) in CD_3CN (3 mL) was stirred at RT over night. ^{1}H-NMR (400 MHz, CD_3CN) δ 8.30 (d, 1H, ^{3}J = 4.4 Hz), 8.23 (d, 1H, ^{4}J = 1.2 Hz), 7.84 (d, 1H, ^{3}J = 7.6 Hz), 7.75 (s, 1H), 7.62 (dd, 1H, ^{3}J = 7.6 Hz), 7.21 (dd, 1H, ^{3}J = 5.2, ^{3}J = 6.8 Hz), 1.33 (s, 9H); ^{13}C-NMR (400 MHz, CD_3CN), δ 157.2, 156.0, 152.3, 150.0, 138.2, 136.1, 132.3, 130.1, 130.0, 128.2, 126.8, 125.5, 125.4, 36.2, 31.8; MS (EI) m/z (%): 1049.7 ($[Ag(C_{32}H_{30}N_4)_2]^+$, 14), 813.4 ($[Ag_2(C_{32}H_{30}N_4)_3]^{2+}$, 21), 618.4 ($[Ag(C_{32}H_{30}N_4)+MeCN]^+$, 100), 578.2 $[Ag_2(C_{32}H_{30}N_4)_2]^{2+}$ (18), 471.3 $[(C_{32}H_{30}N_4)+H]^+$ (46), 455.2 $[(C_{32}H_{30}N_4)-Me+H]^+$ (36%).

$[Ag_4(158)_4][SbF_6]_4$. Mixture of 2,5-di-*tert*-butyl-7,10-di(pyridin-2-yl)-8,9-diazafluoran-thene **158** (0.03 g, 0.064 mmol) and $AgSbF_6$ (0.22 g, 0.064 mmol) in CD_3CN (3 mL) was

stirred at RT over night. ^{1}H-NMR (400 MHz, CD_3CN) δ 8.30 (d, 1H, ^{3}J = 4.0 Hz), 8.22 (s, 1H), 7.85 (d, 1H, ^{3}J = 7.6 Hz), 7.76 (s, 1H), 7.62 (dd, 1H, ^{3}J = 7.2 Hz), 7.20 (dd, 1H, ^{3}J = 6.8, ^{3}J = 6.8 Hz), 1.33 (s, 9H); ^{13}C-NMR (500 MHz, CD_3CN) δ 155.2, 153.8, 153.3, 151.6, 138.5, 137.0, 130.6, 130.6, 130.0, 128.9, 127.5, 126.6, 126.4, 36.4, 31.8; MS (EI) m/z (%): 1049.7 ($[Ag(C_{32}H_{30}N_4)_2]^+$, 14), 813.4 ($[Ag_2(C_{32}H_{30}N_4)_3]^{2+}$, 21), 618.4 ($[Ag(C_{32}H_{30}N_4)$+MeCN$]^+$, 100), 578.2 ($[Ag_2(C_{32}H_{30}N_4)_2]^{2+}$, 18), 471.3 ($[C_{32}H_{30}N_4$+H$]^+$, 46), 455.2 ($[C_{32}H_{30}N_4$-Me+H$]^+$, 36%).

$[Cu_4(158)_4][PF_6]_4$. Mixture of 2,5-di-*tert*-butyl-7,10-di(pyridin-2-yl)-8,9-diazafluoranthene **158** (0.02 g, 0.0424 mmol) and $Cu(CH_3CN)_4PF_6$ (0.016 g, 0.0424 mmol) in acetone-d_6 (3 mL) was stirred at RT over night. The mixture turned dark red right after the addition of the solvent. ^{1}H-NMR (500 MHz, CD_3CN) δ 8.51 (s, 1H), 8.24 (s, 1H), 8.11 (s, 1H), 8.08 (s, 1H), 7.85 (s, 1H), 7.44 (s, 1H), 1.35 (s, 9H); ^{13}C-NMR (500 MHz, CD_3CN) δ 153.5, 153.3, 153.0, 150.7, 138.4, 136.8, 130.7, 130.2, 128.8, 127.8, 127.4, 126.3, 126.3 36.4, 31.7; MS (EI) m/z (%): 1476.4 ($[Cu(C_{32}H_{30}N_4)_3]^+$, 0.2), 1211.7 ($[Cu_2(C_{32}H_{30}N_4)_2PF_6]^+$, 0.3), 1004.0 ($[Cu(C_{32}H_{30}N_4)_2]^+$, 11), 769.3 ($[Cu_2(C_{32}H_{30}N_4)_3]^{2+}$, 6), 574.5 ($[Cu(C_{32}H_{30}N_4)$+MeCN$]^+$, 87), 534.5 ($[Cu_2(C_{32}H_{30}N_4)_2]^{2+}$, 8), 471.4 ($[C_{32}H_{30}N_4$+H$]^+$, 100%).

2,5-Di-*tert*-butyl-7,10-di(pyrimidin-2-yl)-8,9-diazafluoranthene (159).

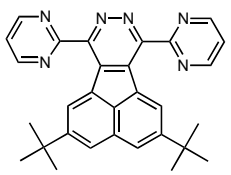

Mixture of 3,6-di(pyrimidin-2-yl)-1,2,4,5-tetrazine (**159**) (0.54 g, 2.3 mmol) and 4,7-di-*tert*-butylace-naphthylene (0.3 g, 1.13 mmol) in DMSO (10 mL) was stirred at 100 °C over night. The mixture was diluted with water (50 mL), precipitate formed and was filtered, washed with methanol and dried to yield of yellow solid (0.45g, 85%). IR (KBr): 2962*s*, 2869*m*, 1627*w*, 1599*w*, 1560*s*, 1445*s*, 1433*m*, 1424*m*, 1395*w*, 1371*s*, 1327*m*, 1264*w*, 1251*w*, 1231*m*, 1213*m*, 1185*w*, 1146*m*, 1132*w*, 1100*m*, 1081*m*, 1008*w*, 990*w*, 934*w*, 892*m*, 814*m*, 807*m*, 755*w*, 698*w*, 679*m*, 642*m*, 621*m*, 590*w*, 566*w*; ^{1}H-NMR (400 MHz, CD_2Cl_2) δ 9.18 (d, 2H, ^{3}J = 4.8 Hz), 8.25 (d, 1H, ^{3}J = 1.2 Hz), 8.10 (d, 1H, ^{3}J = 1.2), 7.63 (dd, 1H, ^{3}J = 4.8, ^{3}J = 4.8 Hz), 1.42 (s, 9H); ^{13}C-NMR (400 MHz, CD_2Cl_2), δ 165.1, 158.3, 154.5, 152.2, 136.2, 131.4, 130.2, 129.9, 127.3, 127.0, 122.0, 36.1, 31.9; MS (EI)

m/z (%): 472.2 (M^+,100), 457.2 (M^+-Me, 98), 441.2 (M^+-2Me+H, 29), 416.2 (M^+-3Me+H, 30), 401.2 (6), 228.6 (19%) ; HRMS (EI) calcd. for $C_{30}H_{28}N_6$: 472.2375; found: 472.2378; mp. over 350 °C decomp.

$[Ag_2(159)_2][PF_6]_2$. Mixture of 2,5-di-*tert*-butyl-7,10-di(pyrimidin-2-yl)-8,9-diazafluoranthene (**159**) (0.03 g, 0.063 mmol) and $AgPF_6$ (0.016 g, 0.063 mmol) in CD_3CN (2 mL) was stirred at RT over night. ^{1}H-NMR (400 MHz, CD_3CN) δ 8.60 (d, 2H, ^3J = 4.5 Hz), 8.39 (s, 1H), 8.17 (s, 1H), 7.39 (dd, 1H, ^3J = 5.0, ^3J = 5.0 Hz), 1.25 (s, 9H); ^{13}C-NMR (500 MHz, CD_2Cl_2) δ 161.7, 159.1, 152.6, 152.5, 139.0, 130.5, 130.4, 129.8, 129.7, 128.8, 124.1, 36.2, 31.9; MS (EI) m/z (%): 1053.8 ($[Ag(C_{30}H_{28}N_6)_2]^+$, 8), 816.8 ($[Ag_2(C_{30}H_{28}N_6)_3]^{2+}$, 6), 620.4 ($[Ag(C_{30}H_{28}N_6)+CH_3CN]^+$, 21), 473.3 ($[(C_{30}H_{28}N_6)+H]^+$, 100), 457.2 ($[(C_{30}H_{28}N_6)-Me]^+$, 21%).

$[Ag_2(159)_2][SbF_6]_2$. Mixture of 2,5-di-*tert*-butyl-7,10-di-(pyrimidin-2-yl)-8,9-diazafluoranthene (**159**) (0.03 g, 0.063 mmol) and $AgSbF_6$ (0.022 g, 0.063 mmol) in CD_2Cl_2 (2 mL) was stirred at RT over night. ^{1}H-NMR (500 MHz, CD_3NO_2, T = 357 K) δ 8.89 (s, 3H), 8.32 (s, 1H), 7.61 (s, 1H), 1.39 (s, 9H); ^{13}C-NMR (500 MHz, CD_2Cl_2, T = 357 K) δ 156.2, 154.8, 148.7, 148.0, 135.3, 127.1, 126.3, 126.1, 125.5, 124.5, 119.5, 31.5, 26.8; MS (EI) m/z (%): 1053.8 ($[Ag(C_{30}H_{28}N_6)_2]^+$, 8), 816.8 ($[Ag_2(C_{30}H_{28}N_6)_3]^{2+}$, 6), 620.4 ($[Ag(C_{30}H_{28}N_6)+CH_3CN]^+$, 21), 473.3 ($[C_{30}H_{28}N_6+H]^+$, 100), 457.2 ($[C_{30}H_{28}N_6–Me]^+$, 21%).

$[Cu_4(159)_4][PF_6]_4$. Mixture of 2,5-di-*tert*-butyl-7,10-di-(pyrimidin-2-yl)-8,9-diazafluoranthene (0.05 g, 0.106 mmol) and $Cu(CH_3CN)_4PF_6$ (0.04 g, 0.106 mmol) in acetone-d_6 (2 mL) was stirred at RT over night. The mixture turned dark red right after the addition of the solvent. ^{1}H-NMR (500 MHz, CD_3CN) δ 9.70 (s, 1H), 8.79 (d, 2H, ^3J = 3.0), 8.41 (d, 1H, ^3J = 3.0 Hz), 7.57 (dd, 1H, ^3J = 4.5, ^3J = 5 Hz), 1.46 (s, 9H); ^{13}C-NMR (500 MHz, CD_3CN), δ 159.9, 158.5, 153.3, 150.4, 140.6, 134.4, 131.8, 131.6, 130.3, 129.7, 125.0, 36.6, 32.2; MS (EI) m/z (%): 1008.0 ($[Cu(C_{30}H_{28}N_6)_2]^+$, 3), 772.5 ($[Cu_2(C_{30}H_{28}N_6)_3]^{2+}$, 20), 576.5 ($[Cu(C_{30}H_{28}N_6)+CH_3CN]^+$, 100), 473.4 ($[C_{30}H_{28}N_6+H]^+$, 50), 457.3 ($[C_{30}H_{28}N_6-Me]^+$, 21%).

2,5-Di-*tert*-butyl-7,10-di(thiazol-2yl)-8,9-diazafluoranthene (160).

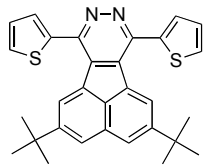

Mixture of 3,6-di(thiazol-2-yl)-1,2,4,5-tetrazine (0.092g, 0.37mmol) and 4,7-di-*tert*-butylacenaphthylene (0.05 g, 0.19 mmol) in dichloromhetane (3 mL) was stirred at reflux for 4 h. The solvent was evaporated, the residue was purified by column chromatography (silica gel, hexane/ethyl acetate 10:1) to yield of yellow solid (0.056 g, 63%). IR (KBr): 3121*w*, 3073*w*, 2948*s*, 2857*s*, 1867*w*, 1725*m*, 1624*w*, 1557*w*, 1525*w*, 1498*m*, 1477*s*, 1463*s*, 1443*s*, 1423*s*, 1395*s*, 1368*s*, 1332*s*, 1323*m*, 1309*s*, 1289*m*, 1268*s*, 1227*s*, 1220*s*, 1208*m*, 1183*m*, 1088*m*, 1059*m*, 1033*s*, 1020*m*, 963*s*, 935*m*, 898*s*, 875*s*, 845*s*, 799*s*, 721*s*, 668*s*, 641*s*, 599*w*, 581*m*, 561*m*, 481*w*; ^{1}H-NMR (500 MHz, $CDCl_3$) δ 10.21 (d, 1H, ^{4}J = 1.5), 8.26 (d, 1H, ^{3}J = 3.0), 8.16 (d, 1H, ^{4}J = 1.0 Hz), 7.68 (d, 1H, ^{3}J = 3.0 Hz) 1.59 (s, 9H); ^{13}C-NMR (400 MHz, CD_2Cl_2) δ 168.2, 152.1, 150.1, 143.9, 134.4, 131.1, 131.0, 130.1, 129.2, 126.9, 123.0, 36.1, 32.0; MS (EI) m/z (%): 482.1 (M^+,60%), 467.1 (M^+-CH_3, 100), 451.1 (16), 427.1 (13%) ; HRMS (EI) calcd. for $C_{28}H_{26}N_4S_2$: 482. 1599; found: 482.1592; mp. 170 °C decomp.

$[Ag_2(160)_2][PF_6]_2$. Mixture of 2,5-di-*tert*-butyl-7,10-di(thiazol-2yl)-8,9-diazafluoranthene **(160)** (0.01 g, 0.021 mmol) and $AgPF_6$ (0.005 g, 0.021 mmol) in CD_3NO_2 (1 mL) was stirred at RT over night. ^{1}H-NMR (500 MHz, $CDCl_3$) δ 9.82 (s, 1H), 8.03 (s, 1H), 8.01 (s, 1H), 7.59 (s, 1H), 1.3 (s, 9H), ^{13}C-NMR (500 MHz, CD_3NO_2); δ 163.6, 155.0, 150.1, 146.0, 139.4, 131.9, 131.3, 130.7, 129.4, 128.8, 126.8, 37.0, 31.8; MS (EI) m/z (%):1073.5 $[Ag(C_{28}H_{26}N_4S_2)_2]^+$, 8), 632.3 ($[Ag(C_{28}H_{26}N_4S_2)+CH_3CN+H]^+$, 100), 483.3 ($[C_{28}H_{26}N_4S_2+H]^+$, 18), 467.2 ($[C_{28}H_{26}N_4S_2-Me+H]^+$, 27%).

$[Ag_2(160)_2][SbF_6]_2$. Mixture of 2,5-di-*tert*-butyl-7,10-di-(thiazol-2yl)-8,9-diazafluoranthene (0.015 g, 0.031 mmol) and $AgSbF_6$ (0.011 g, 0.031 mmol) in CD_3NO_2 (1 mL) was stirred at RT over night. ^{1}H-NMR (500 MHz, $CDCl_3$) δ 9.90 (d, 1H, ^{4}J = 1.2 Hz), 8.03 (d, 1H, ^{3}J = 3.2 Hz), 7.99 (d, 1H, ^{4}J = 1.6 Hz), 7.57 (d, 1H, ^{3}J = 3.2 Hz)1.5 (s, 9H), ^{13}C-NMR (500 MHz, CD_2NO_2) δ 163.2, 155.0, 149.9, 145.9, 139.2, 131.9, 131.3, 130.7, 129.4, 128.8, 126.5, 37.0, 31.8; MS (EI) m/z (%): 1073.5 ($[Ag(C_{28}H_{26}N_4S_2)_2]^+$, 8), 632.3

([Ag($C_{28}H_{26}N_4S_2$)+CH_3CN+H]$^+$, 100), 483.3 ([$C_{28}H_{26}N_4S_2$+H]$^+$, 18), 467.2 ([$C_{28}H_{26}N_4S_2$-Me+H]$^+$, 27%).

7.7 Crystal data

All X-ray crystal structure measurements were made on a *Nonius KappaCCD* area-detector diffractometer[7] or on an *Oxford Diffraction SuperNova Duo* diffractometer[8] using graphite monochromated Mo $K\alpha$ radiation ($\lambda = 0.71073$ Å).

2,5-Di-*tert*-butyl-7,10-di(pyridin-2-yl)-8,9-diazafluoranthene (158), **$C_{32}H_{30}N_4$**. Obtained from acetone, M = 470.62, space group: $P\bar{1}$ (triclinic), a = 10.2436(3), b =10.6985(2), c = 12.3052(3) Å, α = 76.310(1), β = 81.337(1), γ = 76.853(2)°, V = 1269.20(5) Å^3, Z = 2, μ(Mo $K\alpha$) = 0.0733 mm^{-1}, D_x = 1.231 g cm^{-3}, $2\theta_{(max)}$ = 55°, T = 160 K, 37154 measured reflections, 5810 independent reflections, 4067 reflections with $I > 2\sigma(I)$, refinement on F^2 with SHELXL97,[9] 332 parameters, $R(F)$ [$I > 2\sigma(I)$ reflections] = 0.0527, $wR(F^2)$ [all data] = 0.1450, goodness of fit = 1.033, $\Delta\rho_{max}$ = 0.25 e Å^{-3}.

[$Cu_4(C_{32}H_{30}N_4)_4$][PF_6]$_4$·8C_3H_6O. Obtained from acetone/pentane, $C_{152}H_{168}Cu_4F_{24}N_{16}O_8P_4$, M = 3181.11, space group: *Pbca* (orthorhombic), a = 23.9121(4), b = 32.2190(4), c = 38.8832(6) Å, V = 29956.6(8) Å^3, Z = 8, μ(Mo $K\alpha$) = 0.693 mm^{-1}, D_x = 1.407 g cm^{-3}, $2\theta_{(max)}$ = 55°, T = 160 K, 127500 measured reflections, 31301 independent reflections, 19963 reflections with $I > 2\sigma(I)$, refinement on F^2 with SHELXL97, 1760 parameters, 2788 restraints, $R(F)$ [$I > 2\sigma(I)$ reflections] = 0.0874, $wR(F^2)$ [all data] = 0.2635, goodness of fit = 1.060, $\Delta\rho_{max}$ = 1.19 e Å^{-3}. The asymmetric unit contains one tetranuclear Cu-complex cation, four PF_6^- anions and an estimated eight acetone molecules, some of which are highly disordered. Disorder was modeled for three of the eight unique *t*-butyl groups in the cation. Some of the anions also show evidence of disorder and the disorder was modelled for one of the PF_6^- anions. As the disorder in many of the solvent molecules could not be modelled adequately, the solvent contribution to the diffraction data was removed using the *SQUEEZE*[10] procedure of the program *PLATON*.[11] Full details of the disorder and solvent treatment are in the deposited CIF data.

$[Ag_4(C_{32}H_{30}N_4)_4][PF_6]_4 \cdot 3C_6H_6 \cdot 4MeCN$. Obtained from acetonitrile/benzene/pentane, $C_{154}H_{150}Ag_4F_{24}N_{20}P_4$, M = 3292.34, space group: $P\bar{1}$ (triclinic), a = 13.9336(2), b =16.3976 (2), c = 19.5316(3) Å, α = 102.2393(6), β = 106.5617(7), γ = 112.3483(7)°, V = 3688.74(9) Å^3, Z = 1, μ(Mo $K\alpha$) = 0.654 mm^{-1}, D_x = 1.482 g cm^{-3}, $2\theta_{(max)}$ = 60°, T = 160 K, 100836 measured reflections, 21456 independent reflections, 14801 reflections with $I > 2\sigma(I)$, refinement on F^2 with SHELXL97, 1097 parameters, 816 restraints, $R(F)$ [$I > 2\sigma(I)$ reflections] = 0.0520, $wR(F^2)$ [all data] = 0.1328, goodness of fit = 1.022, $\Delta\rho_{max}$ = 1.33 e Å^{-3}. The asymmetric unit contains one half of the cationic Ag-complex, which lies across a centre of inversion, two PF_6^- anions, two MeCN molecules, one disordered benzene molecule, which lies in a general position and one half of another benzene molecule, which lies across a centre of inversion. The *t*-butyl groups of the cation are all disordered. Full details of the disorder treatment are in the deposited CIF data.

$[Ag_4(C_{32}H_{30}N_4)_4][SbF_6]_4 \cdot 4C_5H_{12}$. Obtained from acetonitrile/acetone/benzene/pentane, $C_{148}H_{168}Ag_4F_{24}N_{16}Sb_4$, M = 3545.30, space group: C2/*m* (monoclinic), a = 34.9940(6), b = 17.4149(4), c = 12.8469(3) Å, β = 92.878(1)°, V = 7819.2(3) Å^3, Z = 2, μ(Mo $K\alpha$) = 1.247 mm^{-1}, D_x = 1.506 g cm^{-3}, $2\theta_{(max)}$ = 55°, T = 160 K, 81452 measured reflections, 9186 independent reflections, 7602 reflections with $I > 2\sigma(I)$, refinement on F^2 with SHELXL97, 418 parameters, $R(F)$ [$I > 2\sigma(I)$ reflections] = 0.0399, $wR(F^2)$ [all data] = 0.0943, goodness of fit = 1.080, $\Delta\rho_{max}$ = 0.76 e Å^{-3}. The asymmetric unit contains one quarter of the cationic tetranuclear Ag-complex, which lies across a site of 2/*m* symmetry (C_{2h}), two independent halves of PF_6^- anions, which lie across mirror planes, and highly disordered solvent molecules. As attempts to model the solvent were unfruitful, the solvent contribution to the structure was removed using the *SQUEEZE* procedure of the program *PLATON*. Full details are in the deposited CIF data.

$[Ag_2(C_{32}H_{30}N_4)_2][CHB_{11}Cl_{11}]_2 \cdot 4C_6H_4Cl_2 \cdot CH_2Cl_2$. Obtained from acetonitrile/1,2-dichlorobenzene/hexane, $C_{91}H_{80}Ag_2B_{22}Cl_{32}N_8$, M = 2873.74, $P\bar{1}$ (triclinic), a = 12.8147(2), b =14.1011(2), c = 18.4969(2) Å, α =75.5567(7), β =74.1397(7), γ = 73.6649(7)°, V = 3031.00(7) Å^3, Z = 1, μ(Mo $K\alpha$) = 1.074 mm^{-1}, D_x = 1.574 g cm^{-3}, $2\theta_{(max)}$ = 60°, T = 160 K, 88798 measured reflections, 17607 independent reflections, 13066

reflections with $I > 2\sigma(I)$, refinement on F^2 with SHELXL97, 620 parameters, $R(F)$ [$I > 2\sigma(I)$ reflections] = 0.0398, $wR(F^2)$ [all data] = 0.1053, goodness of fit =1.059, $\Delta\rho_{max}$ = 0.53 e Å^{-3}. The asymmetric unit contains half of a centrosymmetric dinuclear cation, one anion, two molecules of 1,2-dichlorobenzene and a half occupied site for a molecule of CH_2Cl_2, which is disordered about a centre of inversion. As attempts to model the solvent were unfruitful, the solvent contribution to the structure was removed using the *SQUEEZE* procedure of the program *PLATON*. Full details are in the deposited CIF data.

2,5-Di-*tert*-butyl-7,10-di(pyrimidin-2-yl)-8,9-diazafluoranthene (159), **$C_{30}H_{28}N_6$**. Obtained from CH_2Cl_2/pentane/benzene, M = 472.59, space group: $P2_1$ (monoclinic), a = 10.1555(2), b =12.3482(3), c = 10.4107(2) Å, β = 98.744(1)°, V = 1290.35(5) Å^3, Z = 2, μ(Mo $K\alpha$) = 0.0744 mm^{-1}, D_x = 1.216 g cm^{-3}, $2\theta_{(max)}$ = 55°, T = 160 K, 26745 measured reflections, 3094 independent reflections, 2843 reflections with $I > 2\sigma(I)$, refinement on F^2 with SHELXL97, 333 parameters, $R(F)$ [$I > 2\sigma(I)$ reflections] = 0.0375, $wR(F^2)$ [all data] = 0.0941, goodness of fit = 1.066, $\Delta\rho_{max}$ = 0.16 e Å^{-3}. The absolute structure was chosen arbitrarily.

$[Cu_4(C_{30}H_{28}N_6)_4][PF_6]_4 \cdot 2.17H_2O$. Obtained from MeCN/MeOH/acetone, $C_{120}H_{116.33}Cu_4F_{24}N_{24}O_{2.17}P_4$, M = 2763.46, space group: $P\bar{1}$ (triclinic), a = 12.4516(4), b =23.6077(8), c = 42.950(2) Å, α = 99.3440(9), β = 94.255(1), γ = 94.401(1)°, V = 12372.9(7) Å^3, Z = 4, μ(Mo $K\alpha$) = 0.827 mm^{-1}, D_x = 1.483 g cm^{-3}, $2\theta_{(max)}$ = 50°, T = 160 K, 149307 measured reflections, 41319 independent reflections, 24116 reflections with $I > 2\sigma(I)$, refinement on F^2 with SHELXL97, 3551 parameters, 2062 restraints, $R(F)$ [$I > 2\sigma(I)$ reflections] = 0.0791, $wR(F^2)$ [all data] = 0.1762, goodness of fit = 1.077, $\Delta\rho_{max}$ = 0.81 e Å^{-3}. The asymmetric unit contains two tetranuclear cations, eight PF_6^- anions, four sites fully occupied by water molecules and one site approximately one-third occupied by a water molecule. Three *tert*-butyl groups in one cation and one in the other are disordered. Some of the anions also show disorder and the disorder was modelled for two of the PF_6^- anions. Full details of the disorder treatment are in the deposited CIF data.

$[Ag_2(C_{30}H_{28}N_6)_2][PF_6]_2 \cdot 0.5CH_2Cl_2 \cdot 0.5C_6H_5Cl \cdot 0.5C_6H_{14}$. Obtained from dichloromethane/chlorobenzene/hexane/MeCN, $C_{66.5}H_{66.5}Ag_2F_{12}N_{12}P_2Cl_{1.5}$, M = 1592.68, space group: $P2_1/c$ (monoclinic), a = 17.7686(1), b =16.8498(2), c = 23.2107(2) Å, β =90.2002(6)°, V = 6949.2(1) Å^3, Z = 4, μ(Mo $K\alpha$) = 0.748 mm^{-1}, D_x = 1.522 g cm^{-3}, $2\theta_{(max)}$ = 52°, T = 160 K, 140014 measured reflections, 13650 independent reflections, 10805 reflections with $I > 2\sigma(I)$, refinement on F^2 with SHELXL97, 915 parameters, 234 restraints, $R(F)$ [$I > 2\sigma(I)$ reflections] = 0.0543, $wR(F^2)$ [all data] = 0.1623, goodness of fit = 1.074, $\Delta\rho_{max}$ = 1.01 e Å^{-3}. The asymmetric unit contains one cation, two disordered anions and some disordered solvent molecules which have been estimated at one half of each of a molecule of CH_2Cl_2, chlorobenzene and hexane per asymmetric unit. As attempts to model the solvent were unfruitful, the solvent contribution to the structure was removed using the *SQUEEZE* procedure of the program *PLATON*. Full details are in the deposited CIF data.

$[Ag_2(C_{30}H_{28}N_6)_2][SbF_6]_2 \cdot C_3H_6O \cdot 0.5C_6H_{14} \cdot 0.5C_6H_6$. Obtained from acetone/benzene/hexane, $C_{69}H_{72}Ag_2F_{12}N_{12}OSb_2$, M = 1772.52 space group: $C2/m$ (monoclinic), a = 23.2507(3), b =17.2660(3), c = 17.6490(3) Å, β =91.746(1)°, V = 7081.8(2) Å^3, Z = 4, μ(Mo $K\alpha$) = 1.380 mm^{-1}, D_x = 1.662 g cm^{-3}, $2\theta_{(max)}$ = 55°, T = 160 K, 75629 measured reflections, 8370 independent reflections, 7293 reflections with $I > 2\sigma(I)$, refinement on F^2 with SHELXL97, 915 parameters, 100 restraints, $R(F)$ [$I > 2\sigma(I)$ reflections] = 0.0456, $wR(F^2)$ [all data] = 0.1161, goodness of fit = 1.080, $\Delta\rho_{max}$ = 3.2 e Å^{-3}. The asymmetric unit contains half of a dinuclear cation, which sits across a mirror plane perpendicular to the Ag···Ag axis, two half anions, both of which sit on mirror planes and one of which is disordered, one half of a molecule of acetone, which also sits across a mirror plane and further highly disordered solvent molecules which have been estimated at one quarter of each of a molecule of hexane and benzene per asymmetric unit. As attempts to model the solvent were unfruitful, the solvent contribution to the structure was removed using the *SQUEEZE* procedure of the program *PLATON*. Full details are in the deposited CIF data.

2,5-Di-*tert*-butyl-7,10-di(thiazol-2yl)-8,9-diazafluoranthene (160), **$C_{28}H_{26}N_4S_2 \cdot 0.67CH_3CN \cdot 0.33C_5H_{12}$**. Obtained from acetonitrile/dichloromethane/pentane,

$C_{31}H_{32}N_{4.67}S_2$, M = 534.07, space group: $P\bar{4}2_1m$ (tetragonal), a = 16.6799(1), c = 15.0127(2) Å, V = 4176.82(6) Å^3, Z = 6, μ(Mo $K\alpha$) = 0.220 mm^{-1}, D_x = 1.274 g cm^{-3}, $2\theta_{(max)}$ = 60°, T = 160 K, 72287 measured reflections, 5846 independent reflections, 3959 reflections with $I > 2\sigma(I)$, refinement on F^2 with SHELXL97, 328 parameters, 343 restraints, $R(F)$ [$I > 2\sigma(I)$ reflections] = 0.0680, $wR(F^2)$ [all data] = 0.2199, goodness of fit = 1.088, $\Delta\rho_{max}$ = 0.57 e Å^{-3}. There are two symmetry-independent fluoranthene molecules in the structure. One of these molecules sits across a mirror plane which bisects the molecule. The other sits in a mirror plane as well as lying across a second mirror plane which bisects this molecule (mm symmetry). The *tert*-butyl groups in each molecule are disordered over two orientations, although the model for this leads to some illogical geometry. One possibility to compensate this might be the presence of whole molecule disorder, although there is also no clear evidence for this. There are voids in the structure, which appear to be partially occupied with solvent molecules. As attempts to model the solvent were unfruitful, the solvent contribution to the structure was removed using the *SQUEEZE* procedure of the program *PLATON*. Full details are in the deposited CIF data.

$[Ag_2(C_{28}H_{26}N_4S_2)_2]_n \cdot 2n[PF_6]_n \cdot nC_3H_6O$. Obtained from benzene/acetonitrile/ hexane/ether/acetone, $C_{59}H_{58}Ag_2F_{12}N_8OP_2S_4$, M = 1529.06, space group: $P\bar{1}$ (triclinic), a = 11.3226(2) , b =11.5685 (1) , c = 24.0375(4) Å, α = 101.105(1), β = 100.426(2), γ = 94.923(1)°, V = 3014.77(8) Å^3, Z = 2, μ(Mo $K\alpha$) = 0.926 mm^{-1}, D_x = 1.684 g cm^{-3}, $2\theta_{(max)}$ = 59°, T = 160 K, 53400 measured reflections, 14806 independent reflections, 13022 reflections with $I > 2\sigma(I)$, refinement on F^2 with SHELXL97, 894 parameters, 741 restraints, $R(F)$ [$I > 2\sigma(I)$ reflections] = 0.0967, $wR(F^2)$ [all data] = 0.2441, goodness of fit = 1.175, $\Delta\rho_{max}$ = 1.97 e Å^{-3}. The cation is a one-dimensional polymeric ribbon. The asymmetric unit contains two Ag^+ cations, two ligands, two PF_6 anions and one acetone molecule. One *t*-Bu group in one of the independent ligands is disordered over two positions and the F-atoms of one of the independent PF_6^- anions are also disordered over two positions. The crystal was non-merohedrally twinned. The twin components are related by a rotation of 1.2° about the (001) plane with a major twin fraction of 0.806(2). Full details are in the deposited CIF data.

7.8 References

1. a) Petty, M. C.; Bryce, M. R.; Bloor, D.; *Introduction to Molecular Electronics*, Oxford University Press, New York **1995**; b) Tour, J. M. *Acc. Chem. Res.* **2000**, *33*, 791-804; c) Pease, A. R.; Jeppesen, J. O.; Stoddart, J. F.; Luo, Y.; Collier, C. P.; Heath, J. R. *Acc. Chem. Res.* **2001**, *34*, 433-444.
2. a) Joachim, C.; Gimzewski, J. K.; Aviram, A. *Nature* **2000**, *408*, 541-548; b) Service, R. F. *Science* **2001**, *293*, 782-785.
3. a) Rojo, J.; Romero-Salguero, F. J.; Lehn, J-M.; Baum, G.; Fenske, D. *Eur. J. Inorg. Chem.* **1999**, 1421-1428; b) Patroniak, V.; Baxter, P. N. W.; Lehn, J-M.; Kubicki, M.; Nissinen, M.; Rissanen, K. *Eur. J. Inorg. Chem.* **2003**, 4001-4009.
4. a) Zhao, L.; Xu, Z.; Thompson, L. K.; Heath, S. L.; Miller. D. O.; Ohba, M. *Angew. Chem.* **2000**, *112*, 3244-3247; *Angew. Chem. Int. Ed.* **2000**, *39*, 3114 - 3117; b) Thompson, L. K.; Zhao, L.; Xu, Z.; . Miller, D. O.; Reiff, W. M. *Inorg. Chem.* **2003**, *42*, 128-139.
5. Barbiou, M.; Lehn, J.-M. *J. Am. Chem. Soc.* **2003**, *125*, 10257-10265.
6. Rahanyan, N.; Linden, A.; Baldridge, K. K.; Siegel, J. S. *Org. Biomol. Chem.* **2009**, *7*, 2082-2092.
7. Hooft, R. *Kappa CCD Collect Software*, Nonius BV, Delft, The Netherlands **1999**.
8. *CrysAlisPro Diffractometer Software*, Oxford Diffraction Ltd, Yarnton, Oxfordshire, England **2010**.
9. Sheldrick, G. M. *Acta Crystallogr., Sect. A* **2008**, *64*, 112-122.
10. van der Sluis, P.; Spek, A. L. *Acta Crystallogr.* **1990**, *A46*, 194-201.
11. Spek, A. L. *PLATON*, *Program for the Analysis of Molecular Geometry*, University of Utrecht, The Netherlands **2009**.